TOP-BAR AND EMBEDMENT LENGTH EFFECTS IN REINFORCED CONCRETE BEAMS

by

Paul R. Jeanty

A Thesis submitted to the Faculty of Graduate Studies and Research in partial fulfillment of the requirements for the Degree of Master of Engineering

Department of Civil Engineering and Applied Mechanics
McGill University
Montreal, Canada
November 1978

TOP-BAR AND EMBEDMENT LENGTH EFFECTS IN REINFORCED CONCRETE BEAMS

ABSTRACT

This thesis presents a state of-the-art report of bond and describes existing bond testing methods. The results of tests on six simply supported beams with central point loading are used to study the "top-bar" effect and the effect of varying embedment lengths of No. 8 (25.4 mm) reinforcing bars. Three specimens with tension bars cast in the top of the beams and three companion specimens with tension bars cast in the bottom of the beams having embedment lengths of 30 in (76.2 cm), 36 in (91.4 cm) and 40 in (101.6 cm) were tested. The beam span is 10 feet (3.05 m) and the overall cross-section dimensions are 9 x 18 in (22.9 x 45.7 cm).

The overall performance of the beams is illustrated in load-deflection curves. The experimental results are compared with the theoretical predictions obtained from general flexural theory assuming perfect bond. Comparisons of the load-deflection responses indicate that specimens with bottom-cast bars are stronger, stiffer and fail in a more ductile manner than their companion specimens with top-cast bars. The experiments also indicate that the strength, stiffness and ductility are increased with an increase in the embedment length.

The strain distributions and bond stress variations along the tension reinforcing bars were obtained from electrical resistance strain gauges for each loading stage. Comparisons of the results indicate that

beams with bottom-cast bars exhibit higher bond strengths and that the increases in embedment lengths result in a reduction of maximum bond stresses developed.

The results of this investigation indicate a strength reduction of 10 to 18 percent as well as a reduction in ductility for specimens containing top-cast bars. Comparisons of the behaviour of the beams tested indicate that top-cast bars require an increased embedment length between 11 and 20 percent longer than bottom-cast bars in order to reach the same stress levels in the bars.

EFFETS D'ARMATURE SUPERIEURE ET DE LONGUEUR D'ANCRAGE DANS LES POUTRES EN BETON ARME

RESUME

Cette thèse présente une synthèse de l'adhérence et de ses paramètres et décrit les méthodes actuelles des essais d'adhérence. Les résultats des essais sur six poutres simplement appuyées avec charge centrale sont utilisés pour étudier l'effet "d'armature supérieure" et l'effet de la variation de la longueur d'ancrage d'une barre d'acier No. 8 (25.4 mm). Trois spécimens avec armatures supérieures de tension et trois autres spécimens semblables avec armatures inférieures de tension, ayant des longueurs d'ancrage de 30 po (76.2 cm), 36 po (91.4 cm) et 40 po (101.6 cm), ont été mises en charge. La portée des poutres est de 10 pieds (3.05 m) et les dimensions transversales sont de 9 x 18 po (22.9 x 45.7 cm).

La performance générale des poutres est illustrée par des courbes charge-déplacement. Les résultats expérimentaux sont comparés avec les prédictions théoriques obtenues à partir de la théorie de flexion basée sur l'adhérence parfaite. Les comparaisons des courbes charge-déplacement indiquent que les poutres avec armatures inférieures sont plus résistantes, plus rigides et sont plus ductiles à la rupture. Les essais montrent également que la résistance, la rigidité et la ductilité augmentent avec une plus grande longueur d'ancrage.

Les distributions des déformations et les variations des contraintes d'adhérence ont été obtenues à partir de jauges électriques,

à chaque étape du chargement. Les comparaisons des résultats indiquent que les poutres avec armatures inférieures démontrent une plus grande résistance d'adhérence et que les augmentations des longueurs d'ancrage conduisent à une réduction des contraintes maximales d'adhérence.

Les résultats de cette recherche indiquent une diminution de la résistance de 10 à 18% ainsi qu'une réduction de la ductilité pour les poutres contenant des armatures supérieures. Le comportement comparé des poutres soumises à l'essai montre que les barres supérieures nécessitent un ancrage 11 à 20% plus long que les barres inférieures afin d'atteindre les mêmes niveaux de contrainte.

ACKNOWLEDGEMENTS

The experimental work presented in this thesis was undertaken under the combined direction of Professor M.S. Mirza and Professor D. Mitchell. The author takes this opportunity to express his sincere thanks to Professor M.S. Mirza for his guidance, encouragement and patience throughout this investigation and during the course of this study. His advice and constructive comments are invaluable.

The writer also extends his deep gratitude to Professor D. Mitchell for his positive discussions, his guidance and his helpful suggestions through all aspects of this research.

Many thanks are due to fellow graduate students: Kostas Marcakis and Yoon Moi Lee for assistance with the experiments. I am also very grateful to Mr. Brian Cockayne and his technical staff for providing the necessary expertise.

The financial assistance provided by the National Research Council and the Québec Department of Education for the continuing research program at McGill University is thankfully acknowledged. Last, but not least, I wish to express my appreciation to Miron Company Limited for the award of the "Miron Fellowship in Concrete Studies".

The experiments reported in this thesis were carried out in the Jamieson Structures Laboratory of the Department of Civil Engineering and Applied Mechanics, McGill University.

LIST OF FIGURES

LIST OF TABLES

LIST OF NOTATIONS

a	Depth of equivalent rectangular stress block
a^*	Lug height
A_b	Area of the steel bar
$A_{b,1}$	Area of #8 Steel bar
$A_{b,2}$	Area of #6 Steel bar
A_{tr}	Area of transverse reinforcement normal to the plane of splitting through the anchored bars
A_v	Area of shear reinforcement within a distance s
b	Beam width
b_w	Web width
c	Inside lug spacing
C	The smaller of C_b or C_s
C_c	Compression force in the concrete
C_b	Clear bottom cover to main reinforcement
C_s	Half clear spacing between bars (or half available concrete width per bar)
d	Local bond slip
d_b	Nominal diameter of the steel bar
d_c	Local concrete displacements
d_s	Local steel displacements
d_t	Distance from extreme compression fiber to centroid of tension reinforcement

d_1	Distance from extreme compression fiber to centroid of #8 bar
d_2	Distance from extreme compression fiber to centroid of #6 bar
d^*	Displacements at the loaded face of the specimen
d^*_c	Concrete displacements at the loaded face of the specimen
d^*_s	Steel displacements at the loaded face of the specimen
E_c	Modulus of elasticity of concrete
E_s	Modulus of elasticity of the steel bar
f'_c	Concrete compressive strength
$\bar{f}'_c$	Average concrete compressive strength of a group of beams containing the same size bar
f_r	Modulus of rupture of concrete
$(f_s)_c$	Steel stress corresponding to u_c
f_u	Ultimate tensile strength of the steel bar
f_y	Yield strength of the steel bar
f_{yt}	Yield strength of transverse reinforcement
F_b	Bearing force against the face of the lug
H^*	Lever arm of the internal couple
I_{cr}	Moment of inertia of cracked section transformed to concrete
I_e	Effective moment of inertia for computation of deflection
I_g	Moment of inertia of uncracked section transformed to concrete
k, k_1, k_2	Empirical coefficients which depend on type of bars, their diameter, embedment length and the type of the test

K_{tr}	An index of the transverse reinforcement provided along the anchored bar, $A_{tr}f_{yt}/600\ s\ d_b$
l_d	(Basic) development length of bottom-cast bars
l^*_d	Minimum permissible anchorage length
l_e	Embedment length
L	Span length of the beam
L*	Lever arm of the external couple
M_{cr}	Cracking moment
M_{ext}	External moment due to applied load
M_{max}	Maximum external moment at load into consideration
M_u	Ultimate design moment
P	Applied concentrated load on a test specimen
P_u	Ultimate design load
s	Spacing of transverse reinforcement centre to centre
T	Total tensile force
u	Nominal bond stress
u_c	Critical bond stress which is the lesser of the two values of bond stress corresponding to a loaded-end slip of 0.01 in (0.25 mm) and a free-end slip of 0.007 in (0.05 mm)
u_f	Flexural bond stress
u_m	Maximum bond stress (or bond strength or bond resistance)
u_t	Average local bond stress obtained in tests
u*	Permissible average bond stress value
u^*_c	Critical bond stress adjusted by multiplying by $\bar{f}'_c/f'_c$
$u_{m,1}$	Maximum bond stress adjusted by multiplying by $\bar{f}'_c/f'_c$

$u_{m,2}$	Maximum bond stress adjusted to $f'_c = 3000$ psi (22.8 MPa) and cover = 1.5 in (3.8 cm)
$u_{m,3}$	Maximum bond stress adjusted to $f'_c = 3000$ psi (22.8 MPa)
$u_{m,b}$	Maximum bond stress for a beam of width b
$u_{m,18}$	Maximum bond stress for a beam 18 in wide (45.7 cm)
U	Unit shearing force acting parallel to the bar axis at the concrete steel interface
v_c	Nominal permissible shear stress carried by concrete
v_u	Nominal shear stress
v'_u	Shear stress carried by web reinforcement
V_a	Force developed through adhesion along the surface of the bar
V^*_c	Shear force acting on the cylindrical concrete surface between adjacent lugs
V_u	Total applied design shear force at section
z	Lever arm of the internal resisting couple
α	Ratio of $u_{m,b}/u_{m,18}$
Δ_{AB}	Distance between two gauges A and B
Δ_{fs}	Change of steel stress over unit length
ΔF_{AB}	Differential force between two gauges A and B
ΔQ	Change of bar force over unit length
ϵ_A, ϵ_B	Strains at gauge A and gauge B
Γ	Ratio of vertical shear reinforcement area to the gross concrete area of a horizontal section
Σo	Total perimeter of the bars at the section
ϕ	Capacity reduction factor

CONVERSION FACTORS

The following is a list of the conversion factors for all imperial units (English System) used throughout this thesis to the "SI System".

1 Foot	=	30.48 centimeters
1 ft^2	=	.09290304 $meter^2$
1 Inch	=	2.54 cm
1 $in.^2$	=	6.4516 cm^2
1 $in.^3$	=	16.387 cm^3
1 $in.^4$	=	41.623 cm^4
1 kip-force	=	453.6 kilograms force = 4448.2 Newtons
1 kip/in^2 (ksi)	=	6.895 Mega-Pascal (1 Pascal = 1 $Newton/m^2$)
1 Pound-force	=	453.5923 grams-force = 4.4482 Newtons
1 Pound-force/inch	=	178.5796 gr/cm
1 Pound-force in.	=	0.112985 Newton-meter
1 Pound-force foot	=	1.355818 Newton-meter
1 Pound-force/ft^2	=	4.88242 kg/m^2
1 Pound-force/in^2 (psi)	=	6.895 kilo-Pascal = 70.3069 gr/cm^2

TABLE OF CONTENTS

Page

CHAPTER

CHAPTER I

STATE OF THE ART OF BOND AND SCOPE OF RESEARCH

1.1 Introduction

Since external loads are very rarely applied directly to the reinforcement, steel can receive its share of the load only from the surrounding concrete. If one defines "slip" as the differential displacement between steel and concrete, the term "bond" is then used to describe the means by which slip between steel and concrete is minimized or prevented. Then, one of the most important prerequisites of reinforced concrete construction is adequate bond between the reinforcement and the concrete. Inadequate bond usually results in premature failure. Therefore, the attainment of satisfactory performance in bond is an important aspect of the design and the detailing of reinforcement in structural components.

Usually "bond stress" is defined as the unit shearing force acting parallel to the reinforcing bar axis at the concrete steel interface and it is given by:

$$U = \frac{\Delta Q}{\pi d_b} = \frac{\Delta f_s A_b}{\pi d_b} = \frac{d_b \Delta f_s}{4} \qquad (1.1)$$

where ΔQ = change of bar force over unit length

πd_b = nominal surface area of a steel bar of unit length

d_b — nominal diameter of the steel bar

Δf_s — change of steel stress of over unit length

A_b — area of the steel bar

Bond stress is less apt to be critical in design today than it was 30 to 35 years ago when only plain reinforcing bars were used. Deformed bars have provided an extra element of strength and safety. On the other hand, bond is probably less throughly understood today than it was in the days of plain bars. The behaviour of deformed bars, in particular the introduction of high-strength steels and large diameter bars, have created some new problems. Also it has required that engineers re-examine their basic knowledge of bond and put more emphasis on some of the parameters affecting bond strength such as development length, the so-called "top-bar" effect, the concrete cover thickness and the clear distance between bars. In this chapter, the evolution of the development length concept will be presented; then, the basic concepts of bond stress-slip relationships will be reviewed and the parameters influencing bond strength will be discussed before defining the objectives of the present experimental research program.

1.2 Conceptual Shift from Bond Stress to Development Length

Prior to 1971, development and anchorage of bars was always treated as a sub-section of the chapter on bond stress in the American and the Canadian Codes (1,2). This bond concept, which has long been used as a measure of bond performance, is the flexural bond stress defined by the following equation:

$$u_f = \frac{V_u}{\Sigma o \cdot z} \tag{1.2}$$

where V_u is the shear, as a measure of the changing moment, Σo is the total perimeter of the bars at the section and z is the arm of the internal resisting couple.

However, Equation (1.2) grossly oversimplifies the situation, and does not even approximately simulate what actually happens in realistic beams. Even in the region of constant bending moment where shear force is zero, bond stresses are developed on account of cracking of the concrete. Studies over the past fifteen years have shown that the bond stress calculations are not helpful in the present state-of-the-art and that Equation (1.2) must be supplemented by development length checks. When a bar has enough embedment in concrete, it does not fail by bond but reaches its yield strength and fails in tension although the concrete may have cracked along its length.

It is noteworthy that bond stress calculations are not mentioned in the present Codes (3,4,5); however this does not mean that "local" bond stress is unimportant. Three main reasons have led to this change in emphasis. Firstly, bond stress is a very complex problem for which there is no immediate dependable solution available for use in design. Secondly strength over a given length seems not to be sensitive to local peak bond stresses, but can be based on an average value. Thirdly, the development length concept summarizes or incorporates most of the present usable knowledge in this area. That is why, according to Watstein and Bresler (6), it is now generally recognized that a more realistic approach to the bond problem is to regard it as a problem of computing the anchorage or development length of a bar necessary to transmit the stress in the steel to the surrounding concrete. This is given by:

$$l^*_d = \frac{f_y d_b}{4u^*} \qquad (1.3)$$

where l^*_d = minimum permissible anchorage length

u^* = permissible average bond stress value

f_y = yield stress of the steel bar

d_b = nominal diameter of the steel bar

1.3 Bond Stress-Slip Relationship

In any bond test either pull-out or beam test, the evolution of bond between steel and concrete depends greatly on the amount of slip that occurs either at the free end or at the load end of the specimen. It is shown qualitatively in Fig. 1.1 where four different stages are distinguished:

Stage AB : The load increases without slip.

Stage BC : There is loss in bond at B over the embedment length and slip occurs at gradually increasing rates with the increase in load.

Stage CD : There is complete rupture at C of the surrounding concrete and slip continues under constant load.

Stage DE : Premature failure of specimen by pulling of the bar or splitting of concrete.

1.3.1 Concepts of Bond Action

1.3.1.1 Plain Bars

Mylrea (7) reported that bond failures in pull-out specimens reinforced with plain bars are characterized by the extraction of the bar from the concrete specimen, once slipping becomes general and bond stress is nearly uniform along the full length of the bar. In the early days of reinforced concrete, the bond resistance of plain bars was often thought of as chemical adhesion between the mortar paste and the surface. However, even a low bar stress causes slip sufficient to break the adhesion immediately adjacent to a crack in the concrete. Once slip occurs, only the frictional resistance remains and the bond stress can be thought of as the overall average of the bond on the section where adhesive bond is still intact, and the lower bond stress at the section where only frictional resistance is present.

Mikhailov (8) studied the relative values of adhesion and frictional bond with hot rolled and smooth cold rolled bars and concluded the following:

a) The adhesive forces between the steel bars and the concrete are quite low and amount only to 70 - 100 psi (0.5 - 0.7 MPa), therefore adhesion itself is of no significance in preventing slip.

b) The adhesion and frictional resistance resulting from shrinkage account for 25 to 30% of the bond strength.

c) The degree of roughness of the surface and the change in the lateral dimension of the bars along their development length account for about 70 to 75% of the total resistance to slip.

1.3.1.2 <u>Deformed Bars</u>

With the advent of modern deformed bars the pattern of bond failure changed radically. Adhesion and friction still exist, however they are secondary because the primary reliance for bond resistance is on the bearing of lugs and the strength of concrete sections between lugs. The bond strength developed between two ribs of a bar (see Fig. 1.2) is associated with the following forces:

a) The forces V_a, developed through adhesion along the surface of the bar which can be ignored for practical purposes because this adhesion breaks down inevitably as the load is increased.

b) Bearing forces F_b, against the face of the lug.

c) Shear forces V^*_c, acting on the cylindrical concrete surface between adjacent lugs.

The relationship between these two important components of bond force development F_b and V^*_c can be expressed as follows:

$$F_b = \frac{c}{a^*} V^*_c \qquad (1.4)$$

where c = inside lug spacing

a^* = lug height

In some situations, where the bar is short, the shear component V^*_c will govern the behaviour of the specimen. This is the case when the ribs are high and spaced too closely, or when small bars are used with concrete of low compressive strength, or when large size bars are used with large concrete cover. The bar will, then, pull-out without yielding and will shear out a sheath of concrete with its outside diameter equal to that of the lugs.

In bond type specimens with usual deformed reinforcing bars, most bond failures are normally splitting failures of the surrounding concrete; this splitting generally results from the wedging action of the lugs against the concrete. Strictly interpreted, splitting is not the same as bond failure according to the "traditional" concept of the bar pulling out of the concrete or the specimen failing by crushing against the lugs. Splitting failure is basically a tension phenomenon but a better knowledge of the strength and the deformation properties of concrete in tension is needed in order to obtain a better understanding of the splitting phenomenon. Until such time, splitting must be grouped together with other aspects of bond and progressive splitting can be considered as the first evidence of bond distress.

1.3.2 The Mechanism of Bond Splitting

In the forties, the development of deformed bars resulted in greatly increased resistance to local slip. With the advent of higher yield strength reinforcement and the consequent increase in the service load stresses of the reinforcing steel, cracking has become one the most important factors in determining the durability of reinforced concrete members (9). Therefore, extensive investigations have been carried out recently on the crack formation in the concrete adjacent to the deformed reinforcing bars which finally results in splitting failures. The mechanism can be described as follows:

When a deformed reinforcing bar is embedded in mass concrete, bond forces across the ribs (bar deformations) need to be transferred to enable the full strength of the bar to be developed. As slip progresses, the average bond resistance increases and consequently the stresses in the concrete adjacent to the deformed reinforcing bar also increase and lead to cracks and deformations of the concrete as shown in Fig. 1.3.

Bresler and Bertero (10) indicated that at low load levels principal tensile stresses at the steel concrete interface are inclined at an angle with the longitudinal axis varying from about 60° at the crack face and decreasing to 0° at the midway section between two adjacent cracks, as shown in Fig. 1.4. Broms (11, 12) and Goto (13) devised ingenious techniques to study the internal cracks. Broms and Lutz (14) from their analytical and experimental data, established the existence of radial cracks originating at the steel concrete interface and not extending to the concrete surface and therefore not visible at the outside surface.

Goto (13) injected red ink into his specimens which were then sawn to examine the crack pattern as illustrated by Fig. 1.5. His experimental studies confirmed that numerous inclined cracks developed around the deformed bars within the concrete prism. These cracks form cones with their apexes near the bar lugs and with their bases generally directed towards the nearest primary crack or towards the specimen end. According to Goto, the formation of internal cracks usually starts at low steel stresses and is influenced by the surface deformations of the reinforcing bar. In the photographs shown in Fig. 1.5 for the crack pattern after removal of the reinforcing bar, the dark areas indicate that adhesion between the steel and the concrete had been lost in these regions. Also it indicates that the bond between the deformed bar and the concrete therefore depends on the mechanical resistance of the lugs and the frictional resistance between the concrete and the steel.

Referring to Fig. 1.6 a comb-like structure is formed and its teeth are deformed by the compressive forces transmitted through the bar lugs as the tensile force in the steel bar is increased. These forces can be resolved into two components:

(i) A component parallel to the bar axis tending to shear a cylinder of concrete, concentric with the bar deformations.

(ii) A radial component which tends to split the concrete like the bursting pressure in a pipe.

Goto also noted that the complete relaxation of the external tensile load on the steel bar after the formation of internal cracks does not return the steel stress to zero. He concluded that, once the comb-like structure is deformed and undergoes plastic deformations, it does not return to its virgin state even when the steel tensile force is relaxed, due to the interlocking friction at the surfaces of the internal cracks.

Lutz, Gergely and Winter (15, 16) studied the fundamental mechanism of bond transfer on machined bars and they established that slips result from the gradual deterioration (crushing) of the concrete under the high bearing pressures and shearing stresses applied by the bar ribs. This conclusion, which is generally accepted by other investigators, is not in agreement with Houde and Mirza's (17) recent findings. Houde (18) tested sixty-two concentric tensile specimens, each reinforced with only one central bar. Thirteen of the tests were conducted on specimens reinforced with special internally instrumented bars. After testing, five of them were sawn parallel to the bar axis to expose the imprint of the bar and examination of the sliced specimens revealed that the bar deformations were sharply stamped into the concrete, as can be seen from Fig. 1.7. There was no detection of powdery areas on account of crushing under the rib pressure or polished surfaces due to the sliding of the bar. Houde (18) concluded that the slip at the steel-concrete interface can be explained by the internal cracking of the first layers of concrete surrounding the reinforcing bar and by bending of the small concrete teeth of the comb-like structure idealized in Fig. 1.6. However, more basic research is needed in this area.

1.3.3 Bond Stress-Slip Relationship

Early investigators and designers of reinforced concrete recognized that slip of the reinforcement had to be prevented in order to minimize cracking, to develop flexural and shearing strengths and to maintain the composite behaviour of reinforced concrete. Therefore in their bond tests, they determined the slip values at one end of the bar at all loading stages, in order to obtain the important load-slip history of the specimens.

Clark (19) conducted some pull-out tests to check the influence of bar deformations on the bond efficiency of deformed bars. He tested 7/8 in (22.2 mm) diameter bar, with 17 different patterns of deformations, using a concrete specimen of 8 x 9 in (20.3 x 22.9 cm) in cross-section and of two lengths, 8 in (20.3 cm) and 16 in (40.6 cm). He compared their load-slip curves and concluded that height of deformations and the inclination of the face of the deformations were important factors in determining the bond resistance, but not the pattern of the deformations.

Menzel (20) also used the "load-slip" curve as a criterion for bond efficiency when he showed the effect of settlement of concrete on bond performance. Bresler and Bertero (10) conducted experiments on tension specimens under repeated load and reported experimental results on both the bond stress distribution and the measured end-slip.

Mathey & Watstein (9), from their investigation of bond strengths of beams and pull-out specimens, considered advisable to establish limiting slip values in terms of maximum permissible crack widths in an effort to ensure that the reinforcement would not rust in an exposed situation. They considered critical, a given fraction of the ultimate bond stress developed in a particular test. According to them this critical bond stress may be defined as the least of the bond stresses associated with either a free-end slip of 0.002 in (0.05 mm) or a loaded-end slip of 0.01 in (0.25 mm) in beam tests.

On the other hand, with the advent of modern computers and the development of finite element techniques, many researchers have attempted to simulate mathematically the behaviour of reinforced concrete elements from zero load up to failure. In order to model the bond conditions at the steel-concrete interface, they tried to define a bond stress slip law of the form: $u = F(d)$ where u is the nominal bond stress and F(d) is a function of the local bond slip d. By differentiating both sides with respect to d, they obtained the bond spring stiffness which can be introduced at the connecting nodes between concrete and steel.

Nilson (21, 22) used the results of Bresler and Bertero (10) to derive a tentative bond stress-slip relationship as follows. The difference between the local steel displacements d_s, and the local concrete displacements d_c gave the local bond slip between the concrete and the steel whose value was difficult to obtain experimentally (Fig. 1.8). He obtained the steel displacement by numerical integration of the measured steel strains. The concrete displacement at the face of the concrete, d_c^*, was evaluated by substracting the measured slip at the ends, d*, from the steel displacement at the same location, d_s^*. Assuming the concrete stress to vary linearly at a rate proportional to the rate of the stress in the steel bar, the concrete displacement was expressed by the curve OP which deviated from the straight line ON parabolically (see Figs. 1.8a, 1.8b and 1.8c). He calculated the bond stress distribution along the length of the bar from the values of the steel stresses measured at closely spaced locations and plotted it against the local bond slip.

Four sets of data were obtained from the four nominally identical bond zones I, II, III, IV, and are reproduced in Fig. 1.9. In spite of the considerable scatter, Nilson (21, 22) fitted the following third degree polynomial to the data:

$$u = 3.606 \times 10^6 d - 5.356 \times 10^9 d^2 + 1.986 \times 10^{12} d^3 \qquad (1.5)$$

Based on the results of the research carried out by Tanner (23), Nilson (24, 25) derived the experimental bond stress-slip curves, as shown in Fig. 1.10, as well as an idealized bond stress-slip relationship which is linear up to the critical slip i.e., that slip where bond becomes nearly constant. The research involved three concentric tension tests conducted on 6" x 6" x 18" (15.2 x 15.2 x 45.7 cm) long prisms reinforced with a 1" (25.4 mm) diameter bar. Contrary to the results of Ngo and Scordelis (26) Nilson (24) showed that far from being constant, the stiffness varied constantly with the bond stress which increased with slip up to a certain maximum value and then decreased progressively.

The recent work of Houde and Mirza (17) gives a more general expression of the bond stress-slip relations. The experimental program consisted of study of the effect of the following parameters:

(i) the load level,

(ii) the size of the concrete restraining the bar,

(iii) the type of test,

(iv) the quality of the concrete, and

(v) the bar size.

Houde (18) calculated local bond stresses for different pull-out specimens reinforced with instrumented bars by measuring the slopes of each bar force variation curve at many load levels. At each of them, especially the higher one, four values of the slopes were recorded and averaged. Slips of the bars at the same locations, for known stress levels, were also evaluated. Using a correction factor, Houde normalized all the curves to a common concrete strength of 5,000 psi (34.5 MPa) and obtained the plot shown in Fig. 1.11 where the bond stress at the steel-concrete interface reached a maximum value corresponding to a slip of 0.0012" (0.03 mm). Before this peak value is reached, Houde expressed the relationship between the bond stress u, and the local slip, d, with the following fourth-degree polynomial:

$$u = 1.95 \times 10^{6}d - 2.35 \times 10^{9}d^{2} + 1.39 \times 10^{12}d^{3} - 0.33 \times 10^{15}d^{4} \quad (1.6)$$

Contrary to Nilson (24, 25) who observed that the bond stress level is related to the distance from the end face, Houde did not note such a relationship and the maximum stress level was attained at all locations at a maximum slip value of 0.0012" (0.03 mm). His bond stress-slip relationship is thus applicable directly at any point along the bar. This constitutes a useful advantage in a finite element analysis where cracks progressively appear in a random manner under increasing loads. Past the peak point, the behaviour was found to depend on the distance from the end face.

1.4 Variables Influencing Bond Strength

Due to the complex nature of the phenomena acting between steel reinforcement and concrete, bond strength depends on a great number of parameters. There is a general agreement among all researchers on the qualitative influence of some of them on bond strength but it is still difficult to compute correctly their quantitative influence because of the diversity of the testing methods and of the difficulty of interpreting many results. For others, it is not easy to show separately their influence on bond, either because they act contrary to bond or they act directly on each other. Nevertheless, four main categories of variables can be distinguished:

(i) variables related to concrete.
(ii) variables related to steel reinforcement.
(iii) variables related to specimen geometry.
(iv) variables related to types of tests.

1.4.1 Variables Related to Concrete

1.4.1.1 Type of Concrete

Tests have been done at University of Missouri (27) on lightweight aggregage concrete to compare its bond characteristics with that of normal-weight concrete using plain and deformed bars. These data cited by Ferguson (28) indicate that their mode of failure is somewhat different. Roughly one-third of the bars, particularly the top-cast bars, pull-out without splitting the concrete: a mode of failure which indicates that in lightweight concrete, the lugs crush and shear the concrete instead of splitting it like in normal concrete.

The first analysis of the data showed lower bond strengths for the lightweight concrete than for regular concrete. The ratio varies considerably with the criterion selected, ranging from 87 percent when based on certain slip comparisons, to 64 percent when the average ultimate bond values are considered. For this reason the Canadian and the American Building Codes (4, 5) recommend a 33% increase in basic development length of deformed bars in lightweight aggregate concrete.

The type of cement has received little attention from the researchers but based on the work of Muline and Astrova (29) in Russia, the following conclusions can be drawn:

a) For plain bars, the Portland Puzzolan cement and the modified Portland cement (au laitier) reduce bond from 25-75% compared to ordinary Portland cement. The type of aggregate is not important and a decrease of the water/cement ratio improves bond.

b) For deformed bars, bond varies significantly with the quality of the cement and the nature of the aggregates. It increases with the amount of gravel, but there is no unanimous agreement on the influence of the cement content on bond between steel and concrete.

Some experimenters like Davis, Brown, Kelly (30) studied the influence of the richness of mix on bond performance. From their work, it is seen that, for the age of 28 days, for all types of cement, the bond strength at initial slip is less for the rich mix than for the lean mix, while the maximum bond strength is greater for the rich mix than for the lean mix. Also for the lean mix, there is little difference between initial and maximum values and among the various cements these values are nearly constant; for the rich mix there is a large difference between initial and maximum values for a given cement and among the several types of cement the differences both in bond strength at initial slip and in maximum bond strength are large. Menzel (20) showed the influence of cement content, fineness of cement and consistency of concrete on load-slip relationships for companion top and bottom cast pull-out specimens.

1.4.1.2 Methods of Placing Concrete

It is generally agreed that the compactness of concrete influences bond between steel and concrete in a manner similar to its influence on the compressive strength. This compactness depends on the methods of placing the concrete: hand rodding, vibration, disturbance during hardening, delayed vibration etc.

According to Larnach (31), direct vibration at the time of concreting does not have any effect. Bichara (32) noted that vibration either improves or reduces bond strength depending if the concrete is dry or saturated. Robinson (33, 34) studied the effect of vibration and concluded that vibration of concrete decreased the differences due to the casting position of the bars in the specimens. Davis, Brown and Kelly (30) using vertical bars in their pull-out tests compared different methods of compaction: hand tamping, external vibration by means of a vibrating table and internal vibration with a 1 in (2.5 cm) diameter shaft. They noted that external vibration increased the bond strengths just slightly over those obtained by hand tamping alone (10-12%) and that the percentage is around 40% with internal vibration. The reason for this is not clearly evident but it seems possible that vibration may have produced a "remixing action" of the cement paste in the immediate vicinity of the bar, and that through this action was formed a more homogeneous paste structure at the contact surfaces. Roughly the same observations were made when the vibration was delayed for a period of 3 to 9 hours. For effect of disturbances during early hardening, Menzel (20) tried many possibilities like:

(i) Specimen allowed to settle for 10 minutes, then subjected for 14 hours to mild vibrational disturbance of small motor clamped to mold table with shaft at right angles to reinforcing bar. The motor speed was 2650 RPM.

(ii) Specimen allowed to settle for 1 hour and 20 minutes then reconsolidated by "rapping" each side of mold 20 times and "ramming" and pressing concrete around top bar with end of stick 2 in (5.1 cm) square.

(iii) Specimen cast with special steel mold and rerodded 2 hours after placing the upper part of specimen, to consolidate the concrete around the upper bar and to eliminate longitudinal cracks formed over this bar 10 minutes after original placing. He concluded that none had enough influence to materially alter the bond resistance in the corresponding undisturbed specimens.

1.4.1.3 Effect of Storage Conditions

This category includes the storage condition besides the temperature effect and weathering conditions (freezing and thawing; wetting and drying). These parameters have been studied by numerous international investigators: Davis and Kelly (30), Bichara (32), Menzel (20), Plowman (35), Koh (36) and Robinson (33). All of them have the same general conclusion that bond strength is more sensitive to certain factors than is the compressive strength.

For example Davis et al (30) showed from their experimental work that regardless of the duration of moist curing, the maximum bond strength for air stored specimens is greater by about 40% that for the specimens maintained continuously moist. They also discovered that bond strength is substantially affected by either an increase or decrease in the room temperature. Their tests are perhaps not sufficiently comprehensive to justify any conclusions, but the decrease in bond strength due either to a raising or lowering of temperature is significant and this suggests more extensive investigations of temperature effects on bond strength.

Koh (36) and Davis et al (30) studied the effect of freezing and thawing at an early age on bond strength of pull-out specimens. They concluded from the results of their pull-out tests the following:

The maximum bond strength is substantially reduced by repetitions of freezing and thawing at an early age. The effect is more pronounced when the concrete contains more water. The temperature during the first three days of hardening has a great influence. A thin layer of ice on the surface of the bar at the time of concreting reduces the bond strength considerably and deformed bars with good surface conditions are advantageous for winter concrete.

1.4.1.4 Strength of Concrete

This parameter is considered of prime importance in the development of bond resistance and has received considerable attention from many researchers. It is generally agreed that the slip resistance of steel reinforcement increases with the concrete strength for both, plain and deformed bars and for any type of bond test. Davis et al (30) attributed this increase in slip resistance to the compressive strength of concrete, but later, with a better understanding of the mechanics of bond failure, new investigators realized that perhaps the tensile strength of concrete was more critical. Some investigators (32, 37) are even considering the shearing strength to have a significant effect on the bond performance.

Some investigators (33, 38, 39, 40) have suggested different equations for the ultimate bond strength as a function of the strength of concrete. In Europe the most common one is the following linear variation:

$$u_m = k_1 f'_c + k_2 \qquad (1.7)$$

where u_m and f'_c represent respectively the bond strength and the concrete compressive strength; k_1 and k_2 are empirical coefficients, which depend on the type of bars, their diameter, embedment length and the type of the test.

Based on his data, Ferguson (41) established that the bond resistance varied approximately as the square root of the compressive strength and proposed the equation:

$$u_m = k\sqrt{f'_c} \qquad (1.8)$$

The effect of the concrete strength on the distribution of steel and bond stress along a reinforcing bar was investigated, in eccentric pull-out specimens and in beams, by Perry (42) and Perry and Thompson (43). Some results of the eccentric pull-out specimens are shown in Fig. 1.12 for a bar tension of 8.4 kips (37.4 kN) at the loaded end. One can note the shifting of the point of maximum bond stress toward the unloaded end for the lower concrete strengths. As the maximum bond stress was reached at some point along the bar, the bar slipped and caused the bond stress on the side of the loaded end to reduce gradually to the value of frictional drag between the bar and the concrete. The point of maximum bond stress is believed to be just ahead of the propagation of the splitting crack.

1.4.2 Variables Related to Steel Reinforcement

1.4.2.1 Effect of Surface Conditions

The bond characteristics of deformed bars do not appear to be adversely affected by varying degrees of surface rust or ordinary mill scale. On the contrary, it can actually be beneficial to bond, and it is practical to consider that metal reinforcement, except prestressing steel, with rust, mill scale or a combination of both shall be considered as satisfactory, provided the unit weight of a cleaned piece of bar meets the minimum requirements of the Standard specifications. This was the conclusion drawn by Kemp et al (44) after an extensive series of bond tests on stub-cantilever concrete beams reinforced with deformed bars with controlled varying amounts of rust and mill scale. They also found that it is not necessary to clean or wipe the bar surface before using it in concrete construction. In a given rust causing environment, the thickness of the rust layer will be about the same for all bar sizes. Therefore larger diameter bars, which have higher ribs, will be less affected by rust. Other tests on artificially rusted deformed reinforcing bars made by Ghaffarzadeh (45) at University of Oklahoma, have exhibited varying effects of rust on bond strength but no significant reduction in the bond strength of moderately rusted bars.

1.4.2.2 Effect of Bar Profiles

This is a more important parameter than the surface conditions of the bar. According to Bichara (32) who studied the effect of the bar profile, bond as a chemical adhesion between steel and concrete does not depend on the shape and deformations of the bar, but as a resistance to slip, it is greatly affected by the bar profiles. Many investigators have analyzed the influence of bar profile on bond strength: Menzel (46), Clark (19, 47), Lutz (48) and Wilhem et al (49).

From the tests reported by Menzel (46), it appears that plain and knurled bars pull through the pull-out specimens tested but deformed bars cause failure by longitudinal splitting. Knurled bars perform well only as bottom-cast bars. Also Menzel made some recommendations with respect to close spacing of lugs to minimize the effect of concrete settlement for vertical bars and lug height, spacing and thickness to furnish a proper ratio of concrete shear area to bearing area. His suggestions have greatly influenced the formulation of the ASTM Specifications (50) for the deformed reinforcing bars presently used.

Later, Clark (19, 47) conducted some tests to determine the resistance to slip in concrete of 17 different designs of deformed reinforcing bars. The tests were of the pull-out type in which the 7/8 in (22.2 mm) diameter bars were cast in a horizontal position. Height of deformations appears as an important factor as far as effect of concrete settlement is concerned. The pattern of deformations does not seem to be of importance in determining the bond resistance, but the slope of the lugs appears to be a critical factor. As suggested by Menzel (46), Clark (47) also found that ratios of shearing areas to bearing areas of less than 10 gave best results.

Wilhelm et al (49) conducted a recent study of the comparative bond efficiency of reinforcing bars with heights and spacings of deformations differing from the ASTM Specifications. The purpose of the study was to determine if the height of deformations could be lowered at a relatively reduced spacing without adversely affecting bond strength. It was found that changes in deformation height do not affect bond strength significantly provided the total bearing area per unit length of the bar is the same.

Hence, the work of the past few years leads one to the conclusion that the bearing area per unit length of bar is probably the critical bond strength parameter for reinforcing bar deformations, with the requirement that the face angle be not less than 45 degrees. Height and spacing of deformations are important in the case of specimens with bottom-cast bars only, insofar as they affect the bearing area.

1.4.2.3 Effect of Bar Diameter

Many authors have used either the pull-out tests or the beam tests to study the influence of the bar diameter on bond strength. In some tests, the embedment length is held constant while the diameter of the bar varies, and in others the ratio of embedment length over the bar diameter is held constant. Nevertheless, results differ greatly depending on the authors. Bernander (51) and Robinson (33) from their pull-out tests on plain and deformed bars concluded that practically, the bar diameter does not have any influence on bond strength. According to reports from Djabry (52), Jonsson et al (40) and Voellmy and Bernadi (53) observations were made that in the majority of the cases the bond strength values decreased with an increase in the bar diameter for a given "embedment length over diameter" ratio. This decrease is less for plain bars than for deformed bars. However, there is no unanimity on an expression of general validity which varies with the authors. Ferguson et al (41, 54) showed that the slips of large bars were somewhat greater than those of smaller bars and that increased loaded-end slip for large bars, roughly in proportion to their diameters, appeared to be a reasonable approximation.

1.4.2.4 Effect of Embedment Length

Using pull-out and flexural tests, many investigators have verified that bond stress is primarly a function of length rather than of the bar size. Mathey and Watstein (9) determined bond strengths in 18 beams and 18 pull-out specimens with No. 4 (12.7 mm) and No. 8 (25.4 mm) deformed reinforcing bars of high yield strength. The lengths of embedment ranged from 7 in (17.8 cm) to 17 in (43.2 cm) for No. 4 bars (12.7 mm) and from 7 in (17.8 cm) to 34 in (86.4 cm) for No. 8 (25.4 mm) bars. Fig. 1.13 (9) shows clearly that both $u_{m,1}$ and u^*_c decrease with an increasing l_e / d_b for a given bar size. For example, u^*_c decreases from 1170 psi (8.1 MPa) to 530 psi (3.7 MPa) for the No. 4 (12.7 mm) bars, and from 650 psi (4.5 MPa) to 470 psi (3.2 MPa) for the No. 8 (25.4 mm) bars, as l_e / d_b increases from 14 to 34. It may be noted that the values of u^*_c for the two size bars approach each other as l_e / d_b increases. Also, Fig. 1.14 (9) shows the relationships between $(f_s)_c$ and l_e / d_b and indicates that it is possible to develop a steel stress of about 70,000 psi (482.7 MPa) with a 14-diameter embedment of No. 4 (12.7 mm) bars whereas a 34-diameter embedment is required with No. 8 (25.4 mm) bars to develop an average stress of about 66,000 psi (455.1 MPa). In these two figures:

$u_{m,1}$, u^*_c — maximum bond stress and critical bond stress adjusted by multiplying by a factor $\bar{f'}_c$ / f'_c

$\bar{f'}_c$ — average concrete compressive strength of a group of beams containing the same size bar

f'_c — concrete compressive strength

u_c — critical bond stress which is the lesser of the two values of bond stress corresponding to a loaded-end slip of

0.01 in (0.25 mm) and a free-end slip of 0.002 in (0.05 mm)

$(f_s)_c$ — steel stress corresponding to u_c

l_e — embedment length

d_b — nominal diameter of the steel bar

Ferguson and Thompson (41) preferred beam tests to study the effects of several variables on bond strength including embedment length. They used mainly high yield strength No. 7 (22.2 mm), No. 3 (9.5 mm) and No. 11 (35.8 mm) bars with beams of varying cross-section dimensions in order to achieve a bond type of failure. Fig. 1.15 shows some of the results obtained by Ferguson and Thompson (41) for $u_{m,2}$, with varying embedment lengths. In Fig. 1.15 $u_{m,2}$ is the maximum bond stress adjusted to a concrete compressive strength of 3300 psi (22.8 MPa) and a clear bar cover of 1.5 in (3.8 cm). They concluded that the bond stress decreased with an increasing embedment length. Nevertheless, this area needs further study, because recent tests on beams by Untrauer and Warren (55) show that the ultimate bond stress increased with an increase in the embedment length.

1.4.2.5 Effect of Detailing

Recent tests by Megget and Park (56) on exterior beam-column joints indicate that the embedment length of the beam reinforcement is extremely important in determining the performance of the beam-column joint under seismic loads. From the work of Ferguson and Thompson (41), it appears that end anchorage by extra lengths either straight or hooked is reasonably good but it usually reduces the available bond stress over the entire length by approximately 7 to 24%, the larger reductions being for the hooked bars.

Development length must therefore be longer if part of the length is in the form of end anchorage. As noted by Hribar and Vasko (57), the inclusion of compressive stresses as a factor in the bond strength of bent bars, produces some marked differences between the behaviour of straight bar embedments and hooked bars of equal embedded length. The position of the bar relative to the direction of concrete casting has a great influence on the slip behaviour of hooked bars as reported by Rehm (58).

Ferguson (41), Brooks (59) and also Ferguson and Husain (60) studied the effect of multiple cut-offs. Their results illustrate the diagonal tension complications which are always incident to cutting off tension steel in a tension zone where some reasonable shear stress already exists. Apparently effective development for the multiple cut-off would call for at least 30% more length than for continuous bars.

Tests on tension splices (61, 62, 63, 64, 65) reveal that the danger of concrete splitting is particularly great in the vicinity of tension splices. It was observed that the free ends of spliced bars form sources of discontinuity and act as crack initiators across a tension zone which in turn trigger splitting cracks. Tests at the Universities of Oklahoma (66) and Colorado (67) show that for No. 11 bars, the ACI Code splice lengths are conservative. They also show that splices in a varying moment region required less embedment length than prescribed, possibly because one end is at a lower stress. Compression splices have not received as much attention as tension splices, however the limited test data (68) illustrates that bearing against the end of the bar strengthens the splice which has a beneficial effect on bond.

1.4.3 Variables Related to Specimen Geometry

As researchers are getting a better understanding of the nature of bond strength they realize the prime importance of the parameters in this group which includes:

1.4.3.1 Effect of Shape and Dimensions of Specimens

Bichara (32) showed that the beam width does not have any effect on bond as it varies from 6 to 12 inches (15.2 to 30.5 cm). Many researchers do not agree with this conclusion. Plowman (35) found that bond resistance varies with the ratio of the beam width to the bar diameter. Voellmy and Bernadi (53) believe that the shape and dimensions of the specimens affect bond behaviour. The work of Ferguson and Thompson (41) proved that the width of the beam has a decisive effect on the type of failure: bond splitting or diagonal tension. Further study of his data showed that the beam width was still a critical factor even when the failure was in splitting. In fact narrower beams failed at bond stress values 7 to 20 percent lower than wider beams. This can be explained by the higher diagonal tension stresses which result, possibly because of the smaller lateral resistance to splitting provided by the narrower beams.

Fig. 1.16 illustrates the variation of bond strength with the beam width as derived by Ferguson and Thompson (41), Lauritzen (69) and Berkman (70). In Fig. 1.16, l_e is the embedment length and α is the ratio of $u_{m,b} / u_{m,18}$ where $u_{m,b}$ is the maximum bond stress for a beam of width b and $u_{m,18}$ is the maximum bond stress for a beam, 18 in (45.7 cm) wide. It is clear that the variation in beam width is more serious when the embedment length is short; which is reasonable because a short length gives high bond stress and results in larger shear stress. Recently Untrauer and Warren (55) reported that the effect of the beam width on tension steel stress development and ultimate bond stress is very significant and that wider beams develop less steel stress than the narrower beams.

1.4.3.2 Effect of Bar Cover

Investigations at the University of Texas on development length of No. 3, No. 7, No. 11 (9.5, 22.2, 35.8 mm) bars have indicated the clear cover over the bar to be an important variable. Clear cover thickness influences slip resistance and large cover results in smaller end slip. Clear cover over a reinforcing bar is also significant in connection with splitting resistance. According to Robinson (33) it is due to the quality of the concrete cover which, when it is thin, is weak because of side effects (effets de paroi). Thin cover can split easily; very thick cover can greatly delay splitting if bars are not too closely spaced laterally. Figure 1.17 from Reference (41) indicates an approximate increase of bond stress of 100 psi (0.7 MPa) per in (2.5 cm) of cover. In this Figure $u_{m,3}$ represents the maximum bond stress adjusted to a concrete compressive strength of 3300 psi (22.8 MPa).

However the improved bond performance is not proportional to the additional cover thickness and it is not economical to increase bond strength by increasing the cover thickness. For large size bars, the beneficial effect is not very significant. For these bars, the effect on the formation and widths of cracks under service load conditions is the governing criterion in selecting an appropriate value for allowable average bond stresses. Extra cover does not provide protection against excessive surface crack widths. From research programs conducted at the Cement and Concrete Association in London (71), it appears that medium size top bars benefit more from the added cover as indicated by Fig. 1.18. When dowel action affects bond, the influence of cover on crack formation and splitting resistance is eliminated.

1.4.3.3 Effect of Bar Spacing

In the early development of the nature of bond strength, Ferguson, Turpin and Thompson (72) realized, from their tests on pull-out and beam specimens, that the maximum bond stress increased approximately linearly with the clear spacing of the bars. Neglected later by most researchers, the clear bar spacing is not even considered in the development length equation in the present Canadian and American Building Codes (4, 5). More recently, Orangun, Jirsa and Breen (73) derived a proposed equation for calculating development and splice lengths, from a nonlinear regression analysis of many test results of beams with lap splices. The effect of clear bar spacing is included in their equation as well as the thickness of the concrete cover. Later, Untrauer and Warren (55) presented some data on the effect of bar spacing, which was obtained from tests on 27 beams. They found that bar spacing has a significant influence on the stress that can be developed in the tension steel. This is illustrated in Fig. 1.19. Based on the results of these two reports, Ferguson (74) emphasized that if the clear spacing between bars is less than 4 in, (10.2 cm), the present ACI Building Code development lengths for Grade 60 bars, and possibly Grade 40, are not conservative. Further study of this phenomenon is needed.

1.4.3.4 Effect of Transverse Reinforcement

Transverse reinforcement in the form of stirrups, particularly when closely spaced, slows the propagation of a splitting crack or prevents the opening of cracks that form along embedded bars and enables greater bond forces to be transmitted. Stirrups cannot prevent splitting cracks, which always form when large bars are used in beams, but they enable frictional forces to be transferred along the cracks. Stirrups resist dowel forces directly and transfer them into the body of the beam, greatly reducing the importance of splitting stresses developed by dowel action across the plane of the bars. Ultimate bond strength of the beam is little influenced by the stirrups if they are simply adequate for the expected shear, although toughness of the beam is considerably improved. If however surplus of stirrups are present, ultimate bond strength is considerably increased because the stirrups can similtaneously perform the functions of shear reinforcement, split retarder and precluder of dowel action. These observations are reported by many European investigators (34, 35, 75, 76) and are in general agreement with the findings of Ferguson et al. However from their tests, Ferguson et al (41, 72, 77) have been unable to show satisfactorily the quantitative increase of bond strength with increase of the stirrups ratio Γ, defined as the ratio of vertical shear reinforcement area to the gross concrete area of a horizontal section. Nevertheless, he noted a bond strength increase of about 18 psi (0.12 MPa) with each 0.0001 increase in Γ

(Fig. 1.20.).

Also it is clear from the test results reported by Tepfers (61), Robinson (34) and others that transverse steel improves ductility of the anchorage. Orangun, Jirsa and Breen's (73) proposed equations show a considerable reduction in the development length with the addition of stirrups. Bond resistance seems to be improved by the presence of spirals over the bars. However this is not commonly used and this area is inadequately explored experimentally.

1.4.3.5 Effect of Casting Position of Bar

Several researchers have studied the importance of the bar position and type of attachment with respect to bond strength. Davis et al (30), Clark (19), Menzel (20), Dutron (78) and Rehm (58), who were the first to present a report of their work on settlement of concrete, used three different pull-out specimens:

(i) Specimens with vertical reinforcement.

(ii) Specimens with horizontal reinforcement cast at the bottom of the formwork: "bottom-cast" specimens.

(iii) Specimens with horizontal reinforcement cast at the top of the formwork: "top-cast" specimens.

Leonhardt (79), Soretz (80) and Ferguson (28, 54) preferred the beam tests with the bars cast horizontally either at the bottom or at the top of the beams. These investigators observed the poor bond performance of some bars, due to their casting position.

The above investigations led to the conclusion that the settlement of concrete in the forms, left the concrete better consolidated on top of the lugs of the vertical bar than beneath the lugs. The slip and the ultimate bond resistance were thus more favorable when the bar was pulled against the direction of casting of the concrete than in the opposite direction. Likewise, a horizontal bar has better consolidated concrete above the bar than under it. According to Clark (19), Menzel (20) and Davis et al (30), these can be classified in the sequence of decreasing strengths as follows:

a) Vertical bar pulled in a direction opposite to that of casting.

b) Horizontal bottom-cast bar.

c) Horizontal top-cast bar.

d) Vertical bar pulled in the same direction as casting.

From their pull-out tests, Ferguson et al (28, 54) observed a significant difference in slip behaviour between top-cast and bottom-cast bar. Top-cast bars slipped at the unloaded end at very low loads and then continued to accept much more load. Bottom-cast bars did not slip at the unloaded end until almost at their ultimate load.

The American and Canadian Codes (4, 5) define "top-bar" as a horizontal bar so placed that more than 12 in (30.5 cm) of concrete is cast below the bar. Based on Clark's experimental work (19), these Codes recognize a loss of bond strength for top-cast bars, of approximately 30% and recommend an increased development length of 1.4 l_d, l_d being the development length for the bottom-cast bars. In recent tests with concrete depths of 12 to 18 in (30.5 to 45.7 cm) below the bars, this loss was observed to be directly related to the difference in the tensile strengths of the concrete in the vicinity of the top and the bottom-cast bars and was of the order of

10 to 20%. This represents a considerable scatter and the magnitude of the loss of bond is thus, not very well documented and further experimental work is necessary, before the designer can really know what bond strength is possible for top bars in ordinary cast-in-place concrete members of standard and high depths. This is an important problem when one considers the tremendous amount of possible savings involved in the lengths of the reinforcing steel used.

1.4.4 Variables Related to Types of Tests

Although these parameters deserve a great deal of consideration, they have not received much attention in the earlier bond studies. This deficiency may be explained by the difficulty involved in analyzing their effect on bond strength. These parameters are:

1.4.4.1 Types of Structural Members

The bond problem in slabs, connections, brackets, corbels and extremely short cantilevers is quite different from that in conventional pull-out and flexural members. However there is a lack of data in this area. Moreover, there is a scarcity of data on bond characteristic between rolled structural steel sections and concrete. This type of bond is important in the design of composite structural members in order to assume composite action of such a structural unit.

1.4.4.2 State of Stress of Concrete

The loading conditions influence the state of stress of the concrete and have a considerable effect on the bond between the steel and the concrete. In this respect, different research works have shown some marked differences between the results of the pull-out and the beam tests. However, the effect of transverse compression or tension which exists in beam-column connections and other structural elements has not been well documented yet. Similarly the effect of shear on bond is not well known, because most of the beam tests have considered only the portion of the beams under constant moment region which is a case of pure flexure.

Bond fatigue is another area not thoroughly explored in research. Bond fatigue is the progressive deterioration of bond and the slip of tensile reinforcement under some form of repetitive and sustained loading and can lead to collapse of the concrete member. However, even without complete failure, progressive slip is of particular importance in rigid frame buildings, where it results in progressive deterioration of the flexural stiffness. Some fatigue tests (81, 82) on reinforced concrete specimens have examined the bond problem, but have not suggested a consistent basis for a specification to prevent bond fatigue. Thus it is necessary to conduct more research in the area of bond failure due to repeated and sustained loads and to investigate the response of critical portions of structures such as splice regions and connections.

1.4.4.3 Repeated and Cyclic Reversing Loading

This is an important parameter which affects not only the stiffness but also the strength of the structural member. When a reinforced concrete member is subjected to repeated and cyclic reversing loading, cracks formed during the tensioning of a bar do not close completely after the removal of the load because the inelastic deformation in the vicinity of the ribs, microcraking in the concrete and the release of shrinkage strains cause some permanent slip. With repeated loading, the frictional resistance diminishes, resulting in a deterioration of the stiffness of the bond mechanism. This loss in bond has been observed by Bresler and Bertero (10) from their carefully instrumented experiments. Recently Ismail and Jirsa (83, 84) observed yield penetration under cyclic overload to a distance of 14 to 18 bar diameters when the concrete in the anchorage zone was simultaneously subjected to 1000 psi (6.9 MPa) transverse compression. Figure 1.21 shows the tensile strain distribution at two levels of stress along a 16 in (40.6 cm) length of deformed bar No. 9 (28.6 mm) embedded in a 6 in (15.2 cm) diameter concrete cylinder after cyclic loading. This is representative of the bond conditions around a bar in a beam under pure flexure, when cracks are spaced at 8 in (20.3 cm) centers. The curves illustrate quite well the loss of bond between cracks after several cycles of loading as the tensile stress tends to become uniform over the full length of the bar. This loss of bond contributes to the overall loss of stiffness in a reinforced concrete structure. Perry and Jundi (85) reported that in their tests 80% of the ultimate static strength was attained after several hundred load cycles. Nevertheless, this problem needs further examination.

1.5 Scope of the Present Research Program

As discussed earlier, the embedment length and the "top-bar" effect have a significant influence on the bond strength and deserve further quantitative experimental investigation. The objectives of the present investigation are to make use of a practical and realistic bond test and, by varying the embedment lengths of the test bar:

(i) to analyse the overall behaviour of specimens having top versus bottom-cast bars from zero load to failure and to evaluate their respective ultimate bond strengths.

(ii) to analyse the distribution of internal strains for both top and bottom-cast bars and also the distribution of bond stresses in both cases as the applied loads are increased from zero until failure.

(iii) to point out any basic differences in strength and behaviour of specimens and compare the results obtained with the current Code provisions and proposed recommendations of Jirsa et al (73).

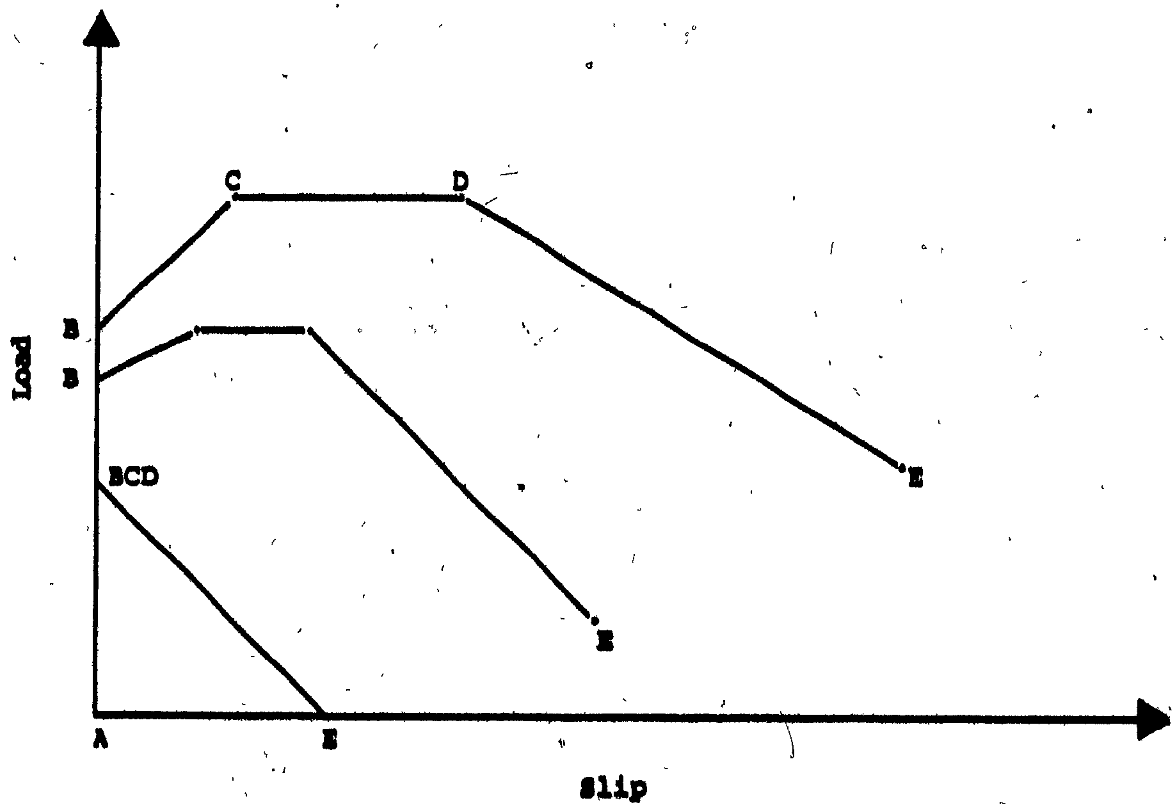

Fig. 1.1 Qualitative Load-Slip Relationship (76)

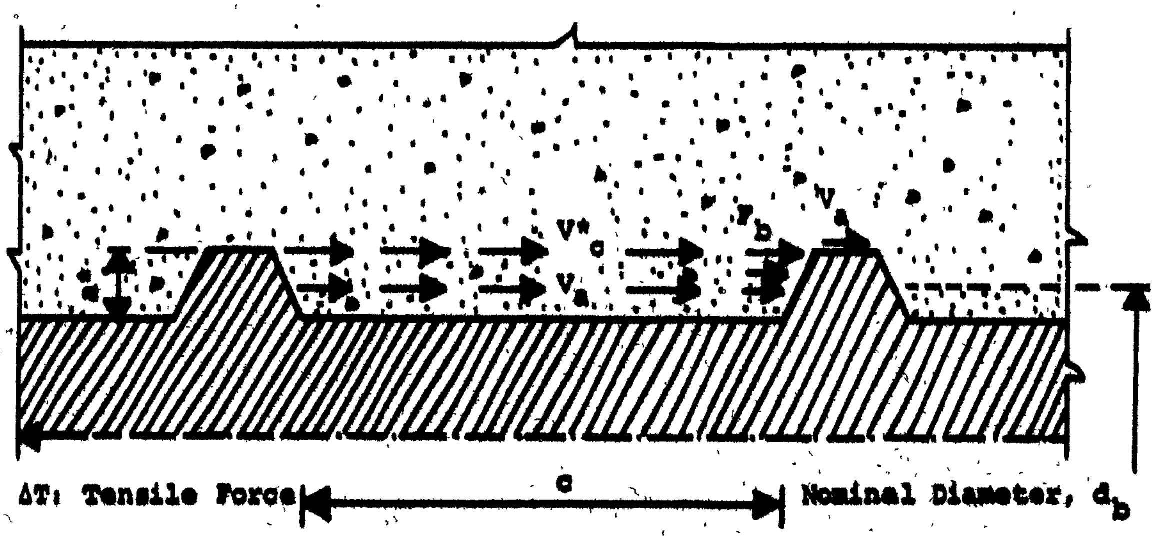

Fig. 1.2 Forces Between two Ribs of a Deformed Bar (86)

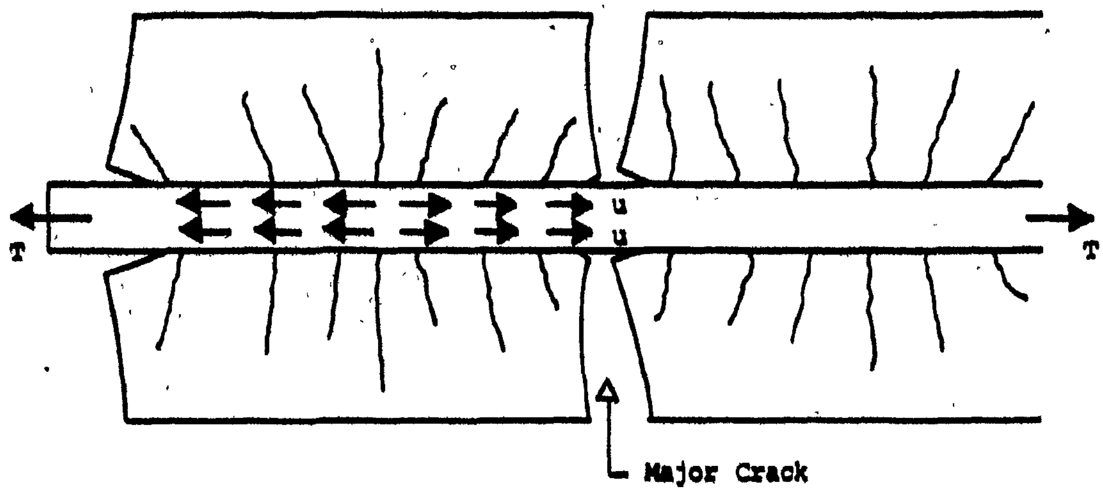

Fig. 1.3 Deformed Concrete Between Transverse Cracks of a Tension Member (16)

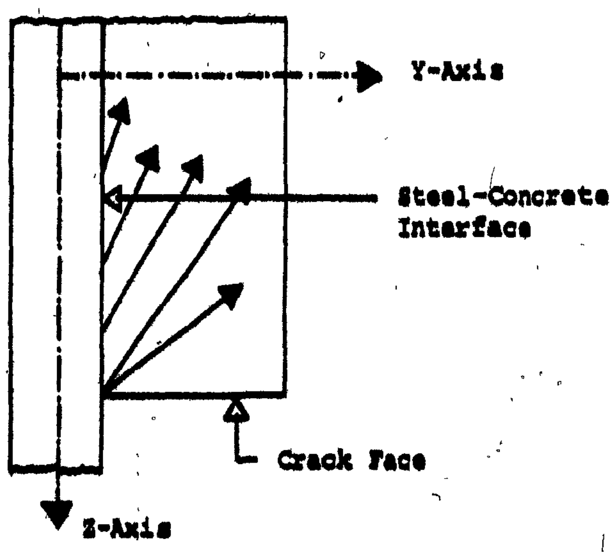

Fig. 1.4 Principal Tensile Stresses at Steel-Concrete Interface in Axially Reinforced Concrete Prism Subjected to Tension (10)

(a) Specimen with 0.75" (1.9 cm) Reinforcing Bar

(b) Specimen after the Removal of the Reinforcing Bar

(a) Specimen with 1.26" (3.2 cm) Reinforcing Bar

(b) Specimen after the Removal of the Reinforcing Bar

Fig. 1.5 Photographs of the Internal Crack Patterns of Goto's Axially Loaded Tensile Specimens (13)

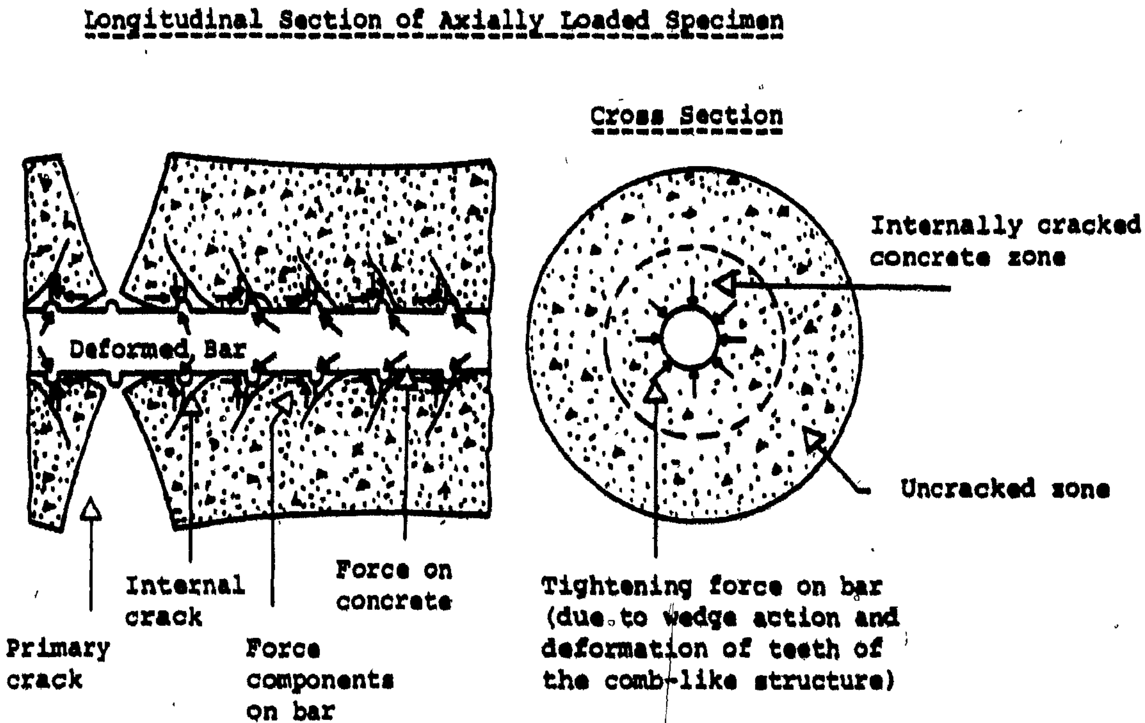

Fig. 1.6 Deformation of Concrete Around Reinforcing Steel Bar after Formation of Internal Cracks (13)

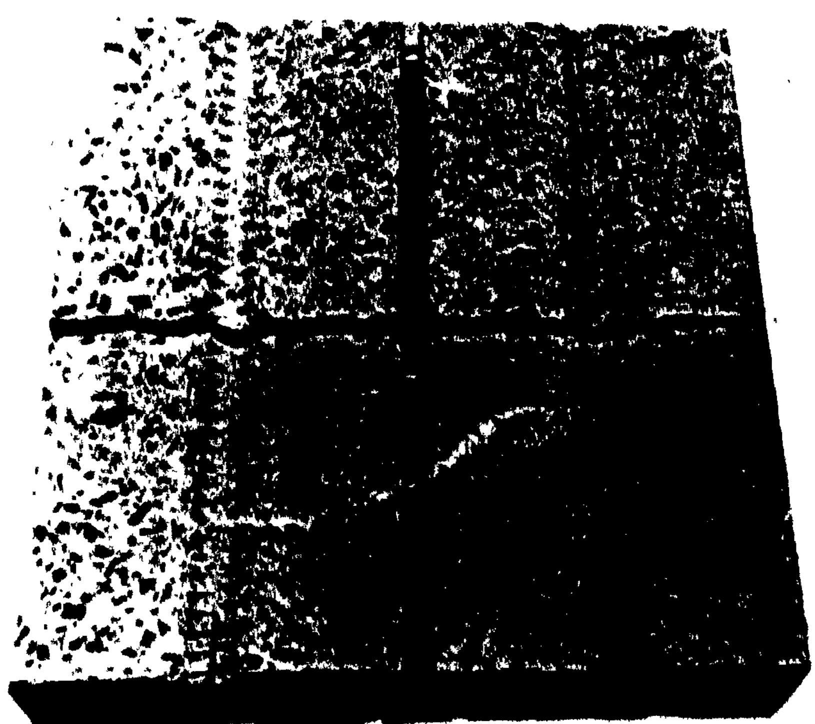

Fig. 1.7 Photograph of the Interior of Houde's Axially Loaded Tensile Specimen #10 after Sawing (18)

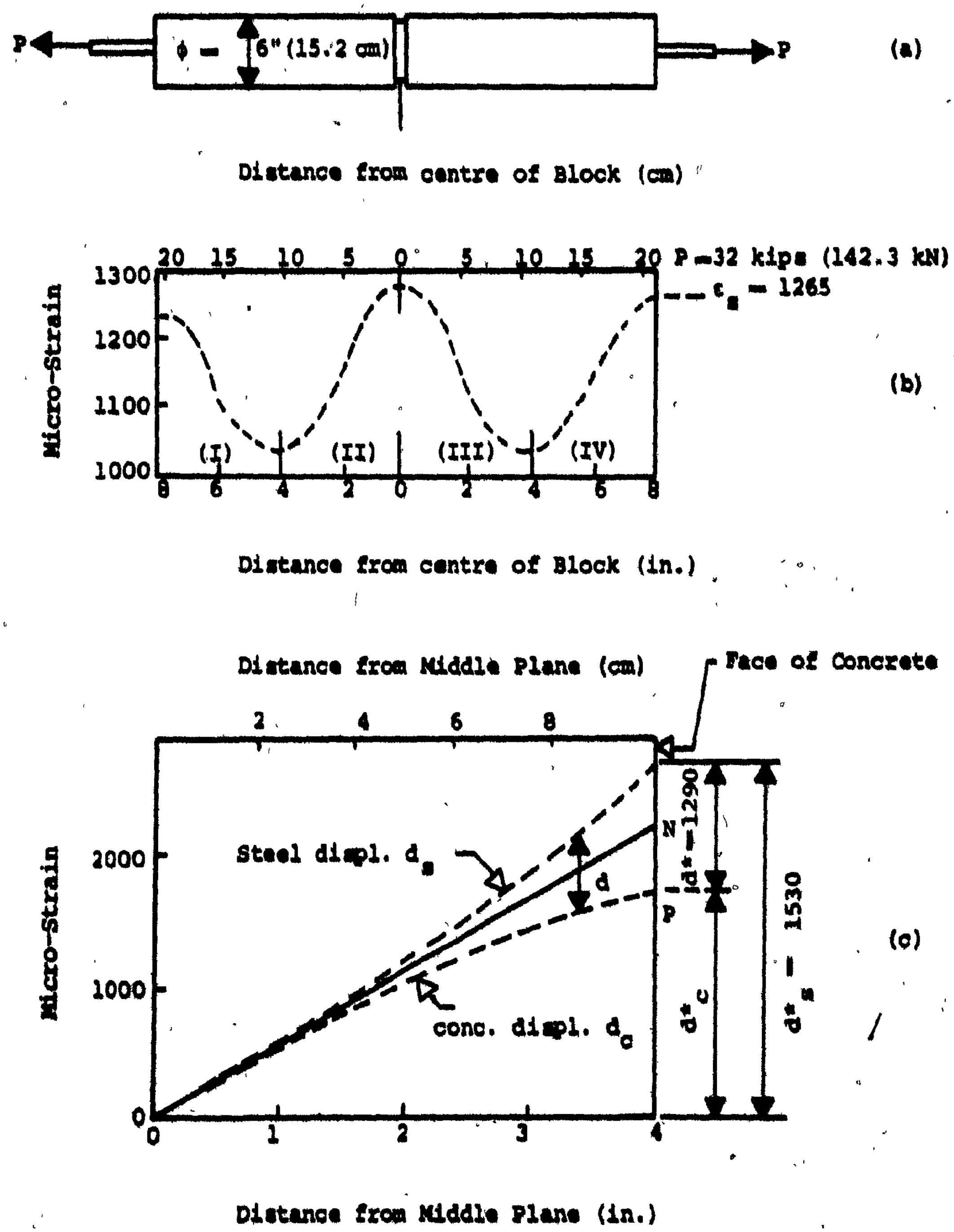

Fig. 1.8 Nilson's Analysis of Bresler and Bertero Tests (22)

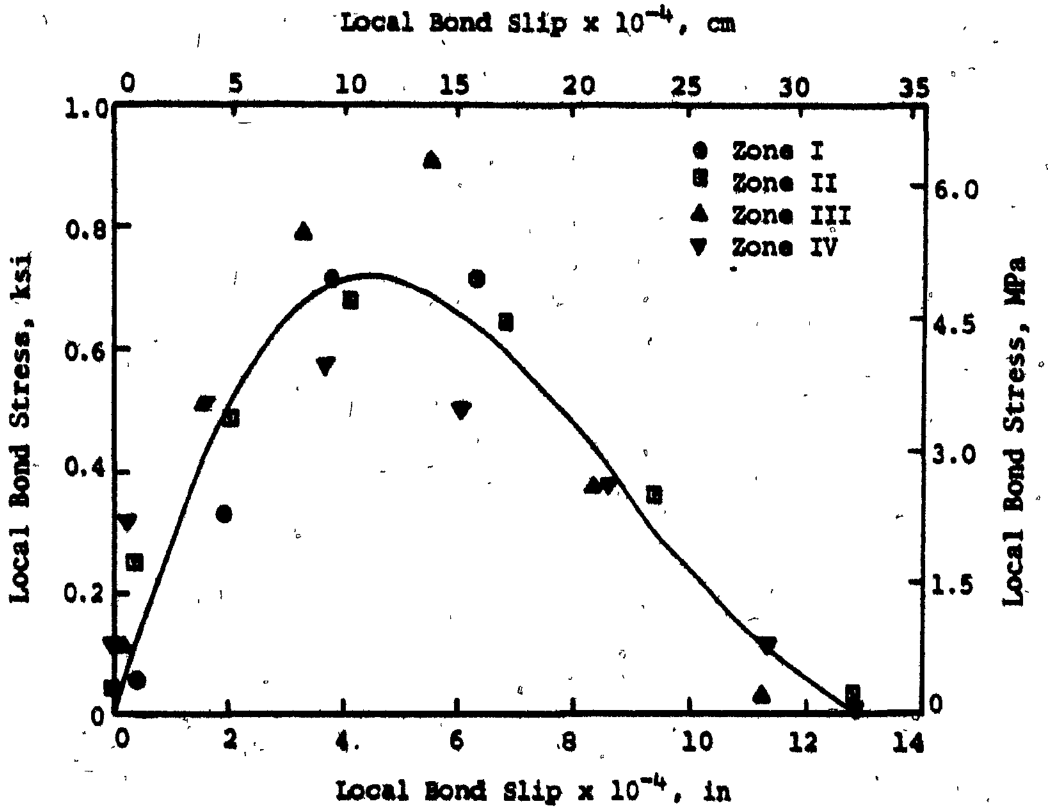

Fig. 1.9 Nilson's Experimental Bond Stress-Slip Curve (22) (Bresler and Bertero Tests)

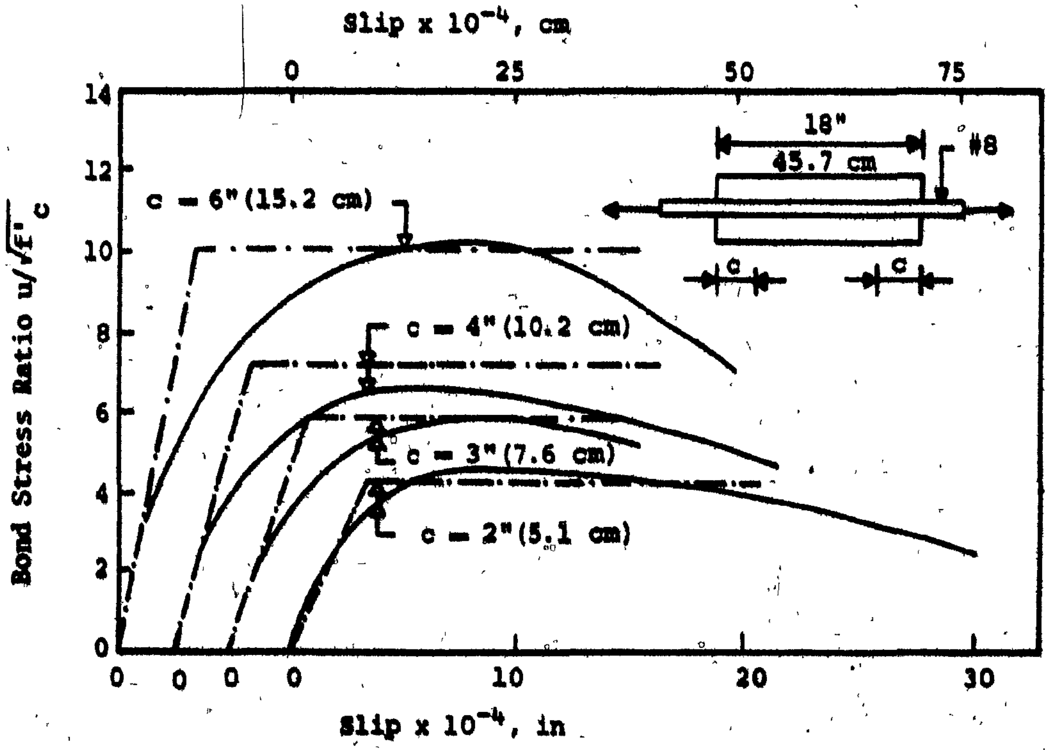

Fig. 1.10 Nilson's Experimental Bond Stress-Slip Curve (24) (Tanner's Tests)

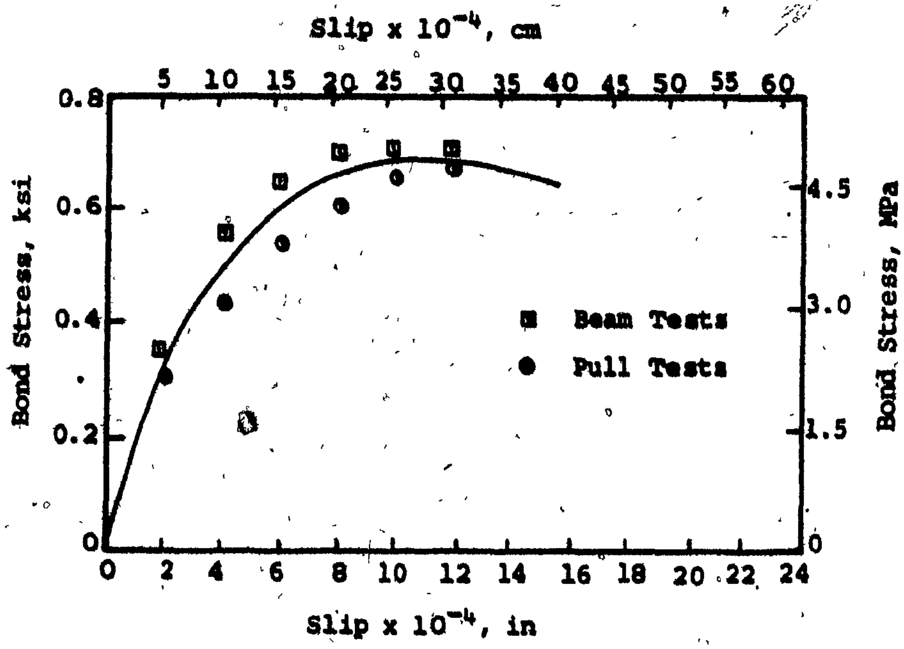

Fig. 1.11 Houde's Bond Stress-Slip Curve (18)

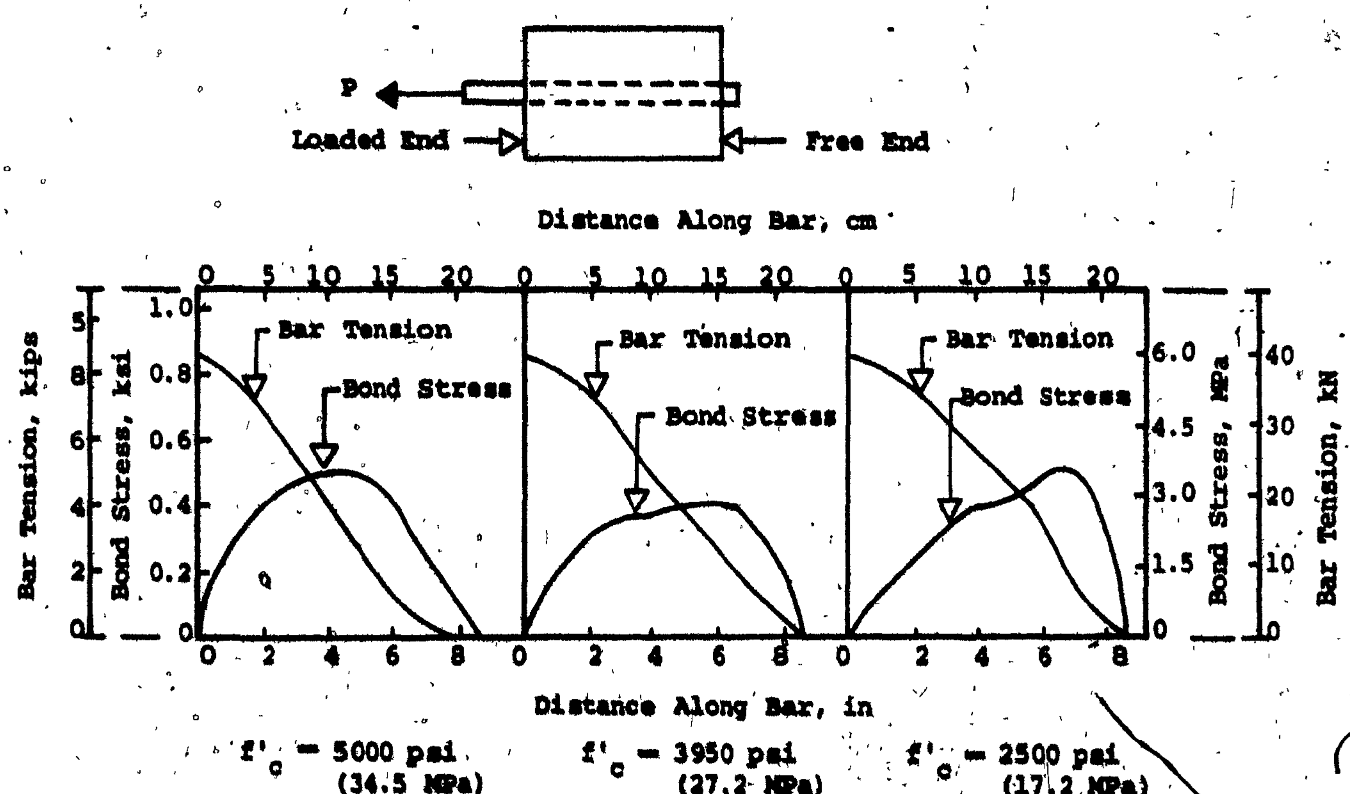

Fig. 1.12 Effect of Concrete Strength on Eccentric Pull-Out Specimens (43)

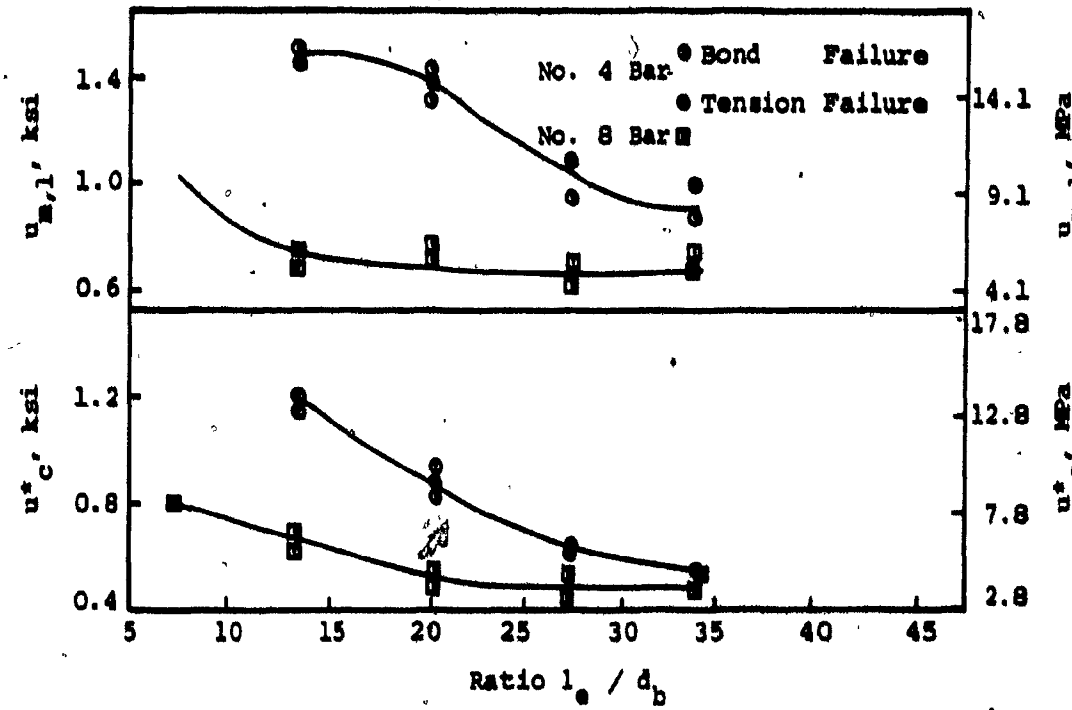

Fig. 1.13 Relationship Between $u_{m,l}$, u^*_c and l_e / d_b (43)

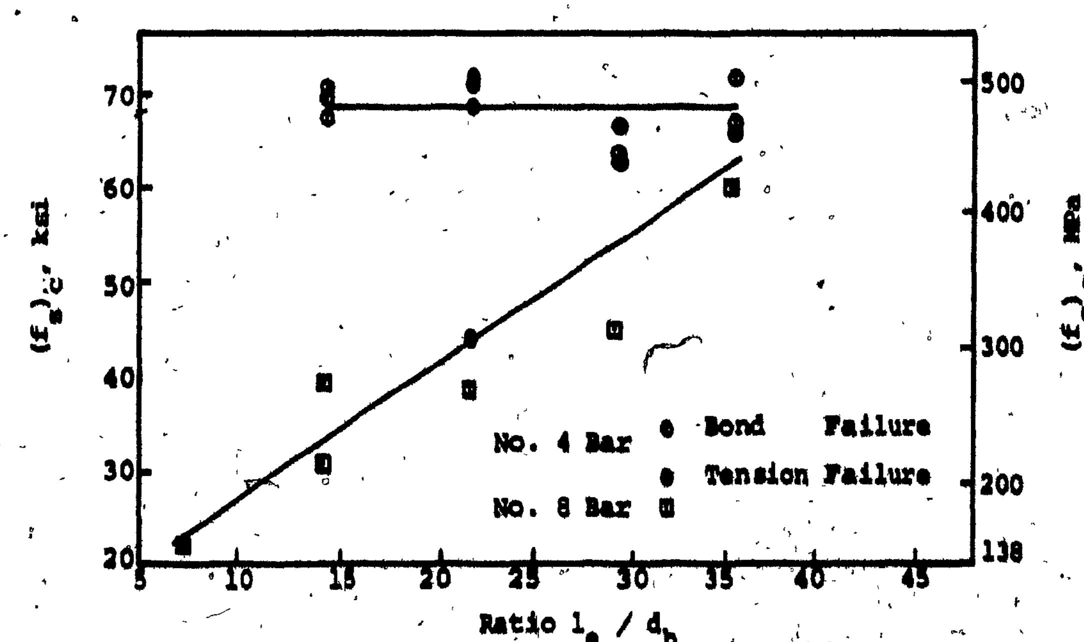

Fig. 1.14 Relationship Between $(f_s)_c$ and l_e / d_b (43)

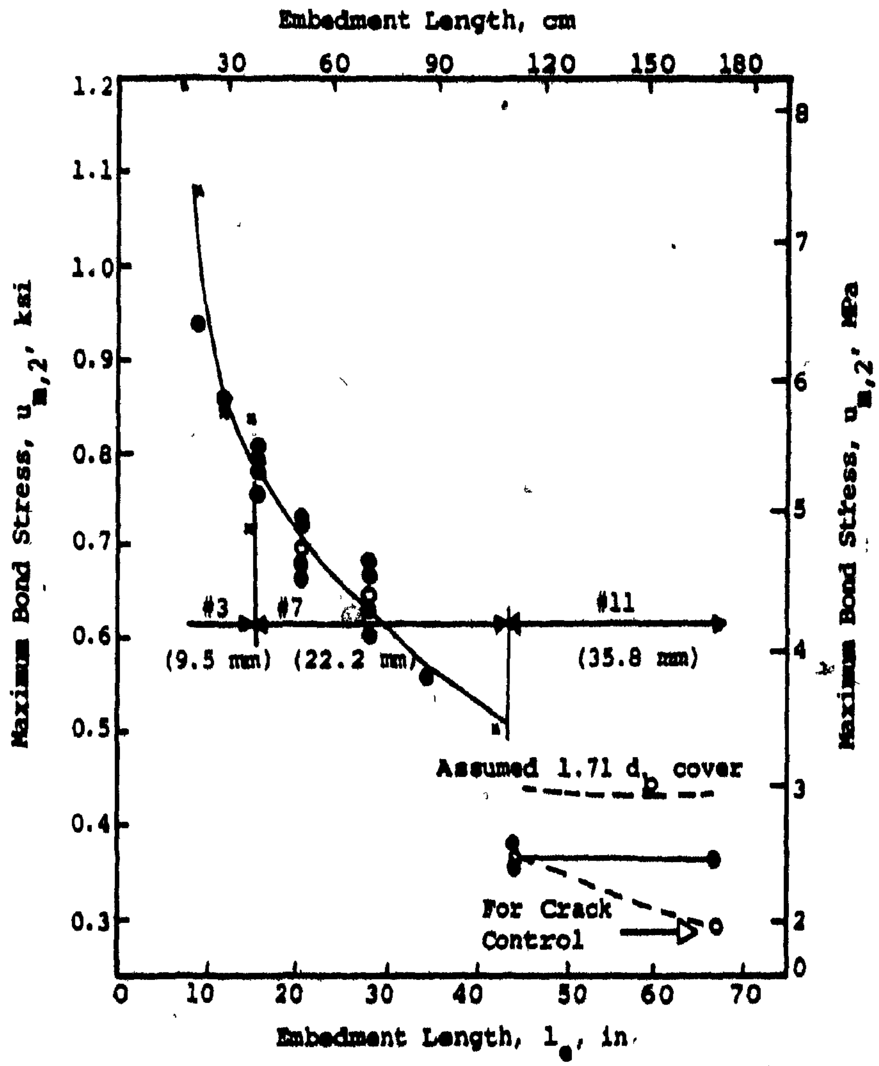

Fig. 1.15 Maximum Bond Stress, $u_{m,2}$, versus Embedment Length (41)

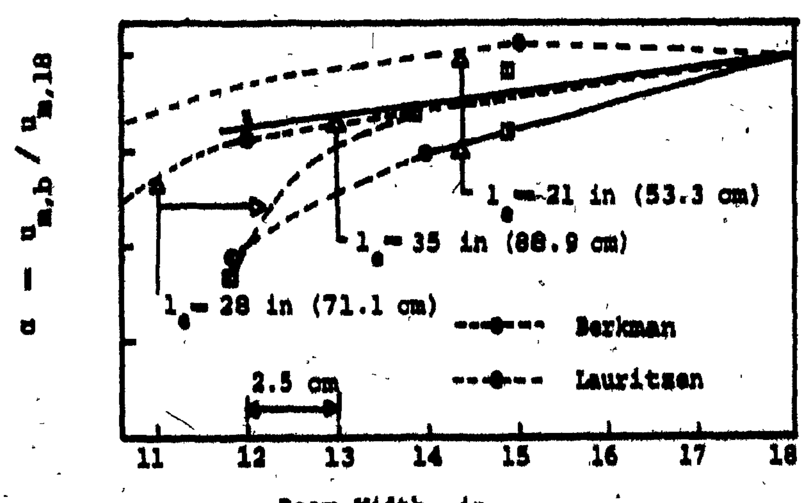

Fig. 1.16 Variation in Bond Strength with Beam Width (41)

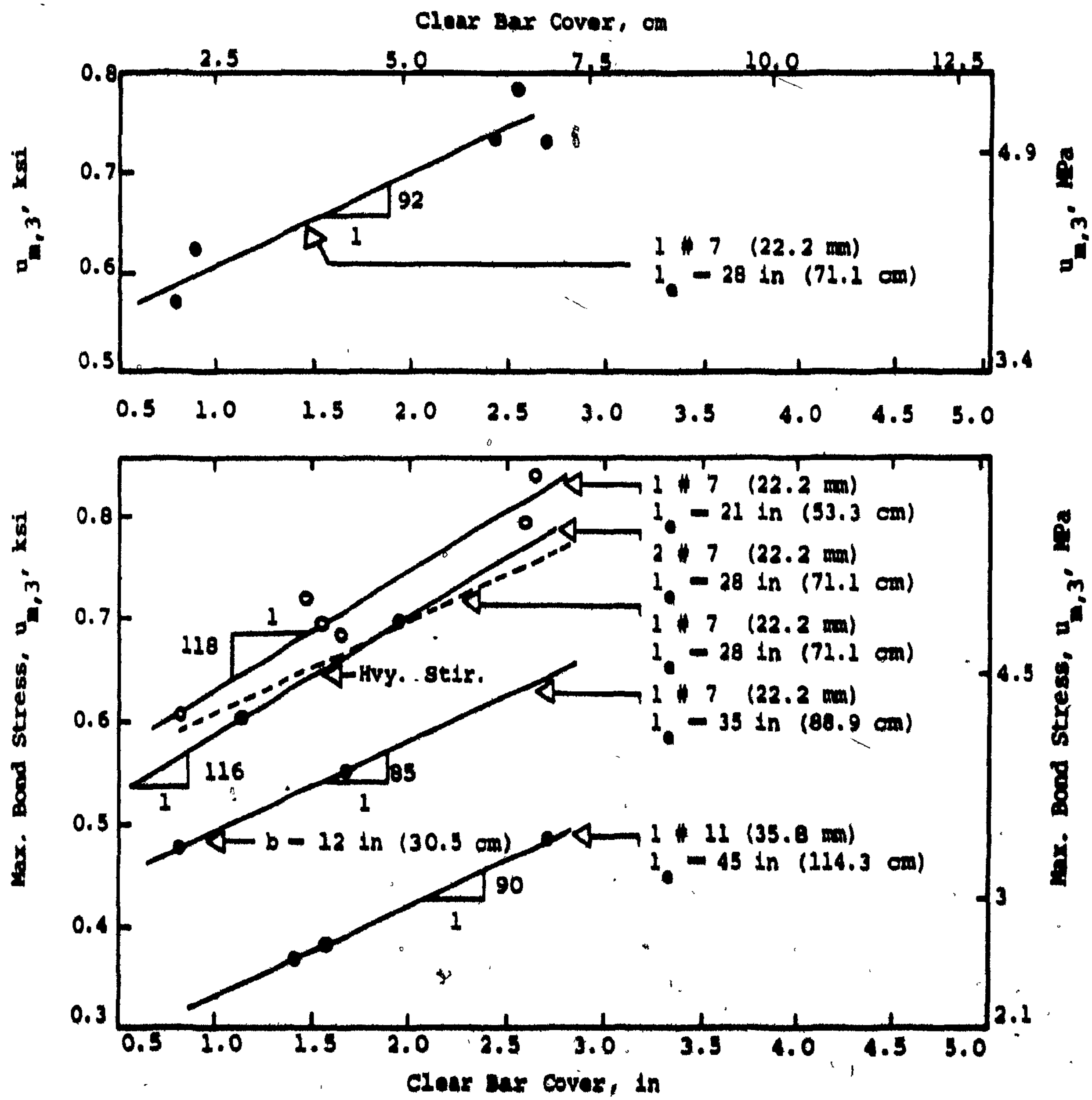

Fig. 1.17 Effect of Clear Bar Cover on Maximum Bond Stress $u_{m,3}$ (41)

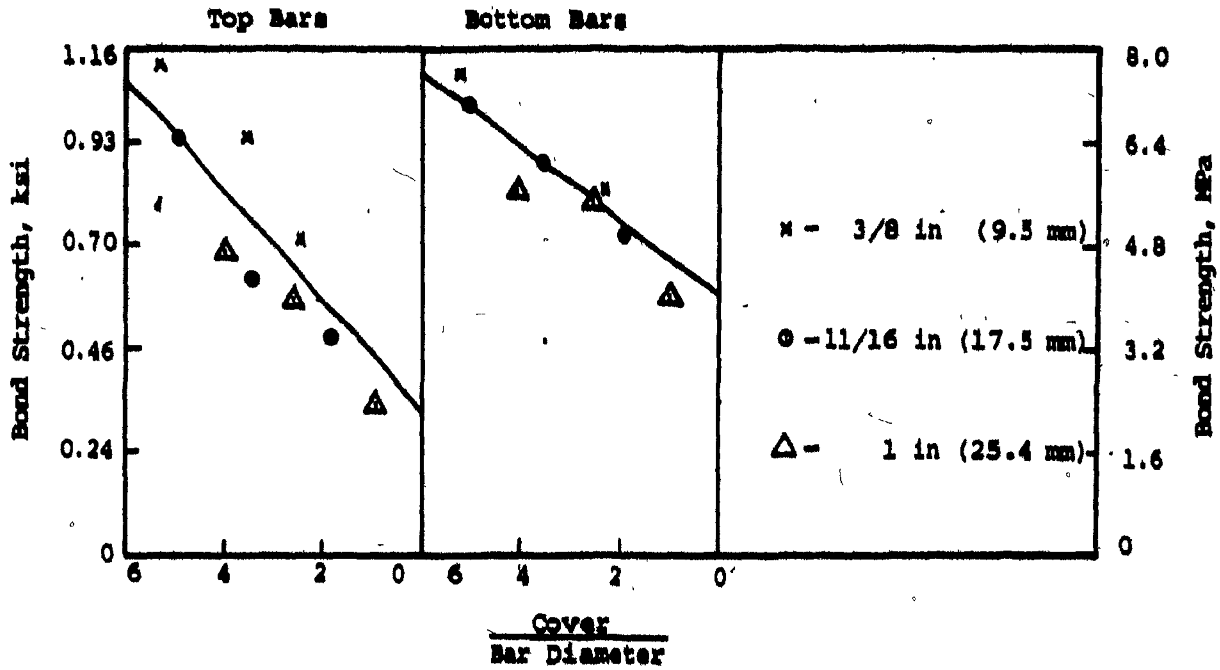

Fig. 1.18 Effect of Clear Bar Cover on Bond Strength (71)

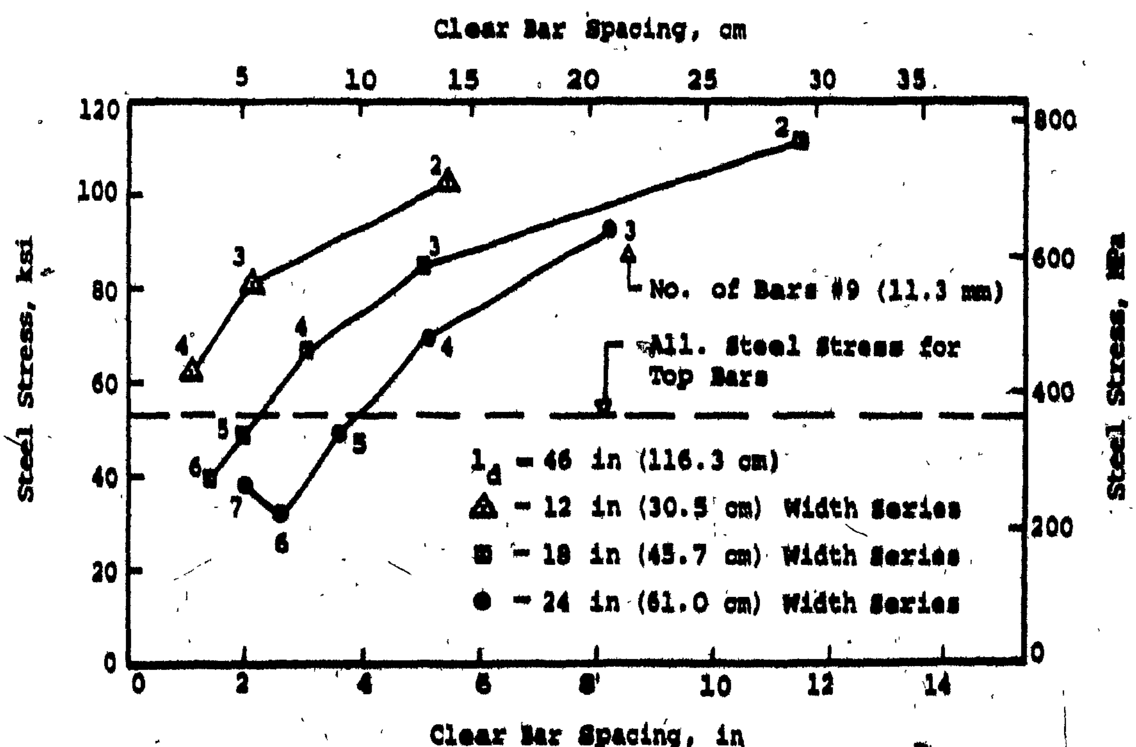

Fig. 1.19 Steel Stress Versus Clear Bar Spacing (55)

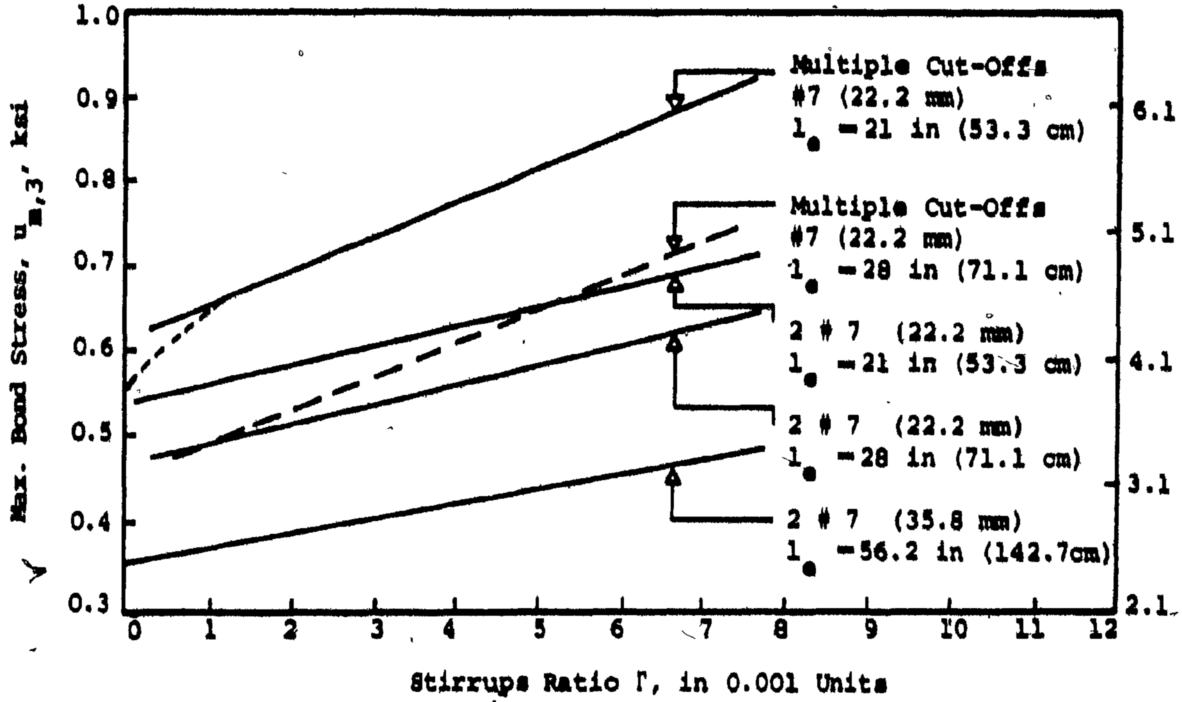

Fig. 1.20 Effect of Stirrups on Maximum Bond Stress, $u_{m,3}$ (41)

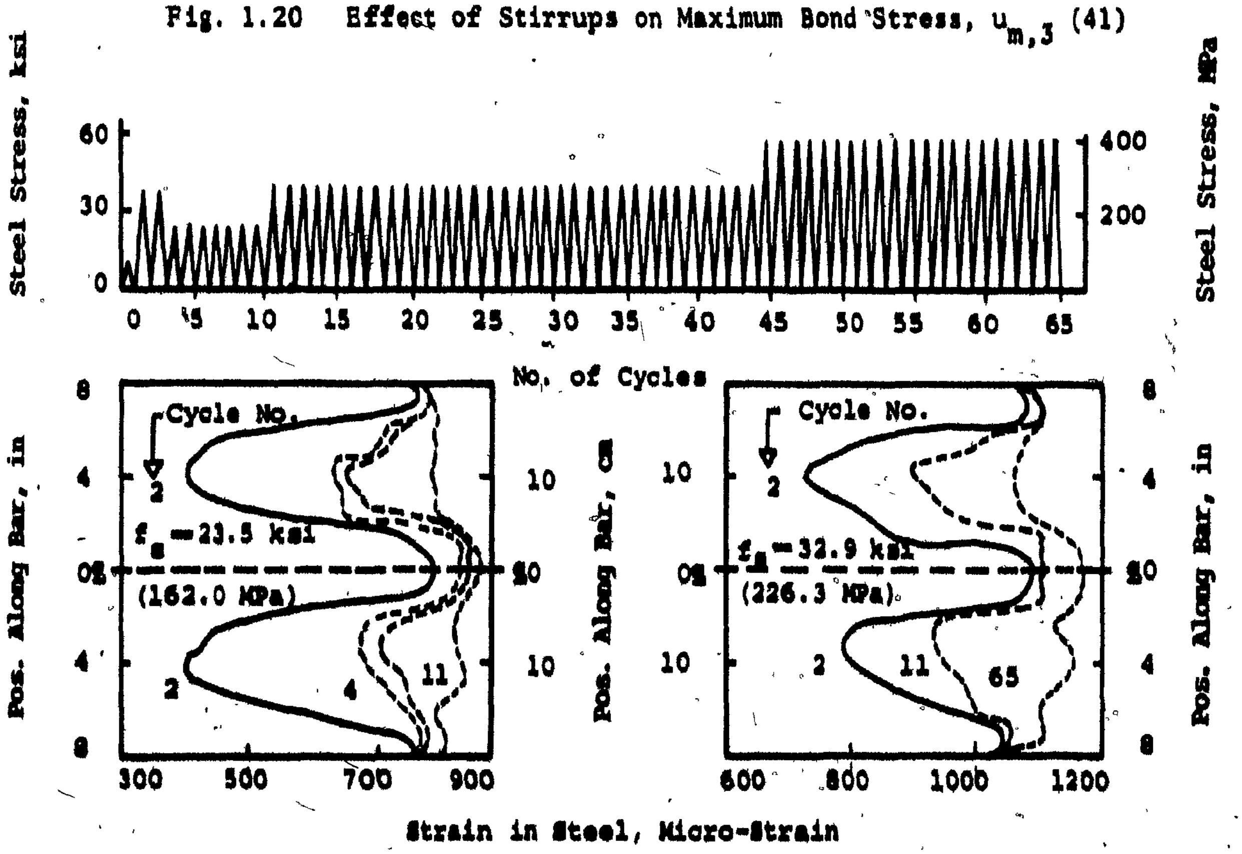

Fig. 1.21 Steel Strains at two Levels of Stress Along a Reinforcing Bar After Cyclic Loading (10)

CHAPTER II

CHOICE OF EXPERIMENTAL BOND TEST

2.1 Requirements of a Bond Test

An evaluation, by members of ACI Committee 408 of the requirements of a bond test, led to the following general conclusions:

(i) The bond test specimen must simulate as closely as possible the actual manner of loading in a concrete structure.

(ii) The bond test specimen must contain a realistic amount of reinforcement with a reasonable bar spacing and concrete cover.

(iii) The bond test specimen must contain some shear reinforcement and must avoid the confinement effect of the loading system and the reaction which influence bond.

(iv) The bond test must be inexpensive and simple.

In the light of the above requirements the existing bond testing methods will be examined in some detail before deciding on the bond test which will be used in this experimental research program.

2.2 Types of Bond Tests

For obvious reasons of simplicity, it would be desirable to establish a "standard method of bond testing". However, this is not an easy task in view of the many variables which influence the usable bond strength and the various physical distresses manifested as bond failures. This is the reason why a survey of the literature indicates a proliferation of the types of bond tests used by different investigators. They can be grouped into five main categories.

(i) the pull-out tests

(ii) the push-out tests

(iii) the axial tension tests

(iv) the beam tests (flexural tests)

(v) the torsional tests

2.2.1 Pull-Out Tests

This is the most common type of test and depending on the position of the bar there can be two types of specimens: the classical pull-out test where the bar is concentric with the axis of specimen, and the modified pull-out where the bar pull-out force is eccentric.

2.2.1.1 Classical Pull-Out Test

This is probably the oldest and simplest of bond tests. In this test, the bar, either plain or deformed is initially cast in the centre of a block, cube, prism or a cylinder of concrete. The specimen is placed in a testing machine and, while the concrete is held by the reaction pressure on one end, the reinforcing bar is pulled out from the same end (see Fig. 2.1). In most cases, the bar is protruding from both ends. While the loading stages are recorded, the relative slip between steel and concrete at one or both ends is measured by means of a dial gauge clamped to either the bar or the concrete block.

In America, various shapes and dimensions of pull-out test specimens are reported in the literature like:

(i) The 8 x 9 in (20.3 x 22.9 cm) and 10 x 10 in (25.4 x 25.4 cm) concrete prisms with varying lengths of 8, 16, 21 in (20.3, 40.6, 53.3 cm).

(ii) The 6 x 12 in (15.2 x 30.5 cm) and 6 x 18 in (15.2 x 45.7 cm) concrete cylinder with a bar protruding from one end.

The European pull-out specimen is more or less standard with a square cross-section of 20 x 20 cm and a length varying from 18 to 60 cm.

Pull-out test can be used for many purposes. For example, Watstein (87) and Mains (88) used it to measure the distribution of tensile and bond stresses along the embedded bar. Clark (19) compared the efficiency of different types of bars by means of pull-out tests. Also Clark (19) and Menzel (20) studied the effect of settlement and water gain on bond by making use of double pull-out specimens. They are rectangular prisms grooved at mid-height in which a top bar and a bottom bar are cast horizontally and centered in the top and bottom halves respectively. After concrete hardening, they are split along the grooves to yield two specimens. The main advantages of this test are its simplicity and low cost.

However, the pull-out test has two major disadvantages:

(i) It does not simulate realistically the bond conditions of a tension steel bar in real-life concrete beams: due to the absence of shear reinforcement and large concrete covers.

(ii) The surrounding concrete of the steel bar in the pull-out specimen is in compression, while in real-life concrete beams it is in tension.

Thus, the pull-out test may be useful only for comparing different shapes of bars, different sizes of bar, different lengths of bar.

2.2.1.2 Modified Pull-Out Test

This is basically the classical pull-out specimen with the difference that the bar is placed eccentrically. The cover is usually about 2 to 2½ in (5.1 to 6.4 cm). It has been used by Ferguson, Breen and Thompson (54), to study the effect of bar size, embedment lengths and casting position on bond performance. Also Perry and Thompson (43) used the eccentric pull-out test to determine the tensile and bond stress distribution by means of strain measurement using electrical resistance strain gauges mounted at specific locations on the steel bar. Several variations of the eccentric pull-out test have been used to study the mechanics of bond and slip, representing more closely the bars in flexural members which is a big advantage over the concentric pull-out test. See Fig. 2.2 for illustration.

2.2.2 Push-Out Tests

The push-out test is a development of the pull-out test in that the loading stages and relative slips are obtained in a similar way. As pointed out by Koh (36) and Plowman (35), they only differ in that in the push-out test, the reinforcing steel and the concrete are both placed in compression by pushing the bar through the concrete as shown in Fig. 2.3. Results differ significantly from those obtained in pull-out test because the dilation of the bar under load increases the pressure between the concrete and the bar surface, whereas in the pull-out test the bar contracts under load, thereby reducing the lateral pressure. The same criticisms apply as for pull-out tests, except that both elements are in compression. This is not a type of bond test commonly used.

2.2.3 Axial Tension Tests

Axial tension specimens, which were not often used in the early development of bond testing, have received considerable attention over the past decade. They can be divided into the following categories:

2.2.3.1 Direct Pull-Out Specimen with Single Embedded Bar

This is the most widely used specimen in this group. The bar is embedded in a prism of concrete and protrudes from both ends. The test consists of applying a pull-out load at the ends of the bar and increasing it until failure occurs (Fig. 2.4). Information as crack spacing and width are recorded. When the bar is instrumented, distribution of tensile stresses and bond stresses can also be obtained.

Houde (18), Nilson (25), Ismail and Jirsa (84) and some other experimenters used the technique used by Mains (88) and by Perry and Thompson (43) which eliminates disruptions in the bonded surface. This technique consists of milling the steel bar to semicircles. A 3/8 x 1/8 in (9.5 x 3.2 mm) groove is then milled in each half bar and electrical resistance strain gauges are mounted in the grooves of each half bar. Following the insulation and checking of the gauges, a few coats of a water resistant silicone resin are applied to all gauges and connections. The grooves are then filled with epoxy resin. After hardening, a new layer of epoxy is applied to fill out the remaining depressions and cover the contact surface of each half-bar which is then clamped together and tack welded at 2 in (5.1 cm) centres using a welding sequence with intermittent cooling to protect the gauges from damage.

The axial tension test, although greatly influenced by the ratio of transverse cross-section dimensions to the bar diameter simulates better the reinforced portion of a constant moment region in a beam. Also, the transverse compression which tends to increase the bond strength of a pull-out or a push-out specimen is relatively small and can be neglected. It is recommended that the specimens be long enough so that at least two cracks can occur in a region not subjected to the end effect of the load. Djabry (52) and Voellmy (53) pointed out that the maximum bond stresses attained with this test are sometimes, approximately three times smaller than values computed from classical pull-out tests.

This type of bond test has enabled researchers to achieve a better understanding of the bond problem. As an example, it helps them to demonstrate that crack widths at the surface of a reinforcing bar will tend to be considerably less than the corresponding surface crack widths. Bresler and Bertero (10) and later Ismail and Jirsa (83, 84) made use of this test to determine the influence of load history on bond and cracking. Their test results indicated that the stress transfer between steel and concrete is influenced by the previous load history and that bond deterioration increases with the peak stress. Other experimenters such as, Houde and Mirza (17) derived their bond stress-slip characteristics for use in finite element analysis of reinforced concrete. In conclusion, this test which does not satisfy all of the requirements previously defined, can be considered to be better than the pull-out or the push-out test.

2.2.3.2 Modified Direct Pull-Out Test

Variations of the direct pull-out tests, as suggested by Hajnal-Konyi (89), Leonhardt (75) and Riessauw (90) are shown in Fig. 2.5. The pull-out load is applied either, at the end of one bar and the hook formed by the other adjacent bars as illustrated in Fig. 2.5a or at both ends of two bars of the same size placed on line with the axis of the specimen (Fig. 2.5b). The sizes of the specimens used for the modified direct pull-out test are usually bigger than those used for the classical pull-out tests. Also the concrete is in tension while it is in compression in the classical pull-out tests. Finally, as reported by Riessauw (90), bond stress results obtained with the modified direct pull-out tests are smaller than those obtained for the classical pull-out tests. However, this type of test is not commonly used.

2.2.3.3 Direct Pull-Out Test with Lapped Bars

In this test, two or more bars are lapped in different ways within a prism of concrete and the pull-out force is applied either to the bars alone or to one bar and the concrete specimen. Fig. 2.6 shows different variations of this type of bond test.

When opposing bars are pulled, the concrete is placed in tension, and the test simulates a portion of a beam between two cracks with zero curvature, since the horizontal extension is the same on all planes. This test is increasing in importance due to extensive use of lapped bars in continuous beams and slabs in modern concrete construction.

2.2.4 Flexural Tests (Beam Tests)

In flexural tests, actual beams of suitable dimensions are loaded to bond failure with a system which consists of applying a bending moment by single or preferably two-point loads. Used for several purposes, they do not fulfill the requirements of low cost, time, material, laboratory space and labour, which very often can prove to be difficult to overcome. These tests have the advantage of being more realistic and also of satisfying most of the bond test requirements.

2.2.4.1 Classical Beam Test

In this test, a simply supported beam which contains a single embedded bar protruding from both ends is subjected to either a central load or a two-point load. The beam, whose cross-section is usually small, may have spirals around the test bar. During the loading stages, the slip is recorded. This beam test can be used to study the experimental relationships between bond stress and slip. From the graphs so obtained, one can compare the bond efficiency of different types of reinforcing bars. Djabry (52) used this beam with the two point load system to determine the distribution of bond stress along reinforcing bars. His results show that, in the region of constant moment, the distribution compares fairly well with that of the axial pull-out test on a single embedded bar. On the other hand, the distribution in the lateral zones is similar to the one obtained from the pull-out test, with comparable values of average bond stress. It has been used also by McHenry and Walker (91) for the same purpose. The schematic representation of their specimens is shown in Fig. 2.7 along with their dimensions. However this beam test has many draw backs: the dimensions are too small, stirrups are absent, the single bar is not representative of practical situations and the high bearing stresses at the ends of the bar increase bond resistance unduly and gives higher values of bond stresses.

2.2.4.2 Beam Test with Lapped Bars

The test specimen, instead of having one single bar, contains two bars of the same size lapped at the middle as illustrated by Fig. 2.8. One potential application is to determine the behaviour of splices which are commonly used in continuous beams. It has the same advantages and disadvantages as the classical beam test.

2.2.4.3 <u>ACI 208 Bond Beam</u>

The ACI 208 Bond Committee (92) developed a test procedure to provide a uniform basis for comparison of flexural bond values of different reinforcing bars. Their proposed Standard called the "ACI 208 Bond Beam" is a simply supported beam, 78 in (198.1 cm) long with a cross-section of 8 in (20.3 cm) wide by 18 in (45.7 cm) deep. It is loaded with two symmetrical concentrated loads at distances varying from 8 in (20.3 cm) to a maximum of 16 in (40.6 cm) from the supports and the tension steel is exposed at two locations so that slip and steel strain can be measured. The beam is shown in Fig. 2.9a and a variation used by Perry and Thompson (43), which has smaller dimensions is illustrated in Fig. 2.9b.

Several potential applications can be found for the Standard beam proposed by the ACI Committee 208, for example, study of the top bar effect. It has the advantage of simulating the bond stress distribution that normally exists in real life beams. However, the single tension bar is not very representative and also the existence of bearing stresses at the supports modifies the bond strength. Finally the Standard beam is rather restrictive since it limits bars to one size, concrete to one strength, and the embedment length to a maximum of 16 in (40.6 cm).

2.2.4.4 <u>Hammerhead Beam</u>

The National Bureau of Standards developed a beam specimen and a test procedure which represents a considerable departure from the ACI Standard 208 (92). This procedure provides flexibility in the design of the recommended test specimen and permits the use of different sizes of bars, different concrete strengths and longer embedment lengths needed to develop stresses equal to the high yield strengths of modern deformed bars. Later, with a few modifications, the National Bureau of Standard beam was adopted by the ACI Committee 408 (93) as a recommended specimen usually termed the "Hammerhead beam". Both specimens are shown in Fig. 2.10.

Both beams have a variable length and shear span and were designed to permit the measurement of the average value of bond stress and the slip at both the loaded and free ends of the portion of the bar between the supports and load points. The beams were provided with T-shaped ends in order to shift the reactions to points where they would not contribute to the restraint of longitudinal splitting. A transverse metal strip embedded in the concrete directly opposite each load point assures formation of a crack at that plane, and slip measurements were made at each load point plane. Used by Mathey and Watstein (9) to study the effect of embedment length on bond strength, the "Hammerhead beam" has the advantage of eliminating the confinement effect of the reaction. However, other criticisms raised against the classical beam test and the ACI 208 Standard beam are also applicable to the "Hammerhead beam".

2.2.4.5 Cantilever or Continuous Beam

Ferguson and Thompson (41), at the University of Texas, developed a cantilever beam for a more realistic bond test, especially in affording the positioning of the unstressed ends of the bars at locations away from the bearing of external reactions. This type of beam is commonly known as "the University of Texas Beam".

The University of Texas beams were designed for investigating bond in the area of bar cut-offs and points of inflection. The embedment length of the test bar, l_e, was placed in a negative moment region between the point of inflection and the point of maximum stress. In some cases, "l_e" included an extension beyond the point of inflection. Different sizes of bars were used: No. 3 (9.5 mm), No. 7 (22.2 mm), No. 11 (35.8 mm), and No. 18 (57.3 mm). Consequently the embedment lengths of the test bar varied considerably and also the overall lengths of the beams with a maximum of 22 feet 6 in. (6.86 m).

The dimensions of the cross-section and clear covers over the main steel were varied considerably, along with the positive moment steel, the auxiliary negative moment steel, the stirrups in the cantilever end, and those between the cantilever and the start of the embedment length. The relative size of the load applied to the cantilever end and to the other load point was also varied.

The University of Texas beams can be used efficiently to study the effect of many variables on bond strength and also to determine the distribution of bond stresses along different reinforcing bars. They are also considered as a good bond research tool, because of the lack of confinement due to loads at the end of the test bar and a realistic build-up of tensile force in the bar. However they are more expensive and more difficult to handle and to test because of their size. The large area of concrete surrounding each bar apparently provides stiff "shoulders" which unduly brace the concrete against longitudinal splitting. Thus, the University of Texas beams test data can be considered to be the upper bound of bond strength while narrower beams with multiple bars at reasonable spacings would constitute the lower bound.

Fig. 2.11 shows the typical details of the University of Texas beam, along with the beam used by Perry and Thompson (43) in their investigation of bond stress distribution along the No. 7 (22.2 mm) deformed bar. Fig. 2.11 also shows a recent variation of the University of Texas beam, as used by Untrawer and Warren (55) in their study of the effect of bar spacing and beam width for "top-cast bars".

2.2.4.6 Symmetrical Beam

Hsu and Mirza (94) and Hsu (95) at Mc-Gill University developed the symmetrical bond beam shown in Fig. 2.12. This is so called because the specimen geometry and the loading conditions are symmetrical, so that only one testing machine can be used to apply the four equal loads. The main characteristics of this flexural bond test specimen are as follows:

(i) The central portion is a region of known length over which the shearing force and the bending moment are zero. This is similar to the free end conditions in the eccentric pull-out test.

(ii) With the two interior loads between the reactions, the top bars may be terminated within the central portion of the beam, thus making it possible to study the development of bond between each interior load and the adjacent reaction.

(iii) It can be used to study bond characteristics of reinforcing bars anchored in zones of zero moment and zero shear.

(iv) It is easier to apply and control the four equal concentrated loads during the test unlike the Texas beams which require evaluation of distances between the supports and the two concentrated loads generally not equal.

However if interior loads are placed directly over the bars being tested, they will have a confinement effect in which case the bond strengths will be over estimated. Also, even if it satisfies fairly well other requirements of a bond test, it is as expensive as the University of Texas beam.

2.2.4.7 Stub-Cantilever Beam

To reduce specimen sizes and expenses, stub-cantilever or beam end specimens, capable of attaining most of the advantages of the Texas beam have been developed (Fig. 2.13). The cantilever beam test represents the bond situation existing between a flexural crack and the end of a simple beam and produces a similar strain gradient. Although several varying details are used, Fig. 2.13 provides a schematic representation. The pull-out force is applied directly to the bar as shown and the bottom reaction may bear against the end of the bar, or may be arranged so as not to be near the bar. The overall length of the specimen and the test length can each be varied. One or several bars may be used, with or without stirrups.

The major advantages of this specimen lie in its simplicity, inexpensiveness and its flexibility of load application since the relationships of bond, shear, moment and dowel force can be easily varied to produce different types of failure, thus facilitating the study of the complicated interactions of bond, shear, and flexure. Its disadvantages lie in the possible confining pressure against the free end of the bar and in the increased length over which splitting resistance tends to be mobilized. Also the validity of these tests with respect to the reported results of pull-out and beam tests, which has been discussed by a few investigators, needs further experimental evidence.

2.2.4.8 Other Beam Tests

A beam widely used at Université de Liège in Belgium (76) is illustrated in Fig. 2.14. The specimen consists of two prisms of concrete attached at their bases by the testing bar and at their tops by a hinge. The loading system is a two part loading system which is the same as in most American beam type tests. Its advantage lies in the precise determination of the tensile force on the steel bar due to the presence of the hinge where the resultant compressive force must necessarily pass. This force is given by:

$$T = P \times \frac{L^*}{H^*} \qquad (2.1)$$

where T is the total tensile force, L* and H* are the respective lever arms of the external and internal couples, and P is the applied concentrated load.

The slips are measured at the ends of the bar and the test can be used for practical evaluations of embedment lengths of reinforcing bars.

2.2.5 Torsional Bond Tests

Torsion tests have been used to a very limited extent to obtain bond strengths (32). This test consists of twisting the bar, embedded in a prism of concrete, about its axis relative to the concrete. The torque applied is obtained from dial gauges measuring the angular deflection of the bar outside the specimen over a suitable gauge length. The rotation of the bar relative to the concrete is also obtained at both loaded and free ends by means of suitable levers and dial gauges. This test can provide a useful approach to the complete understanding of the mechanism of bond.

2.2.6 Choice of Bond Test

Keeping in mind the objectives of the present experimental program and after comparing the advantages of the various bond tests, it was decided not to preclude possibility of shear force in the bond test specimens since the interaction of bond and shear occurs under most usage conditions in practice. Thus it was considered that a continuous beam, with a few bars at reasonable spacings and designed not to fail in shear, would be more suitable than other tests not only for fundamental bond research but also for reliable quantitative results.

But the preliminary design with cross-sections of 9 x 18 in (22.9 x 45.7 cm) gave a length of beam varying from 25 feet (7.6 m) to 30 feet (9.1 m) depending on the size of the test bars, if confinement effect from loading reaction has to be avoided. To cut the relatively high costs of such a beam it was decided to truncate all but the negative moment region which results in a simply supported beam with a concentrated load at the middle as shown in Fig. 2.15. It was also decided to use a reasonable amount of tension steel reinforcement and adequate shear reinforcement to prevent shear failures. This beam test, which eliminates confinement effects from direct bearing of reaction load against the ends of the test bar, can be considered a good choice for satisfying the objectives of this research program. Fabrication and testing of the specimens are discussed in the next chapter.

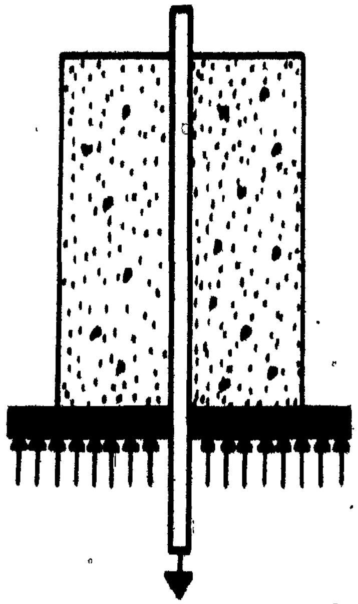

Fig. 2.1 Classical Pull-Out Test, Schematic (19, 20, 88)

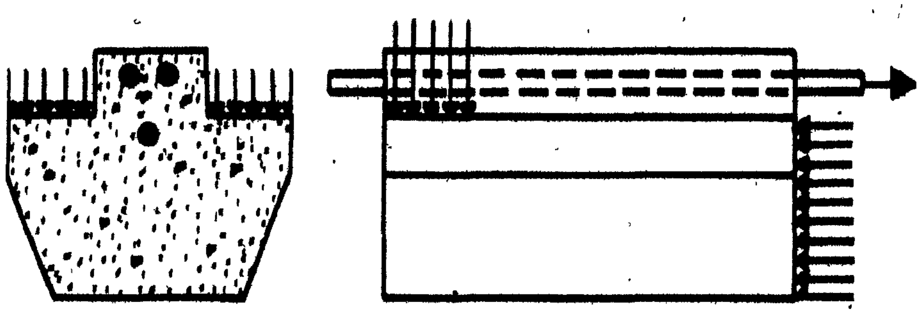

Fig. 2.2 Modified Pull-Out Test, Schematic (41, 43, 54)

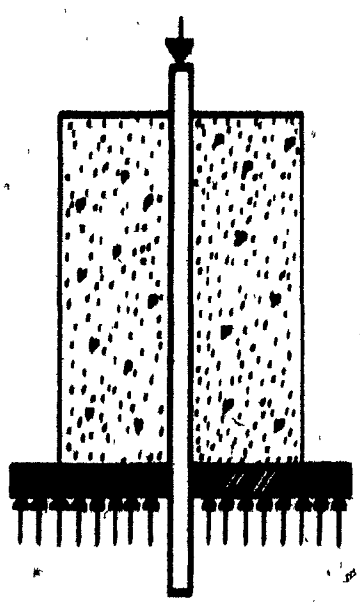

Fig. 2.3 Push-Out Test, Schematic (34, 35, 52)

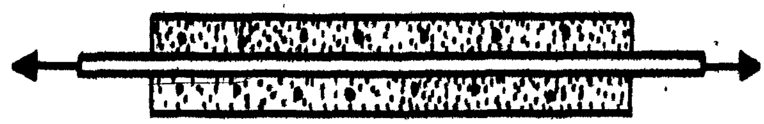

Fig. 2.4 Direct Pull-Out Test with Single Bar, Schematic (10, 18, 25)

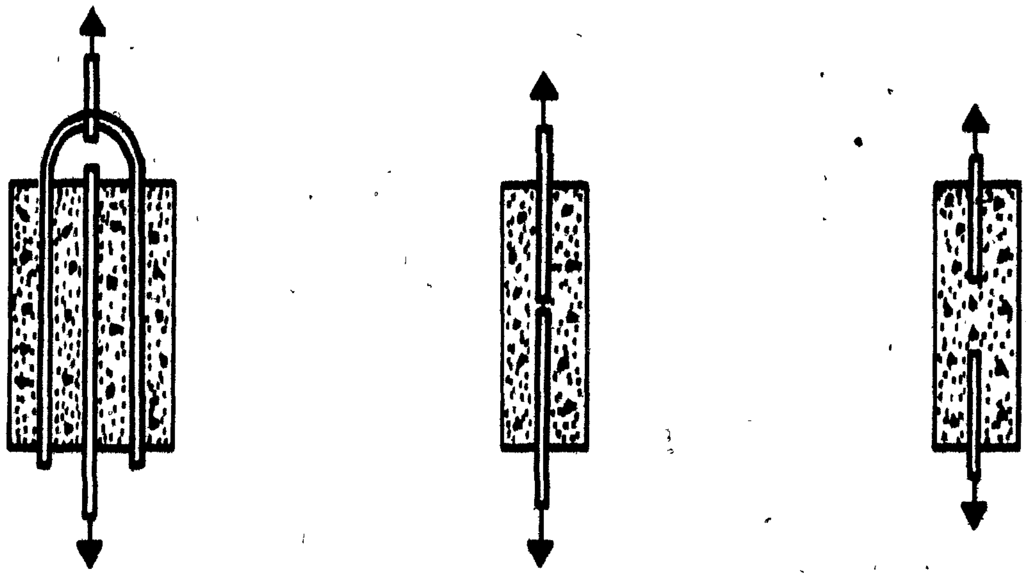

Fig. 2.5 Modified Direct Pull-Out Tests, Schematic

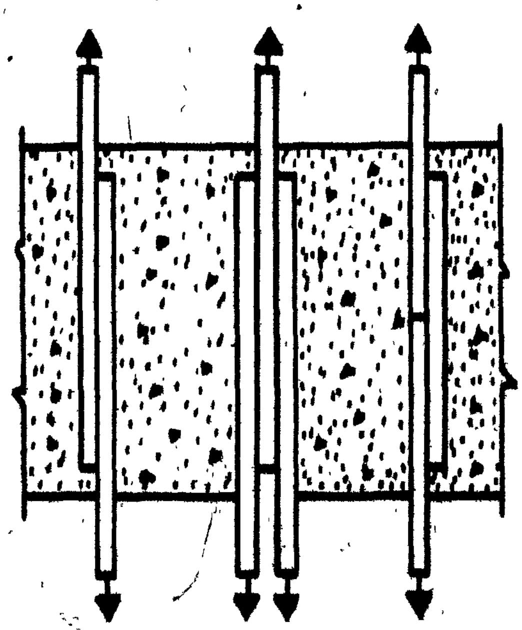

Fig. 2.6 Direct Pull-Out Tests with Lapped Bars, Schematic

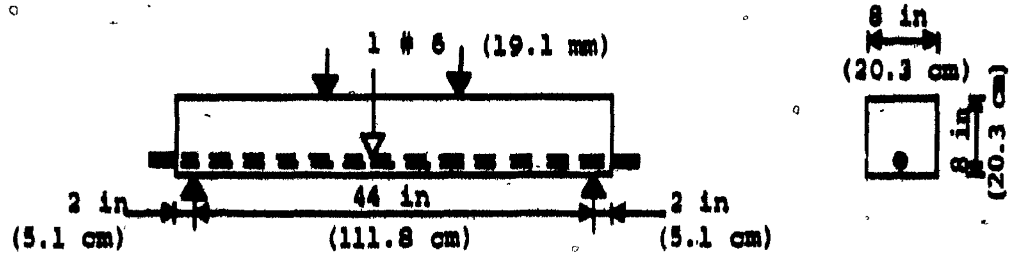

Fig. 2.7 Classical Bond Beam (52,91)

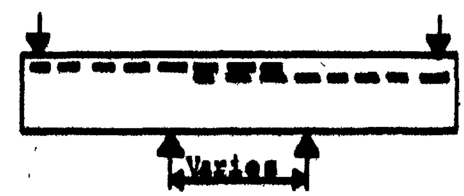

Fig. 2.8 Bond Beam with Lapped Bars (96)

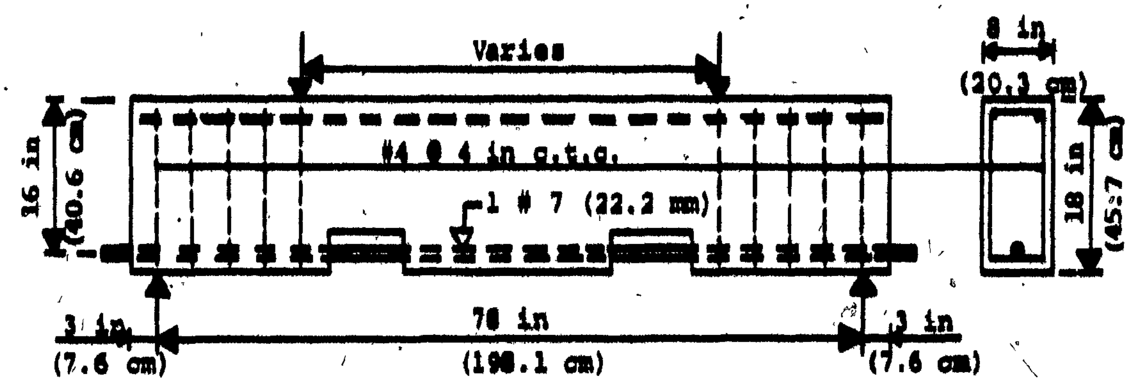

Fig. 2.9a ACI Committee 208 Bond Beam (92)

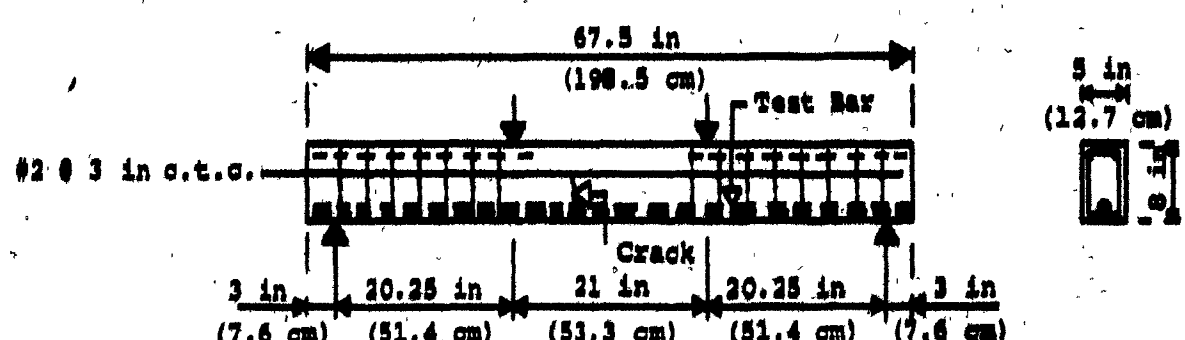

Fig. 2.9b Variation of ACI Committee 208 Bond Beam (43)

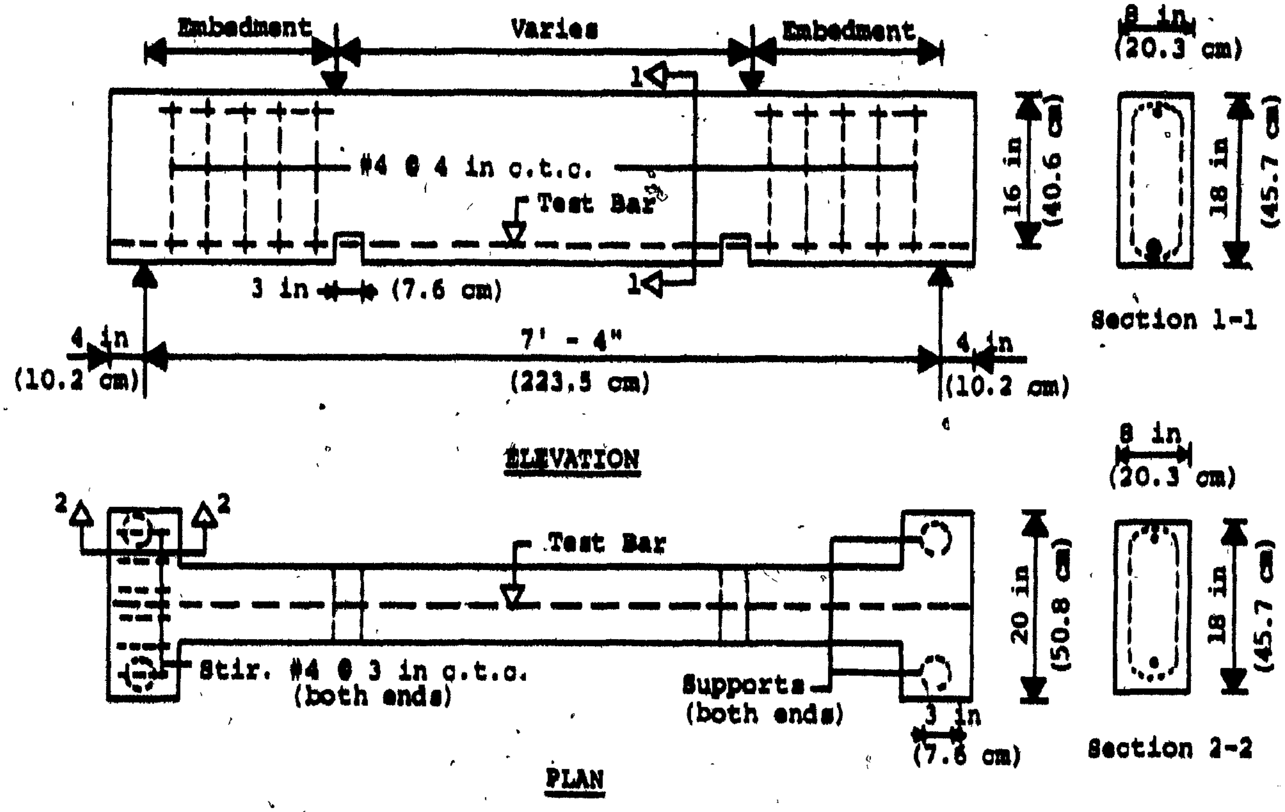

Fig. 2.10a National Bureau of Standards Bond Beam

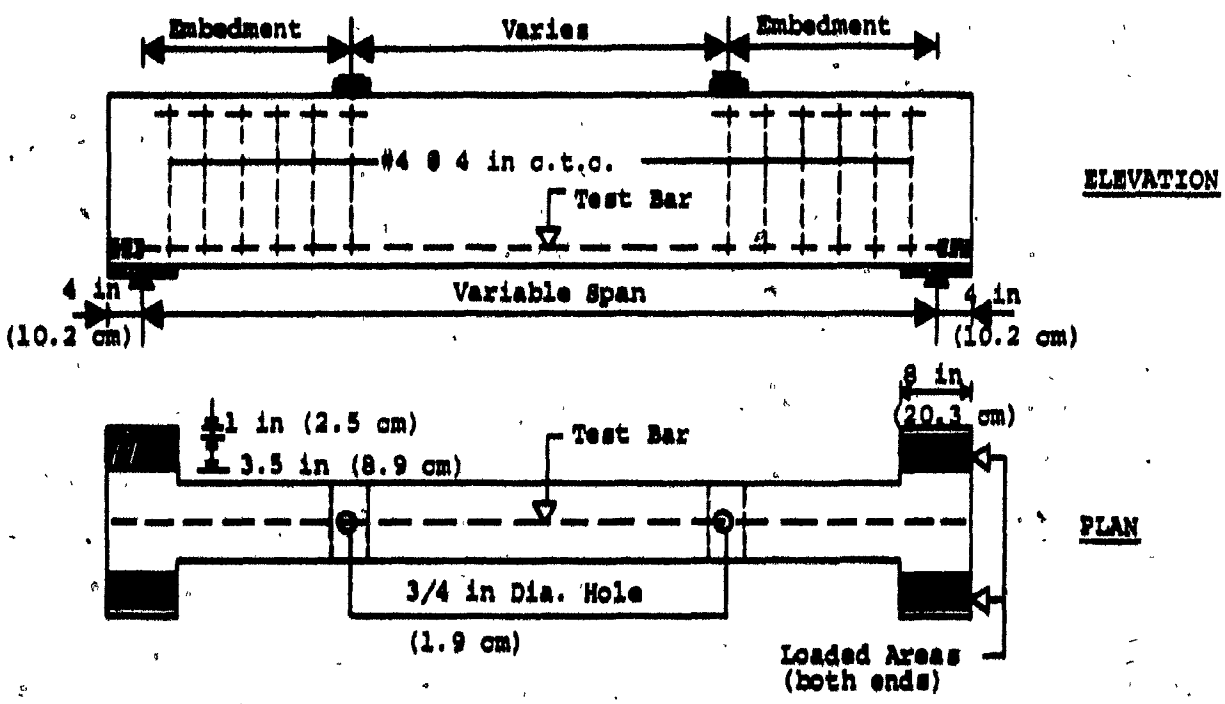

Fig. 2.10b ACI Committee 408 Bond Beam (93)

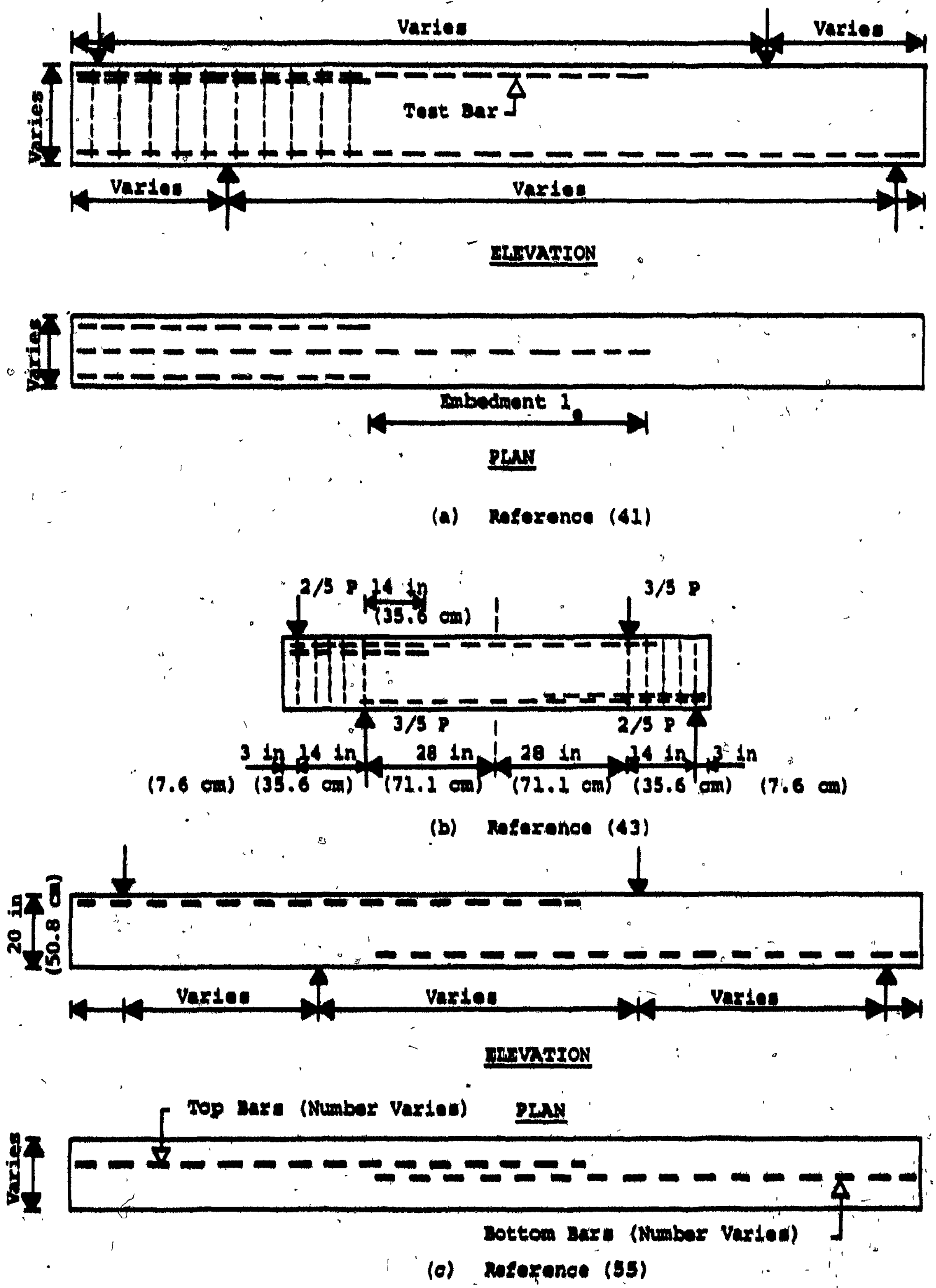

Fig. 2.11 The University of Texas Beam

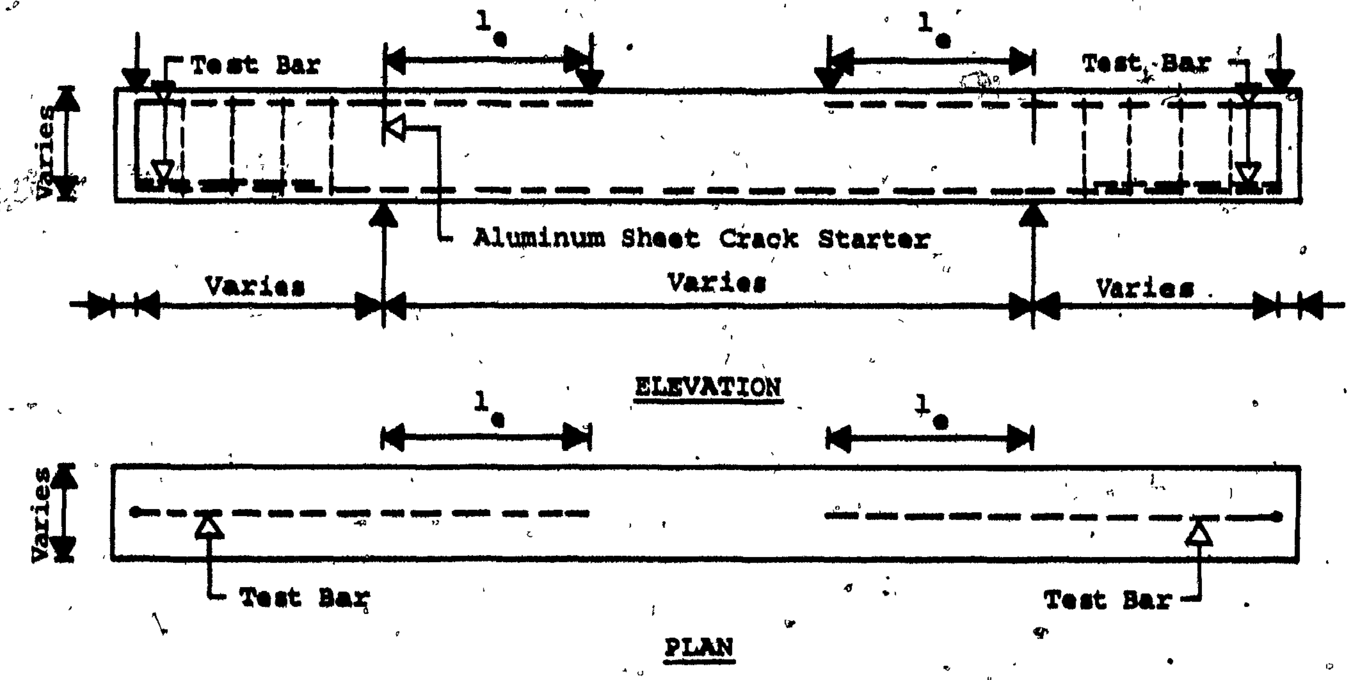

Fig. 2.12 Symmetrical Bond Beam (95)

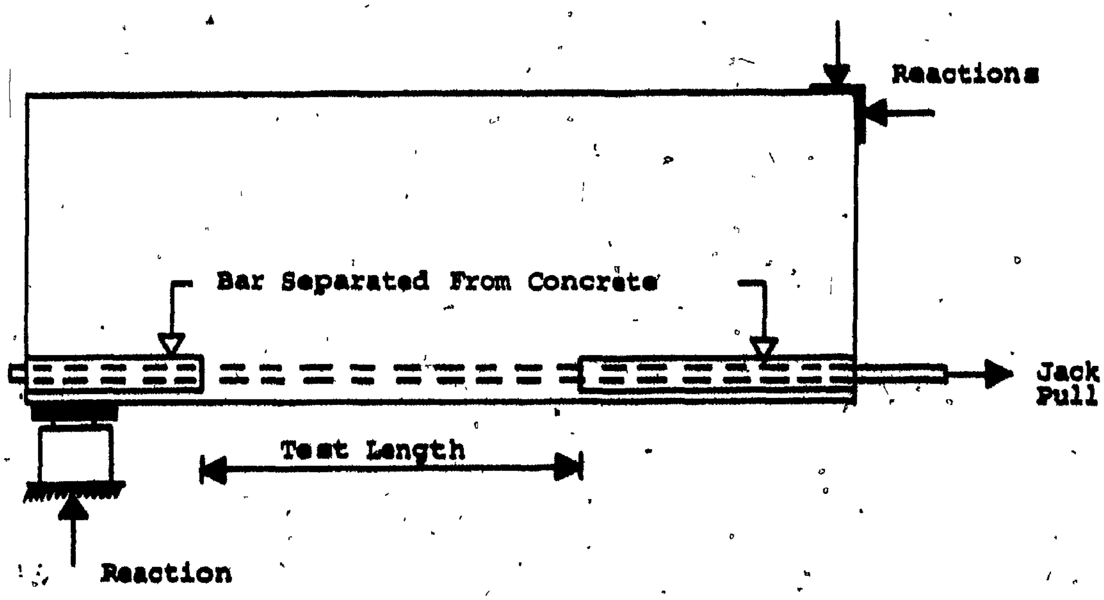

Fig. 2.13 Stub-Cantilever Beam

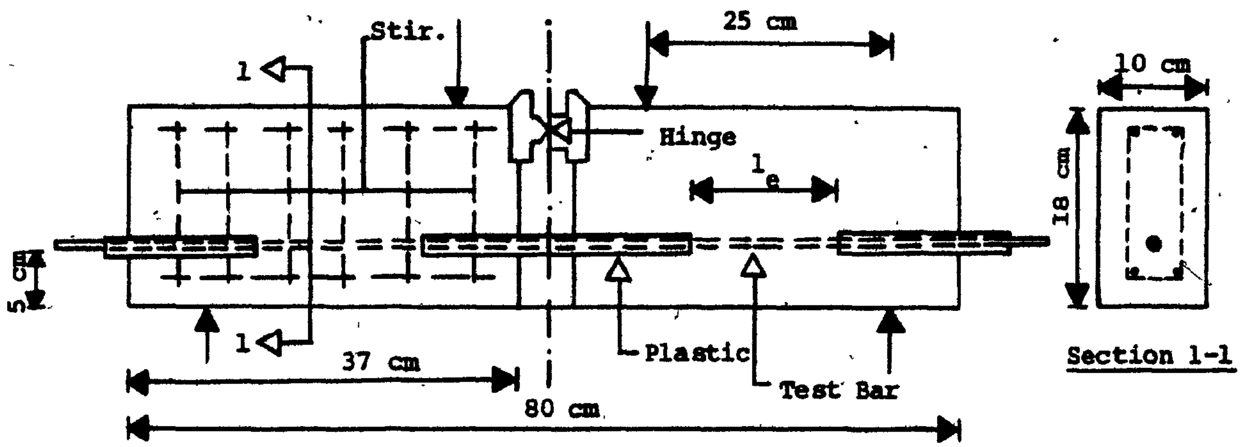

Fig. 2.14 Bond Beam of Université de Liège (76)

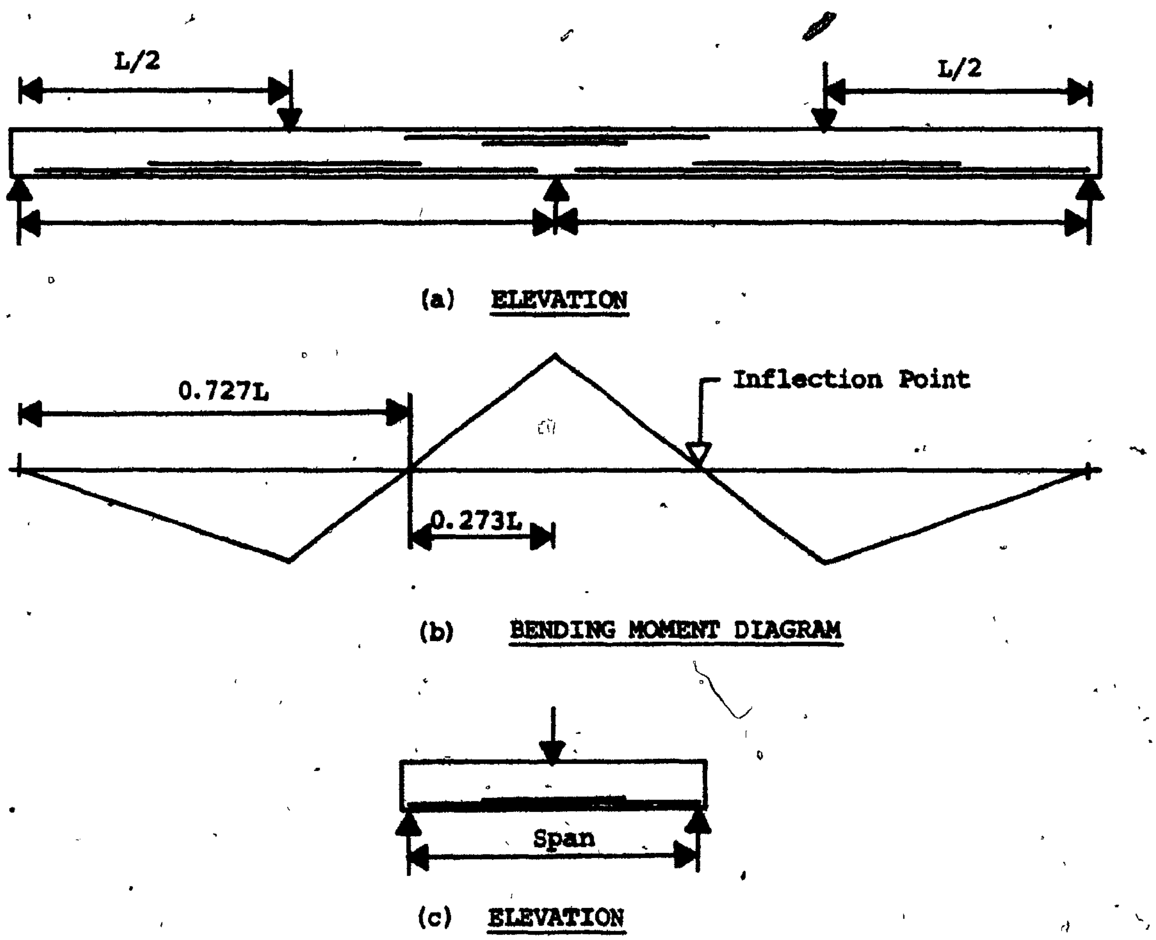

Fig. 2.15 Tentative Continuous Bond Beam and Simply Supported Bond Beam with Central Point Loading

CHAPTER III

EXPERIMENTAL TEST PROGRAM

3.1 Introduction

Having outlined the general requirements of the bond beam to be used, the first step was to decide on the size and type of the test bar to be used. The commercialy available, standard No. 8 (25.4 mm) deformed bar, which is commonly used in practice, was selected as the test bar. The second step was to design and detail the beam in order to ensure a bond failure. This is developed in the next section.

3.2 Design and Details of Test Specimens

After some trials the beam cross-section was set at 9 x 18 in (22.9 x 45.7 cm). The design was based on flexural and shear requirements of the American and Canadian Codes (4, 5). The beam details are shown in Fig. 3.2.

(i) Flexural Requirements

Given f'_c = 4,000 psi (27.6 MPa)

f_y = 60,000 psi (413.7 MPa)

$A_{b,1}$ = 0.79 in^2 (5.1 cm^2)

$A_{b,2}$ = 0.44 in^2 (2.84 cm^2)

d_1 = 16 in (40.6 cm)

d_2 = 15.75 in (40 cm)

d_t = 15.9 in (40.3 cm)

$$b = 9 \text{ in } (22.9 \text{ cm})$$

where f'_c = concrete compressive strength

f_y = yield strength of the steel bar

$A_{b,1}$ = area of the #8 steel bar

$A_{b,2}$ = area of the #6 steel bar

d_1 = distance from extreme compression fiber to centroid of #8 bar

d_2 = distance from extreme compression fiber to centroid of #6 bar

d_t = distance from extreme compression fiber to centroid of tension reinforcement

b = beam width

From the rectangular stress distribution shown in Fig. 3.1, the compression force in the concrete (C_c) and the total tensile force in the reinforcement (T) are given respectively by:

$$C_c = 0.85\, f'_c ba = 30.6\, a \tag{3.1}$$

$$T = (f_y \times A_{b,1}) + 2(f_y \times A_{b,2}) = 100.2 \tag{3.2}$$

From internal equilibrium ($C_c = T$):

$$a = \frac{100.2}{30.6} = 3.275 \text{ in}$$

The ultimate design moment is given by:

$$M_u = \frac{\phi T(d_t - a/2)}{12} \tag{3.3}$$

ϕ = capacity reduction factor (0.9 for flexure)

$$M_u = \frac{0.9 \times 100.2(15.9 - 1.638)}{12} = 107.2 \text{ kips-ft}$$

The external moment is given by:

$$M_{ext} = \frac{P_u.L}{4} \quad (3.4)$$

where P_u = ultimate design load

L = span length of the beam

but $M_{ext} = M_u$

Hence $\frac{P_u L}{4} = 107.2$ and $P_u L = 420.7$ kips-ft

assuming L = 10 feet

P_u = 42.1 kips (187.3 kN)

(ii) <u>Shear Requirements</u>

The nominal shear stress of the beam is computed by:

$$v_u = \frac{V_u}{\phi b_w d_t} \quad (3.5)$$

Due to the cut-off of the No. 8 bar, and to satisfy clause (12.1.6.1) of the ACI Code (4)

$$v_u = \frac{2}{3}(v_c + v'_u) \quad (3.6)$$

where
$$v_c = 2\sqrt{f'_c} \quad (3.7)$$

$$v'_u = \frac{f_{yt}.A_v}{b_w.s} \quad (3.8)$$

In the above Equations

V_u	=	total applied design shear force at section
b_w	=	web width
v_c	=	nominal permissible shear stress carried by concrete
v'_u	=	shear stress carried by web reinforcement
f'_c	=	concrete compressive strength
f_{yt}	=	yield strength of transverse reinforcement
A_v	=	area of shear reinforcement within a distance s
s	=	spacing of transverse reinforcement centre to centre
ϕ	=	capacity reduction factor (0.85 for shear)

Assuming #3 stirrups at 8 in (20.3 cm) centre to centre

$$v'_u = \frac{60,000 \times 0.22}{9 \times 8} = 183 \text{ psi}$$

$$v_c = 2\sqrt{4000} = 127 \text{ psi}$$

$$v_u = \frac{2}{3}(183 + 127) = 206 \text{ psi}$$

$$v_u = \frac{V_u}{0.85 \times 9 \times 15.9} = \frac{V_u}{121.6} \text{ psi}$$

then $$\frac{V_u}{121.6} = 206 \text{ psi}$$

$$V_u = 25.1 \text{ kips}$$

but $$V_u = P_u/2$$

Hence $$P_u = 2 \times 25.1 = 50.2 \text{ kips (223.3 kN)}$$

(iii) The ultimate design capacity of the beam is governed by flexure and is given by:

$$P_u = 42.1 \text{ kips} \quad (87.3 \text{ kN})$$

3.3 Description of Test Specimens

Bond type of failure in reinforced concrete beams subjected to a moment gradient is usually difficult to obtain, due to the close interaction of bond with shear and flexure. Therefore, it was decided to use the first beam as a pilot test and to make the necessary modifications if the results were not satisfactory. The pilot test consisted of a simply supported beam, 11 ft (3.35 m) long with the reaction loads at 6 in (15.2 cm) from both ends. The beam cross-section was 9 x 18 in (22.9 x 45.7) and was reinforced with Grade 60 steel reinforcement as follows:

(i) The test bar consisting of one No. 8 (25.4 mm) deformed bar with an embedment length of 30 in (76.2 cm). This is the length required by both American and Canadian Codes (4, 5) for the No. 8 (25.4 mm) "bottom-cast" bar of Grade 60 to develop its full yield stress.

(ii) Two No. 6 (19.1 mm) deformed bars, as adjacent bars, which run the full length of the beam specimen. The No. 8 (25.4 mm) bar is tied to the No. 6 (19.1 mm) bars and held in position at three locations along its length, by means of a small cross-bar 1/8 in (3.2 mm) diameter, approximately 8 in (20.3 cm) long.

(iii) Two No. 3 (9.5 mm) deformed bars placed on the opposite face and running the full length of the beam, help as hangers to tie the shear reinforcement.

(iv) The shear reinforcement which consists of stirrups, made with No. 3 (9.5 mm) deformed bars, placed at 8 in (20.3 cm) centre to centre. The stirrups conformed to the American and Canadian Code specifications except for the hooks around the No. 6 (19.1 mm) bars which had a diameter and a length slightly less than prescribed. The test bar had a clear spacing of at least 1.25 in (3.2 cm) from the adjacent bars and was left completely free from the stirrups.

The pilot test beam had a side cover of 0.75 in (19.1 mm). Cast with the tension bars on the top of the specimens, it had a depth of concrete of 15.5 in (39.4 cm) below the No. 8 (25.4 mm) test bar. According to the American and Canadian Code specifications, a "top bar" is a bar cast with at least 12 in (30.5 cm) of concrete below the bar. Therefore, the pilot test, named beam B1 was considered as a specimen with "top-cast bars" or simply a "top-cast specimen". Later, it was turned upside down for testing. Having performed very well, the same design and detailing were kept for the rest of the experimental program. The beams whose details are shown in Fig. 3.2 are classified as follows:

(i) Beams B1 and B2 are respectively the "top-cast" and the "bottom-cast" specimens. The embedment length of the test bar is 30 in (76.2 mm).

(ii) Beam B3 is a "top-cast" specimen while beam B4 is a "bottom-cast" specimen. They both have an embedment length of 36 in (91.4 cm) for the test bar.

(iii) Beams B5 and B6, which have an embedment length of 40 in (101.6 cm), for the test bar are cast respectively with their main bars at the top and at the bottom of the specimens.

3.4 Material Properties

3.4.1 Steel Reinforcement

Each group of the steel reinforcing bars used in this research program, had the same heat treatment and was from the same stock. They were all standard deformed bars corresponding to ASTM 615-68 specifications. For each size of bar at least three randomly cut specimens 18 in (45.7 cm) long, were selected for an axial tension test. These specimens were instrumented with electrical resistance strain gauges in a manner similar to that of the bars used in the specimens. Two gauges, diametrically opposed, were placed at mid-length of each coupon, which was later held in the jaws of a 60 kip (266.9 kN) capacity testing machine and tested until failure. The physical properties of the reinforcing bars were then determined; their average values are summarized in Table 3.1. Results of the tensile tests of the coupons are presented in Appendix A.

TABLE 3.1

PROPERTIES OF REINFORCING BARS

BAR NO.	d_b in (mm)	A_b in^2 (cm^2)	f_y psi (MPa)	f_u psi (MPa)	E_s 10^6psi (10^3MPa)
No. 8	1.000 (25.4)	0.790 (4.030)	59,500 (410.3)	88,600 (610.9)	30.5 (210.3)
No. 6	0.750 (19.1)	0.440 (1.250)	58,500 (403.4)	89,100 (614.3)	31.0 (213.7)
No. 3	0.375 (9.5)	0.110 (0.078)	60,300 (415.8)	91,900 (633.7)	30.8 (212.4)

3.4.2 Concrete

Normal Portland Cement, meeting the current standard specifications of the ASTM C150 - 69a for type I (or C.S.A. type 10) was used. The fine aggregate consisted of natural concrete sand while the coarse aggregate consisted of crushed limestone with a maximum size of 3/4 in (19.1 mm). The mix (97) designed for a slump of 4 in (10.2 cm) and a water-cement ratio of 0.54, consisted of the following by weight of one cubic yard of concrete:

Fine aggregate	:	Sand	-	1610 lbs
Coarse aggregate	:	1/4" Stone	-	510 lbs
		1/2" Stone	-	840 lbs
		3/4" Stone	-	340 lbs
Coarse aggregate	:	Total	-	1690 lbs
Portland Cement Type I	:		-	500 lbs
Water	:		-	270 lbs
Water reducing agent	:	(W.R.D.A.)	-	35 oz

The ready-mixed concrete was delivered into the laboratory and for each specimen six standard 6 x 12 in (15.2 x 30.5 cm) concrete cylinders were cast at the same time. They were stored and cured in the same manner as the beam specimen and were tested on the following day, to determine the physical characteristics of the concrete. Prior to testing, the control cylinders were capped at both ends with a strong industrial plaster. In a few tests, electrical resistance strain gauges were used and a typical concrete stress-strain curve is illustrated in Fig. 3.3. The concrete compression test results are listed in Appendix A. The average values of the compressive strength and the modulus of elasticity of the concrete used for each beam are shown in Table 3.2.

TABLE 3.2

PROPERTIES OF CONCRETE

BEAM NO.	f'_c psi (MPa)	$E_c = 57{,}000\sqrt{f'_c}$ 10^6 psi (10^3 MPa)	$f_r = 7.5\sqrt{f'_c}$ psi (MPa)
B1	4,040 (27.9)	3.63 (25.0)	478 (3.3)
B2	3,890 (26.8)	3.56 (24.5)	468 (3.2)
B3	4,070 (28.1)	3.63 (25.0)	478 (3.3)
B4	4,240 (29.2)	3.71 (25.6)	488 (3.4)
B5	4,030 (27.8)	3.63 (25.0)	478 (3.3)
B6	4,070 (28.1)	3.63 (25.0)	478 (3.3)

3.5 Fabrication and Curing of Specimens

All specimens were cast in the McGill Civil Engineering laboratory. After making the stirrups, the reinforcing cage was fabricated by tying each junction of longitudinal and transverse reinforcement together with wire. The day before casting, the cage was placed in wooden forms made of 3/4" (19.1 mm) stiffened plywood formwork.

Prior to placing the cage, the inner faces of the forms were given two-coats of liquid plastic (form grease), which facilitated the removal of the forms after casting. Later, the cage was held rigidly in its exact position to satisfy all cover requirements and the lead wires from the instrumented bars were carefully tucked away to the outside of the forms through holes drilled in the forms. The concrete was carried by a wheel barrow from the truck and deposited by shovel into the forms in a few layers, starting from one end to the other. Each layer, approximately 6 in (15.2 cm), was vibrated carefully with a portable electric vibrator 1 in (2.5 cm) diameter to remove air voids and special attention was paid in the vicinity of the strain gauge sections. During the concreting, external vibration was also applied a few times to the outside faces of the forms using the same needle vibrator. The slump of the concrete was recorded and averaged 4.5 in (11.4 cm) for the six beam specimens.

The exposed surface of the concrete was finished with a trowel approximately half an hour after placing. The specimens were then covered with burlap which was wetted each day and a layer of polyethylene. The forms were then stripped and the specimens were laid horizontally on the floor and were moist-cured under the polyethylene sheets for seven days. Subsequently, they were allowed to cure, without any special protection, in the dry air of the laboratory until they were moved into the strong floor for testing.

3.6 Instrumentation

3.6.1 Basic Measurements

In any experimental study, it is important to measure the loads, reactions, deflections and strains. Loads and reactions give a check on the static equilibrium and the accuracy of the applied loads. Deflection readings are very significant, as they indicate the ranges of linear and non-linear response. Strains are a measure of the extent of deformation at any point in the structure and constitute the basis for all further calculations and evaluation of internal forces and moments. Also, bond stresses can be derived from the internal strain deformations.

3.6.2 Choice of Instrumentation

As far as the load is concerned, there was no need for using load cells because of the high precision of the "Roylyn" pressure gauge model 2554-38C53 series. Also, the beam being simply supported the reactions were not measured. Only the vertical deflection readings at the centre-line of the specimen were made by using a two-inch travel dial gauge. The instrumentation for the measurement of strains on the reinforcing bars and on the surface of concrete consisted of electrical resistance strain gauges. This strain gauge scheme was divided into three parts. Its main objective was to obtain information which would enable plotting the entire strain and bond stress distribution along the length of the instrumented bars. Also, at critical sections such as the section with the maximum bending moment and bar cut-offs, a check could be made on the equilibrium between internal couple and external moment to verify the validity of the basic assumptions:

3.6.2.1 Test Bar

The gauge type and their mode of application were uniform for all test bars. Application of the gauge required grinding of two bar deformations over a length of approximately 3/4 in (19.1 mm). Then the bar surface at the gauge area was sanded to obtain a smooth surface for the installation of the strain gauge. Degreasing was done by cleaning the area with acetone. After the gauge was set and tested with a D.C. ohm meter, the area was covered with waterproofing to protect the gauge from getting damaged during the concreting operation and to prevent bonding between the gauge and the concrete. Lead wire connection, waterproofing and other disturbances to bond action were confined to this narrow region. The gauges on the test bars were all PL-5-11 and were typically placed 4 inches (10.2 cm) apart starting from the centre-line. The layout of strain gauges is shown in Figs. 3.4 and 3.5 and also in Fig. B.1 in Appendix B.

3.6.2.2 Adjacent Bars

Only one of the adjacent bars was instrumented along part of its length, in the same manner as the test bar. However the gauge distance varied from 6 to 12 in (15.2 to 30.5 cm) as can be seen from the layout shown in Figs. 3.4 and 3.5 (or in Fig. B.2 in Appendix B).

3.6.2.3 Concrete Strains

For the first beam, Demec gauges were used to measure the concrete compressive strains at selected stations. For the rest of the beam, PL-20-11 electrical resistance strain gauges were preferred, and were installed at locations along the span length, as illustrated in Figs. 3.4 and 3.5, and in Fig. B.3 in Appendix B. Their installation was simpler than the gauges on steel bars because it did not require any special protective coatings.

3.7 Test Set Up

3.7.1 Loading Arrangement

The beam was simply supported with a span length of 10'-0" (3.05 m). Each support reaction consisted of a 2 in (5.1 cm) steel roller placed between two bearing plates 1½ in (3.8 cm) thick. The roller was fixed at one end and free at the other end. These systems were supported on two steel I-beams, seated on two concrete blocks which were resting on the strong floor. A neat mortar of industrial plaster was applied between the lower faces of the beam specimen and the top surface of each bearing plate, to provide a true bearing surface for the end reaction. These caps were allowed to harden one day before testing.

A double channel steel beam was seated on top of the specimen at mid-span, which was capped at this location. Two high strength steel threaded rods, 1-1/8 in (28.6 mm) diameter, with a tensile strength of 125 ksi (861.9 MPa) and corresponding to ASTM Standard A193 were symmetrically placed, 19 inches (48.5 cm) apart on both sides of the test beam. They extented from the top of the loading beam to the bottom of the strong floor and were connected to a 30 ton (266.9 kN) hydraulic jack. They were bolted on both ends. The hand pump applied a given pressure through a system of hoses to the Simplex jacks and was measured by a "Roylyn" pressure gauge. The Simplex jacks in turn applied the tensile force to the steel rods, resulting in a central reaction on the top of the beam specimen (Fig. 3.6).

3.7.2 Testing Procedure

The load was applied with the system described above in increments of 200 psi (1.4 MPa) corresponding approximately to a midspan load of 2.61 kip (11.6 kN). All strain gauges were calibrated before the test. The strain readings were obtained by means of an electronic multi-channel strain indicator, model SY161 series. The indicator controlled and synchronized all scanning and printing operation and gave strain readings in micro-inches per inch. At each load increment, the printing unit provided all readings of strains acting on the concrete surfaces and the reinforcing bars. The deflection readings were also recorded. In addition to these measurements, the location, extent, type (transverse flexural, longitudinal splitting etc) and width of cracks were recorded immediately after the application of each increment of load. Near failure load, deflections increased more rapidly and the test procedure was switched from load control to a control of deflection. On the average, each test required approximately three hours. The test data (Appendix C) is presented and discussed in the next two chapters.

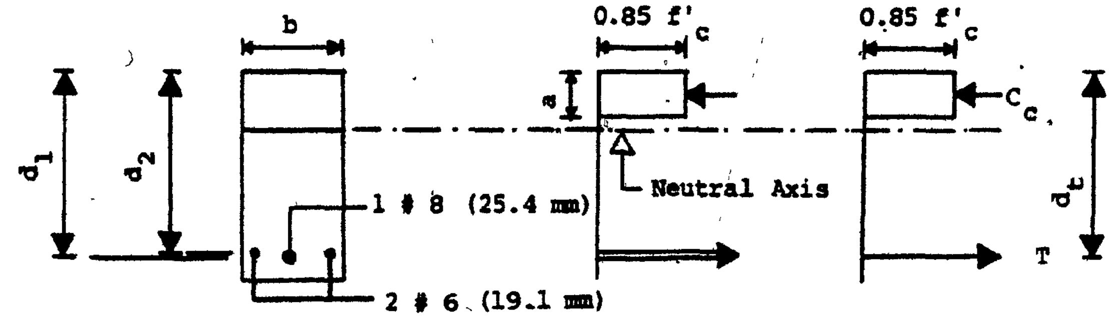

Fig. 3.1 Rectangular Stress Distribution

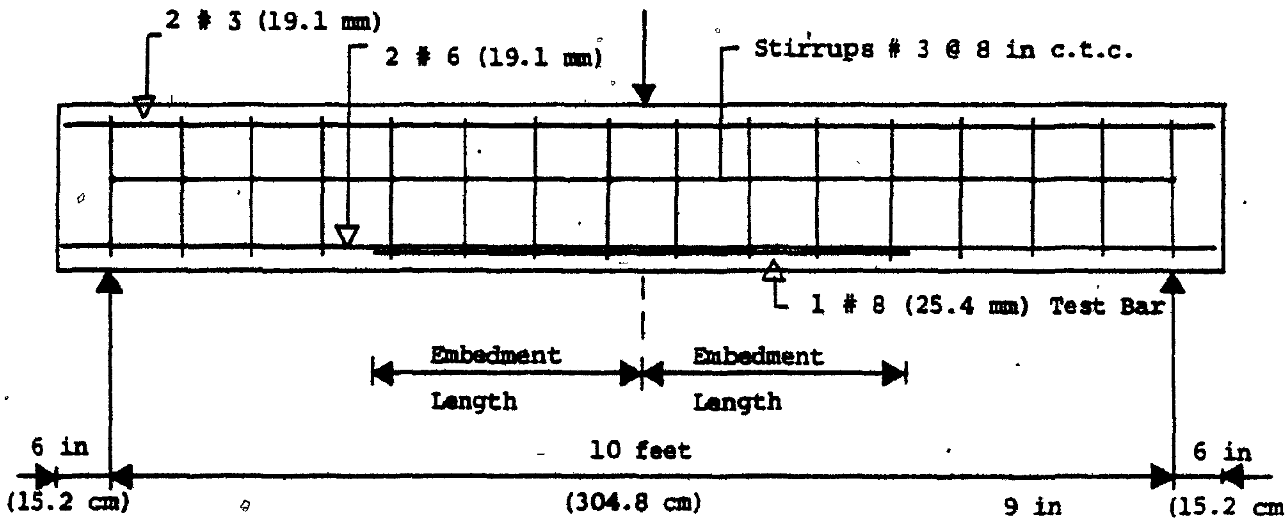

BEAM CLASSIFICATION	EMBEDMENT LENGTH
Beam B1 : Top-Cast Specimen	30 in (76.2 cm)
Beam B2 : Bottom-Cast Specimen	30 in (76.2 cm)
Beam B3 : Top-Cast Specimen	36 in (91.4 cm)
Beam B4 : Bottom-Cast Specimen	36 in (91.4 cm)
Beam B5 : Top-Cast Specimen	40 in (101.6 cm)
Beam B6 : Bottom-Cast Specimen	40 in (101.6 cm)

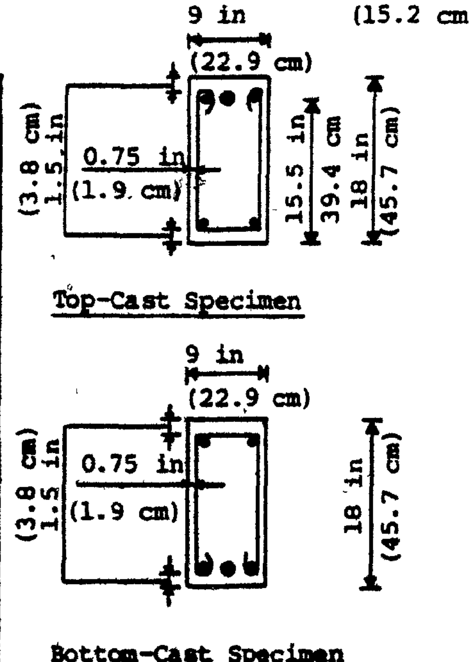

Fig. 3.2 Beam Specimens

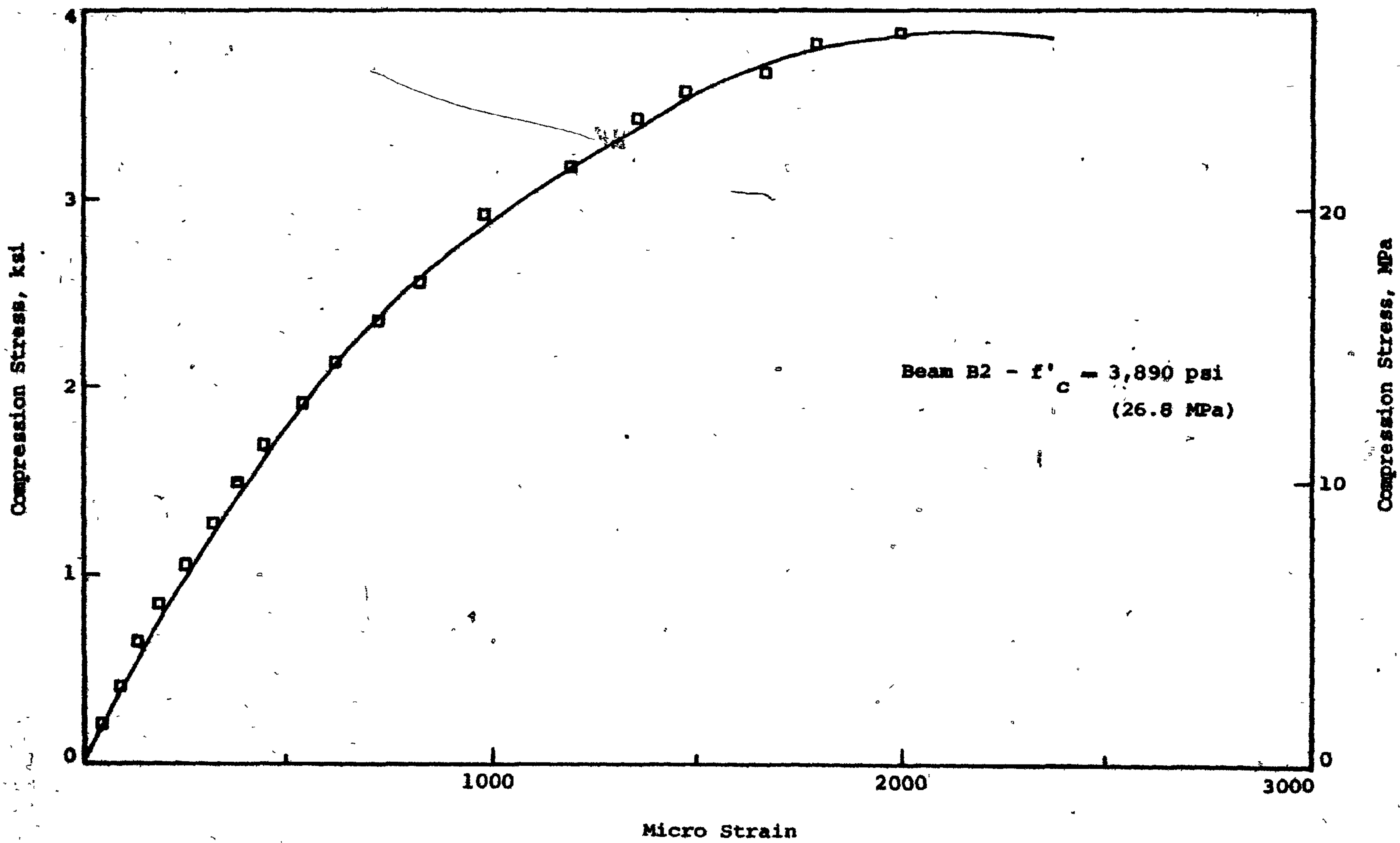

Fig. 3.3 Concrete Stress-Strain Curve

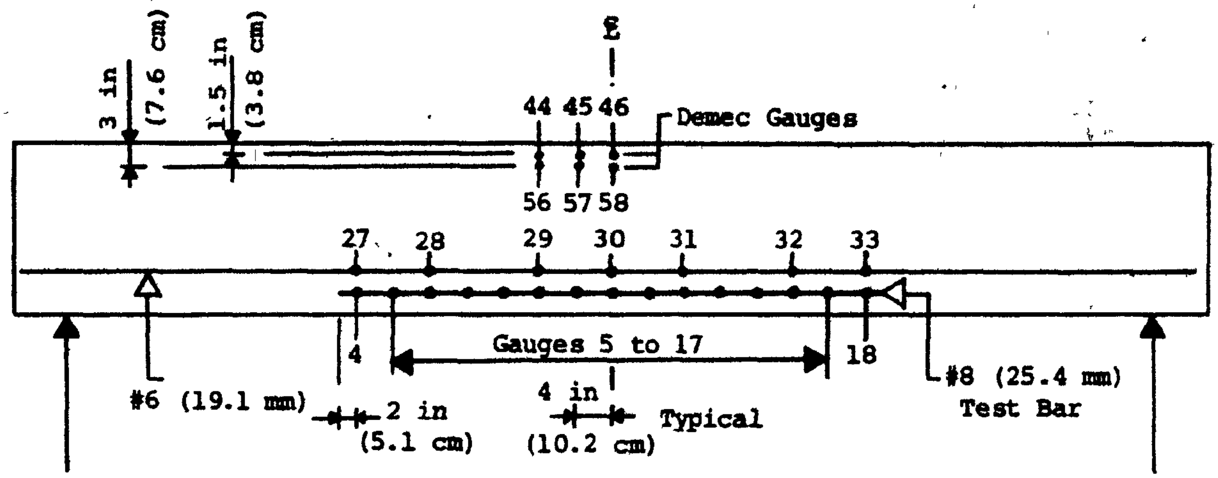

(a) BEAM B1 - ELEVATION

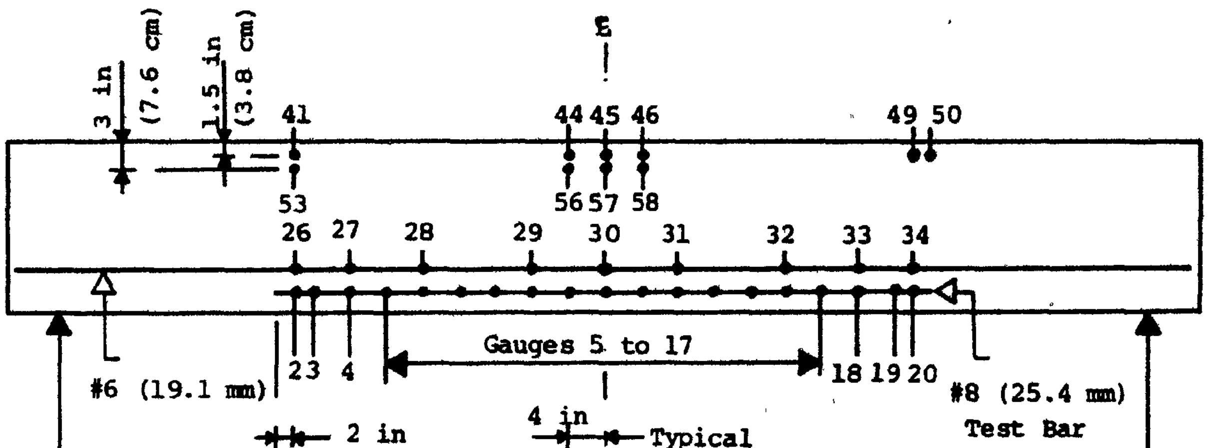

(b) BEAM B3 - ELEVATION

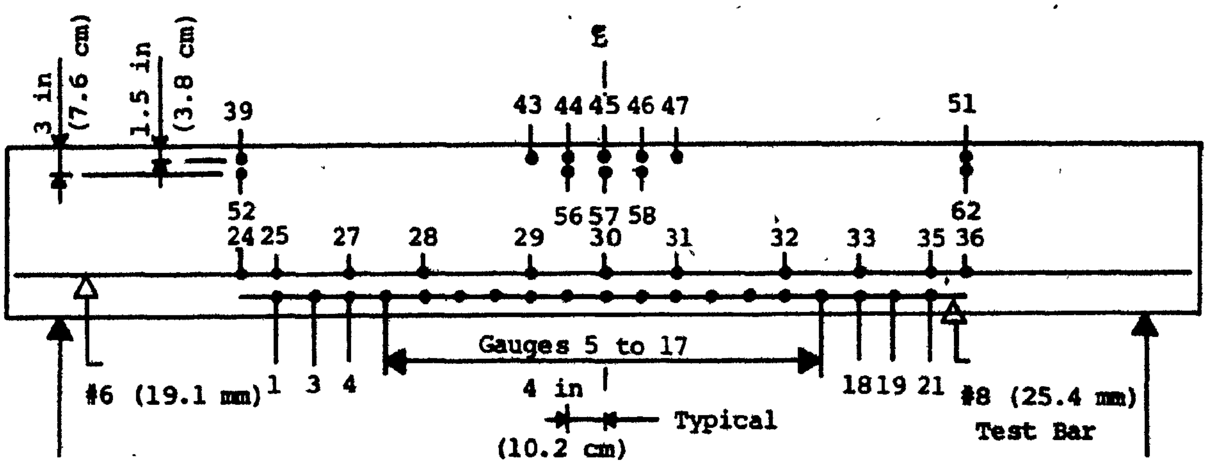

(c) BEAM B5 - ELEVATION

Fig. 3.4 Locations of Strain Gauges for Top-Cast Beams

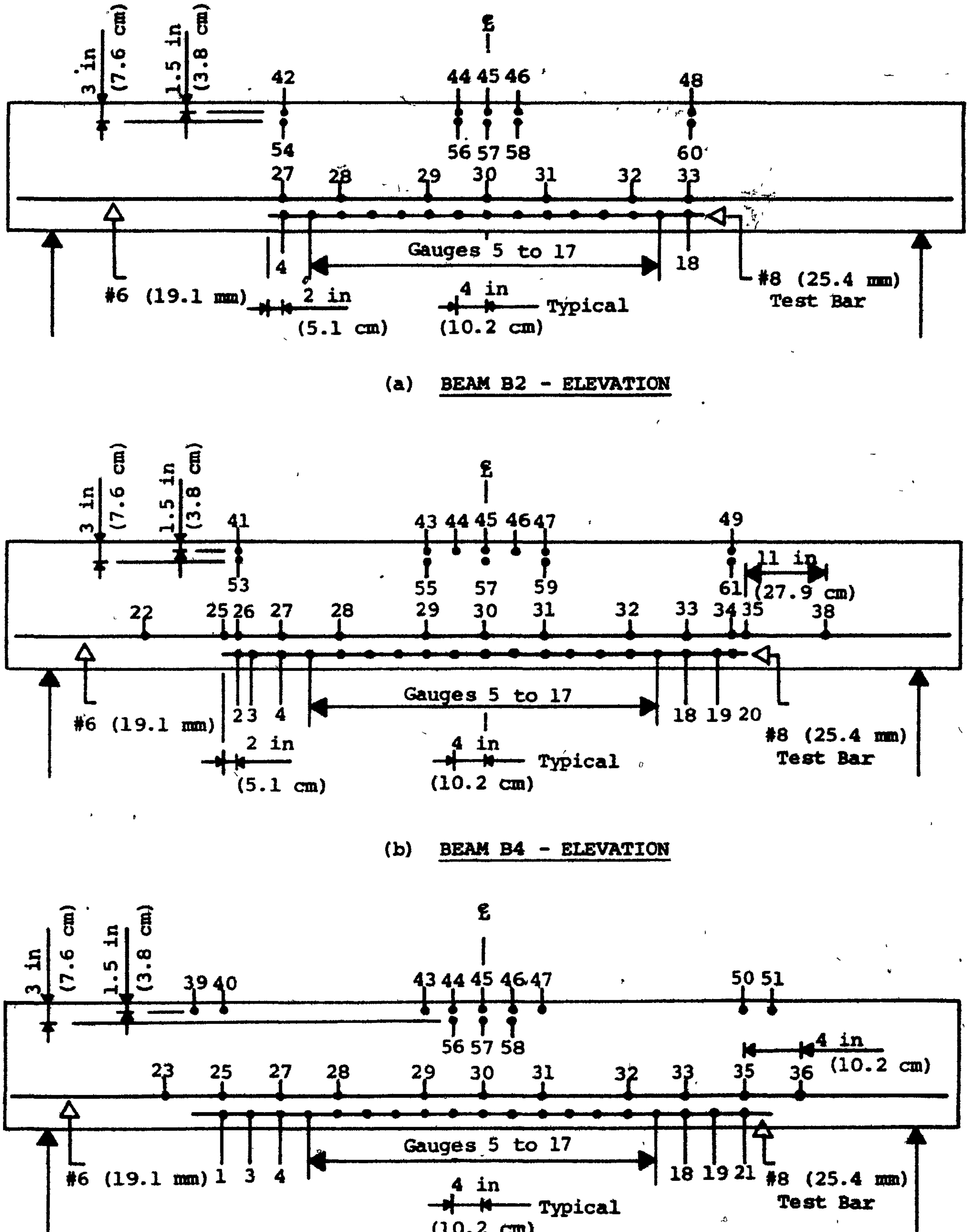

(a) BEAM B2 - ELEVATION

(b) BEAM B4 - ELEVATION

(c) BEAM B6 - ELEVATION

Fig. 3.5 Locations of Strain Gauges for Bottom-Cast Specimens

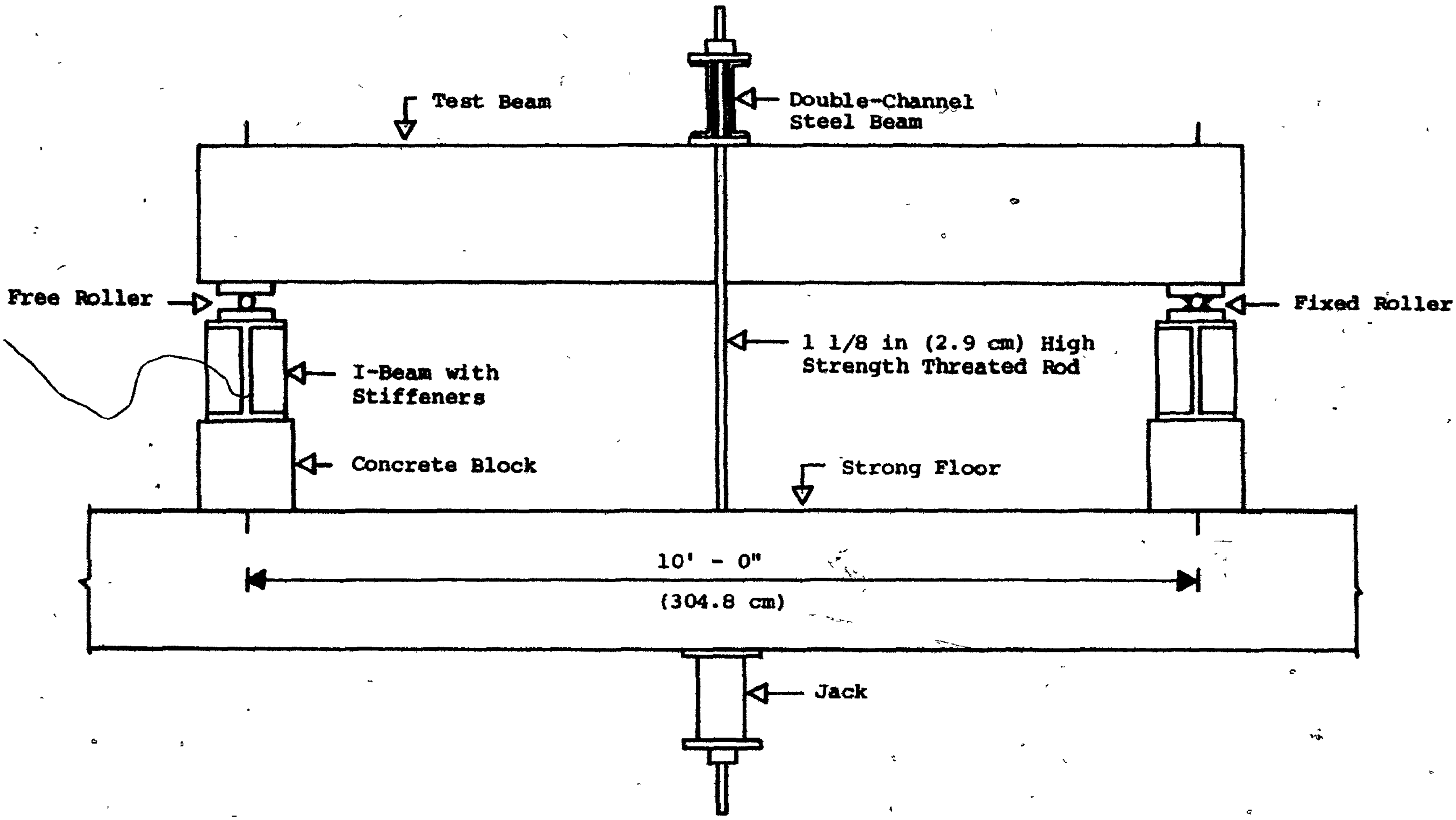

Fig. 3.6 Beam Test Set-Up

CHAPTER IV

TEST RESULTS AND EXPERIMENTAL BEHAVIOUR

This chapter presents the experimental results of the six beams tested in terms of load-deflection responses, strain distributions in both concrete and steel, cracking behaviour and failure mechanisms.

The measured steel strains on the No. 8 (25.4 mm) test bar were used to calculate the variation of bond stresses in each beam. The behaviour of the beams is discussed in three groups having embedment lengths of 30 in (76.2 cm), 36 in (91.4 cm) and 40 in (101.6 cm). This enables a direct comparison of the "top-cast" vs. "bottom-cast" bars having the same embedment length. The behaviour of the three "top-cast" specimens, B1, B3 and B5, is then compared to study the influence of different embedment lengths. A similar comparison is then made for the three "bottom-cast" specimens, B2, B4 and B6.

4.1 Response of Beams with Top-Cast and Bottom-Cast Bars

4.1.1 Beams B1 and B2. Embedment Length of 30 in (76.2 cm)

4.1.1.1 Response of Beam B1

The load-deflection response of beam B1 ("top-cast") is shown in Fig. 4.1. Beam B1 deflected almost linearly under the first four load increments, without any sign of flexural cracking. At the load of 10.4 kips (46.3 kN), a hairline transverse crack appeared right at the centre-line of the beam. As the applied load was increased, a few more cracks were formed on each side of the centre-line in a fairly symmetrical manner. Their widths were approximately 0.002 in (0.05 mm). When the load reached 23.5 kips (104.5 kN) a flexural crack appeared at each cut-off location and widened, with the next load increment, to a width of 0.008 in (0.20 mm), while other cracks were finer. Another increase of the load moved most of the cracks higher up into the compression zone of the beam with a slight inclination towards the centre.

Finally longitudinal splitting cracks started appearing on both ends of the No. 8 (25.4 mm) test bar at a load of 36.6 kips (162.8 kN). Their length was approximately 6 in (15.2 cm) and their width 0.03 in (0.7 mm). With further increase of the load, a large flexural shear crack appeared suddenly at one end of the No. 8 (25.4 mm) bar as can be seen in Fig. 4.2a and the load dropped off. The maximum load recorded was 37.0 kips (164.6 kN). The final splitting cracks had propagated to a length of 14 in (35.6 cm) on one side and 8 in (20.3 cm) on the other side. The maximum widths of the splitting and the major shear cracks were measured and were both 0.25 in (6.4 mm). This brittle failure was aggravated by the presence of diagonal tension due to the cut-off of the No. 8 (25.4 mm) bar in the tension zone. The maximum deflection reached before the load dropped was 0.444 in (1.13 cm).

The theoretical load deflection and the ACI yield prediction are also shown in Fig. 4.1 with the P-Δ curve of beam B1. For the deflection at yielding, Branson's equation is used to compute the effective moment of inertia: I_e

$$I_e = \left(\frac{M_{cr}}{M_{max}}\right)^3 I_g + \left[1 - \left(\frac{M_{cr}}{M_{max}}\right)^3\right] I_{cr} \quad (4.1)$$

where M_{cr} = cracking moment

M_{max} = maximum external moment at load into consideration

I_g = moment of inertia of uncracked section transformed to concrete

I_{cr} = moment of inertia of cracked section transformed to concrete

It is apparent from Fig. 4.1 that beam B1 did not reach the ACI yield prediction, having a maximum capacity of only 78% of the ACI yield prediction. This is explained by the fact that beam B1 does not have perfect bond between steel and concrete and does not develop its yield stress of 60 ksi (413.7 MPa) because the embedment length is too short.

An examination of Fig. 4.3, which shows the variation of tensile strain along the test bar of beam B1 at different load stages, confirms that the maximum strain reached at centre is only 1430 micro in/in. This is less than the yield strain of 1950 micro in/in. The theoretical strain distribution is obtained before cracking and after cracking. This is almost a straight line going from zero at the end of the bar to a maximum value at centre. Before cracking, at a load of 5.2 kips (23.1 kN), the strains are low and quite close to the predicted values. For the subsequent load stages, cracks occur along the beam length and their locations govern the magnitude and the distribution of the tensile strains. Crack locations are close to the measured peaks in the bar strain curves due to the increased tensile force carried by the steel at crack locations.

Between cracks, the concrete helps to carry tension and the steel strain drops off in a compensating manner as illustrated by these distributions.

The bar strain curves may very well not show the true peak in the strain curve unless the crack happens to occur within about ½ in (1.27 cm) or less of the gauge length. The strain curves increase gradually with the applied load and most strain values at the ends of the test bar are much higher than the predicted values. The tensile strains along the continuous No. 6 (19.1 mm) bars are presented in Table C.3 in Appendix C. This table indicates a yielding of the No. 6 (19.1 mm) at the cut-off locations, at failure of the specimen. This is due to the large moment and the stress concentration at the cut-off location. No yielding of the No. 6 (19.1 mm) bars was recorded at the centre of the beam.

Bond stress is the slope of the "force in-bar" curve. The average local bond stresses can be derived between two gauge locations by the following equation:

$$u_t = \frac{\Delta F_{AB}}{\pi d_b \ \Delta_{AB}} = \frac{E_S A_b \ (\varepsilon_B - \varepsilon_A)}{\pi d_b \ \Delta_{AB}} \qquad (4.2)$$

where u_t = average local bond stress obtained in tests

ΔF_{AB} = differential force between two gauges A and B

d_b = diameter of the steel bar

Δ_{AB} = distance between two gauges A and B

E_S = modulus of elasticity of the steel bar

A_b = cross-section area of the steel bar

$\varepsilon_B, \varepsilon_A$ = strains at gauge A and gauge B

The bond stress distributions of beam B1 are shown in Fig. 4.4. As expected from the strain variation, the average local bond stresses are higher at the ends of the test bar at all load levels due to the increased build up of steel tension at the bar ends. At failure, the average local bond stresses at the ends of the test bar are 1572 psi (10.8 MPa) and 1534 psi (10.6 MPa) which resulted in a brittle longitudinal splitting failure.

4.1.1.2 Response of Beam B2

Fig. 4.1 also shows the load-deflection response of beam B2 ("bottom-cast"). Beam B2 undergoes a small deflection, under application of the first load increments. As the load is increased to 13.1 kips (58.3 kN), two flexural cracks occurred close to the centre of the beam. Afterwards, cracks continued to form and at a load of 23.4 kips (104 kN) flexural cracks appeared at the ends of the test bar. Beam B2 continued deflecting slowly under load, as more fine cracks continued developing and the previous cracks progressed towards the compression zone.

At a load of 34.0 kips (151.2 kN), an additional flexural crack formed approximately 10 in (25.4 cm) from one end of the test bar. It transformed into a flexural shear crack with signs of splitting on the side of the beam near the end of the bar, as illustrated in Fig. 4.2a. At this stage most cracks attained a width of 0.006 in (0.15 mm). After the next load stage of 36.6 kips (162.8 kN), the following observations were made indicating a near failure by bond splitting.

(i) An increase in deflection shown in the P-Δ curve of Fig. 4.1.

(ii) A large widening of the flexural shear crack at one end of the test bar. The recorded width is 0.125 in (3.2 mm).

(iii) A formation of longitudinal splitting cracks 0.03 in (0.8 mm) wide at both ends of the test bar with lengths of 7 in (17.8 cm).

A very large deflection is observed in the P-Δ curve with further increase of the load. Beam B2 reached an ultimate capacity of 39.0 kips (173.5 kN). Then the load dropped off slightly and deflection continued until failure occurred at a maximum deflection of 0.60 in (15.2 mm). After failure, the major shear crack was 0.22 in (5.6 mm) wide. The longitudinal splitting cracks on both ends of the test bar, had propagated to a length of 10 in (25.4 cm) approximately, with a width of 0.22 in (5.6 mm). This is shown in Fig. 4.2b.

As observed in the load-deflection curves beam B2 reaches only 82% of the ACI yield prediction. The variation of tensile strain presented in Fig. 4.5 also shows that the No. 8 test bar (25.4 mm) did not attain its yield strain of 1950 micro in/in. The maximum strain developed at the centre was 1485 micro in/in which represents 76% of the yield strain. The tensile strain variations at all load stages resemble a parabolic curve with zero strain at the ends of the bar and a peak strain at the centre. Before cracking, the variation was flat and after cracking, the peak strain at centre increased with the load. As observed with beam B1, the strains at the ends of the test bar exceed the predicted strain values. In addition, the strains along the continuous No. 6 (19.1 mm) bars also indicate a yielding at the cut-off locations without yielding at the centre of the beam (see Appendix C). Average local bond stresses are also obtained for beam B2 and are shown in Fig. 4.6. Their maximum values at failure, attained at the ends of the test bar are 1600 psi (11 MPa) and 1580 psi (10.9 MPa).

4.1.1.3 Comparison of Beam B1 and B2

The behaviour of beams B1 and B2 is very similar in the sequence of physical distresses associated with loss of bond strength. However, beam B2 showed signs of visible cracks at a load of 13.1 kips (58.3 kN) while beam B1 cracked at a load of 10.4 kips (46.3 kN). This indicates a higher tensile strength for the "bottom-cast" concrete. In its response to the applied load, beam B2 exhibited more rigidity than its companion beam B1, as shown in Fig. 4.1. Beam B1 failed at 37.0 kips (164.6 kN) in a very brittle way while beam B2 showed more ductility after reaching its ultimate capacity of 39.0 kips (173.5 kN). Although the difference in ultimate capacities is only 5%, the difference in ductility is quite significant. The observed maximum deflections were respectively 0.444 in (11.3 mm) for beam B1 and 0.60 in (15.2 mm) for beam B2.

The cracking pattern of both beams after failure, shown in Figs. 4.2a and 4.2b, indicates more flexural cracks for beam B2 than for beam B1 providing further evidence of the better bond performance of the "bottom-cast" specimen.

Also the splitting and major shear cracks at failure were 0.22 in (5.6 mm) wide for beam B2 and 0.25 in (6.4 mm) wide for beam B1. When the tensile strain curves along the test bars of both beams are compared at the same load level, higher strains are observed for beam B1 at lower load levels. This may be attributed to the lower tensile strength of the "top-cast" concrete in beam B1. The tensile strain variations of both beams at respective ultimate strengths, are compared in Fig. 4.7. Beam B2 shows slightly higher strains than its companion beam B1. The bond stress distributions of both beams, are also presented in Fig. 4.8 indicating that beam B2 developed higher bond stresses than beam B1 at the ends of the test bar.

4.1.2 Beams B3 and B4. Embedment Length of 36 in (91.4 cm)

4.1.2.1 Response of Beam B3

After a load of 7.8 kips (34.7 kN) was reached, a slight change in the slope of the load-deflection curve of beam B3 shown in Fig. 4.9 is noticed. At a load of 10.4 kips (46.3 kN) a couple of hairline flexural cracks appeared in the central region of the beam. They were followed later, at a load of 20.9 kips (93 kN), by additional flexural cracks at both ends of the test bar. At the same time, most cracks widened and progressed towards the top of the beam at a small inclination. At a load of 31.3 kips (139.2 kN), the average crack width was 0.006 in (0.25 mm) except for the one close to the cut-off locations that had a width of 0.01 in (0.25 mm).

An additional flexural crack appeared at a load of 34 kips (151.2 kN), approximately 12 in (30.5 cm) from one end of the test bar and was accompanied by some longitudinal splitting cracks on the bottom face of the beam. This flexural crack transformed into a major shear crack at the following load increment of 36.6 kips (162.8 kN), as it formed with previous cracks a critical region of "debonding action" at one end of the test specimen. The maximum widths of cracks were observed in that region and averaged 0.02 in (0.5 mm) for both longitudinal splitting and major shear cracks. These cracks widened to a width of 0.19 in (4.8 mm), as the beam attained a maximum load capacity of 40 kips (177.9 kN) and failed abruptly with a drop in load. The cracking pattern at failure, illustrated in Figs. 4.10a and 4.10b, shows a length of splitting cracks of 10 in (25.4 cm) and 12 in (30.5 cm) at the ends of the test bar. The numbers written on the sides of the beams in Fig. 4.10 indicate the load stage number.

As illustrated in the load-deflection curve of beam B3, it did not reach the ACI yield prediction of 47.0 kips (209.1 kN). It attained only 85% of this value at a maximum observed deflection of 0.486 in (12.3 mm).

The variations of tensile strain along the test bar of beam B3 are shown in Fig. 4.11, at selected load levels. The increase in strains, as load is applied, is readily noticed and also the importance of cracking pattern on the magnitude of the tensile strains. The increase in tensile strains at the ends of the test bar is also observed at a load of 36.6 kips (162.8 kN), corresponding to the appearance of longitudinal splitting cracks. At failure, beam B3 reaches a maximum tensile strain, at the centre of the test bar, of 1750 micro in/in which is 90% of the yield strain.

Average local bond stresses are derived for the same load stages and their distributions are shown in Fig. 4.12, where very high bond stresses are noticed at the ends of the test bar when failure is approached. The maximum bond stresses calculated were 1296 psi (8.9 MPa) and 1227 psi

(8.5 MPa). Finally, the tensile strains of the adjacent No. 6 (19.1 mm) bars, presented in Appendix C, indicate that yielding only occurred at the cut-off locations.

4.1.2.2 Response of Beam B4

The load-deflection readings of beam B4 are also plotted in Fig. 4.9. Beam B4 showed the first sign of visible cracking around the centre at a load of 13.1 kips (58.3 kN) accompanied by a drop in stiffness. At a load of 23.5 kips (104.5 kN), the first flexural cracks occurred at both ends of the test bar. Within the next four load increments, a lot of fine flexural cracks developed and moved towards the neutral axis, as illustrated by Fig. 4.10a. With further increase of the load to 36.6 kips (162.8 kN), hairline splitting cracks, 3 in (7.6 cm) long, appeared along the length of the test bar. As the load was increased, the flexural cracks widened and extended towards the compression zone. At a load of 41.8 kips (185.9 kN) the cracks at the cut-off locations also widened and transformed into major shear cracks, as they progressed towards the top of the beam. Side splitting cracks were also noticed near the ends of the test bar. The largest crack width measured at a load of 45.7 kips (203.3 kN), was 0.09 in (2.3 mm) along one of the major shear cracks. At the same time, the splitting propagated along the length of the No. 8 (25.4 mm) bar between transverse flexural cracks. Also a considerable increase in deflection was observed at this stage and can be seen in the load-deflection curve. A small increment of load to 47.0 kips (209.1 kN) resulted in increased deflections with the widening of all cracks.

Before failure occurred, beam B4 showed a fairly ductile behaviour with a lot of cracking and reached a maximum estimated deflection of 0.656 in (16.7 mm). An examination of the bottom face at failure, indicated that splitting cracks propagated along the length of the test bar and reached a length of 7 in (17.8 cm) at one end, as can be seen in Fig. 4.10b. The major shear cracks had a maximum width of 0.13 in (3.3 mm). The splitting cracks were finer and about 0.09 in (2.3 mm) wide.

Fig. 4.9 shows that the deflections of beam B4 are very close to the predicted values at the early load stages up to 23.5 kips (104.5 kN) approximately. Afterwards, beam B4 loses stiffness until if failed at 47.0 kips (209.1 kN), when it reached the ACI yield prediction. In Fig. 4.13 it is easily observed how the tensile strains along the length of the test bar are rapidly increasing with loads, especially at the ends where they always exceed the theoretical strain values. The maximum strain reached at centre is 1965 micro in/in at failure, and also indicates that beam B4 reached the yield strain of 1950 micro in/in. The distribution of bond stresses shown in Fig. 4.14, is again derived from the strain variation. As for the previous beams, the maximum values of the average bond stress are attained near the ends of the test bar. For beam B4, they are 1553 psi (10.7 MPa) and 1476 psi (10.2 MPa) at failure. As for beam B3, yielding of the No. 6 (19.1 mm) bars only occurred at the cut-off locations. However, the No. 6 bars reached 95 percent of their yield strain at the beam centreline.

4.1.2.3 Comparison of Beam B3 and Beam B4

From the load-deflection plots in Fig. 4.9 a few comparisons can be made.

(i) The "bottom-cast" concrete of beam B4 has a higher tensile strength than the "top-cast" concrete of beam B3, as indicated by the larger cracking load for beam B4.

(ii) Beam B4 shows higher stiffness than beam B3 during the loading history with a maximum difference of 25% at the load of 40 kips (177.9 kN).

(iii) Beam B4 exhibits greater ductility than beam B3, having maximum measured deflections of 6.656 in (16.7 mm) and 0.486 in (12.3 mm) respectively.

(iv) Beam B4 failed at a load of 47.0 kips (209.1 kN) while beam B3 failed at a load of 40 kips (177.9 kN), resulting in an 18% strength increase for the "bottom-cast" specimen.

The better bond performance of beam B4 can also be observed in the cracking pattern shown in Figs. 4.10a and 4.10b. More fine flexural cracks are developed in beam B4. Also the splitting cracks and the major shear cracks are not as wide. Tensile strains are compared at different load levels and show less strains in the test bar of beam B4 due to the difference in tensile strengths. Finally the compared tensile strains and bond stresses at failure are presented in Fig. 4.15 and Fig. 4.16 respectively. Tensile strains at failure are higher for beam B4. The strains at the centre of each beam at failure load were 1965 micro in/in for beam B4 and 1750 micro in/in for beam B3. Average local bond stresses, developed at the ends of the test bar at failure, are also higher for beam B4.

4.1.3 Beams B5 and B6. Embedment Length of 40 in (101.6 cm)

4.1.3.1 Response of Beam B5

After the appearance of a few cracks in the central region of the beam at a load of 10.4 kips (46.3 kN), beam B5 showed a decrease in its flexural rigidity as more cracks formed and elongated. The cracks propagated to the ends of the test bar at a load of 23.5 kips (104.5 kN), as illustrated in the load-deflection curve shown in Fig. 4.17. At the load of 31.3 kips (139.2 kN), some flexural cracks at the ends of the beam inclined towards the centre-line. At a load of 34.0 kips (151.2 kN), fine splitting cracks initiated from flexural cracking at the cut-offs. The flexural cracks showed a maximum width of 0.006 in (0.15 mm) at this stage.

At a load of 40 kips (177.9 kN) a wide flexural shear crack rapidly developed approximately 16 in (40.6 cm) from one end of the test bar. It became a major shear crack at the load of 43.1 kips (191.7 kN), and formed a definite "debonding region" at this end where longitudinal splitting cracks were larger and averaged 0.04 in (1 mm) in width. The beam reached a peak load of 45.0 kips (200.2 kN), as observed in the P-Δ curve; then, the load dropped off slightly and, after an increase in deflection under constant load, the specimen failed abruptly. The maximum crack width was noticed at the major flexural shear crack and the splitting cracks close to it. When measured, these cracks averaged a width of 0.06 in (1.5 mm) while others were approximately 0.008 in (2 mm) wide. Figs. 4.18a and 4.18b illustrate the cracking pattern of beam B5, which exhibited a maximum deflection of 0.588 in (14.9 mm). The deflections of beam B5 started deviating considerably from the theoretical values after a load of 23.5 kips

(104.5 kN), and continued the same way until failure where it attained 96% of the ACI yield prediction.

The tensile strain readings obtained for the test bar are plotted, at selected load stages, in Fig. 4.19. The same general shape of the distributions is also found for beam B5. The maximum strain at the centre, at failure is 1865 micro in/in. This represents 96% of the yield strain which is exactly the same percentage obtained from the comparison of ultimate capacities. The maximum calculated bond stresses were 1114 psi (7.7 MPa) and 1170 psi (8.1 MPa) at the ends of the test bar (see Fig. 4.20). When the tensile strains of the No. 6 (19.1 mm) bars are examined (see Appendix C), they do not show any yielding at failure either at the cut-off location nor at the centre of the beam.

4.1.3.2 Response of Beam B6

Flexural cracking for beam B6 occurred at a load of 13.1 kips (58.3 kN) with cracks on both sides of the centre-line. The cracking load is displayed in Fig. 4.17 with the cracking pattern of beam B6 illustrated in Figs. 4.18a and 4.18b. Thereafter, new cracks formed and all progressed slowly towards the compression zone. At a load of 26.1 kips (116.1 kN), many fine flexural cracks were observed on the tension side. Flexural cracks appeared at the cut-offs at a load of 28.7 kips (127.7 kN) and started sloping at the next load stage to become flexural shear cracks. Further increments of the load up to 36.6 kips (162.8 kN) caused some fine splitting cracks, 2 in (5.1 cm) long, at both ends of the test bar. These cracks propagated with subsequent increases of the load to reach 6 in (15.2 cm) each, at a load of 40.5 kips (180.2 kN) where they were 0.004 in (1 mm) wide. The maximum flexural shear crack at one of the cut-off locations measured 0.007 in (1.8 mm). The propagation continued until a major shear crack suddenly appeared 16 in (40.6 cm) from the end of the test bar, at a load of 45.7 kips (203.3 kN), as shown in Fig. 4.18a.

Further increases in load led to increasing deflections with a maximum load occurring at 49.5 kips (220.2 kN) and at a deflection of 0.792 in (20.1 mm). The resulting failure was ductile, as shown in Fig. 4.17, after two symmetrical flexural cracks close to the centre widened considerably indicating possible yielding. The average width of these two cracks was 0.06 in (15 mm) at failure. The longitudinal splitting cracks indicated a maximum width of 0.02 in (0.5 mm). Branson's equation predicts the pre-yielding response very well and ultimate capacity of beam B6 is 5% higher than the ACI yield prediction. The tensile strain variations shown in Fig. 4.21 indicate that yielding of the No. 8 (25.4 mm) bar had occurred at failure. Average local bond stresses derived from the tensile strain variations are presented in Fig. 4.22. The maximum bond stresses at the ends of the test bar are 1304 psi (9 MPa) and 1342 psi (9.3 MPa). Table C.2 in Appendix C indicates a yielding of the No. 6 (19.1 mm) bars only at the centre of the beam.

4.1.3.3 Comparison of Beam B5 and Beam B6

The load-deflection responses of the beams are first compared and show several important differences as indicated below:

(i) The "bottom-cast" concrete of beam B6 has a higher tensile strength than the "top-cast" concrete of beam B5. This is demonstrated by the higher cracking load observed for beam B6.

(ii) Beam B6 is stiffer than its companion beam B5 at all load levels.

(iii) The failure of beam B6 is more ductile than the corresponding failure of beam B5. At failure, beams B6 and B5 show respectively maximum deflections of 0.792 in (20.1 mm) and 0.588 in (14.9 mm).

(iv) Beam B6 attained a higher capacity than beam B5. They failed at 49.5 kips (220.2 kN) and 45 kips (200.2 kN) respectively, resulting in a difference of 10%.

The cracking patterns are compared in Fig. 4.18, and it is observed that beam B6 exhibited a larger number of smaller flexural cracks than beam B5. This is another indication of the better bond performance of beam B6. At failure, beam B6 developed a maximum tensile strain at the centre which was 8% higher than that of beam B5 (see Fig. 4.23). Finally average local bond stresses are compared in Fig. 4.24. Beam B6 indicated a maximum bond stress which was about 15-18% larger than the bond stresses calculated for beam B5.

4.2 Effect of Embedment Lengths on the Response

4.2.1 Comparison of Beams with Top-Cast Bars: B1, B3 and B5

The load-deflection curves of these beams are compared in Fig. 4.25. Some of the common characteristics are compared below:

(i) All of the "top-cast" beams cracked at the same load level.

(ii) All beams showed signs of splitting cracks at about the same load level.

(iii) All three beams did not reach the ACI predicted ultimate load.

Some of the differences in behaviour are compared below:

(i) The stiffness at all load levels increases as the embedment length increases.

(ii) Beam B5 with the largest embedment length displayed a more ductile failure than the failure displayed by beams B1 and B3.

(iii) The strength increases as the embedment length increases.

The cracking pattern of these three beams is shown in Figs. 4.26a and 4.26b. It can be seen that an increase in embedment length leads to a larger number of more closely spaced, finer flexural cracks. Thus an increase in embedment length leads to a more desirable cracking and bond behaviour resulting in larger stress being developed in the cut-off bar. The development of larger bar stresses is confirmed in Figs. 4.3, 4.11, 4.19 and 4.27. For example, beam B5 develops 7% higher stress than beam B3 and Beam B3 develops 22% higher stress than beam B1. However, as illustrated in Fig. 4.28, lower bond stresses are obtained at failure for beams with longer embedment lengths. Beam B5 has a maximum local bond stress of 1170 psi (8.1 MPa) compared to 1296 psi (8.9 MPa) for beam B3 and 1572 psi (10.8 MPa) for beam B1.

4.2.2 Comparison of Beams with Bottom-Cast Bars: B2, B4 and B6

When specimens B2, B4 and B6 are compared, the following significant differences are observed:

(i) As shown in the P-Δ curves of Fig. 4.29, the stiffness increases as the embedment length is increased.

(ii) Beam B6, B4 and B2 failed in the same ductile manner, but a significant difference is observed between the deflections reached at the maximum loads of B6, B4 and B2. They are respectively 0.792 in (20.1 mm), 0.656 in (16.7 mm) and 0.600 in (15.2 mm). The ductility therefore increases with increasing embedment lengths.

(iii) Beam B6 exceeds the ACI yield prediction of 47 kips (209.1 kN) by 5%, and beam B4 just reaches it while beam B2 attains only 83% of the predicted strength.

(iv) The cracking patterns illustrated in Figs. 4.30a and 4.30b indicate that a larger number of smaller cracks are formed in specimens with longer embedment lengths. This provides visual evidence of better bond behaviour as the embedment length is increased.

(v) The difference in tensile strains and obviously the tensile stresses is illustrated in Fig. 4.31. Beam B2 attains a maximum tensile strain at centre of 1485 micro in/in while beam B4 reaches the yield strain at 1965 micro in/in, and beam B6 exceeds the yield strain with a value of 2018 micro in/in.

(vi) The average local bond stresses shown in Fig. 4.32, indicate maximum values at the ends of the test bar of 1600 psi (11 MPa), 1553 psi (10.7 MPa) and 1342 psi (9.3 MPa) respectively for beams B2, B4 and B6. This indicates a decrease in bond stress with longer embedment lengths.

4.3 Summary of Experimental Results

Tables 4.1 and 4.2 summarize the basic experimental test results and can be easily referred to when comparisons are made to show the "top-bar" effect and the "embedment length" effect.

TABLE 4.1

SEQUENCE OF PHYSICAL DISTRESSES ASSOCIATED WITH BOND FAILURE

PHYSICAL DISTRESS		BEAM B1	BEAM B2	BEAM B3	BEAM B4	BEAM B5	BEAM B6
First Flexural Crack	kips (kN)	10.4 (46.3)	13.1 (58.3)	10.4 (46.3)	13.1 (58.3)	10.4 (46.3)	13.1 (58.3)
First Flexural Crack at Cut-Off	kips (kN)	20.9 (93.0)	23.5 (104.5)	20.9 (93.0)	23.5 (104.5)	23.5 (104.5)	28.7 (127.7)
First Splitting Crack	kips (kN)	36.6 (162.8)	36.6 (162.8)	34.0 (151.2)	36.6 (162.8)	34.0 (151.2)	36.6 (162.8)
Major Shear Crack	kips (kN)	37.0 (164.6)	39.0 (173.5)	36.6 (162.8)	41.8 (185.9)	43.1 (191.7)	45.7 (203.3)
Failure	kips (kN)	37.0 (164.6)	39.0 (173.5)	40.0 (177.9)	47.0 (209.1)	45.0 (200.2)	49.5 (220.2)

TABLE 4.2

BEAM TEST RESULTS

RESULTS		BEAM B1	BEAM B2	BEAM B3	BEAM B4	BEAM B5	BEAM B6
First Flexural Crack	kips (kN)	10.4 (46.3)	13.1 (58.3)	10.4 (46.3)	13.1 (58.3)	10.4 (46.3)	13.1 (58.3)
Maximum Deflection	in (mm)	0.444 (11.3)	0.600 (15.2)	0.486 (12.3)	0.656 (16.7)	0.588 (14.9)	0.792 (20.1)
Maximum Capacity	kips (kN)	37 (164.6)	39 (173.5)	40 (177.9)	47 (209.1)	45 (200.2)	49.5 (220.2)
Splitting Crack at Failure	in (mm)	0.25 (6.4)	0.22 (5.6)	0.13 (3.3)	0.09 (2.3)	0.06 (1.5)	0.02 (0.5)
Major Shear Crack at Failure	in (mm)	0.25 (6.4)	0.22 (5.6)	0.18 (4.6)	0.13 (3.3)	0.06 (1.5)	0.02 (0.5)
Type of Failure		Brittle	Ductile	Brittle	Ductile	Brittle	Ductile
Strain at Centre of #8 Bar at Failure	micro in/in	1430	1485	1750	1965	1865	2018
Local Bond Stress at Ends of #8 Bar at Failure	psi (MPa)	1572 10.8	1600 11.0	1296 8.9	1553 10.7	1114 7.7	1304 9.0
	psi (MPa)	1534 10.6	1580 10.9	1227 8.5	1476 10.2	1170 8.1	1342 9.3

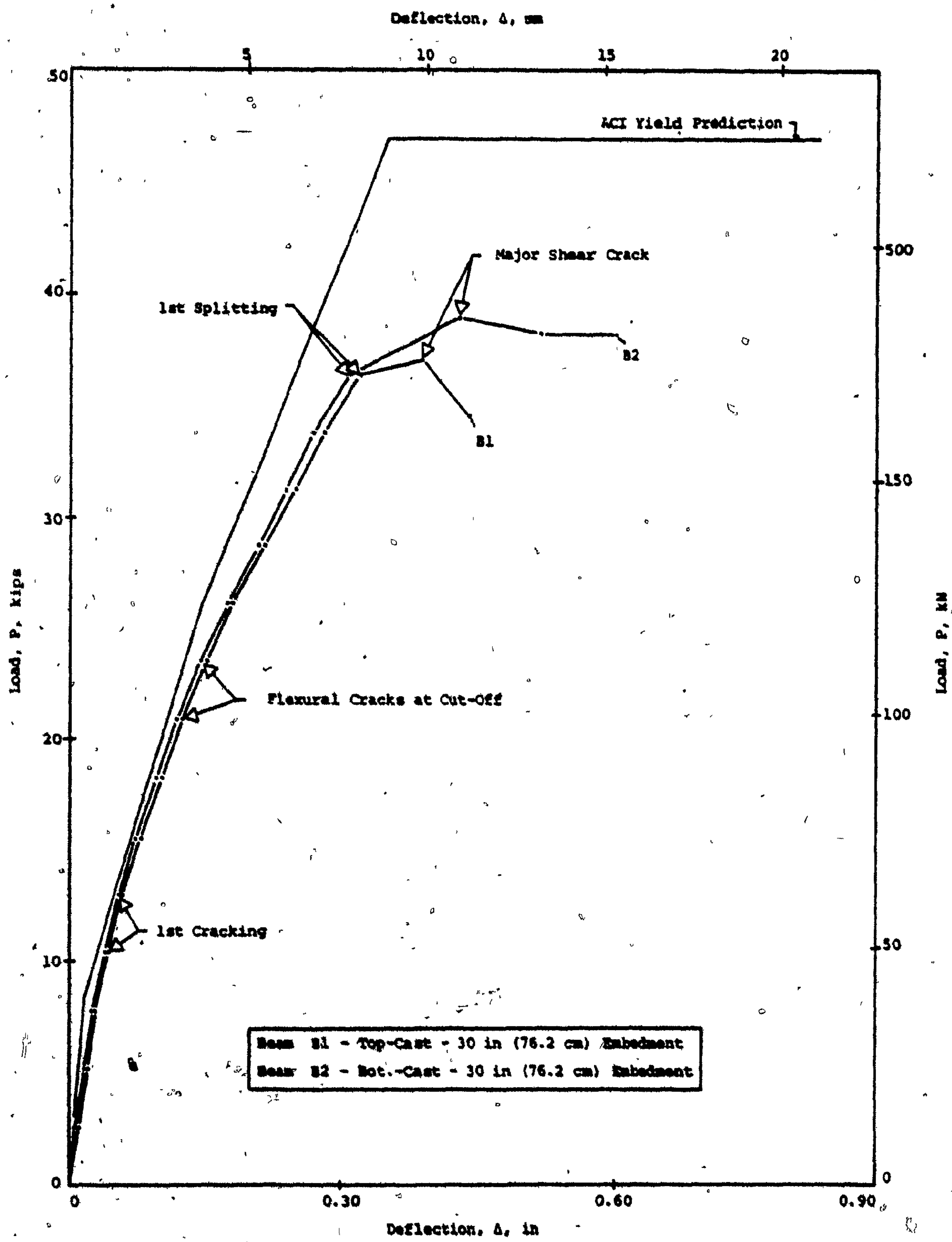

Fig. 4.1 Effect of Casting Position of Reinforcement on the Load-Deflection Responses of Beams B1 and B2

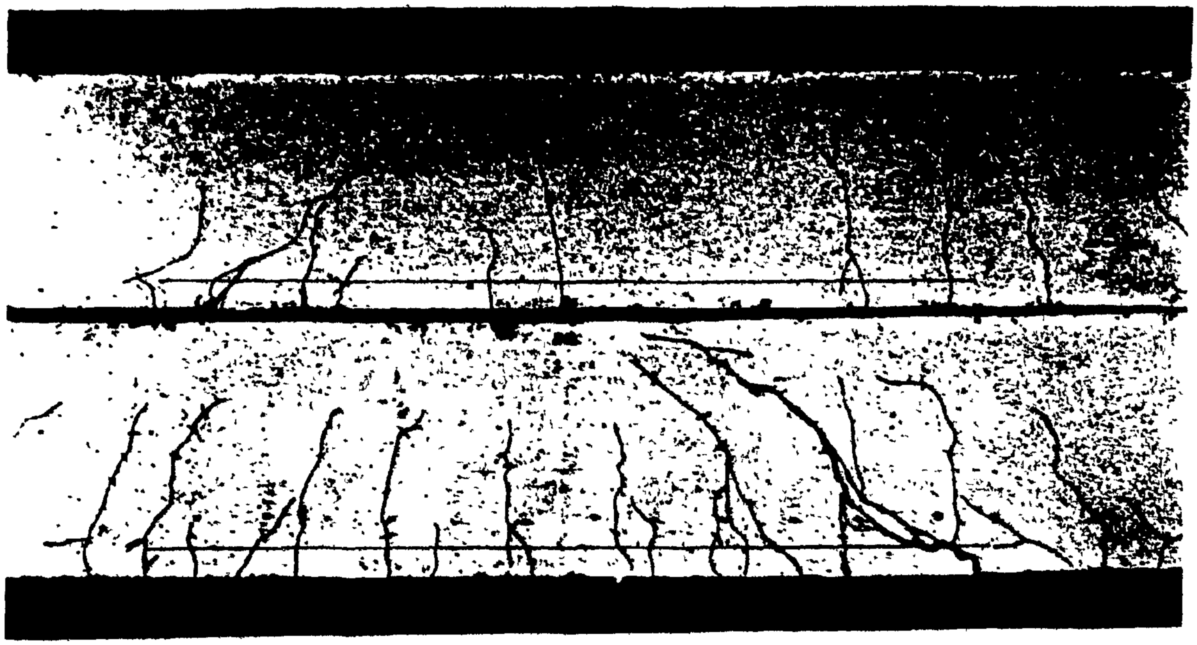

(a) Side Faces

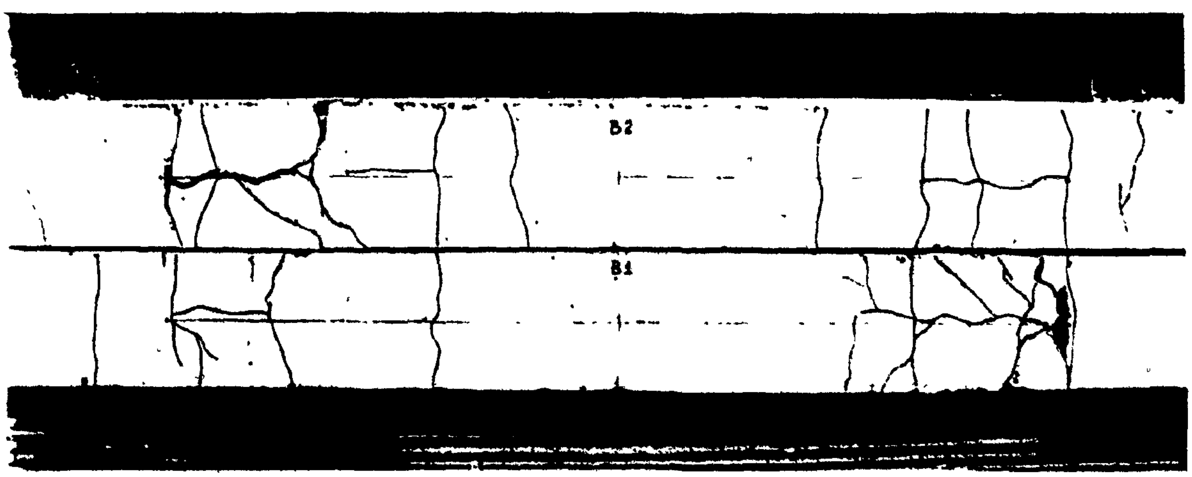

(b) Bottom Faces

Fig. 4.2 Effect of Casting Position of Reinforcement on the Crack Patterns of Beams B1 and B2

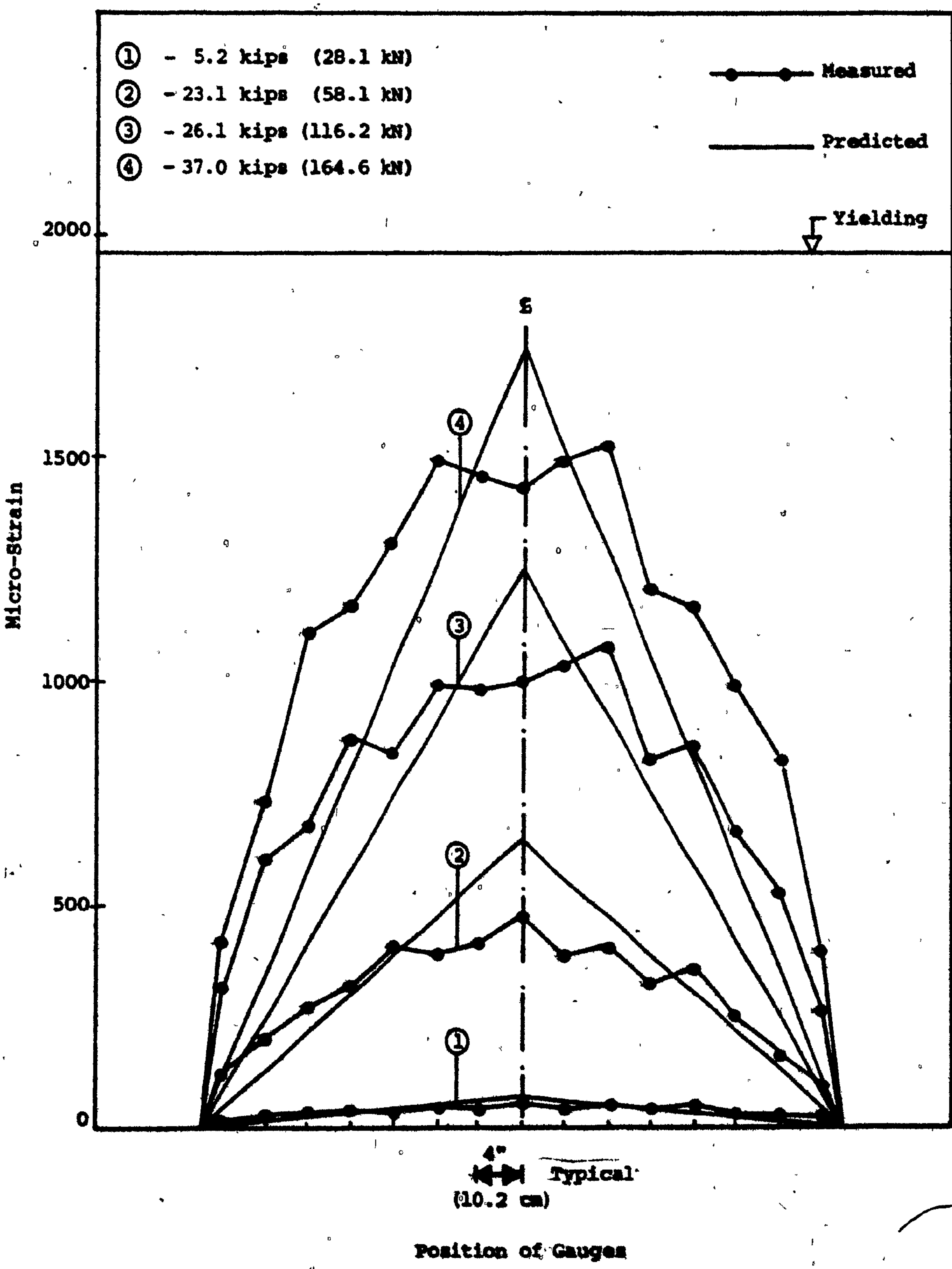

Fig. 4.3 Tensile Strains on #8 Bar - Beam B1

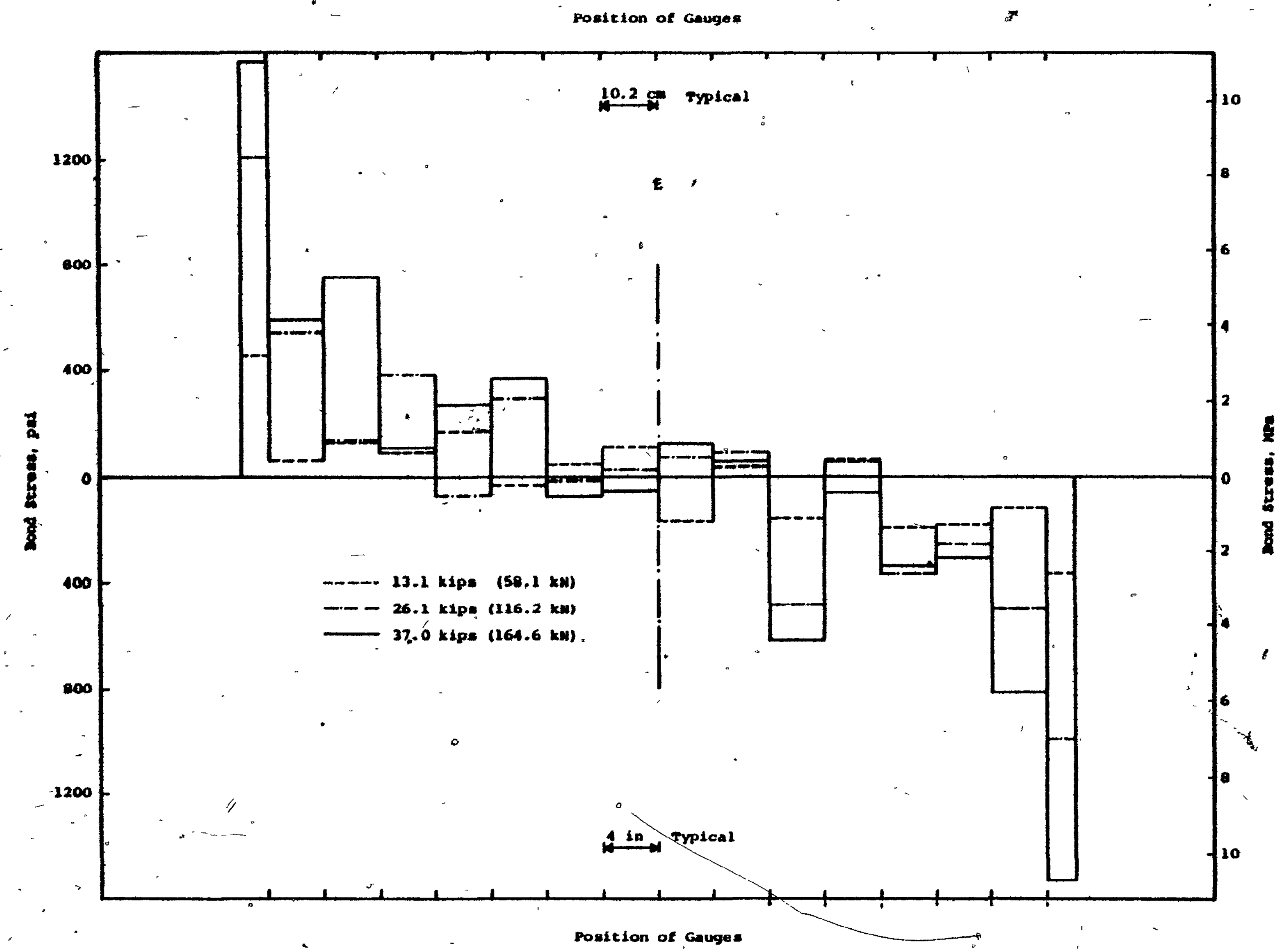

Fig. 4.4 Bond Stresses in #8 Bar - Beam B1

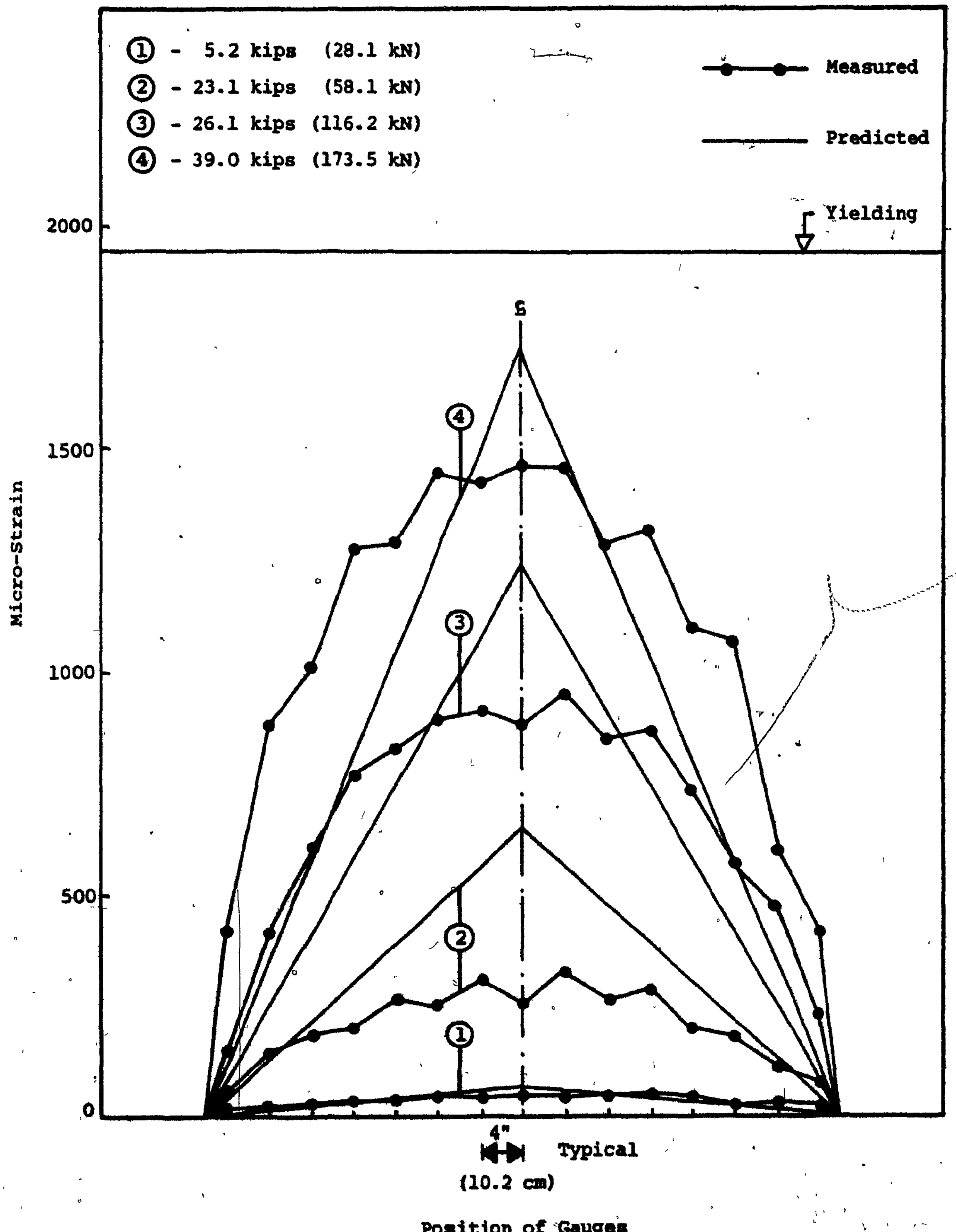

Fig. 4.5 Tensile Strains in #8 Bar - Beam B2

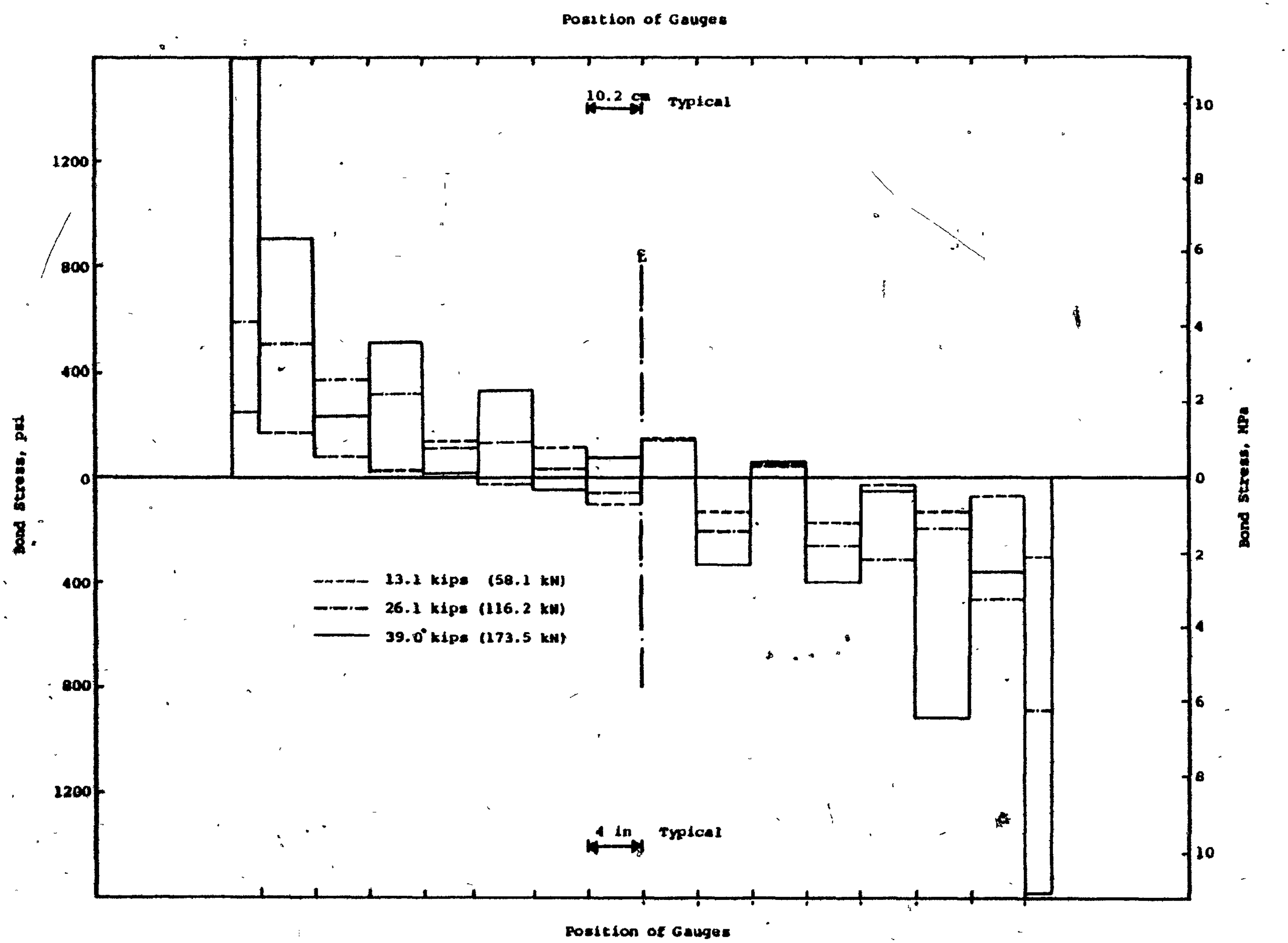

Fig. 4.6 Bond Stresses in #8 Bar - Beam B2

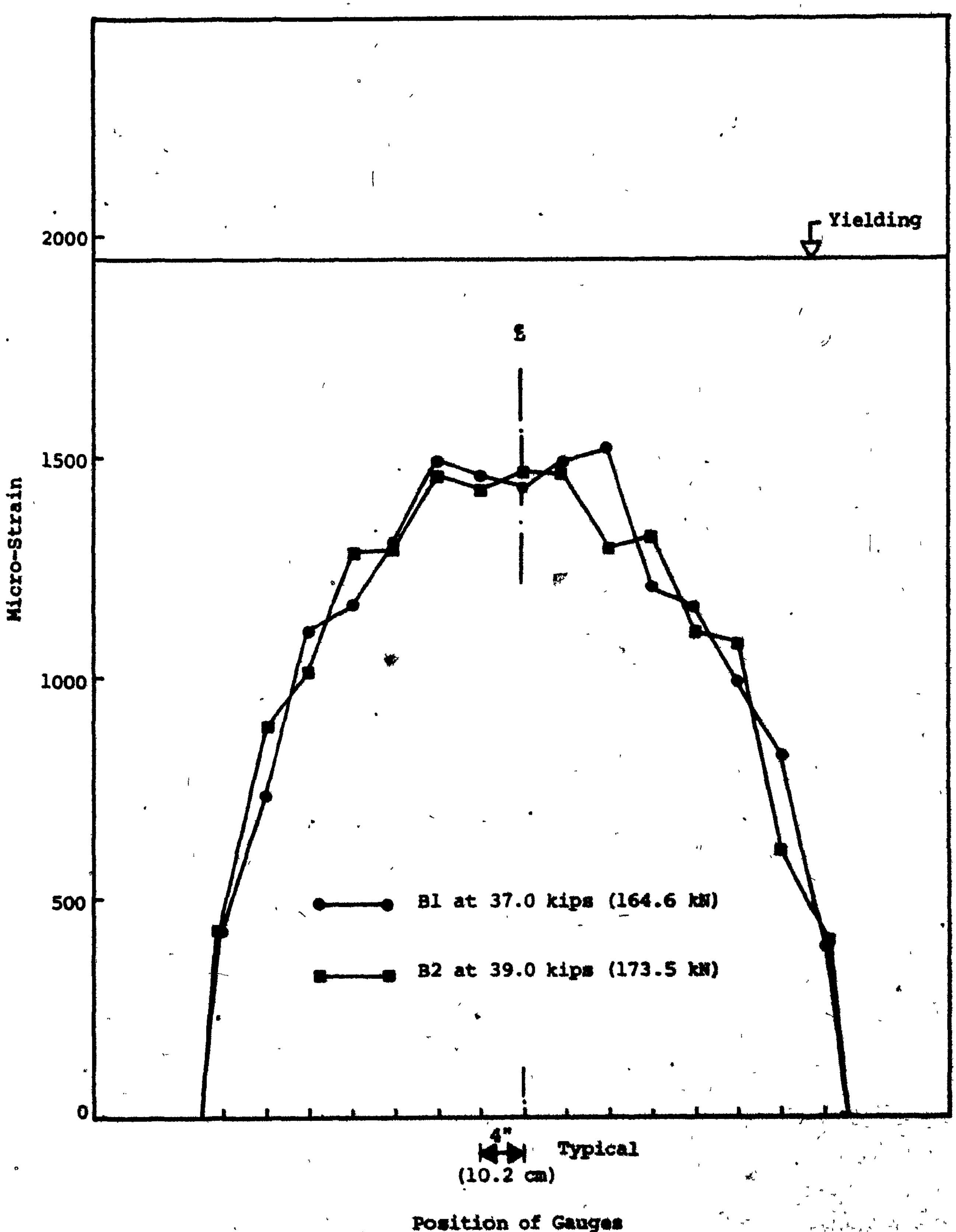

Fig. 4.7 Tensile Strains in #8 Bar at Failure - Beams B1 and B2

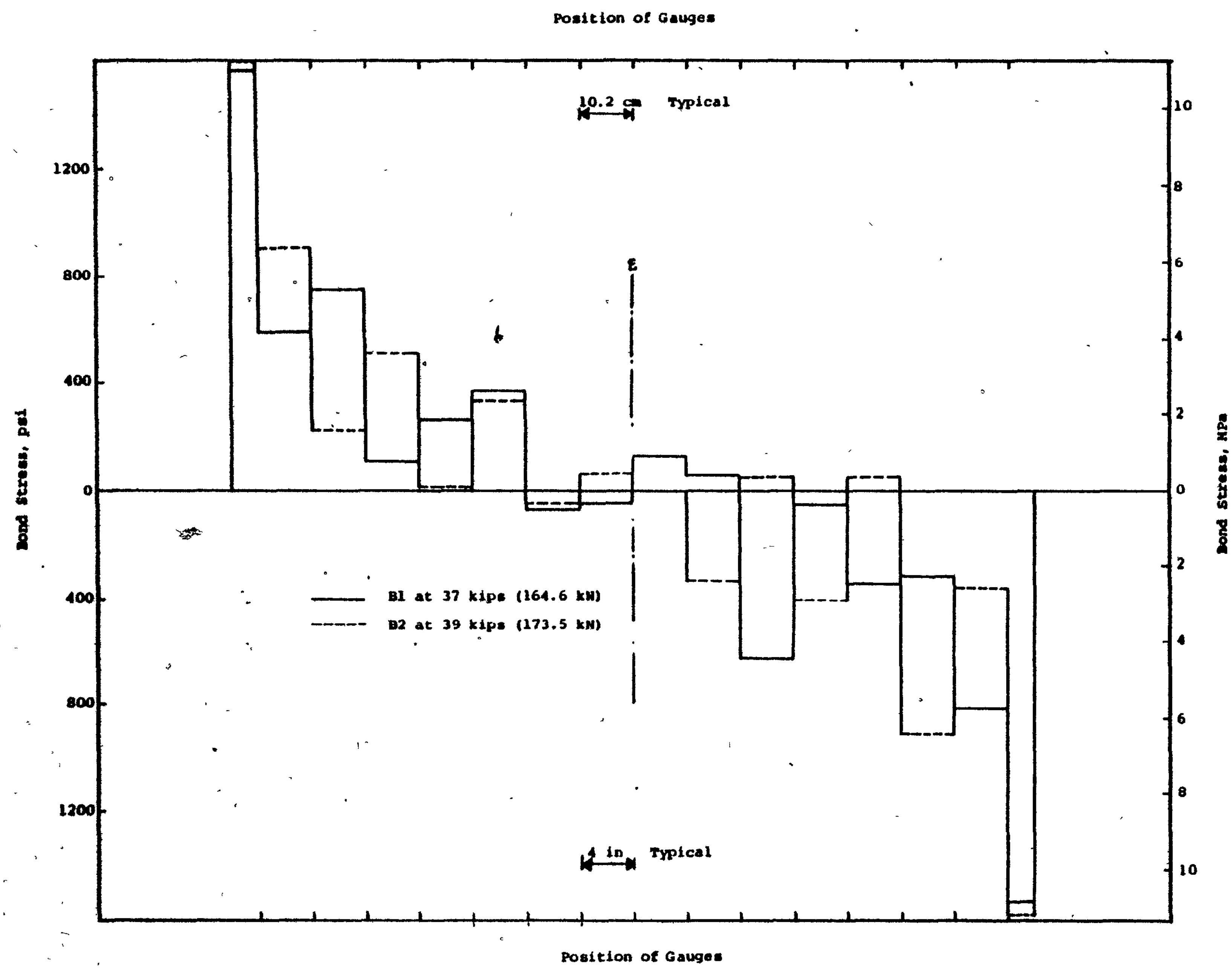

Fig. 4.8 Bond Stresses in #8 Bar at Failure - Beams B1 and B2

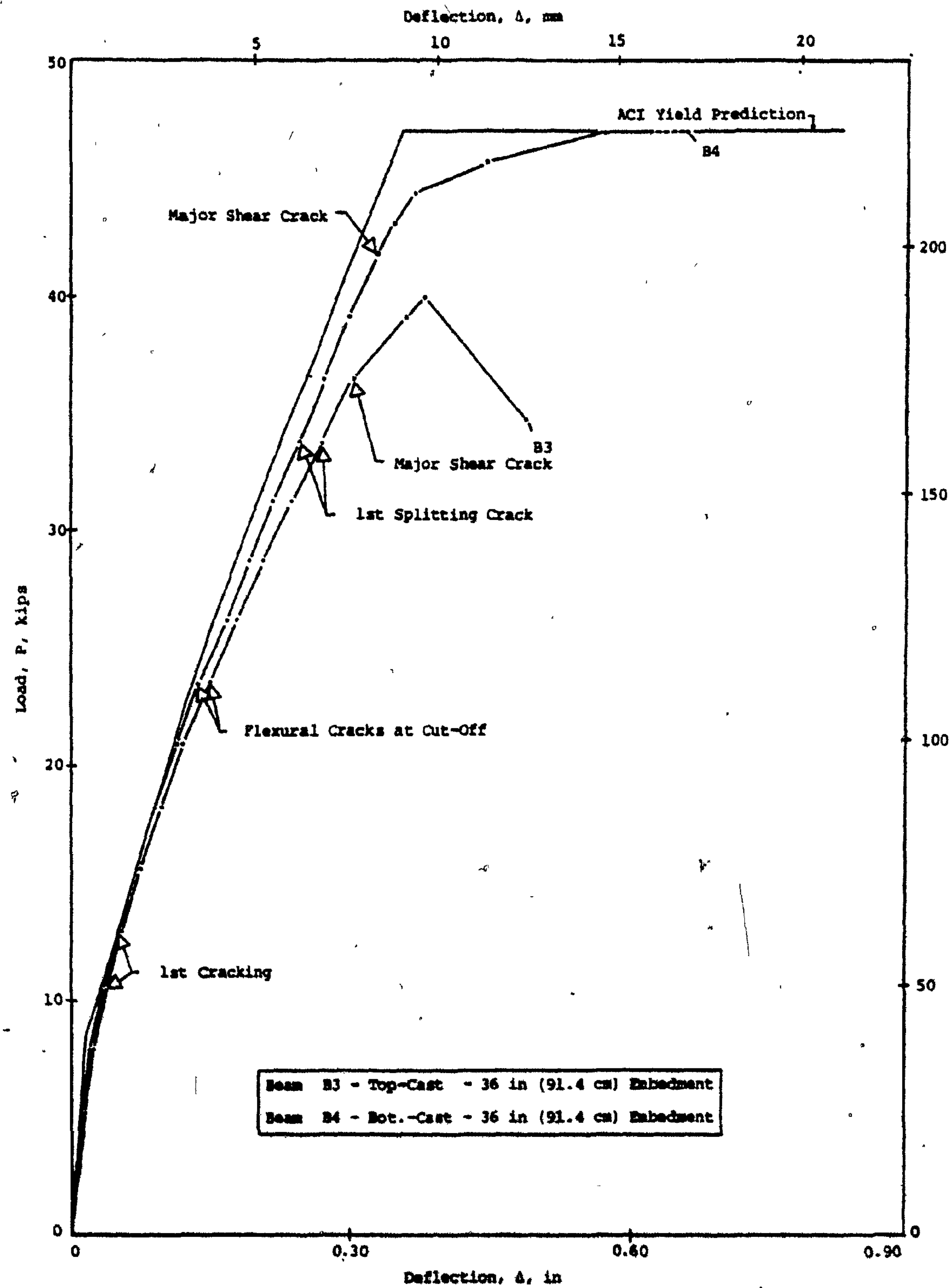

Fig. 4.9 Effect of Casting Position of Reinforcement on the Load-Deflection Responses of Beams B3 and B4

(a) Side Faces

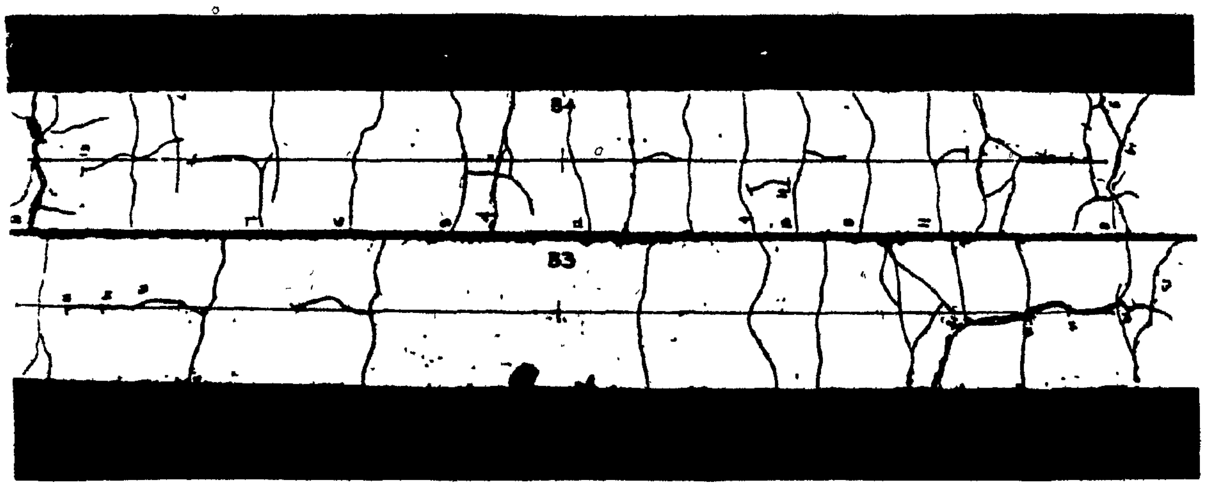

(b) Bottom Faces

Fig. 4.10 Effect of Casting Position of Reinforcement on the Crack Patterns of Beams B3 and B4

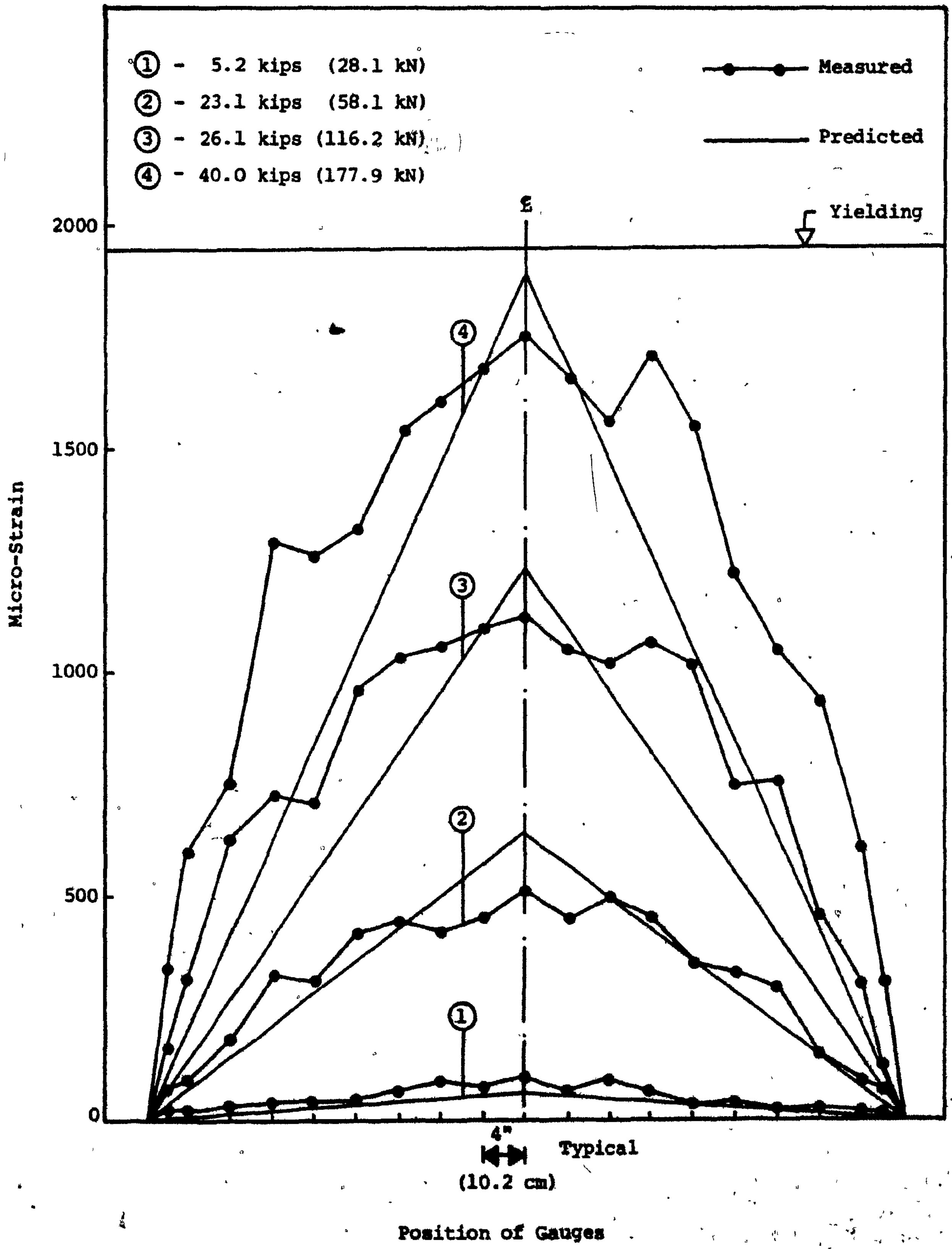

Fig. 4.11 Tensile Strains in #8 Bar - Beam B3

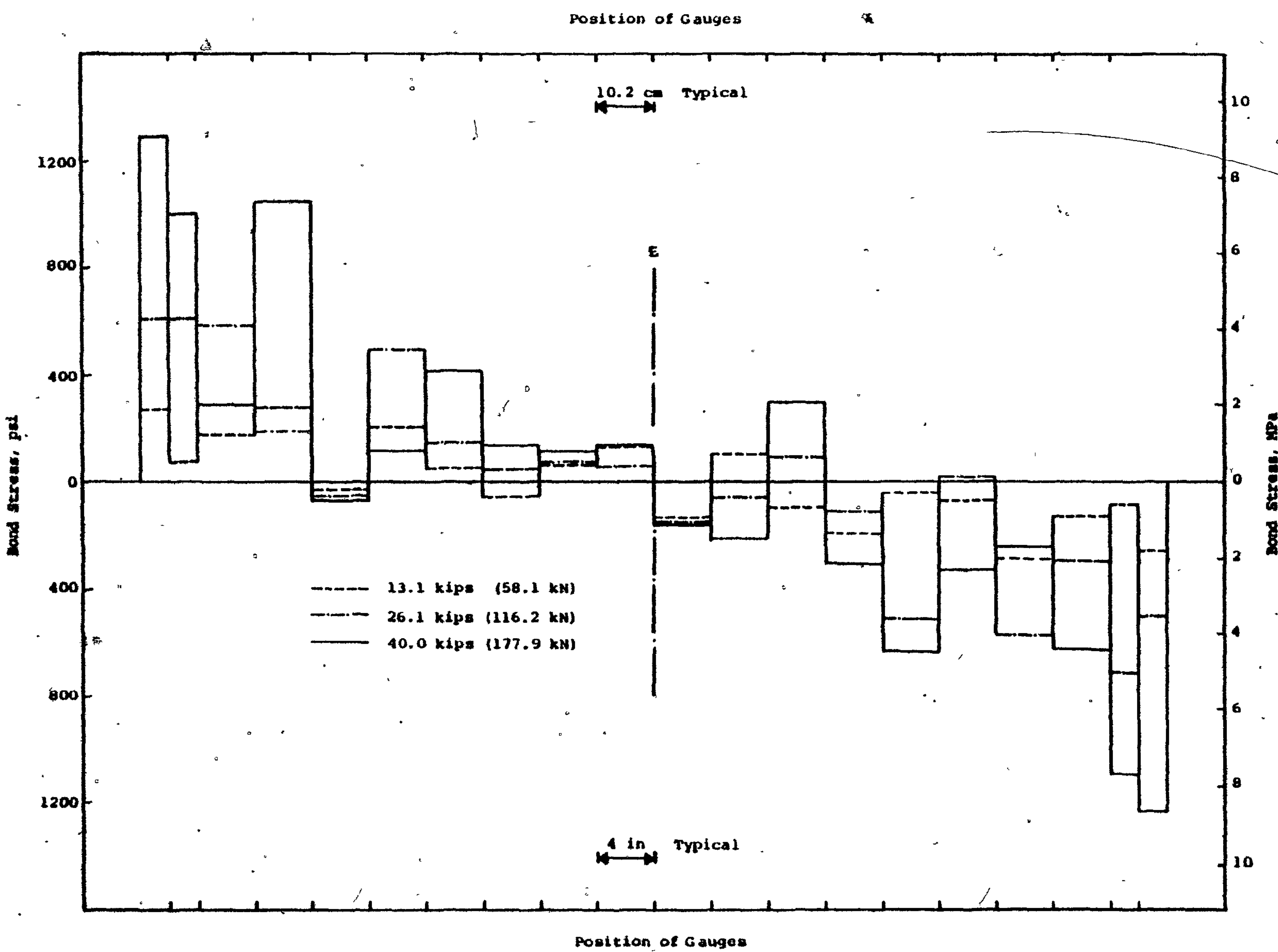

Fig. 4.12 Bond Stresses in #8 Bar - Beam B3

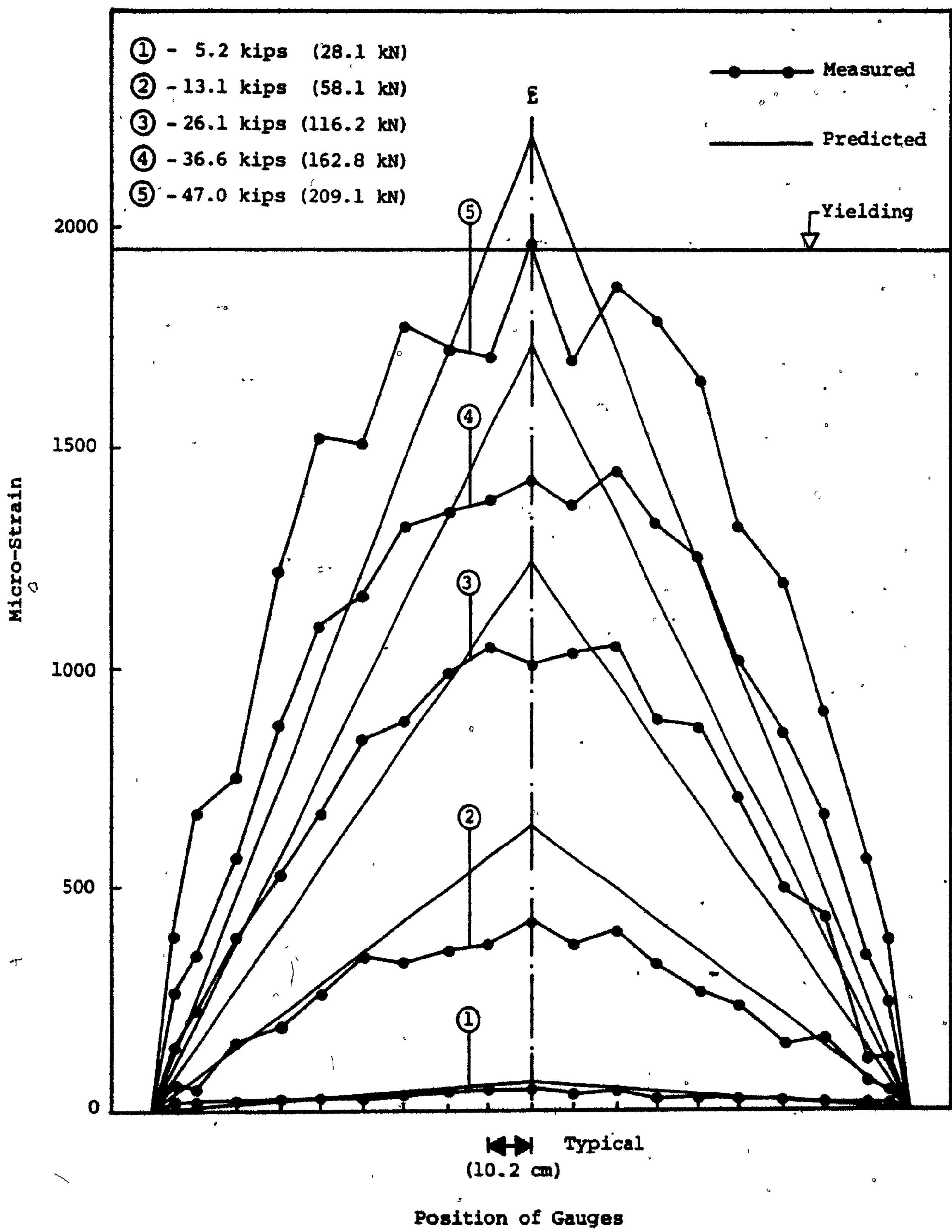

Fig. 4.13 Tensile Strains in #8 Bar - Beam B4

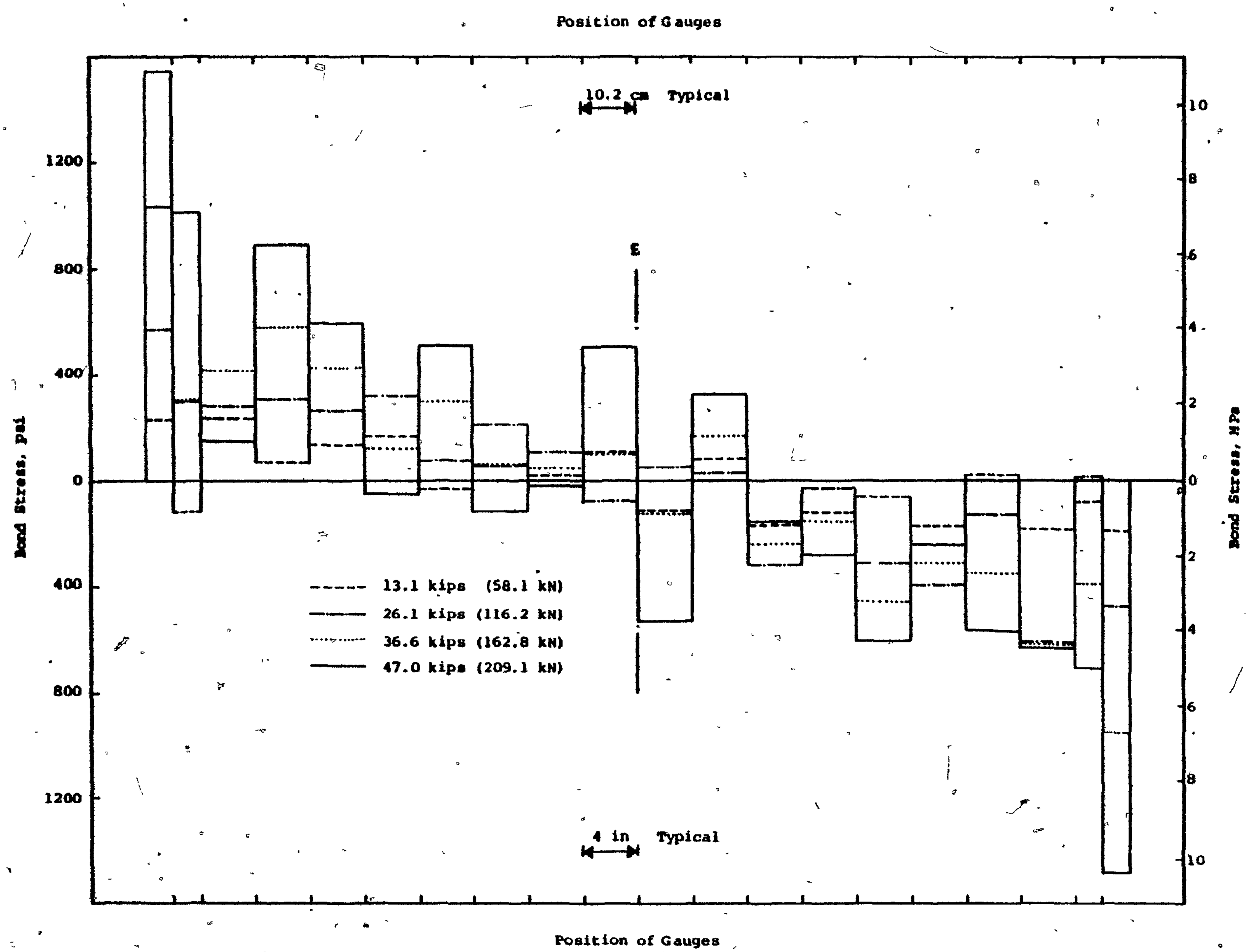

Fig. 4.14 Bond Stresses in #8 Bar - Beam B4

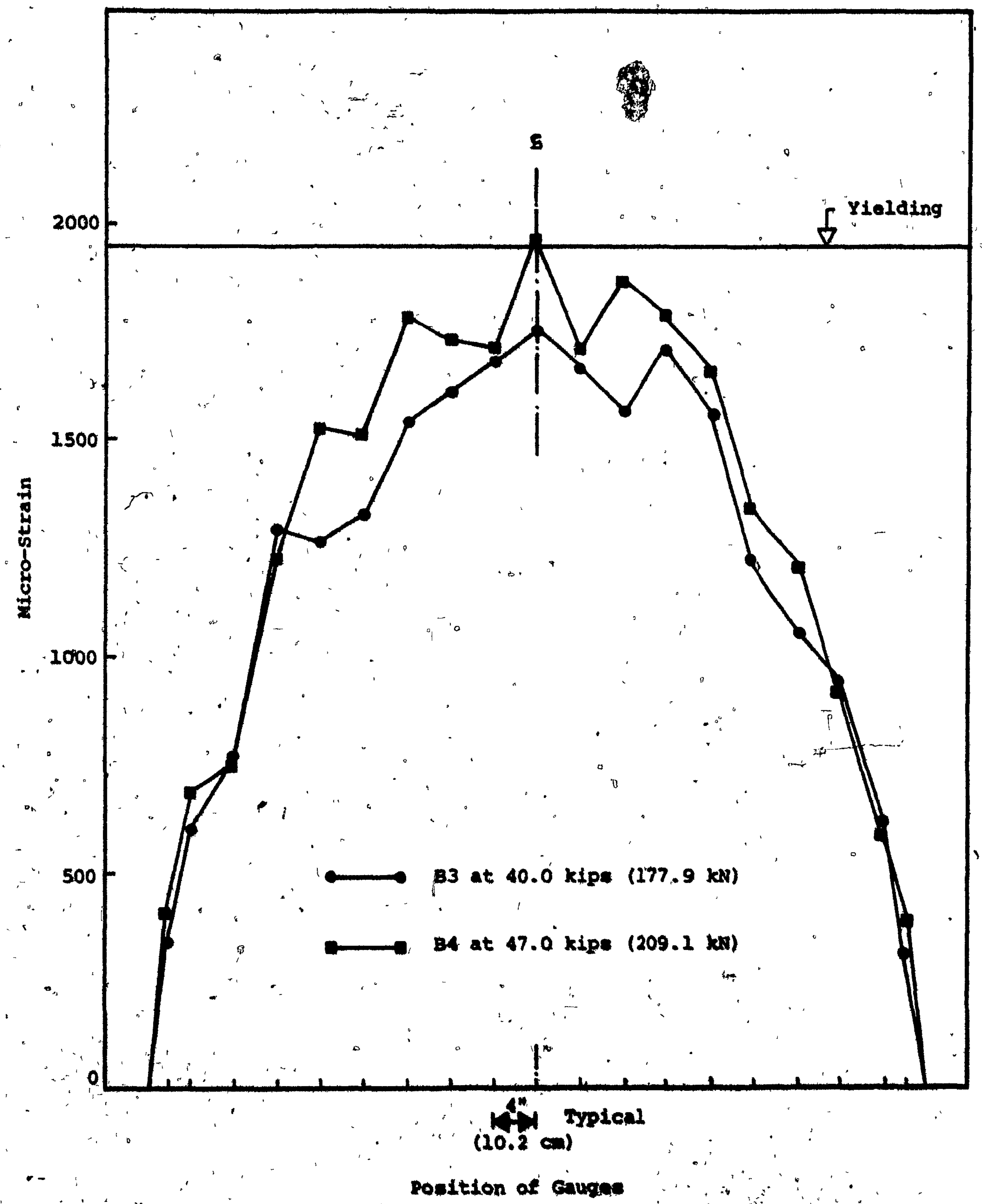

Fig. 4.15 Tensile Strains in #8 Bar at Failure - Beams B3 and B4

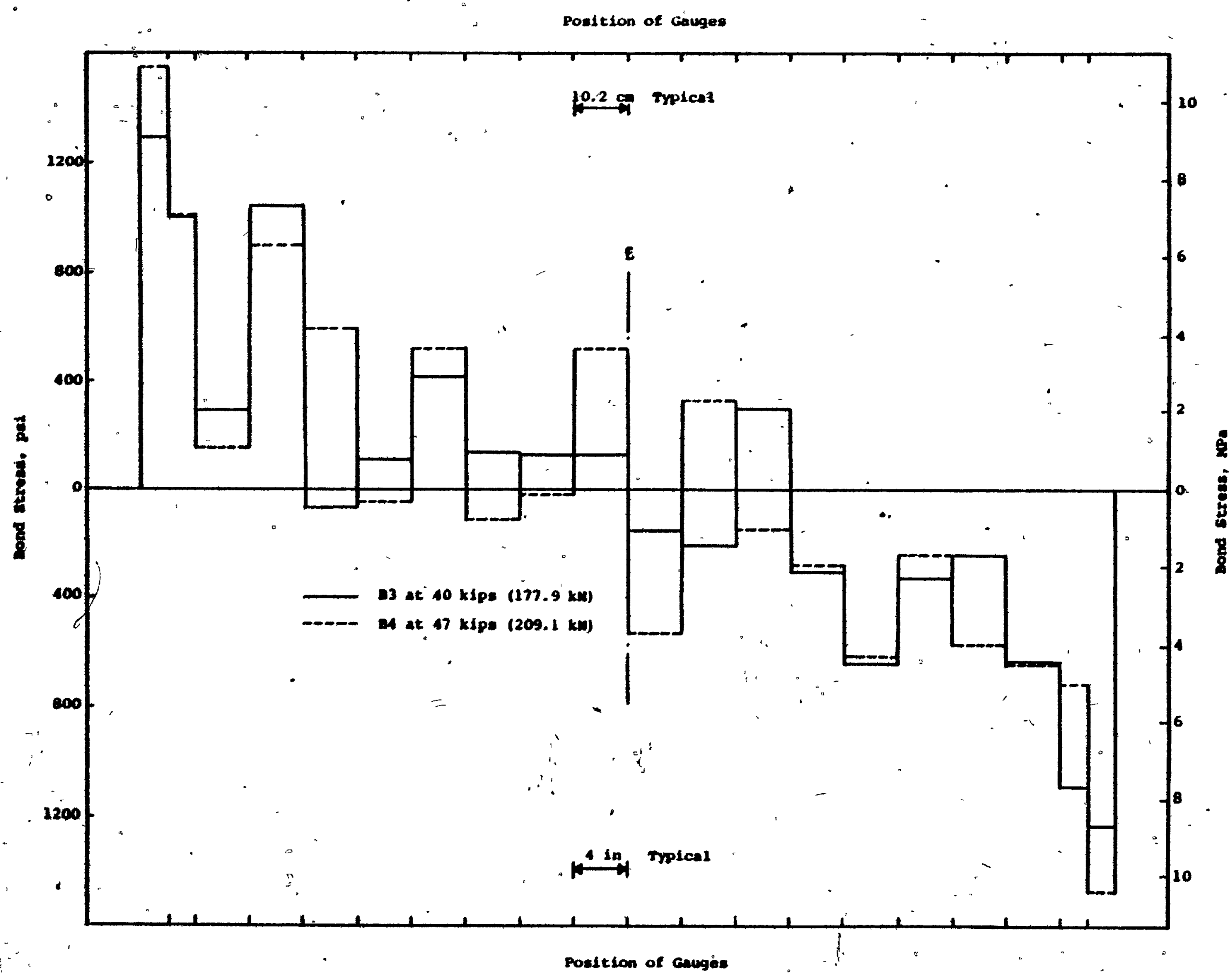

Fig. 4.16 Bond Stresses in #8 Bar at Failure - Beams B3 and B4

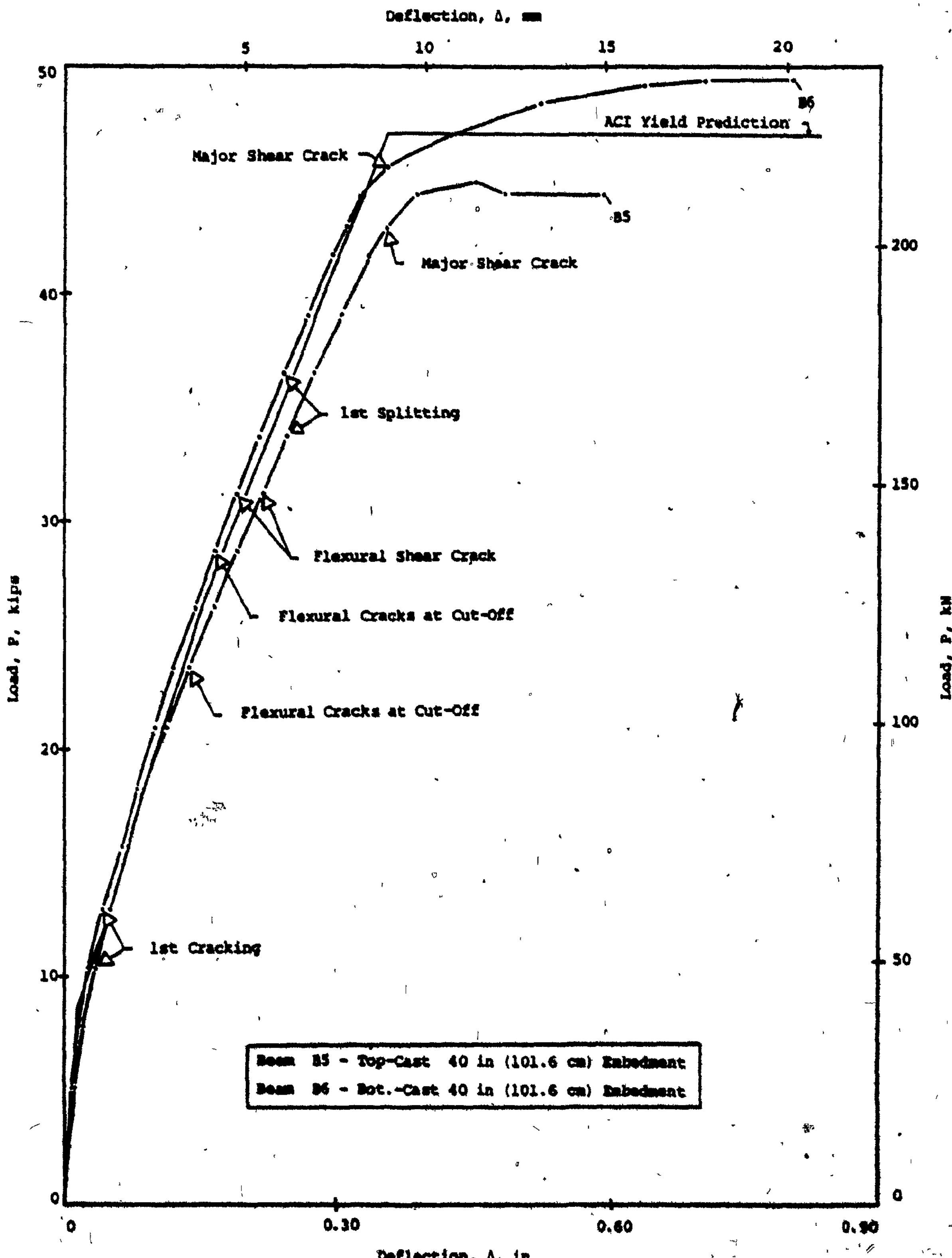

Fig. 4.17 **Effect of Casting Position of Reinforcement on the Load-Deflection Responses of Beams B5 and B6**

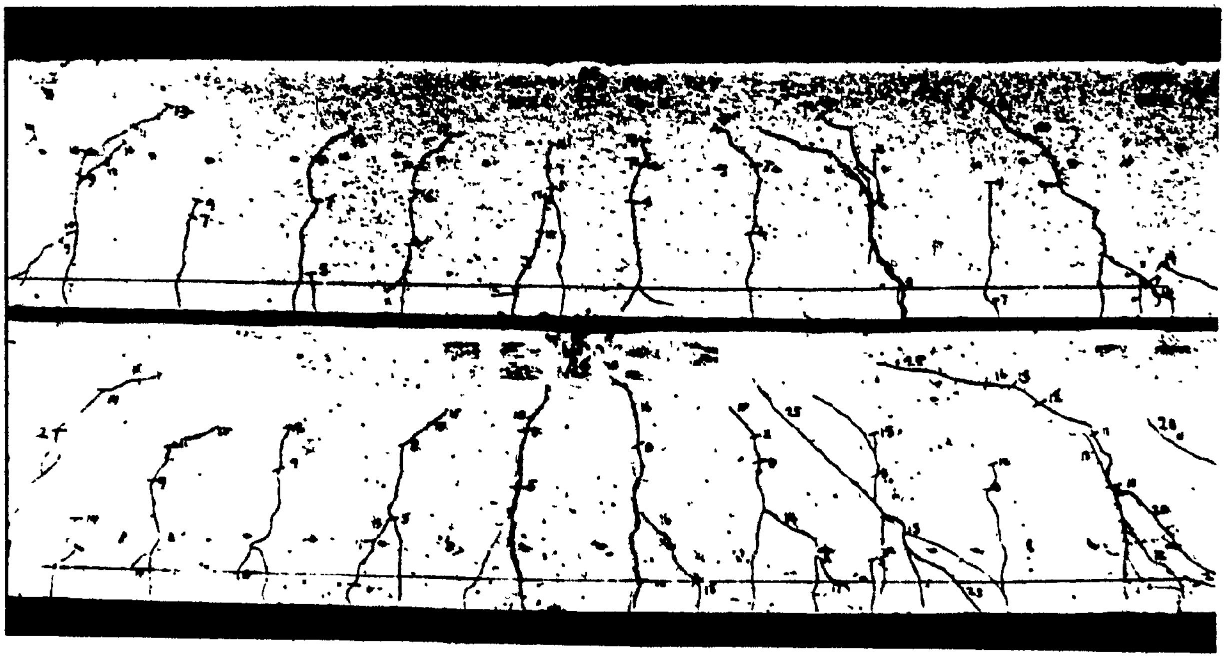

(a) Side Faces

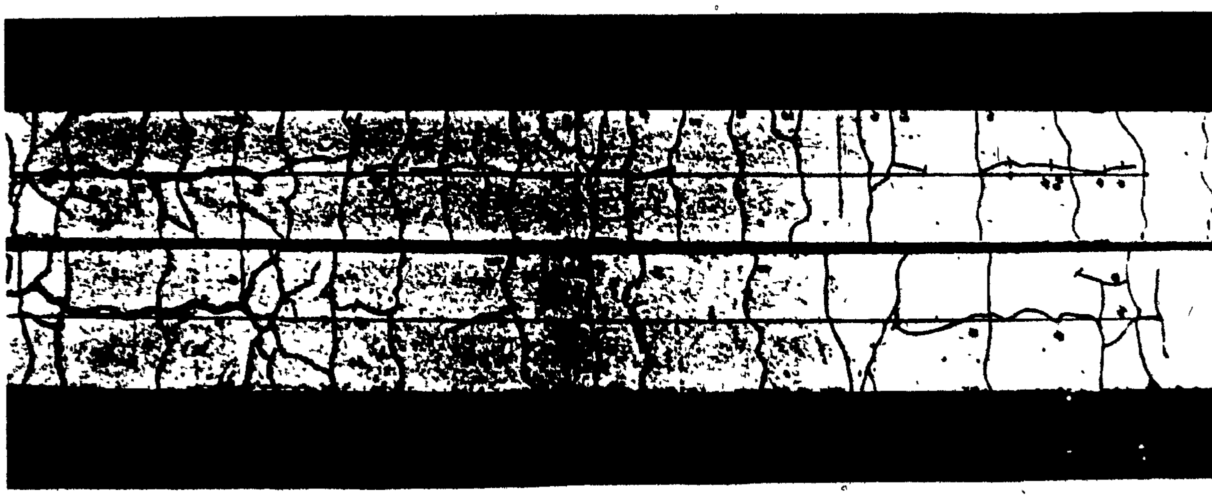

(b) Bottom Faces

Fig. 4.18 Effect of Casting Position of Reinforcement on the Crack Patterns of Beams B5 and B6

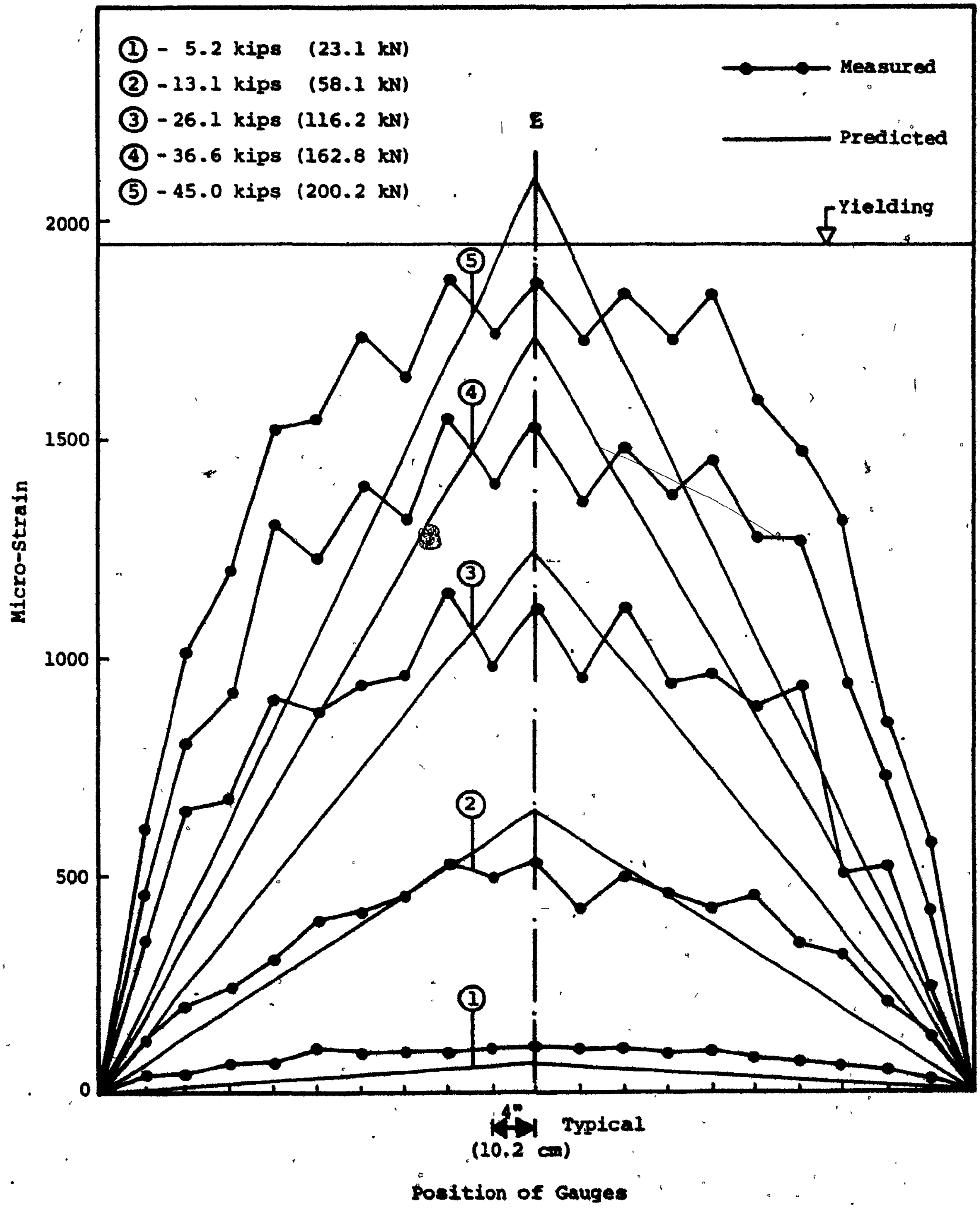

Fig. 4.19 Tensile Strains in #8 Bar - Beam BS

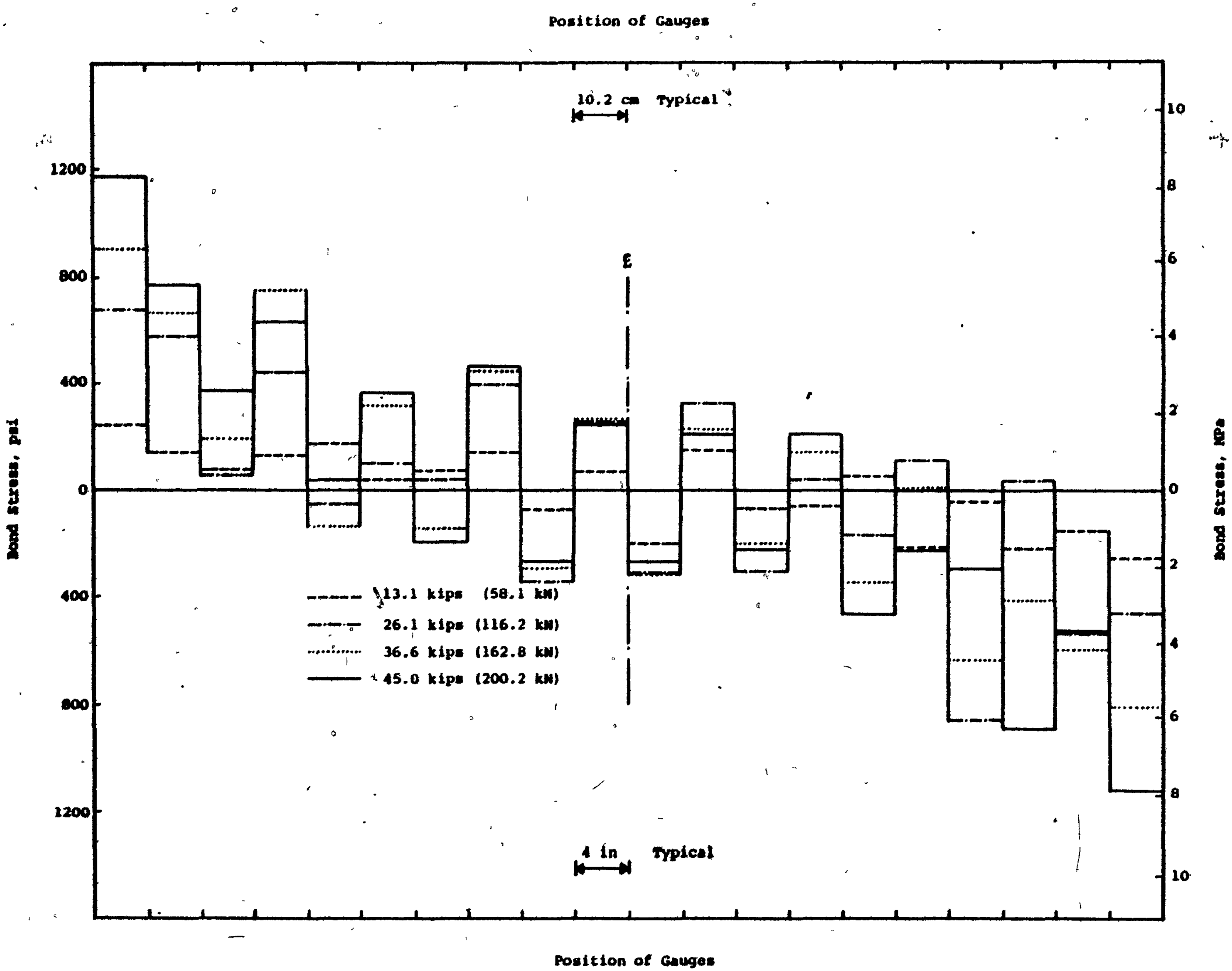

Fig. 4.20 Bond Stresses in #8 Bar - Beam B5

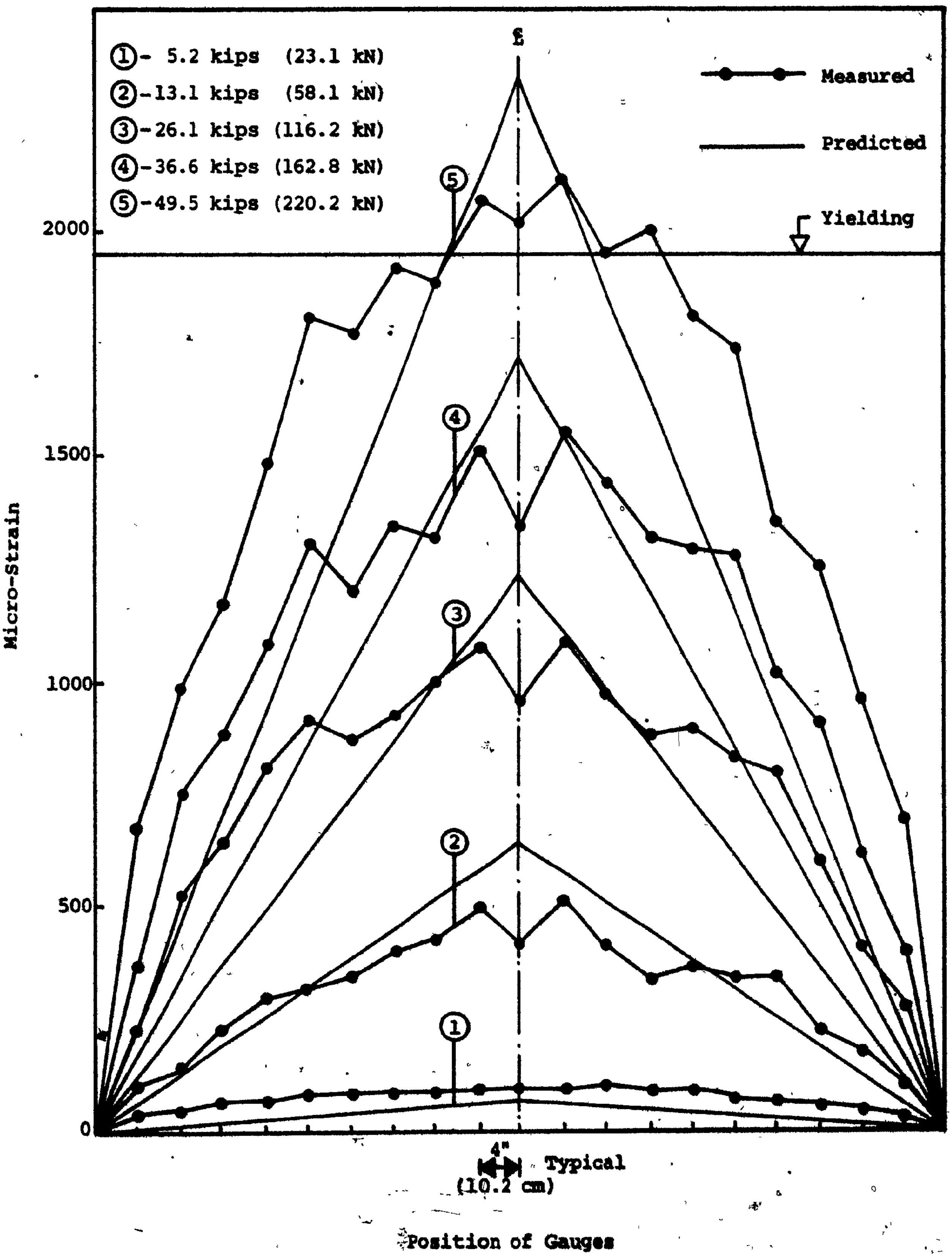

Fig. 4.21 Tensile Strains in #8 Bar - Beam B6

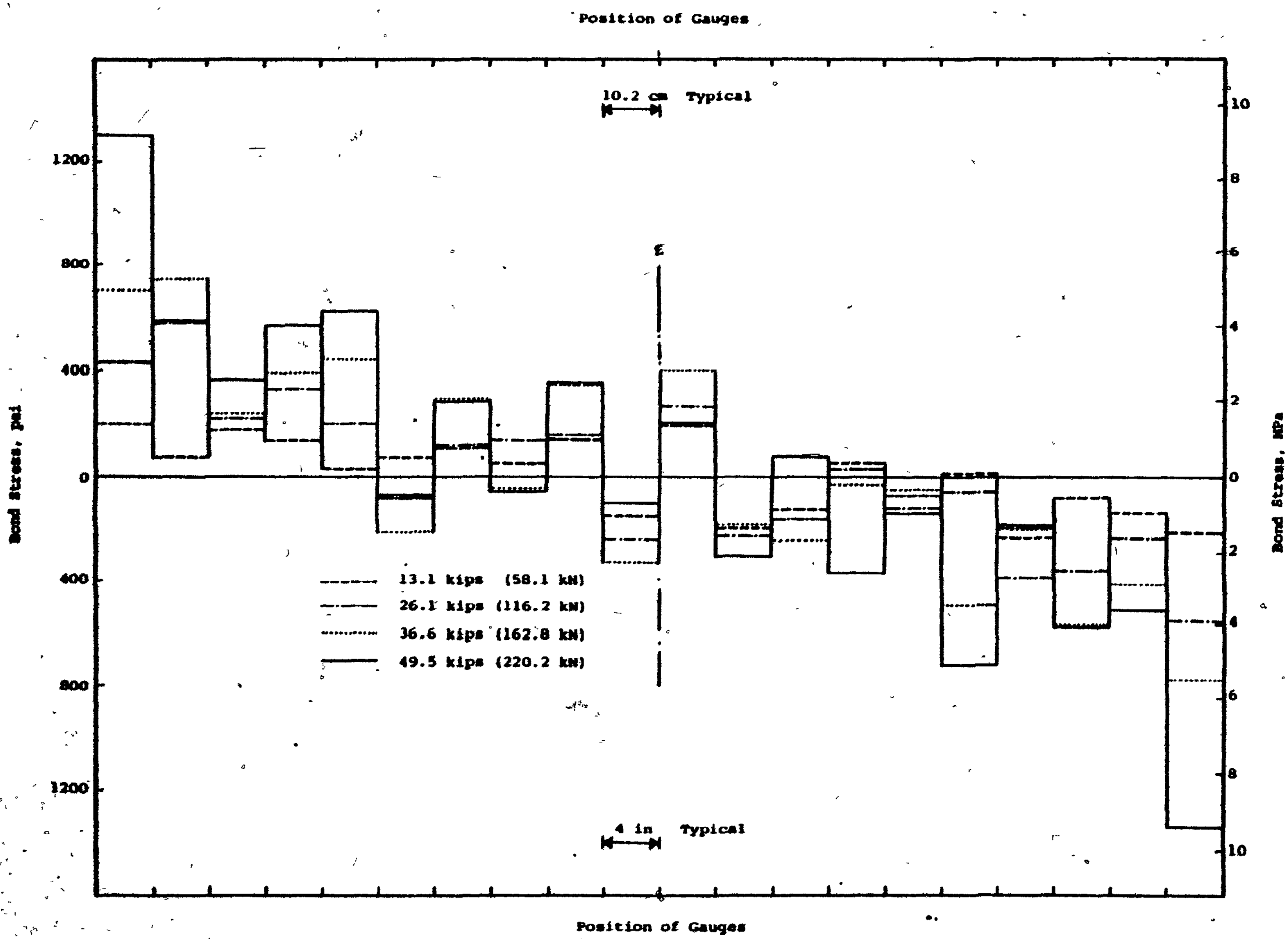

Fig. 4.22 Bond Stresses in #8 Bar - Beam B6

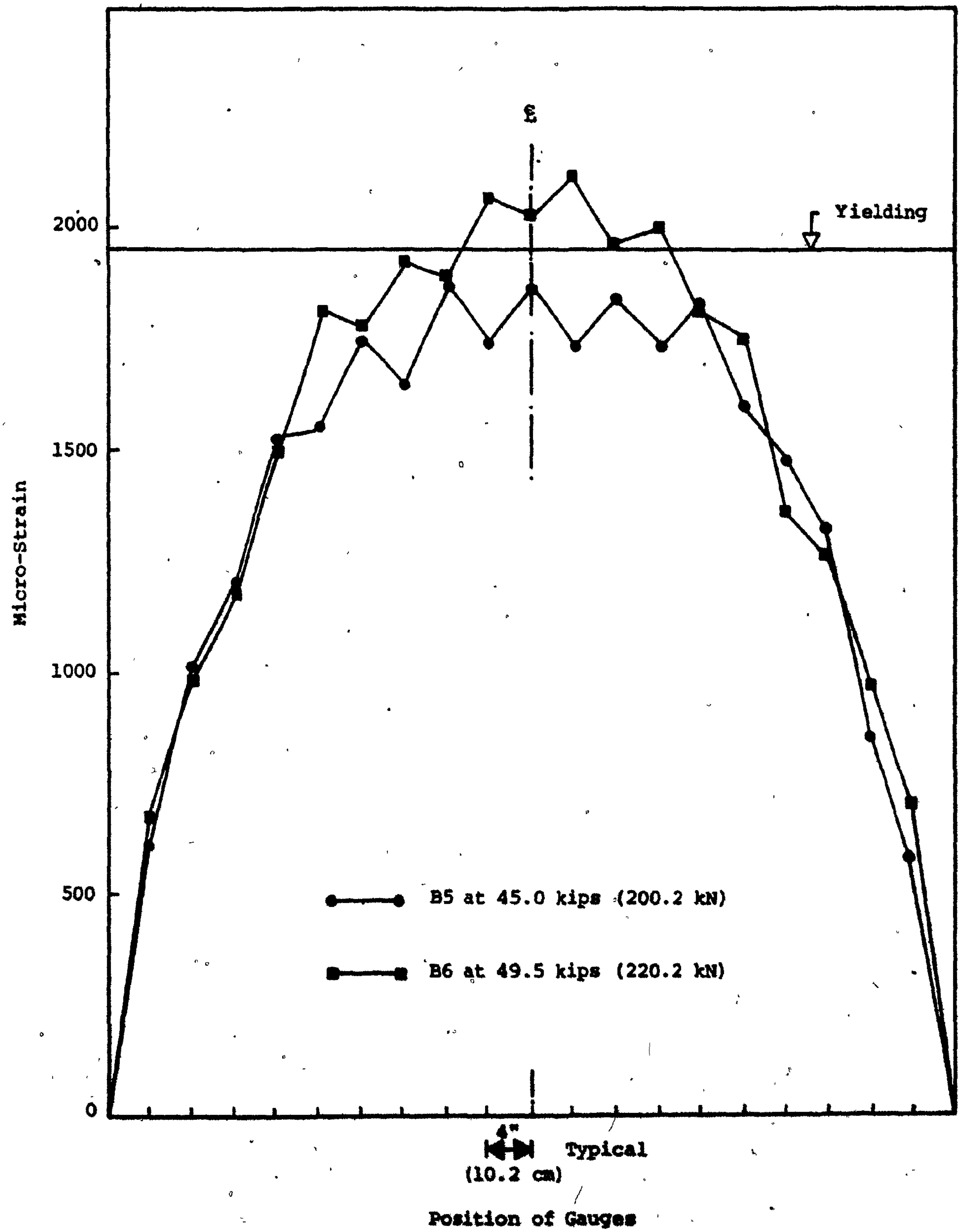

Fig. 4.33 Tensile Strains in #8 Bar at Failure - Beams B5 and B6

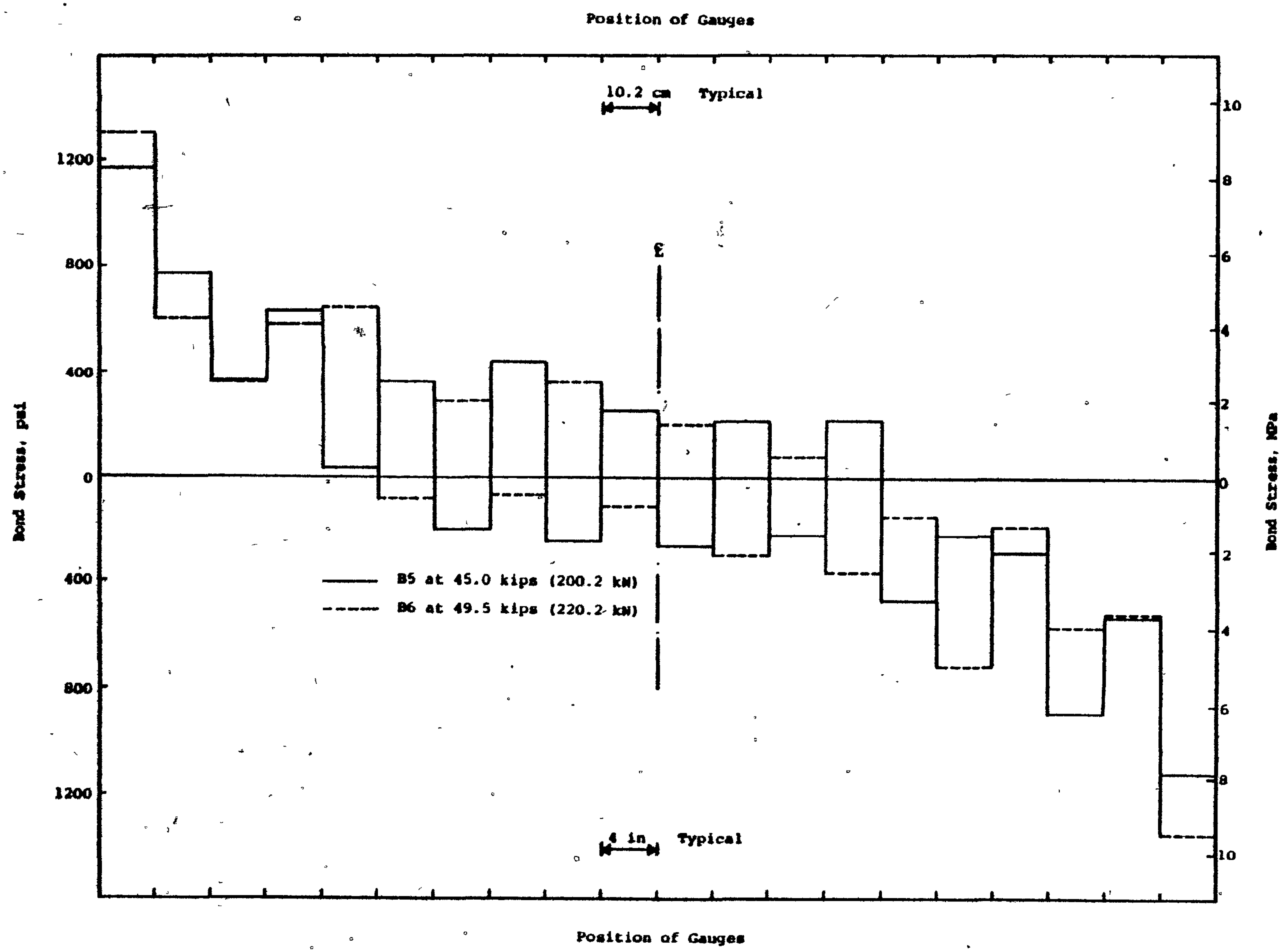

Fig. 4.24 Bond Stresses in #8 Bar at Failure - Beams B5 and B6

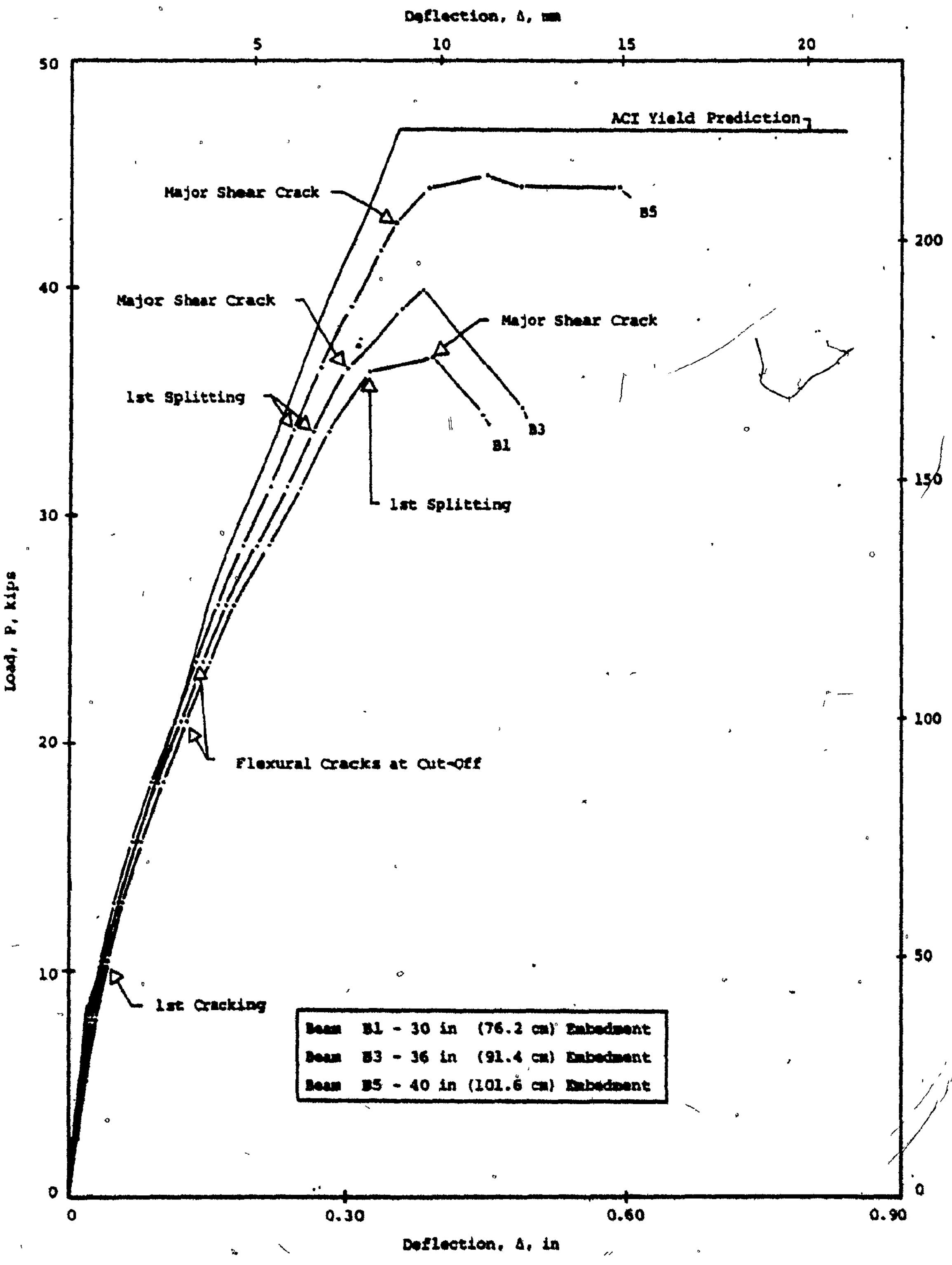

Fig. 4.25 Effect of Embedment Length on the Load-Deflection Responses of Top-Cast Beams B1, B3 and B5

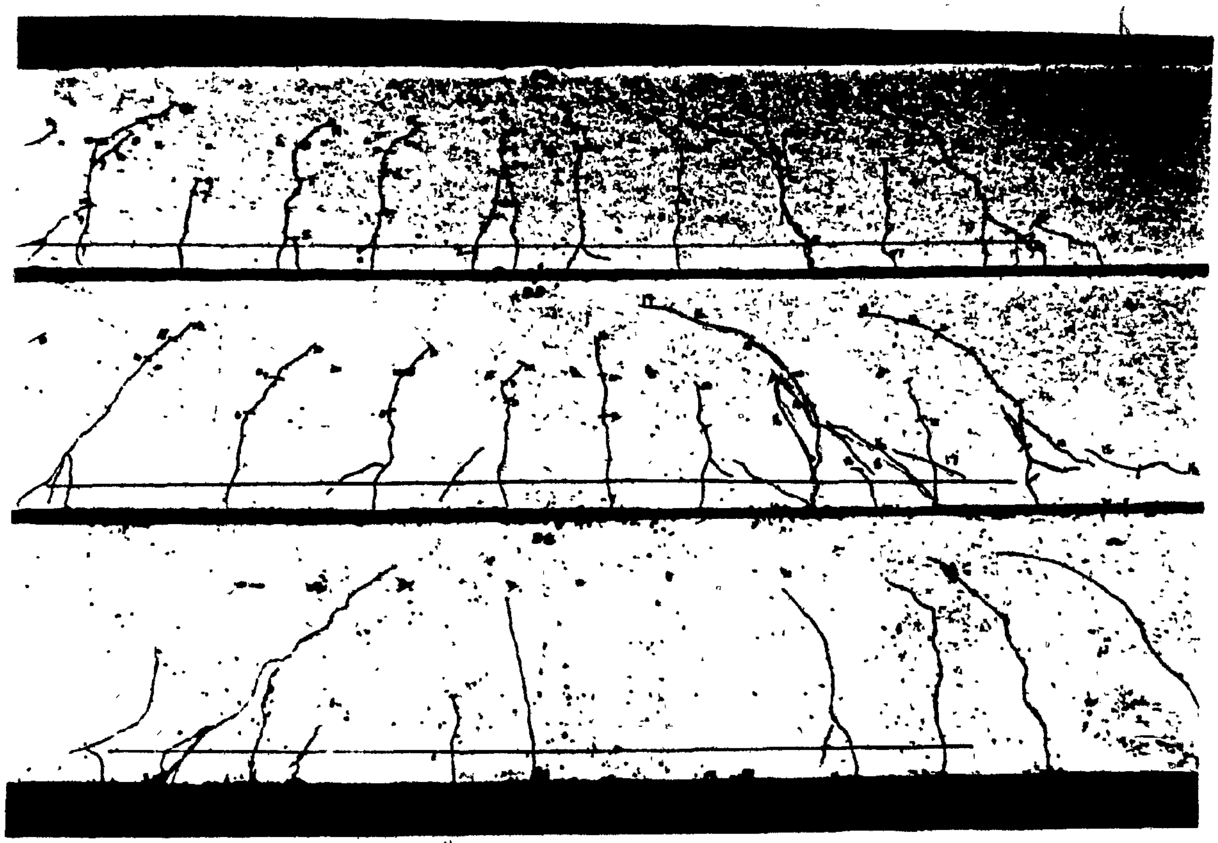

(a) Side Faces

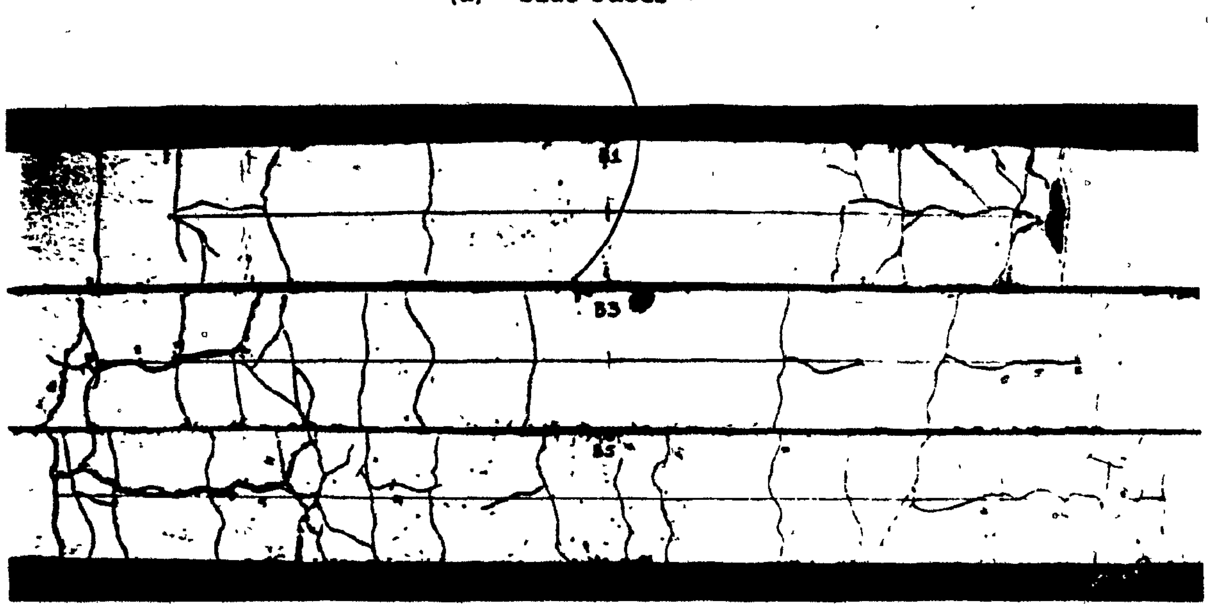

(b) Bottom Faces

Fig. 4.26 Effect of Embedment Length on the Crack Patterns of Top-Cast Beams B1, B3 and B5

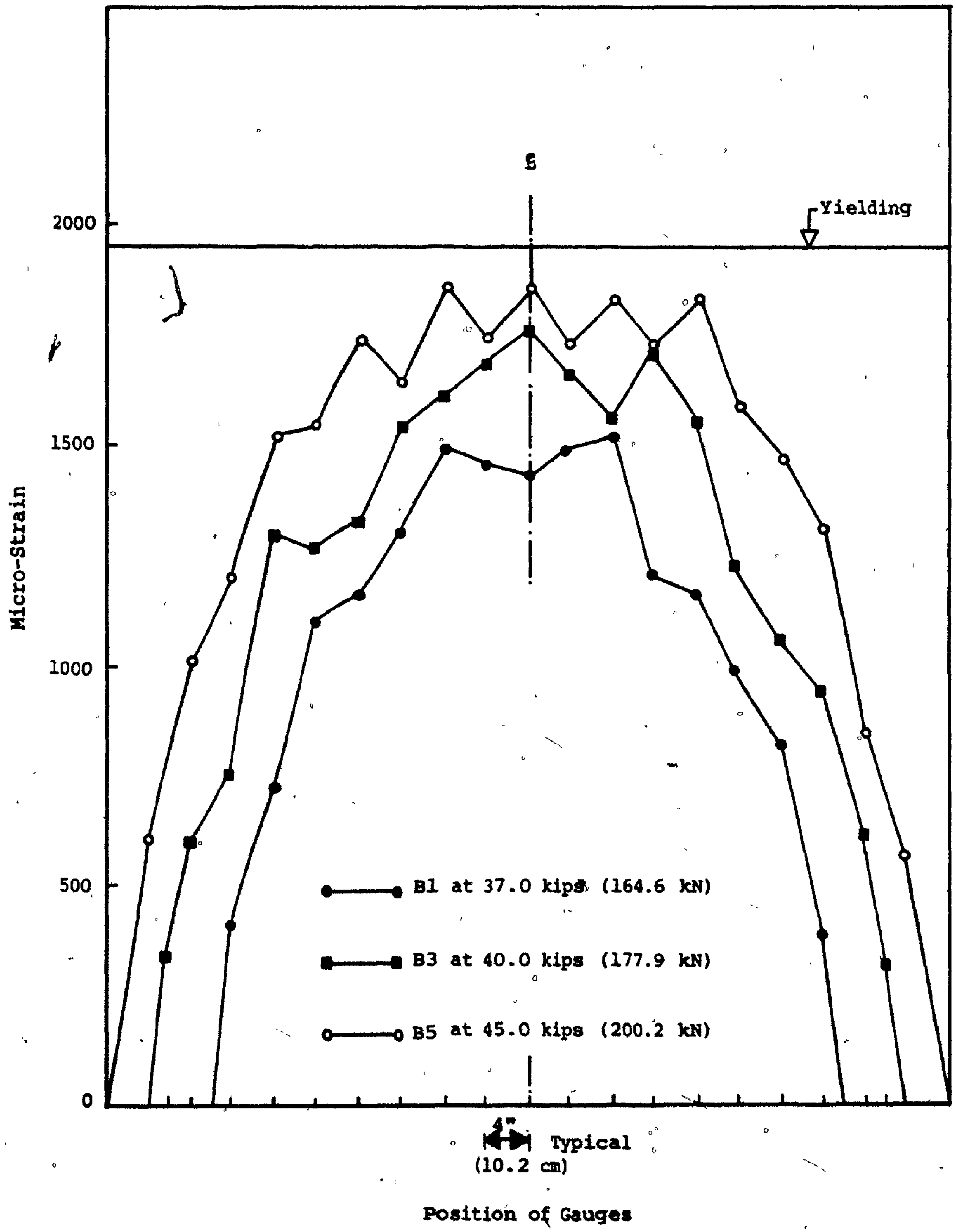

Fig. 4.27 Tensile Strains in #8 Bar at Failure - Beams B1, B3 and B5

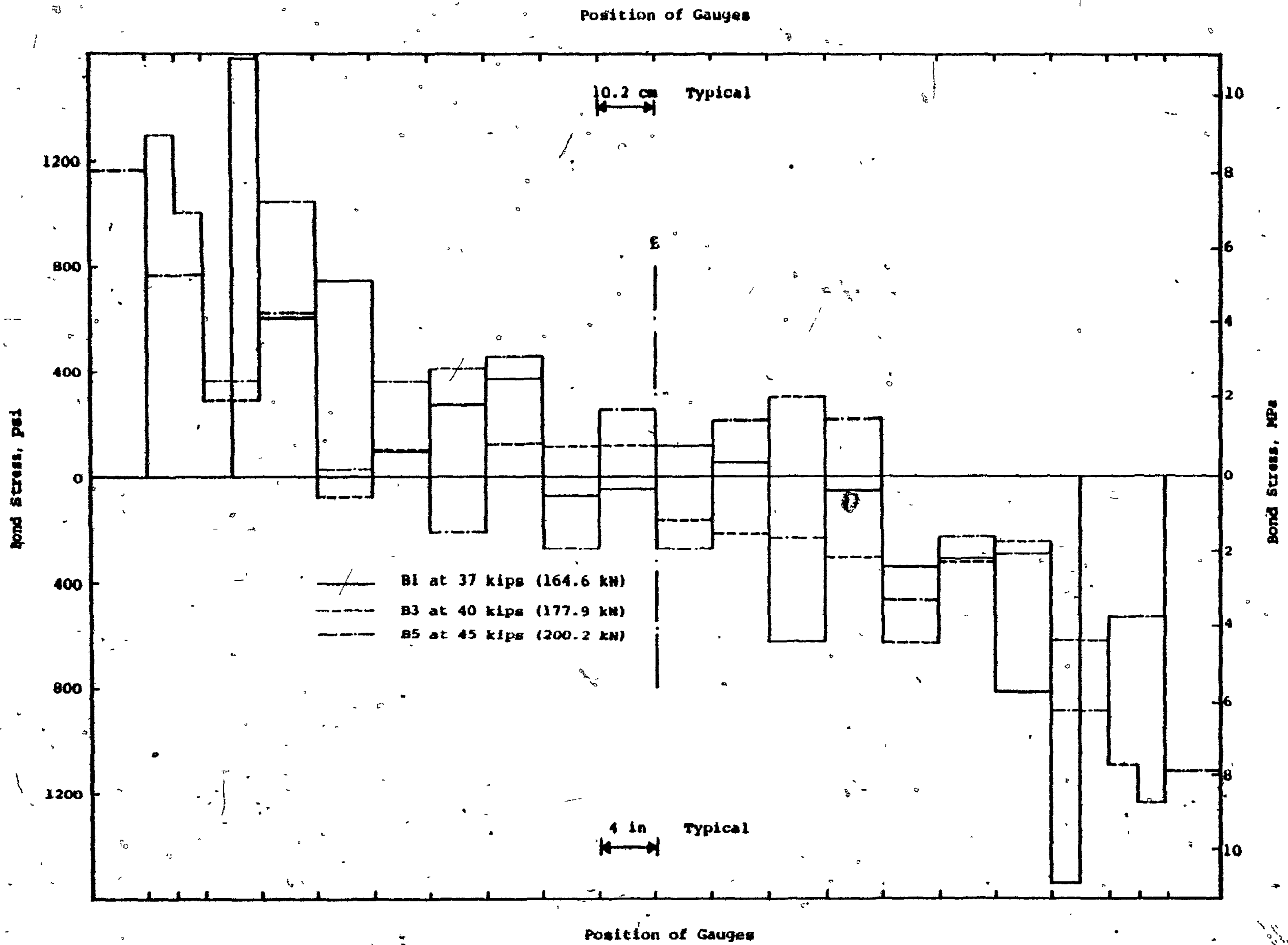

Fig. 4.28 Bond Stresses in #8 Bar at Failure - Beams B1, B3 and B5

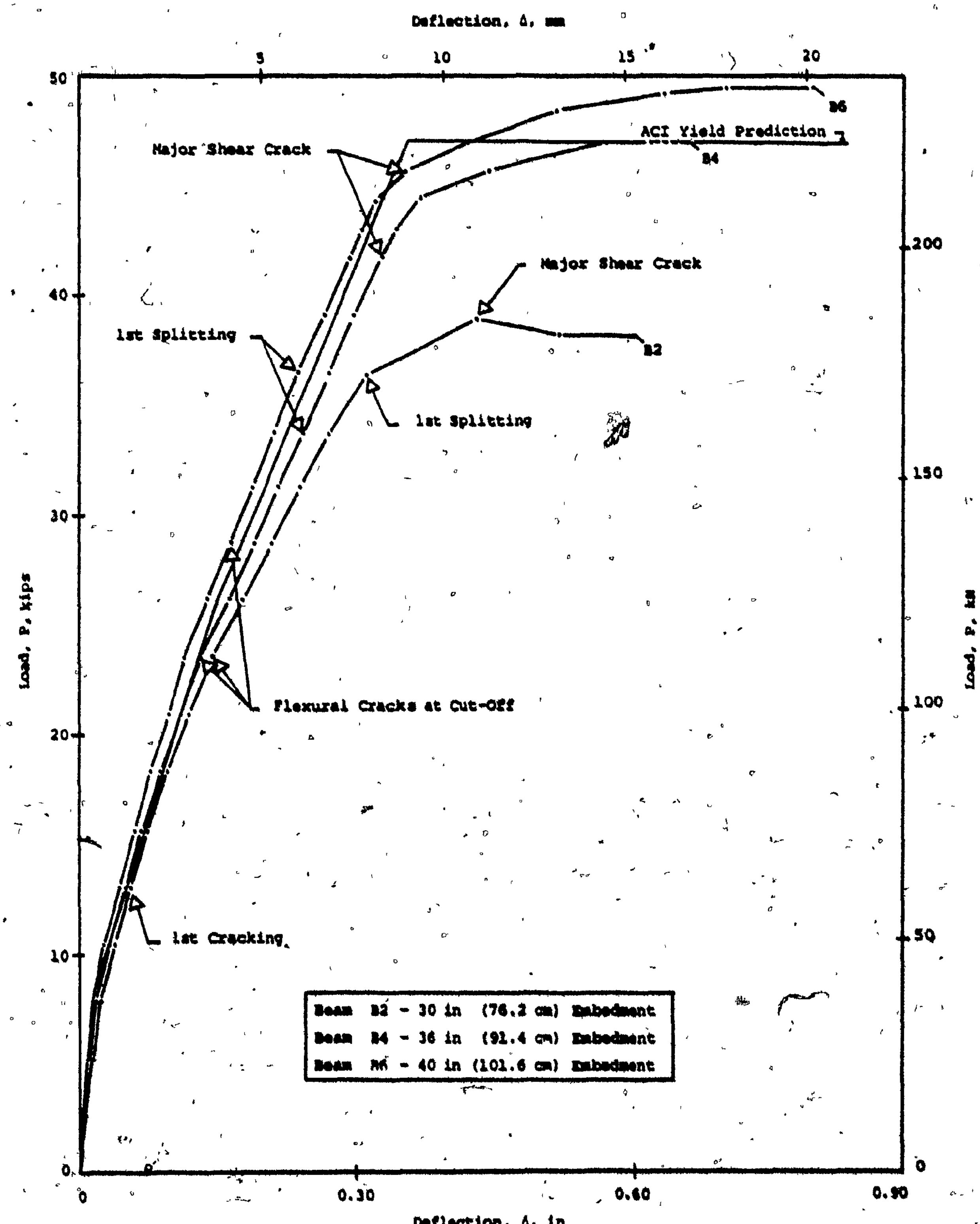

Fig. 4.29 Effect of Embedment Length on the Load-Deflection Responses of Bottom-Cast Beams B2, B4 and B6

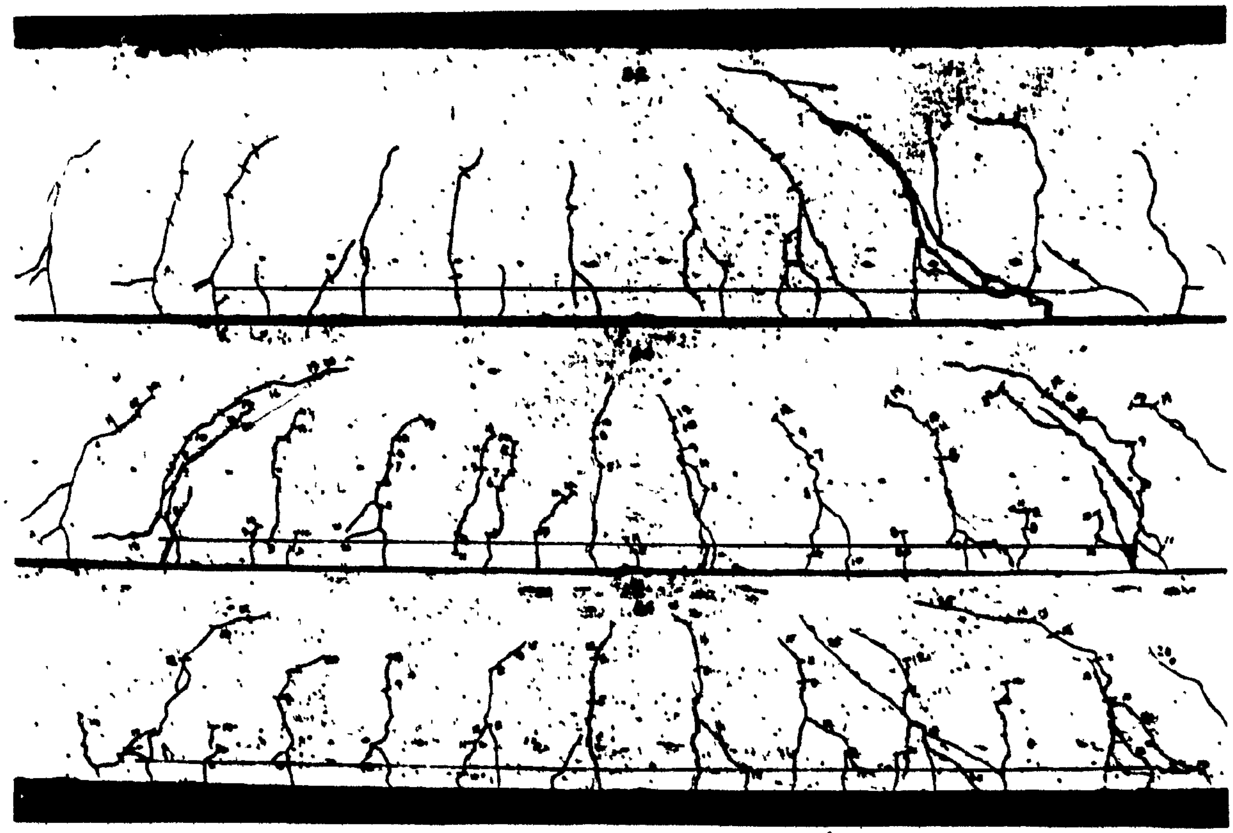

(a) Side Faces

(b) Bottom Faces

Fig. 4.30 Effect of Embedment Length on the Crack Patterns of Bottom-Cast Beams B2, B4 and B6

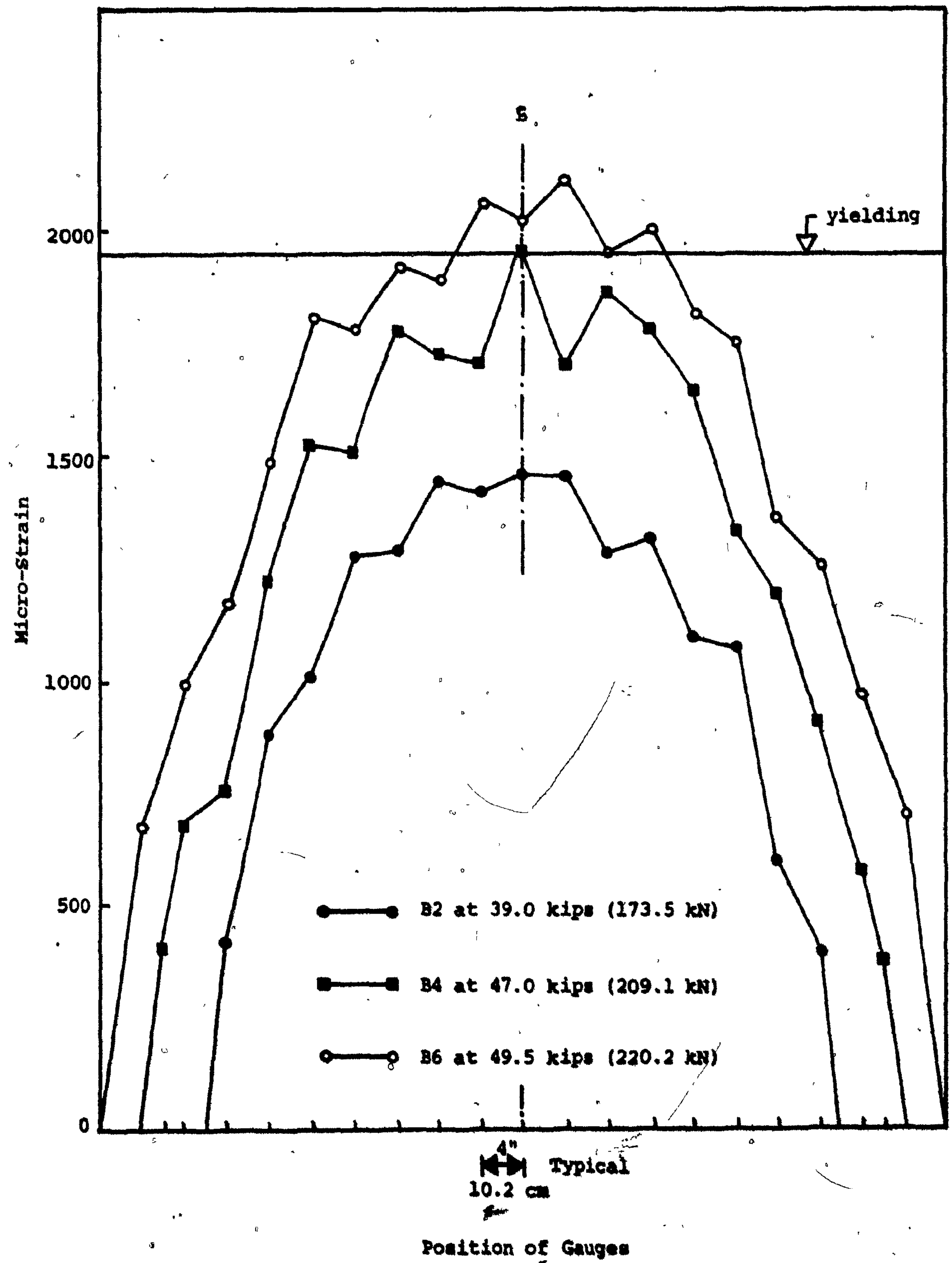

Fig. 4.31 Tensile Strains in #8 Bar at Failure - Beams B2, B4 and B6

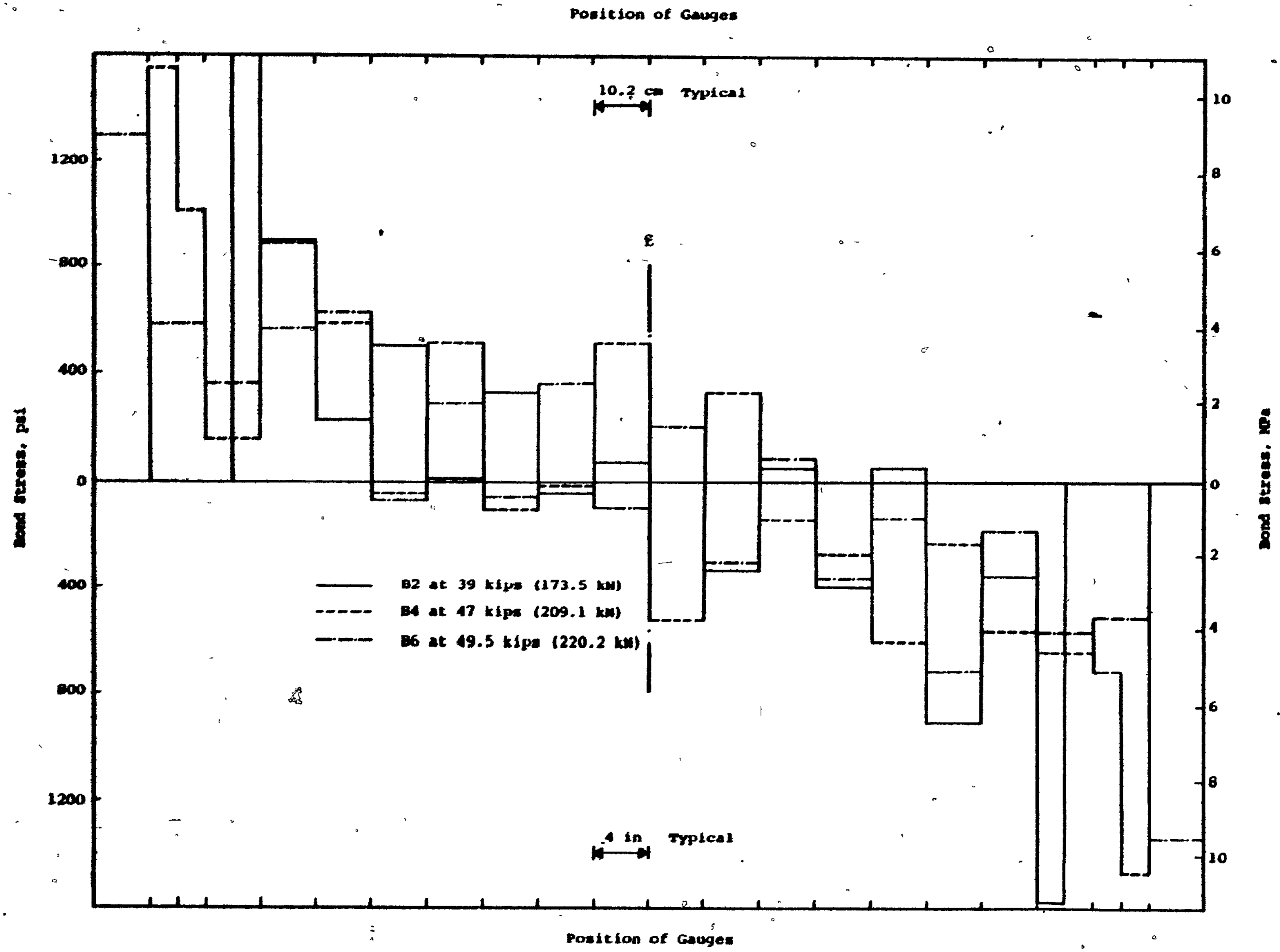

Fig. 4.32 Bond Stresses in #8 Bar at Failure - Beams B2, B4 and B6

CHAPTER V

DISCUSSION OF TEST RESULTS

5.1 Comparisons with ACI 1977

The results of beam B4 with an embedment length of 36 in (91.4 cm) indicate that the bottom-cast bar just yielded while the beam reached the theoretical moment capacity. None of the beams with top-cast bars reached the theoretical moment capacity. Beam B5, with an embedment length of 40 in (101.6 cm) had a maximum strain equal to 96 percent of the yield strain and failed at a load corresponding to 96 percent of the theoretical moment capacity.

For normal weight concrete and for Grade 60 steel reinforcement, the ACI (4) formula for the development length, l_d, of bottom-cast bars smaller than No. 11 (35.8 mm) is expressed by:

$$l_d = \frac{0.04\, A_b\, f_y}{\sqrt{f'c}} \qquad (5.1)$$

but not less than $0.0004\, d_b\, f_y$ (5.2)

where A_b = area of the steel bar

f_y = yield strength of the steel bar

f'_c = concrete compressive strength

d_b = nominal diameter of steel bar

The ACI provisions (from Equations 5.1 and 5.2) require a development length of 30 in (76.2 cm) for the bottom-cast bars. The Code also requires that the reinforcement continue a distance d_t or $12d_b$ beyond the theoretical cut-off point. This requirement would result in an embedment length of 45.5 in (115.6 cm). The results of beam B4 indicate that an embedment length of 36 in (91.4 cm) is required to develop the yielding of the bottom-cast reinforcing bar. The ACI Code requires a development length of 1.4 l_d for top-cast bars. In order to assess the top-bar effect, it is of interest to compare bottom-cast specimen B2, with 30 in (76.2 cm) embedment length with top-cast specimen B3 having a 36 in (91.4 cm) embedment length. Both beams failed at approximatively the same load. This suggests that top-cast bars require an embedment length equal to 1.20 times the embedment length for bottom-cast bars in order to develop the same stress. A similar comparison between beams B4 and B5 indicates a factor of 1.11.

5.2 Orangun, Jirsa and Breen's Equations

Orangun, Jirsa and Breen (67) have derived from a non-linear regression analysis of many beam test results an equation for splice length and development length of steel reinforcement. This equation considers the effects of bar diameter, steel stress and concrete strength and in addition accounts for the effects of concrete cover, bar spacing and the amount of shear reinforcement which have been neglected by current Code specifications. This results in a basic development length for a "bottom-cast steel bar" having a yield stress of 60 ksi (413.7 MPa) calculated as follows:

$$l_d = \frac{10,200\ d_b}{\phi\ \sqrt{f'c}\ (1 - 2.5\ c/d_b - K_{tr})} \qquad (5.3)$$

where ϕ = capacity reduction factor taken as 0.8

C = the smaller of C_b and C_s

C_b = clear bottom cover to main reinforcement

C_s = half clear spacing between bars

K_{tr} is an index of the amount of transverse reinforcement along the embedded bar and is given by:

$$K_{tr} = \frac{A_{tr}\ f_{yt}}{600\ s\ d_b} < 2.5 \qquad (5.4)$$

where A_{tr} = area of transverse reinforcement normal to the plane of splitting througth the embedded bar

f_{yt} = yield strength of transverse reinforcement

s = spacing of transverse reinforcement centre to centre

For this series of beams $C = C_b = 1.5$ in (3.8 cm) and due to the details of the stirrups $K_{tr} = 0$.

The predicted basic development length for the No. 8 (25.4 mm) bottom-cast bar is 34 in (86.4 cm) from Equation (5.3) with $\phi = 1.0$. This basic development length is greater than the 30 in (76.2 cm) required by the ACI Code (4). Also Orangun, Jirsa and Breen proposed a factor of 1.3 for top-cast bars.

5.3 Consideration for Future Research

The simply supported beam with central point loading has been used in this experimental program to study the top-bar effect with varying embedment lengths. The ACI Code approach with a top-bar factor of 1.4 and a required extension of d_t or 12 b_d beyond the theoretical cut-off point is conservative for this series of tests. However more research is needed in order to quantify the top-bar effect.

Other variables that could be investigated are:

(i) different depths of concrete below the top bar,

(ii) different strengths and types of concrete,

(iii) different sizes of reinforcing bars,

(iv) different percentages of transverse reinforcement, and

(v) different orientations of reinforcement (e.g. vertical bars in walls)

These investigations would help to quantify the top-bar effect and would add to the knowledge of this complex bond problem.

CHAPTER VI

CONCLUSIONS

The behaviour of specimens containing top-cast bars was compared with the behaviour of companion specimens containing bottom-cast bars. The results of the tests indicate that beams containing top-cast bars do not perform as well as beams with bottom-cast bars. The observed top-bar effects on the behaviour are as follows:

(1) A decrease in the ultimate strength (10 to 18 percent for this series),

(2) A decrease in ductility,

(3) Lower bond stresses at failure,

(4) Lower stiffness at all load levels, and

(5) Lower cracking loads due to the reduction of tensile strength for top-cast concrete.

Comparisons of the behaviour of the beams tested indicate that top-cast bars require an increased embedment length between 11 and 20 percent longer than bottom-cast bars in order to reach the same stress levels in the bars.

The three beams containing top-cast bars and the three beams containing bottom-cast bars indicate that increases in embedment length resulted in higher strength, higher stiffness and higher ductility.

BIBLIOGRAPHY

1. ACI Committee 318, "Building Code Requirements for Reinforced Concrete (ACI 318-63)", American Concrete Institute, Detroit, Michigan, 1963, 144 pp.

2. Joint CSA/NBC Committee, "Code for the Design of Plain or Reinforced Concrete Structures (CSA Standard A 23.2-1970)", Canadian Standards Association, 1970, 107 pp.

3. ACI Committee 318, "Building Code Requirements for Reinforced Concrete (ACI 318-71)", American Concrete Institute, Detroit, Michigan, 1971, 78 pp.

4. ACI Committee 318, "Building Code Requirements for Reinforced Concrete (ACI 318-77)", American Concrete Institute, Detroit, Michigan, 1977, 78 pp.

5. Joint CSA/NBC Committee, "Code for the Design of Concrete Structures for Buildings (CSA Standard A 23.3-1973)", Canadian Standards Association, 1973, 123 pp.

6. Watstein, D., and Bresler, B., "Bond and Cracking in Reinforced Concrete", Reinforced Concrete Engineering, Edited by Boris Bresler, New York, Wiley, 1974.

7. Mylrea, T.D., "Bond and Anchorage", ACI Journal, Proceedings, Vol. 44, No. 7, March 1948, pp. 521-552.

8. Mikhailov, K.V., "Stzepleniye Armatury & Betonom", ("Bond of Reinforcement to Concrete" in Russian) Moscou, 1952.

9. Mathey, Robert, G., and Watstein, D., "Investigation of Bond in Beams an Pull-Out Specimens with High-Yield Strength Deformed Bars", ACI Journal, Proceedings, Vol. 57, No. 9, March 1961, pp. 1071-1090.

10. Bresler, B., and Bertero, V., "Behaviour of Reinforced Concrete Under Repeated Load", Journal of the Structural Division, ASCE, Vol. 94, ST6, June 1968, pp. 1567-1590.

11. Broms, B.B., "Technique for Investigation of Internal Cracks in Reinforced Concrete Members", ACI Journal, Proceedings, Vol. 62, No. 1, January 1965, pp. 35-44.

12. Broms, B.B., "Stress Distribution in Reinforced Concrete Members with Tension Cracks", ACI Journal, Proceedings, Vol. 62, No. 9, September 1965, pp. 1095-1108.

13. Goto, Y., "Cracks Formed in Concrete Around Deformed Tension Bars", ACI Journal, Proceedings, Vol. 68, No. 4, April 1971, pp. 244-251.

14. Broms, B.B., and Lutz, Leroy, A., "Effect of Arrangement of Reinforcement on Crack Width and Spacing in Reinforced Concrete Members", ACI Journal, Proceedings, Vol. 62, No. 11, November 1965, pp. 1395-1410.

15. Lutz, L.A., Gergely, P., and Winter, G., "The Mechanics of Bond and Slip of Deformed Bars in Concrete", Report 324, Structural Engineering Department, Cornell University.

16. Lutz, L.A., and Gergely, P., "Mechanics of Bond and Slip of Deformed Bars in Concrete", ACI Journal, Proceedings, Vol. 64, No. 11, November 1967, pp. 711-721.

17. Houde, J., and Mirza, M.S., "A Study of Bond Stress-Slip Relationship in Reinforced Concrete", Structural Concrete Series No. 72-8, McGill University, Montreal, April 1972.

18. Houde, J., "Study of Force Displacement Relationships for the Finite Element Analysis of Reinforced Concrete", Ph. D. Thesis, McGill University, Montreal, October 1973.

19. Clark, A.P., "Comparative Bond Efficiency of Deformed Concrete Reinforcing Bars", Journal of Research of the National Bureau of Standards, Vol. 37, RP 1755, December 1946, pp. 399-407.

20. Menzel, C.A., "Effect of Settlement of Concrete on Results of Pull-Out Bond Tests", Portland Cement Association, No. 41, November 1952.

21. Nilson, A.H., "Non-Linear Analysis of Reinforced Concrete by the Finite Element Method", ACI Journal, Proceedings, Vol. 65, No. 9, September 1968, pp. 757-766.

22. Nilson, A.H., "Finite Element Analysis of Reinforced Concrete", Ph. D. Thesis, University of California at Berkeley, 1968.

23. Tanner, J.A., "An Experimental Investigation of Bond Slip in Reinforced Concrete", M.S. Thesis, Cornell University, Ithaca, N.Y., November 1971.

24. Nilson, A.H., "Bond Stress-Slip Relations in Reinforced Concrete", Report 345, School of Civil and Environmental Engineering, Cornell University, Ithaca, New York, December 1971, 22 pp.

25. Nilson, A.H., "Internal Measurement of Bond Slip", ACI Journal, Proceedings, Vol. 69, No. 7, July 1972, pp. 439-441.

26. Ngo, O., and Scordelis, A.C., "Finite Element Analysis of Reinforced Concrete Beams", ACI Journal, Proceedings, Vol. 64, No. 3, March 1967, pp. 152-163.

27. Baldwin, J.W., "Bond of Reinforcement in Lightweight Aggregate Concrete", Preliminary Report, University of Missouri, March 1965, 10 pp.

28. Ferguson, P.M., "Bond Stress - The State of the Art" (ACI Committee 408), ACI Journal, Proceedings, Vol. 63, No. 11, November 1966, pp. 1161-1190.

29. Muline, N.M., Astrova, T.I., "Etude de l'Influence de la Composition du Béton sur l'Adhérence Acier-Béton", Bulletin d'Information du C.E.B. No. 48, April 1965.

30. Davis, R.E., Brown, E.H., and Kelly, J.W., "Some Factors Influencing the Bond Between Concrete and Reinforcing Steel", Proceedings ASTM, Vol. 38-11, 1938, pp. 394-409.

31. Larnach, W.J., "Changes in Bond Strength Caused by Re-Vibration of Concrete and the Vibration of Reinforcement", Magazine of Concrete Research No. 10, July 1952.

32. Bichara, A., "Etude du Problème de l'Adhérence dans le Béton Armé, Cahiers du Centre Scientifique et Technique du Bâtiment Nos. 117/127, Paris, 1951.

33. Robinson, J.R., "Cours de Béton Armé - III - Adhérence - Jonctions et Ancrages", Ecole Nationale des Ponts et Chaussées, Paris 1962-1963.

34. Robinson, J.R., "Premiers Résultats d'Essais de Coutures", Bulletin d'Information du C.E.B. No. 49, Mai 1965.

35. Plowman, J.M., "The Measurement of Bond Strength", Rilem Symposium on Bond and Crack Formation in Reinforced Concrete, Stockholm 1957, Vol, II, pp. 347-359.

36. Koh, Y., "Bond Between Concrete and Reinforcement (With Particular Reference to Cold Weather Concreting)", Rilem Symposium on Bond and Crack Formation in Reinforced Concrete, Stockholm 1957, Vol. I, pp. 177-190.

37. Saillard, Y., "Mécanisme de la Liaison Béton-Acier", Arckiwum Inzynierii Ladowey - Tome VI-4, Varsovie, 1960.

38. Baus, R., "Proposition de Détermination des Longueurs Pratiques d'Ancrage à partir des Contraintes de Rupture d'Adhérence données par le Beam Test", Bulletin d'Information du C.E.B. No. 48, Avril 1965.

39. Kuuskoski, V., "Uber die Haftung Zwischen Beton und Stahl" The State Institute for Technical Research, Helsinki, 1950.

40. Jonsson, P.O., Osterman, J., and Wastlund, G., "Background of the Swedish Tentative Standard Specifications for Limitation of Crack Widths in Reinforced Concrete Structures", Rilem Symposium on Bond and Crack Formation in Reinforced Concrete, Stockholm 1957, Vol. II, pp. 319-340.

41. Ferguson, P.M., Thompson, J.N., "Development Length of High Strength Reinforcing Bars in Bond", ACI Journal, Proceedings, Vol. 59, No. 7, July 1962, pp. 887-922.

42. Perry, Ervin, S., "Bond Stress Distribution in Concrete Beams and Eccentric Pull-Out Specimens", M.S. Thesis, The University of Texas, May 1961.

43. Perry, E.S., Thompson, J.N., "Bond Stress Distribution on Reinforcing Steel in Beams and Pull-Out Specimens", ACI Journal, Proceedings Vol. 63, No. 8, August 1966, pp. 865-875.

44. Kemp, E.L., Brezny, F.S., and Unterspan, J.A., "Effect of Rust and Scale on the Bond Characteristics of Deformed Reinforcing Bars", ACI Journal, Proceedings, Vol. 65, No. 9, September 1968, pp. 743-756.

45. Ghaffarzadeh, M., "Effect of Corrosion and Bar Spacing on Bond Properties of Reinforcing Bars in Concrete", Ph.D. Dissertation, University of Oklahoma, 1968.

46. Menzel, C.A., "A Proposed Standard Deformed Bar for Reinforcing Concrete", Paper Presented at the 17th Semi-Annual Meeting, Concrete Reinforcing Steel Institute, Colorado Springs, Colorado, September 1941, pp. 1-63.

47. Clark, A.P., "Bond of Concrete Reinforcing Bars", ACI Journal, Proceedings, Vol. 46, November 1949, pp. 161-184.

48. Lutz, L.A., "Information on the Bond of Deformed Bars from Special Pull-Out Tests", ACI Journal, Proceedings, Vol. 67, No. 11, November 1970.

49. Wilhelm, W.J., Kemp, E.L., and Lee, Y.T., "Influence of Deformation Height and Spacing on the Bond Characteristics of Steel Reinforcing Bars", Civil Engineering Studies Report No. 2013, Department of Civil Engineering, West Virginia University, 1971, Federal Clearinghouse No. PB-200635.

50. ASTM Standards in Building Codes, "Standard Specification for Deformed and Plain Billet-Steel Bars for Concrete Reinforcement", ASTM : A 615-77, American Society for Testing and Materials, 1977.

51. Bernander, K.G., "An Investigation of Bond by Means of Strain Measurements in High Tensile Bars Embedded in Long Cylindrical Pull-Out Specimens", Rilem Symposium on Bond and Crack Formation in Reinforced Concrete, Stockholm 1957, Vol. I, pp. 203-214.

52. Djabry, W., "Contribution à l'Etude de l'Adhérence des Fers d'Armature au Béton", Laboratoire Fédéral d'Essai des Matériaux, Zurich, Rapport No. 184, 1952.

53. Voellmy, A., Bernardi, B., "Remarques sur l'Adhérence et la Formation des Fissures dans le Béton Armé", Rilem Symposium on Bond and Crack Formation in Reinforced Concrete, Stockholm 1957, Vol. II, pp. 347-359.

54. Ferguson, P.M., Breen, J.E., Thompson, J.N., "Pull-Out Tests on High Strength Reinforcing Bars", ACI Journal, Proceedings, Vol. 62, No. 8, August 1965, pp. 933-950.

55. Untrauer, R.E., Warren, G.E., "Stress Development of Tension Steel in Beams", ACI Journal, Proceedings, Vol. 74, No. 8, August 1977, pp. 368-372.

56. Megget, L.M., and Park, R., "Reinforced Concrete Exterior Beam-Column Joints under Seismic Loading", New Zealand Engineering, November, 15, 1971, p. 341.

57. Hribar, J.A., and Vasko, R.C., "End Anchorage of High-Strength Steel Reinforcing Bars", ACI Journal, Proceedings, Vol. 66, No. 11, November 1969, pp. 875-883.

58. Rehm, G., "The Basic Principles of the Bond Between Steel and Concrete", Translation No. 134, Cement and Concrete Association, London, 1968, 66 pp.

59. Brooks, Larry, T., "Stress Distribution in Steel at Cut-Off Points in Reinforced Concrete Beams", M.Sc. Thesis, University of Texas, Austin, August 1959.

60. Ferguson, P.M., and Husain, S.T., "L'Etat des Recherches de l'I.R.A.B.A. sur les Aciers de Couture du Béton Armé", Supplément des Annales de l'Institut Technique du Bâtiment et des Travaux Publics, Paris, France, Juin 1968.

61. Tepfers, Ralejs, "A Theory of Bond Applied to Overlapped Tensile Reinforcement Splices for Deformed Bars", Publication No. 73-2, Division of Concrete Structures, Chalmers University of Technology, Goteborg, Sweden, 1978, 328 pp.

62. Chamberlin, S.J., "Spacing of Spliced Bars in Beams", ACI Journal, Proceedings, Vol. 54, February 1958.

63. Ferguson, P.M., and Briceno, E.A., "Tensile Lap Splices - Part I: Retaining Wall Type, Varying Moment Zone", Research Report 113-2, Center for Highway Research, The University of Texas at Austin, July 1969.

64. Ferguson, P.M., and Krishnaswamy, C.N., "Tensile Lap Splices - Part II: Design Recommendations for Retaining Wall Splices and Large Bar Splices", Research Report 113-3, Center for Highway Research, The University of Texas at Austin, April 1971.

65. Thompson, M.A., Jirsa, J.O., Breen, J.E., and Meinheit, D.F., "The Behaviour of Multiple Lap Splices in Wide Sections", Research Report 154-1, Center for Highway Research, The University of Texas at Austin, February 1975.

66. Segmer, E.P., Jr., "Splices in Tensile Reinforcing Bars", Report No. 1468, University of Oklahoma Research Institute, August 1965.

67. Judd, T.H., "Strength of Lapped Splices in Concrete Beams Using Hooks", M.S. Thesis, University of Colorado, 1965.

68. Pfister, J.F., and Mattock, A.H., "High Strength Bars as Concrete Reinforcement, Part 5, Lapped Splices in Concentrically Loaded Columns", Journal of the PCA Research and Development Laboratories, Vol. 5, No. 2, July 1963, pp. 27-40.

69. Lauritzen, Charles, A., "Relation Between Bond and Shear Strength of Reinforced Concrete Beams", M.S. Thesis, University of Texas, May 1960.

70. Berkman, R.M., "Diagonal Tension and Bond in Rectangular Reinforced Concrete Beams with Varying Beam Width", M.S. Thesis, University of Texas, June 1960.

71. "An Investigation of the Bond of Deformed Steel Bars with Concrete", Translation No. 112, Cement and Concrete Association, London 1964, 28 pp.

72. Ferguson, P.M., Turpin, R.D., and Thompson, J.N., "Minimum Bar Spacing as a Function of Bond and Shear Strength", ACI Journal, Proceedings, Vol. 50, No. 10, June 1954, pp. 869-887.

73. Orangun, C.O., Jirsa, J.O., Breen, J.E., "A Reevaluation of Test Data on Development Length and Splices", ACI Journal, Proceedings, Vol. 74, No. 3, March 1977, pp. 114-122.

74. Ferguson, P.M., "Small Bar Spacing or Cover - A Bond Problem for the Designer", ACI Journal, Proceedings, Vol. 74, No. 9, September 1977, pp. 435-439.

75. Leonhardt, F., "On the Need to Consider the Influence of Lateral Stresses on Bond", Rilem Symposium on Bond and Crack Formation in Reinforced Concrete, Stockholm 1957, Vol. I, pp. 29-34.

76. Louis, H., Baus, R., "L'Adhérence au Béton des Armatures en Acier Mi-Dur", Annales des Travaux Publics de Belgique, No. 1, 1962.

77. Ferguson, P.M., Breen J.E., "Lapped Splices for High Strength Reinforcing Bars", ACI Journal, Proceedings, Vol. 62, No. 9, September 1965, pp. 1063-1078.

78. Dutron, R., "Adhérence des Armatures au Béton", Revue des Matériaux de Construction et de Travaux Publics, Nos. 514 à 517, Paris, 1958.

79. Leonhardt, F., Walther, R., "Schubversuche an Plattenbalken mit Unterschiedlicher Schubbewehrung", Auschuss fur Stahlbeton, Heft 156, Berlin 1963.

80. Dr. Soretz, S., "Contribution à la Recherche sur les Aciers à Béton et sur le Béton Armé", Annales I.T.B.T.P., Série Béton Armé No. 64, Novembre 1961.

81. Verna, J.R., and Stelson, T.E., "Repeated Loading Effect on Ultimate Static Strength of Concrete Beams", ACI Journal, Proceedings, Vol. 60, No. 6, June 1963, pp. 743-750.

82. Barnoff, R.M., "Bond Fatigue Strength of Reinforced Concrete Beams", Ph.D. Thesis, Department of Civil Engineering, Carnegie Institute of Technology, May 1966.

83. Ismail, A.F., and Jirsa, J.O., "Bond Deterioration in Reinforced Concrete Subject to Low Cycle Loads", ACI Journal, Proceedings, Vol. 69, No. 6, June 1972, pp. 334-343.

84. Ismail, A.F., and Jirsa, J.O., "Behaviour of Anchored Bars under Low Cycle Overloads Producing Inelastic Strains", ACI Journal, Proceedings, Vol. 69, No. 7, July 1972, pp. 433-438.

85. Perry, E.S., and Jundi, N., "Pull-Out Bond Stress Distribution under Static and Dynamic Repeated Loadings", ACI Journal, Proceedings, Vol. 66, No. 5, May 1969, pp. 377-380.

86. Park, Paulay, "Bond and Anchorage", Reinforced Concrete Structures, N.Y., Wiley, 1975.

87. Watstein, David, "Bond Stress in Concrete Pull-Out Specimens", ACI Journal, Proceedings, Vol. 38, September 1941, pp. 37-50.

88. Mains, R.M., "Measurement of the Distribution of Tensile and Bond Stresses along Reinforcing Bars", ACI Journal, Proceedings, Vol. 48, No. 3, November 1951, pp. 225-252.

89. Hajnal-Konyi, K., "Suggestions for the Comparison of the Bond Resistance of Various Types of Reinforcing Bar", Rilem Symposium on Bond and Crack Formation in Reinforced Concrete, Stockholm 1957, Vol. I, pp. 137-146.

90. Riessauw, F.G., "Essais Comparatifs d'Adhérence entre Acier Tor 40 (avec verrous) et Acier A.37", Rilem Symposium on Bond and Crack Formation in Reinforced Concrete, Stockholm 1957.

91. McHenry, Douglas, Walker, W.T., "Laboratory Measurements of Stress Distribution in Reinforcing Steel", ACI Journal, Proceedings, Vol. 44, June 1948, pp. 1041-1054.

92. ACI Committee 208, "Proposed Test Procedure to Determine Relative Bond Values of Reinforcing Bars", ACI Journal, Proceedings, Vol. 55, No. 1, July 1958, pp. 1-6.

93. ACI Committee 408, "A Guide for the Determination of Bond Strength in Beam Specimens", ACI Journal, Proceedings, Vol. 61, No. 2, February 1964, pp. 129-135.

94. Mirza, M.S., and Hsu, C.T., "Investigation of Bond in Reinforced Concrete Models - Eccentric Pull-Out Test", Proceedings, International Conference on Shear, Torsion and Bond in Reinforced and Prestressed Concrete, Coimbatore, India, January 1969.

95. Cheng-Tzu Hsu, "Investigation of Bond in Reinforced Concrete Models", M. Eng. Thesis, McGill University, April 1969.

96. Hillerborg, A., "Bond in, and Safety of Reinforced Concrete Structures", Stockholm, January 1958.

97. Association Ciment Portland, "Dosage et Contrôle des Mélanges de Béton", Montréal, Québec, 1976.

98. Report by ACI Committee 408, "Development of Bond Testing".

99. Report by ACI Committee 408, "Towards an Understanding of the Mechanics of Bond Failures.

100. Baus, R., et Claude, M.G., "Etat des Connaissances sur le Mécanisme de l'Adhérence et des Ancrages", Essai de Synthèse Bibliographique, C.E.B. Bulletin No. 66, Octobre 1966, pp. 185-213.

101. Kriz, L.B., and Raths, C.H., "Connections in Precast Concrete Structures-Strength of Corbels", PCA Research and Development Laboratories, Bulletin D85, February 1965, pp. 16-61.

102. Slutter, R.G., and Driscoll, G.C., "Flexural Strength of Steel Concrete Composite Beams", ASCE, Journal of the Structural Division, Vol. 91, ST2, April 1965, pp. 71-99.

APPENDIX A

TEST OF MATERIALS

TABLE A.1

VALUES OF f_y AND f_u FOR REINFORCING BARS

TEST No.	BAR SIZE	AREA in^2 (cm^2)	YIELD LOAD kips (kN)	AV. YIELD LOAD kips (kN)	ULT. LOAD kips (kN)	AV. ULT. LOAD kips (kN)	f_y psi (MPa)	f_u psi (MPa)
1			6.8 (30.2)		10.3 (45.8)			
2	#3 (9.5 mm)	0.11 0.71	6.6 (29.4)	6.6 (29.4)	10.0 (44.5)	10.1 (44.9)	60.3 (415.8)	91.9 (633.7)
3			6.4 (28.5)		10.0 (44.5)			
1			25.6 (113.9)		39.3 (174.8)			
2	#6 (19.1 mm)	0.44 2.84	25.8 (114.8)	25.7 (114.3)	39.0 (173.5)	39.2 (174.4)	58.5 (403.4)	89.1 (614.3)
3			25.8 (114.8)		29.3 (174.8)			
1			46.8 (208.2)		69.0 (306.9)			
2	#8 (25.4 mm)	0.79 (5.10)	47.0 (209.1)	47.0 (209.1)	70.5 (313.6)	70.0 (311.4)	59.5 (410.3)	88.6 (610.9)
3			47.3 (210.4)		70.5 (313.6)			

TABLE A.2

COMPRESSION TEST RESULTS

BEAM No.	CYLINDER No.	AREA in^2 (cm^2)	ULTIMATE LOAD lbs	AV. ULT. LOAD lbs (kN)	AVERAGE STRENGTH psi (MPa)
B1	1 2 3 4 5 6	28.27 (182.4)	114,500 113,500 113,000 114,960 113,300 116,000	114,200 (508)	4040 (27.9)
B2	1 2 3 4 5 6	28.27 (182.4)	108,920 109,500 110,980 108,300 110,200 111,920	109,970 (489.2)	3890 (26.8)
B3	1 2 3 4 5 6	28.27 (182.4)	115,310 113,690 116,600 115,700 114,200 114,860	115,060 (511.8)	4070 (28.1)
B4	1 2 3 4 5 6	28.27 (182.4)	119,290 120,200 121,500 118,650 120,900 118,650	119,865 (533.2)	4240 (29.2)
B5	1 2 3 4 5 6	28.27 (182.4)	113,900 112,500 115,000 114,070 113,000 115,100	113,928 (506.8)	4030 (27.8)
B6	1 2 3 4 5 6	28.27 (182.4)	116,000 115,500 113,900 113,460 116,500 115,000	115,060 (511.8)	4070 (28.1)

APPENDIX B

INSTRUMENTATION

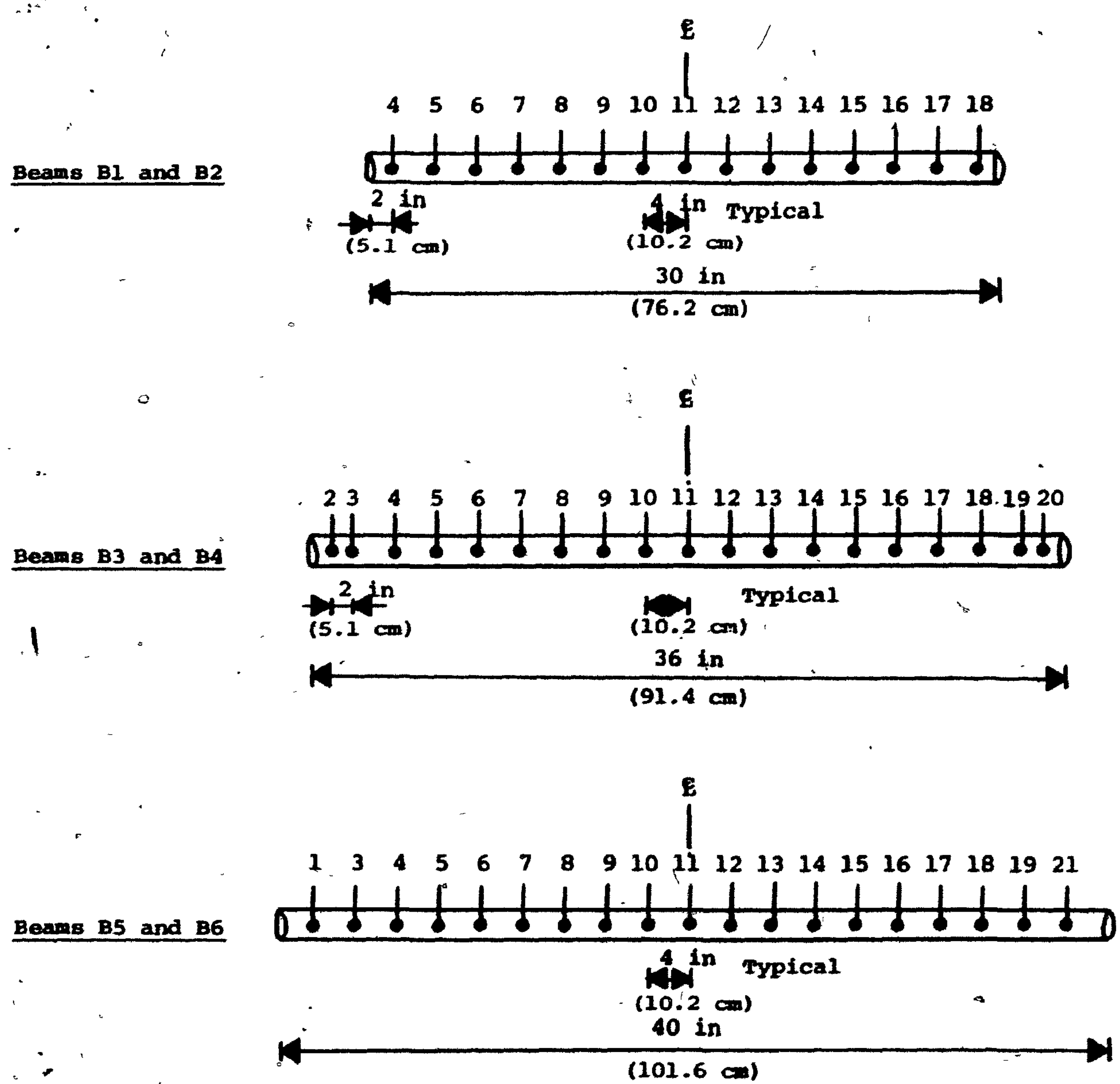

Fig. B.1 Locations of Steel Strain Gauges (#8 Bar)

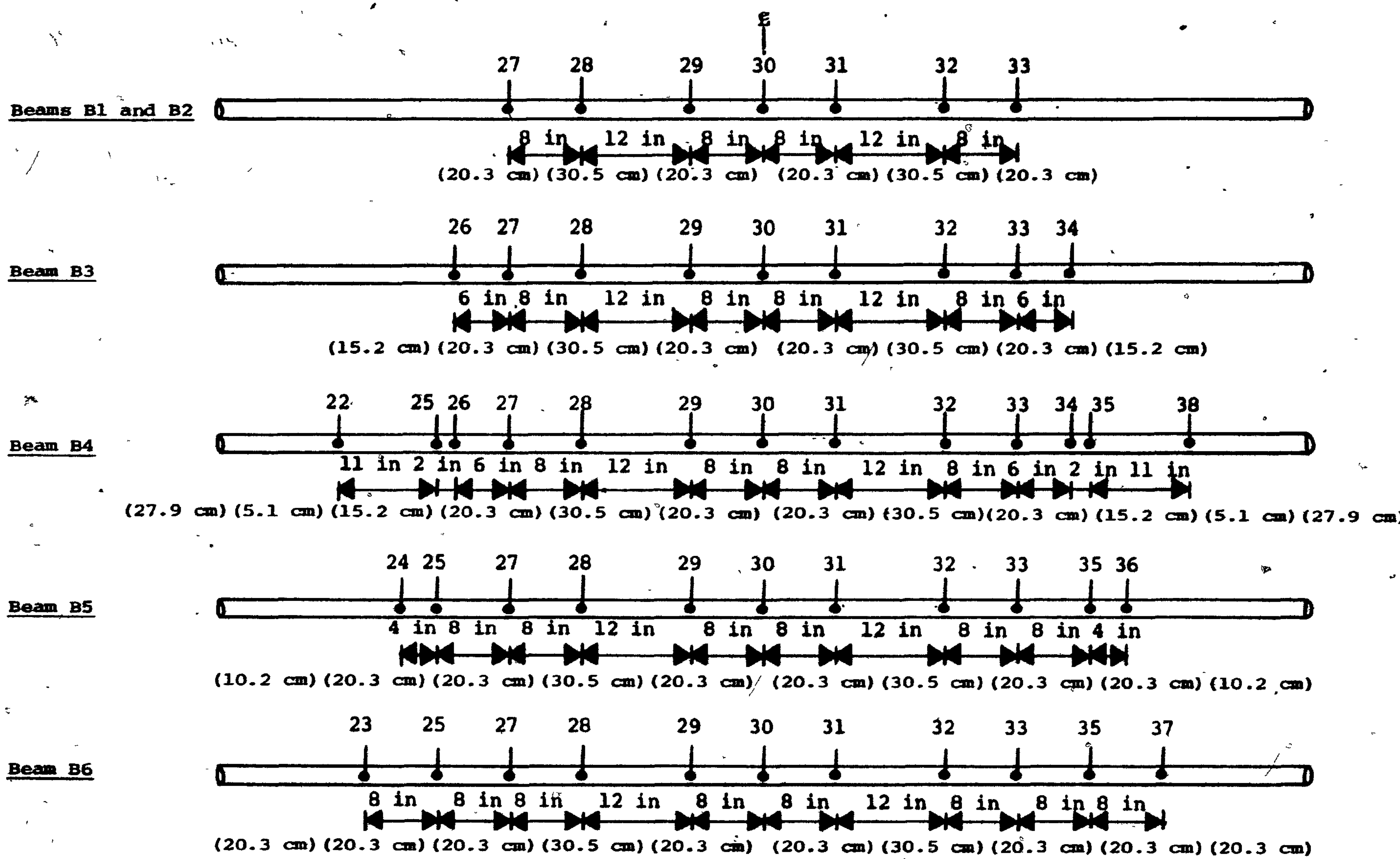

Fig. B.2 Locations of Steel Strain Gauges (#6 Bar)

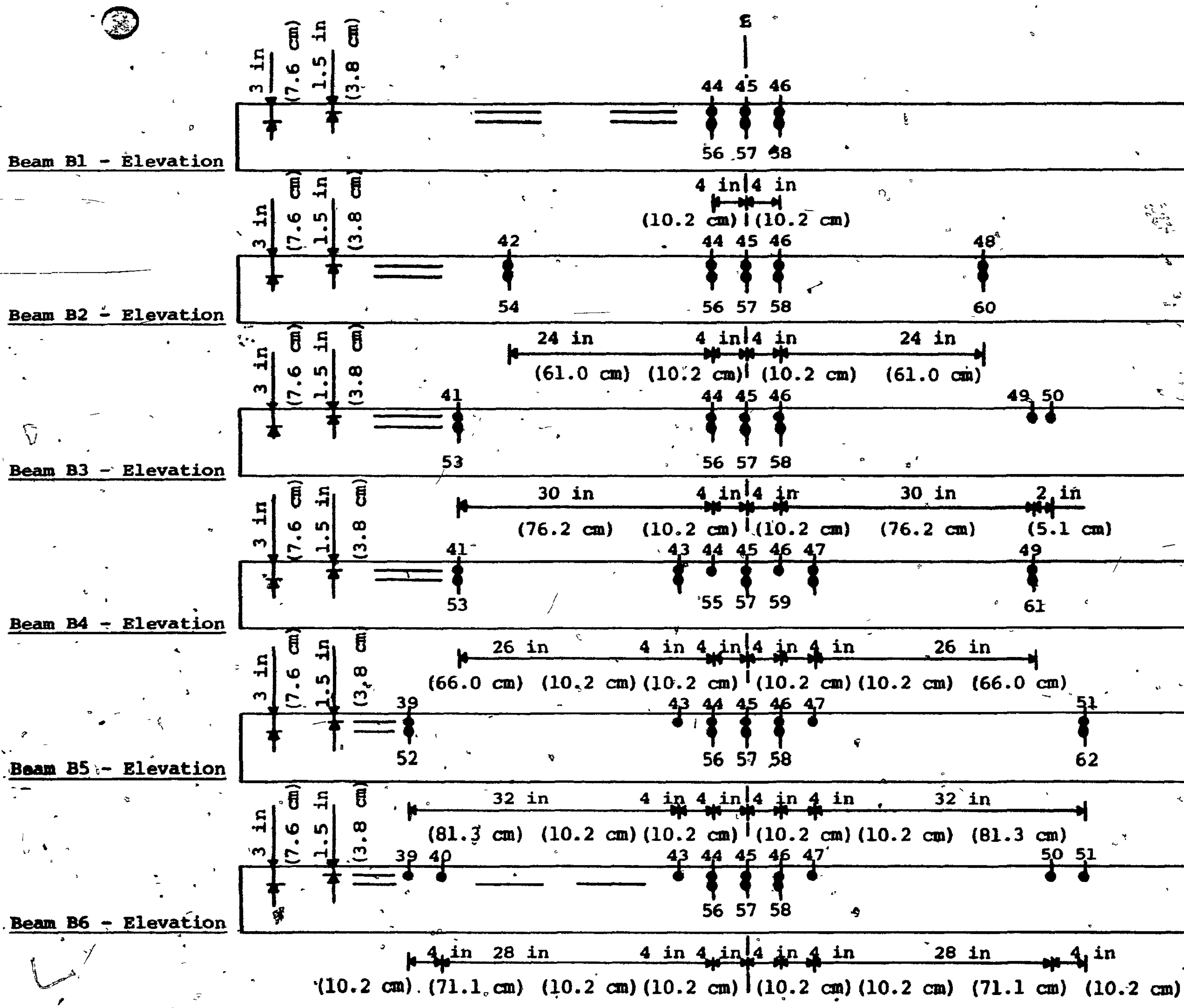

Fig. B.3 Locations of Concrete Strain Gauges

APPENDIX C

EXPERIMENTAL DATA

TABLE C.1

LOAD, P		DEFLECTION, Δ												COMMENTS
		BEAM B1		BEAM B2		BEAM B3		BEAM B4		BEAM B5		BEAM B6		
kips	kN	in	mm	in	mm	in	mm	in	mm	in	mm	in	mm	
0	0	0	0	0	0	0	0	0	0	0	0	0	0	
2.61	11.62	0.0120	0.304	0.0065	0.165	0.0064	0.162	0.0060	0.152	0.0060	0.152	0.0040	0.101	
5.22	23.24	0.0220	0.558	0.0170	0.431	0.0180	0.457	0.0140	0.355	0.0140	0.355	0.0100	0.254	
7.84	34.86	0.0290	0.736	0.0240	0.609	0.0260	0.660	0.0210	0.533	0.0230	0.584	0.0160	0.406	
10.45	46.47	0.0480	1.219	0.0410	1.041	0.0400	1.016	0.0350	0.889	0.0350	0.889	0.0260	0.660	
13.06	58.09	0.0620	1.574	0.0570	1.447	0.0570	1.447	0.0520	1.320	0.0500	1.270	0.0380	0.965	
15.67	69.71	0.0820	2.082	0.0760	1.930	0.0750	1,905	0.0710	1.803	0.0700	1.778	0.0620	1.574	
18.28	81.33	0.1060	2.692	0.0980	2.489	0.1000	2.540	0.0900	2.286	0.0900	2.286	0.0780	1.981	
20.90	92.95	0.1260	3.200	0.1200	3.048	0.1230	3.124	0.1140	2.895	0.1160	2.946	0.0980	2.489	
23.51	104.57	0.1540	3.911	0.1480	3.759	0.1470	3.733	0.1340	3.403	0.1380	3.505	0.1180	2.997	
26.12	116.19	0.1830	4.648	0.1770	4.495	0.1750	4.445	0.1660	4.216	0.1620	4.114	0.1390	3.530	
28.73	127.81	0.2160	5.486	0.2080	5.283	0.2040	5.181	0.1920	4.876	0.1900	4.826	0.1610	4.089	
31.34	139.42	0.2500	6.350	0.2400	6.096	0.2350	5.969	0.2150	5.461	0.2160	5.486	0.1870	4.749	
33.96	151.04	0.2810	7.137	0.2700	6.858	0.2650	6.731	0.2430	6.172	0.2400	6.096	0.2110	5.359	
36.59	162.66	0.3180	8.077	0.3060	7.772	0.3000	7.620	0.2700	6.858	0.2740	6.959	0.2380	6.045	
37.00	164.58	0.3860	9.804											Maximum capacity and Failure of Beam B1
34.61	153.95	0.4440	11.277											
39.00	173.48			0.4300	10.922									Maximum capacity and Failure of Beam B2
38.25	170.14			0.5200	13.208									
38.25	170.14			0.6000	15.240									
39.18	174.28					0.3540	8.991	0.2980	7.569	0.3040	7.721	0.2640	6.705	
40.00	177.93					0.3780	9.601							Maximum capacity and Failure of Beam B3
34.75	154.57					0.4860	12.344							
41.79	185.89							0.3280	8.331	0.3320	8.432	0.2910	7.391	
43.10	191.72							0.3420	8.686	0.3500	8.890	0.3060	7.772	
44.40	197.52							0.3660	9.296	0.3840	9.753	0.3180	8.077	
45.00	200.17									0.4460	11.328			Maximum capacity and Failure of Beam B5
44.40	197.52									0.4800	12.192			
45.68	203.19							0.4440	11.277			0.3510	8.915	
46.98	208.98							0.5700	14.478			0.4200	10.668	
46.98	208.98							0.6180	15.697					Maximum capacity and Failure of Beam B4
46.98	208.98							0.6560	16.662					
48.50	215.74											0.5180	13.157	
49.25	219.07											0.6300	16.002	
49.50	220.19											0.6980	17.729	Maximum capacity and Failure of Beam B6
49.50	220.19											0,7920	20.116	

TABLE C.2

TENSILE STRAINS ALONG #8 REINFORCING BAR (MICRO IN/IN)

DISTANCE FROM CENTRE	in	36	34	32	28	24	20	16	12	8	4	CENTRE	4	8	12	16	20	24	28	32	34	36
	cm	91.4	86.4	81.3	71.1	61.0	50.8	40.6	30.5	20.3	10.2	0	10.2	20.3	30.5	40.6	50.8	61.0	71.1	81.3	86.4	91.4
LOAD	GAUGE NUMBER	1	2	3	4	5	6	7	8	9	10	11	12	13	14	15	16	17	18	19	20	21
kips kN																						
	BEAM B1				0008	0014	0018	0018	0018	0020	0033	0035	0028	0020	0022	0018	0015	0009	0012			
	BEAM B2				0008	0015	0016	0021	0020	0026	0023	0026	0023	0025	0028	0025	0014	0016	0006			
2.6 11.6	BEAM B3		0010	0010	0016	0019	0021	0026	0031	0049	0042	0050	0036	0044	0034	0023	0024	0017	0014	0010	0010	
	BEAM B4		0010	0010	0012	0015	0016	0017	0020	0020	0025	0030	0022	0026	0017	0016	0014	0017	0010	0010	0012	
	BEAM B5	0023		0023	0015	0038	0056	0050	0052	0050	0053	0058	0053	0055	0050	0050	0045	0038	0040	0030		0018
	BEAM B6	0015		0028	0035	0038	0045	0038	0048	0045	0048	0060	0055	0052	0045	0048	0037	0030	0030	0032		0010
	BEAM B1				0016	0030	0035	0041	0036	0047	0044	0054	0040	0050	0039	0046	0030	0025	0023			
	BEAM B2				0022	0030	0032	0041	0038	0052	0045	0051	0047	0050	0055	0048	0028	0032	0026			
5.2 23.2	BEAM B3		0020	0020	0033	0038	0040	0045	0068	0090	0080	0100	0070	0095	0070	0040	0045	0032	0030	0020	0020	
	BEAM B4		0017	0020	0024	0030	0032	0033	0038	0045	0050	0054	0042	0050	0030	0032	0029	0022	0021	0022	0022	
	BEAM B5	0041		0048	0020	0073	0103	0095	0100	0098	0106	0110	0103	0105	0095	0100	0082	0079	0063	0055		0032
	BEAM B6	0044		0050	0070	0071	0088	0085	0092	0090	0093	0100	0098	0108	0090	0096	0073	0069	0065	0056		0034
	BEAM B1				0055	0045	0105	0075	0136	0089	0076	0120	0136	0135	0075	0118	0092	0035	0045			
	BEAM B2				0040	0071	0055	0090	0071	0080	0105	0090	0140	0120	0104	0065	0045	0061	0055			
7.8 34.9	BEAM B3		0042	0032	0090	0095	0090	0146	0119	0141	0179	0150	0145	0196	0185	0085	0139	0075	0070	0045	0040	
	BEAM B4		0035	0028	0060	0090	0118	0140	0120	0135	0165	0120	0150	0170	0080	0109	0089	0071	0070	0045	0030	
	BEAM B5	0075		0075	0105	0105	0150	0132	0149	0165	0210	0195	0150	0208	0196	0166	0150	0121	0150	0105		0060
	BEAM B6	0060		0080	0133	0090	0106	0106	0185	0183	0196	0210	0226	0130	0135	0150	0150	0135	0100	0095		0055
	BEAM B1				0090	0090	0185	0166	0284	0150	0180	0238	0255	0240	0165	0225	0148	0070	0075			
	BEAM B2				0051	0110	0091	0121	0136	0141	0195	0139	0221	0170	0165	0099	0074	0089	0066			
10.4 46.5	BEAM B3		0058	0045	0135	0180	0180	0254	0285	0210	0306	0225	0230	0342	0319	0182	0233	0121	0106	0070	0053	
	BEAM B4		0045	0028	0090	0148	0196	0255	0211	0212	0269	0195	0270	0268	0166	0195	0171	0109	0100	0060	0040	
	BEAM B5	0105		0105	0170	0164	0225	0196	0269	0285	0375	0363	0276	0358	0320	0239	0256	0195	0239	0150		0105
	BEAM B6	0090		0105	0179	0165	0153	0137	0300	0299	0326	0310	0375	0197	0210	0210	0250	0225	0150	0133		0096

TABLE C.2 (continued)

TENSILE STRAINS ALONG #8 REINFORCING BAR (MICRO IN/IN)

DISTANCE FROM CENTRE		in	36	34	32	28	24	20	16	12	8	4	CENTRE	4	8	12	16	20	24	28	32	34	36
		cm	91.4	86.4	81.3	71.1	61.0	50.8	40.6	30.5	20.3	10.2	0	10.2	20.3	30.5	40.6	50.8	61.0	71.1	81.3	86.4	91.4
LOAD	GAUGE NUMBER		1	2	3	4	5	6	7	8	9	10	11	12	13	14	15	16	17	18	19	20	21
kips kN																							
	BEAM B1					0120	0202	0270	0315	0404	0389	0411	0470	0384	0403	0320	0352	0250	0156	0095			
	BEAM B2					0063	0150	0190	0200	0270	0252	0310	0255	0330	0264	0288	0200	0183	0116	0078			
13.1	BEAM B3			0071	0090	0182	0327	0313	0421	0448	0420	0452	0518	0450	0503	0454	0355	0334	0300	0152	0088	0067	
58.1	BEAM B4			0060	0030	0154	0192	0265	0351	0335	0365	0375	0432	0376	0418	0332	0270	0239	0151	0163	0069	0049	
	BEAM B5		0128		0201	0242	0308	0400	0419	0455	0530	0490	0525	0420	0500	0461	0429	0455	0346	0323	0210		0132
	BEAM B6		0103		0142	0231	0300	0313	0349	0403	0428	0500	0417	0517	0412	0345	0373	0345	0348	0225	0183		0110
	BEAM B1					0165	0285	0361	0434	0481	0411	0532	0569	0510	0441	0419	0459	0329	0235	0120			
	BEAM B2					0085	0209	0275	0316	0375	0375	0436	0406	0466	0391	0420	0301	0255	0179	0109			
15.7	BEAM B3			0090	0120	0269	0420	0390	0535	0558	0550	0585	0646	0569	0609	0586	0496	0422	0390	0220	0135	0080	
69.7	BEAM B4			0075	0075	0181	0276	0360	0448	0451	0500	0512	0556	0506	0556	0452	0389	0335	0226	0225	0080	0061	
	BEAM B5		0180		0290	0330	0436	0496	0610	0550	0662	0573	0632	0529	0628	0560	0645	0546	0469	0359	0269		0150
	BEAM B6		0120		0208	0330	0405	0450	0450	0510	0556	0612	0525	0637	0523	0451	0486	0450	0445	0300	0232		0150
	BEAM B1					0210	0375	0452	0526	0586	0615	0645	0692	0645	0658	0523	0545	0421	0310	0150			
	BEAM B2					0104	0255	0358	0434	0495	0510	0548	0526	0574	0510	0526	0406	0334	0255	0151			
18.3	BEAM B3			0112	0140	0370	0495	0470	0645	0680	0675	0719	0760	0692	0713	0708	0619	0508	0495	0285	0180	0100	
81.3	BEAM B4			0091	0120	0226	0332	0435	0555	0552	0630	0647	0658	0635	0673	0562	0508	0435	0300	0273	0106	0075	
	BEAM B5		0218		0376	0422	0552	0601	0615	0643	0776	0677	0758	0629	0742	0662	0658	0629	0578	0399	0335		0175
	BEAM B6		0150		0302	0405	0500	0572	0548	0617	0673	0735	0630	0755	0640	0560	0582	0523	0542	0370	0273		0185
	BEAM B1					0240	0450	0515	0660	0688	0750	0759	0795	0778	0809	0629	0661	0495	0376	0175			
	BEAM B2					0121	0306	0439	0556	0603	0645	0673	0650	0707	0615	0640	0525	0418	0329	0166			
20.9	BEAM B3			0129	0210	0450	0570	0542	0750	0810	0810	0853	0886	0822	0810	0837	0750	0586	0585	0345	0224	0115	
92.9	BEAM B4			0122	0152	0258	0406	0510	0657	0674	0752	0784	0790	0762	0793	0680	0628	0526	0358	0329	0112	0096	
	BEAM B5		0260		0469	0495	0672	0688	0710	0735	0898	0780	0877	0737	0871	0758	0764	0722	0710	0436	0400		0196
	BEAM B6		0170		0368	0478	0599	0675	0662	0722	0780	0850	0750	0870	0749	0663	0693	0630	0633	0425	0325		0216

TABLE C.2 (continued)

TENSILE STRAINS ALONG #8 REINFORCING BAR (MICRO IN/IN)																						
DISTANCE FROM CENTRE	in	36	34	32	28	24	20	16	12	8	4	CENTRE	4	8	12	16	20	24	28	32	34	36
	cm	91.4	86.4	81.3	71.1	61.0	50.8	40.6	30.5	20.3	10.2	0	10.2	20.3	30.5	40.6	50.8	61.0	71.1	81.3	86.4	91.4
LOAD	GAUGE NUMBER	1	2	3	4	5	6	7	8	9	10	11	12	13	14	15	16	17	18	19	20	21
kips kN																						
	BEAM B1				0290	0525	0598	0764	0762	0870	0871	0900	0902	0945	0735	0735	0586	0451	0220			
	BEAM B2				0149	0360	0526	0661	0722	0776	0794	0756	0827	0734	0750	0630	0495	0404	0195			
23.5 104.6	BEAM B3		0151	0260	0540	0655	0628	0855	0919	0946	0976	1003	0943	0918	0962	0886	0675	0676	0408	0270	0125	
	BEAM B4		0130	0191	0316	0470	0600	0736	0763	0868	0920	0902	0902	0925	0775	0767	0623	0432	0390	0120	0105	
	BEAM B5	0310		0557	0586	0789	0784	0828	0830	1024	0885	0975	0841	1000	0852	0868	0812	0835	0475	0467		0225
	BEAM B6	0200		0446	0570	0703	0793	0765	0825	0890	0960	0855	0991	0865	0770	0790	0738	0720	0522	0373		0240
	BEAM B1				0315	0600	0672	0870	0835	0987	0980	0991	1028	1075	0820	0850	0658	0523	0260			
	BEAM B2				0153	0415	0609	0775	0830	0898	0912	0880	0953	0848	0870	0735	0570	0472	0230			
26.1 116.2	BEAM B3		0161	0322	0632	0730	0705	0965	1040	1063	1101	1130	1053	1022	1071	1018	0750	0761	0465	0315	0130	
	BEAM B4		0149	0228	0375	0535	0673	0840	0881	0992	1049	1010	1035	1050	0883	0871	0709	0503	0438	0120	0123	
	BEAM B5	0353		0650	0679	0908	0879	0930	0950	1154	0975	1110	0945	1113	0954	0975	0889	0950	0502	0520		0240
	BEAM B6	0225		0528	0641	0816	0919	0873	0930	1000	1080	0954	1091	0972	0885	0900	0833	0801	0600	0413		0289
	BEAM B1				0345	0640	0765	0949	0958	1096	1079	1095	1125	1193	0898	0931	0751	0604	0290			
	BEAM B2				0210	0510	0675	0871	0921	1000	1005	0991	1051	0946	0954	0810	0675	0510	0255			
28.7 127.8	BEAM B3		0200	0390	0655	0840	0810	1034	1143	1163	1215	1247	1170	1125	1200	1115	0840	0820	0571	0375	0179	
	BEAM B4		0181	0270	0406	0626	0795	0928	0990	1083	1131	1121	1114	1153	1002	0976	0795	0589	0500	0189	0155	
	BEAM B5	0375		0692	0730	1006	0960	1052	1020	1250	1085	1210	1050	1205	1052	1100	0986	1030	0620	0570		0300
	BEAM B6	0251		0590	0705	0870	1020	0945	1035	1080	1170	1050	1201	1080	0994	0992	0945	0855	0675	0460		0300
	BEAM B1				0360	0660	0901	1011	1065	1214	1215	1200	1260	1282	1005	1006	0815	0660	0330			
	BEAM B2				0249	0598	0741	0975	1010	1095	1096	1112	1152	1036	1045	0885	0778	0525	0286			
31.3 139.4	BEAM B3		0240	0445	0675	0945	0930	1108	1232	1272	1322	1350	1288	1232	1318	1220	0930	0871	0646	0431	0219	
	BEAM B4		0213	0298	0462	0703	0900	1014	1100	1185	1215	1230	1200	1257	1110	1066	0868	0682	0548	0241	0192	
	BEAM B5	0412		0730	0794	1110	1049	1155	1130	1353	1192	1310	1156	1307	1160	1215	1078	1110	0722	0632		0338
	BEAM B6	0283		0650	0750	0945	1125	1020	1143	1165	1288	1156	1321	1206	1094	1095	1068	0917	0750	0518		0325

TABLE C.2 (continued)

TENSILE STRAINS ALONG #8 REINFORCING BAR (MICRO IN/IN)

DISTANCE FROM CENTRE		36	34	32	28	24	20	16	12	8	4	CENTRE	4	8	12	16	20	24	28	32	34	36
	cm	91.4	86.4	81.3	71.1	61.0	50.8	40.6	30.5	20.3	10.2	0	10.2	20.3	30.5	40.6	50.8	61.0	71.1	81.3	86.4	91.4
LOAD	GAUGE NUMBER	1	2	3	4	5	6	7	8	9	10	11	12	13	14	15	16	17	18	19	20	21
kips kN																						
34.0 151.0	BEAM B1				0380	0692	0990	1095	1183	1351	1320	1320	1364	1410	1095	1079	0910	0748	0360			
	BEAM B2				0300	0705	0810	1080	1100	1200	1201	1215	1250	1120	1135	0960	0884	0556	0320			
	BEAM B3		0270	0519	0701	1050	1031	1172	1316	1380	1438	1433	1408	1333	1444	1320	1000	0931	0738	0479	0255	
	BEAM B4		0244	0329	0513	0796	1003	1095	1215	1275	1290	1335	1278	1350	1225	1152	0946	0765	0618	0298	0218	
	BEAM B5	0436		0770	0856	1206	1140	1270	1220	1455	1293	1407	1265	1410	1275	1333	1172	1182	0838	0690		0326
	BEAM B6	0330		0705	0822	1010	1216	1110	1244	1245	1393	1246	1439	1332	1214	1200	1170	0970	0847	0573		0370
36.6 162.7	BEAM B1				0390	0710	1088	1150	1281	1472	1440	1415	1470	1505	1181	1150	0962	0810	0378			
	BEAM B2				0331	0800	0878	1173	1190	1300	1281	1322	1350	1203	1226	1025	0980	0564	0350			
	BEAM B3		0300	0531	0715	1155	1126	1230	1416	1480	1542	1592	1520	1425	1555	1423	1105	0978	0813	0534	0290	
	BEAM B4		0271	0350	0570	0872	1100	1165	1322	1353	1376	1432	1369	1455	1331	1253	1015	0853	0670	0350	0248	
	BEAM B5	0465		0809	0911	1303	1230	1395	1320	1550	1395	1530	1365	1485	1380	1455	1275	1275	0945	0730		0420
	BEAM B6	0370		0759	0881	1085	1315	1200	1352	1328	1510	1339	1549	1450	1322	1305	1280	1020	0915	0620		0405
37.0 164.6	BEAM B1				0410	0720	1108	1162	1301	1492	1455	1430	1495	1525	1195	1165	0987	0825	0400			
	BEAM B2				0345	0820	0900	1195	1210	1335	1305	1345	1371	1225	1240	1050	1002	0575	0365			
	BEAM B3		0310	0540	0723	1175	1148	1246	1430	1505	1571	1620	1539	1460	1581	1440	1121	0992	0830	0543	0300	
	BEAM B4		0285	0370	0585	0900	1118	1184	1340	1369	1390	1468	1380	1469	1345	1269	1033	0872	0685	0360	0260	
	BEAM B5	0480		0824	0930	1318	1245	1406	1335	1573	1420	1550	1395	1510	1395	1472	1280	1290	0960	0742		0435
	BEAM B6	0380		0770	0891	1100	1335	1215	1370	1350	1628	1362	1575	1470	1340	1320	1295	1035	0930	0635		0415
39.0 173.5	BEAM B2				0418	0890	1010	1275	1280	1452	1425	1460	1460	1285	1310	1100	1073	0600	0412			
	BEAM B3		0323	0582	0735	1260	1225	1300	1500	1579	1650	1709	1639	1529	1672	1521	1191	1035	0900	0585	0305	
	BEAM B4		0305	0432	0605	0758	1197	1249	1425	1441	1456	1570	1440	1559	1456	1342	1096	0940	0732	0406	0286	
	BEAM B5	0509		0865	1000	1355	1320	1488	1407	1650	1498	1608	1468	1607	1478	1568	1366	1338	1063	0768		0465
	BEAM B6	0405		0790	0930	1158	1423	1305	1440	1502	1608	1488	1659	1538	1455	1393	1365	1090	0992	0688		0449

TABLE C.2 (continued)

TENSILE STRAINS ALONG #8 REINFORCING BAR (MICRO IN/IN)

DISTANCE FROM CENTRE	in	36	34	32	28	24	20	16	12	8	4	CENTRE	4	8	12	16	20	24	28	32	34	36
	cm	91.4	86.4	81.3	71.1	61.0	50.8	40.6	30.5	20.3	10.2	0	10.2	20.3	30.5	40.6	50.8	61.0	71.1	81.3	86.4	91.4
LOAD	GAUGE NUMBER	1	2	3	4	5	6	7	8	9	10	11	12	13	14	15	16	17	18	19	20	21
kips kN																						
40.0 177.9	BEAM B3		0338	0600	0750	1296	1260	1320	1538	1610	1680	1750	1668	1560	1715	1557	1225	1055	0930	0605	0320	
	BEAM B4		0320	0463	0628	0997	1241	1287	1470	1485	1485	1620	1470	1590	1485	1383	1122	0973	0752	0418	0300	
	BEAM B5	0524		0883	1030	1392	1348	1531	1452	1688	1538	1652	1510	1632	1517	1605	1394	1367	1095	0785		0490
	BEAM B6	0420		0812	0960	1187	1456	1349	1500	1520	1649	1546	1696	1590	1500	1430	1402	1112	1007	0710		0465
41.8 185.9	BEAM B4		0340	0519	0659	1050	1308	1334	1545	1540	1545	1708	1523	1665	1576	1438	1185	1020	0778	0465	0320	
	BEAM B5	0556		0933	1090	1435	1427	1606	1516	1755	1605	1725	1575	1712	1592	1690	1469	1402	1180	0810		0513
	BEAM B6	0450		0850	1005	1245	1530	1429	1580	1618	1726	1647	1770	1668	1580	1505	1458	1158	1050	0760		0485
44.4 197.5	BEAM B4		0370	0600	0700	1140	1408	1425	1650	1635	1620	1832	1605	1760	1680	1545	1255	1112	0850	0525	0349	
	BEAM B5	0590		0985	1160	1495	1510	1708	1605	1858	1710	1833	1689	1800	1697	1800	1575	1465	1303	0841		0560
	BEAM B6	0500		0900	1063	1323	1632	1545	1700	1763	1845	1808	1898	1765	1735	1622	1552	1228	1129	0829		0525
45.0 200.2	BEAM B4		0385	0615	0715	1155	1440	1440	1665	1650	1634	1868	1620	1785	1700	1560	1275	1125	0865	0540	0360	
	BEAM B5	0610		1010	1203	1527	1546	1735	1633	1872	1732	1865	1724	1835	1720	1833	1591	1475	1320	0855		0581
	BEAM B6	0520		0915	1080	1335	1650	1565	1730	1780	1870	1840	1920	1800	1760	1640	1575	1252	1150	0850		0545
47.0 209.1	BEAM B4		0405	0670	0750	1215	1525	1500	1770	1710	1700	1965	1690	1860	1780	1635	1320	1195	0900	0570	0385	
	BEAM B6	0585		0950	1125	1400	1725	1665	1820	1830	1965	1910	2010	-1875	1855	1710	1650	1306	1200	0900		0615
49.5 220.2	BEAM B6	0680		0990	1180	1480	1810	1770	1918	1886	2073	2018	2123	1965	2006	1815	1740	1365	1265	0970		0700

TABLE C.3

TENSILE STRAINS ALONG #6 REINFORCING BAR (MICRO IN/IN)																		
DISTANCE FROM CENTRE	in	47	44	40	36	34	28	20	8	CENTRE	8	20	28	34	36	40	44	47
	cm	119.4	111.8	101.6	91.4	86.4	71.1	50.8	20.3	0	20.3	50.8	71.1	86.4	91.4	101.6	111.8	119.4
LOAD	GAUGE NUMBER	22	23	24	25	26	27	28	29	30	31	32	33	34	35	36	37	38
kips kN																		
	BEAM B1						0014	0018	0010	0025	0018	0015	0012					
	BEAM B2						0018	0025	0025	0024	0028	0023	0018					
2.6 11.6	BEAM B3					0015	0020	0025	0020	0024	0020	0017	0020	0015				
	BEAM B4	0016			0030	0042	0018	0038	0035	0047	0035	0038	0018	0022	0018			0014
	BEAM B5			0018	0032		0018	0038	0040	0046	0035	0038	0027		0032	0018		
	BEAM B6		0016		0025		0028	0047	0034	0040	0034	0044	0032		0025		0016	
	BEAM B1						0022	0036	0025	0060	0034	0030	0026					
	BEAM B2						0022	0048	0048	0045	0054	0043	0030					
5.2 23.2	BEAM B3					0018	0038	0040	0038	0050	0053	0038	0036	0019				
	BEAM B4	0024			0062	0062	0030	0070	0070	0093	0090	0055	0030	0034	0038			0019
	BEAM B5			0030	0062		0034	0084	0080	0084	0075	0062	0060		0045	0030		
	BEAM B6		0031		0045		0058	0094	0075	0081	0057	0090	0073		0045		0030	
	BEAM B1						0036	0064	0055	0160	0060	0060	0045					
	BEAM B2						0038	0075	0068	0080	0082	0070	0055					
7.8 34.9	BEAM B3					0030	0048	0064	0069	0120	0090	0060	0042	0031				
	BEAM B4	0041			0071	0077	0042	0120	0100	0164	0135	0077	0045	0048	0058			0037
	BEAM B5			0045	0088		0059	0152	0134	0135	0128	0108	0089		0064	0051		
	BEAM B6		0045		0060		0075	0135	0104	0122	0083	0132	0103		0075		0045	
	BEAM B1						0048	0107	0105	0345	0105	0100	0075					
	BEAM B2						0055	0120	0094	0120	0128	0105	0078					
10.4 46.5	BEAM B3					0041	0072	0150	0150	0228	0172	0106	0058	0053				
	BEAM B4	0052			0092	0103	0060	0180	0151	0270	0210	0092	0065	0069	0065			0048
	BEAM B5			0070	0108		0075	0252	0226	0196	0195	0181	0118		0089	0075		
	BEAM B6		0062		0090		0106	0182	0152	0174	0121	0182	0136		0108		0057	

TABLE C.3 (continued)

TENSILE STRAINS ALONG #6 REINFORCING BAR (MICRO IN/IN)

DISTANCE FROM CENTRE	in			47	44	40	36	34	28	20	8	CENTRE	8	20	28	34	36	40	44	47		
	cm			119.4	111.8	101.6	91.4	86.4	71.1	50.8	20.3	0	20.3	50.8	71.1	86.4	91.4	101.6	111.8	119.4		
LOAD	GAUGE NUMBER			22	23	24	25	26	27	28	29	30	31	32	33	34	35	36	37	38		
kips kN																						
	BEAM B1								0160	0128	0175	0470	0330	0125	0120							
	BEAM B2								0078	0175	0140	0221	0200	0140	0135							
13.1 58.1	BEAM B3							0059	0120	0272	0245	0380	0318	0178	0079	0091						
	BEAM B4			0064			0159	0127	0072	0256	0235	0390	0388	0138	0075	0090	0101			0058		
	BEAM B5					0120	0146		0106	0356	0348	0300	0304	0314	0169		0119	0127				
	BEAM B6				0078		0120		0134	0272	0225	0311	0150	0253	0190		0137		0063			
	BEAM B1								0258	0168	0280	0585	0548	0160	0258							
	BEAM B2								0168	0240	0248	0357	0324	0220	0226							
15.7 69.7	BEAM B3							0089	0159	0360	0410	0558	0465	0268	0121	0121						
	BEAM B4			0077			0234	0223	0102	0406	0375	0570	0541	0196	0105	0135	0186			0073		
	BEAM B5					0151	0182		0150	0464	0474	0405	0434	0449	0255		0153	0156				
	BEAM B6				0093		0150		0166	0337	0348	0465	0242	0300	0249		0168		0075			
	BEAM B1								0366	0240	0450	0690	0702	0212	0408							
	BEAM B2								0286	0300	0390	0487	0435	0270	0338							
18.3 81.3	BEAM B3							0139	0225	0438	0525	0750	0690	0378	0210	0236						
	BEAM B4			0098			0345	0290	0135	0496	0494	0690	0646	0300	0135	0195	0255			0086		
	BEAM B5					0190	0235		0257	0555	0614	0542	0562	0570	0390		0195	0195				
	BEAM B6				0120		0166		0242	0420	0458	0577	0375	0389	0319		0196		0107			
	BEAM B1								0755	0364	0600	0790	0856	0256	0602							
	BEAM B2								0438	0406	0545	0600	0570	0374	0522							
20.9 92.9	BEAM B3							0229	0330	0512	0660	0870	0810	0487	0300	0352						
	BEAM B4			0121			0510	0370	0180	0586	0600	0834	0750	0377	0210	0328	0375			0092		
	BEAM B5					0286	0328		0350	0645	0736	0662	0700	0675	0482		0256	0286				
	BEAM B6				0149		0196		0318	0558	0581	0722	0494	0491	0419		0244		0125			

TABLE C.3 (continued)

TENSILE STRAINS ALONG #6 REINFORCING BAR (MICRO IN/IN)

DISTANCE FROM CENTRE	in			47	44	40	36	34	28	20	8	CENTRE	8	20	28	34	36	40	44	47		
	cm			119.4	111.8	101.6	91.4	86.4	71.1	50.8	20.3	0	20.3	50.8	71.1	86.4	91.4	101.6	111.8	119.4		
LOAD	GAUGE NUMBER			22	23	24	25	26	27	28	29	30	31	32	33	34	35	36	37	38		
kips kN																						
	BEAM B1								0975	0470	0735	0895	0992	0390	1005							
	BEAM B2								0860	0498	0645	0722	0720	0476	0860							
23.5 104.6	BEAM B3							0551	0420	0590	0765	1005	0920	0560	0378	0620						
	BEAM B4			0152			0676	0525	0285	0675	0706	0960	0870	0482	0320	0452	0522			0124		
	BEAM B5					0391	0450		0432	0728	0862	0794	0855	0772	0558		0390	0406				
	BEAM B6				0168		0247		0442	0710	0706	0855	0600	0647	0494		0298		0158			
	BEAM B1								1170	0550	0858	0990	1118	0512	1188							
	BEAM B2								1070	0586	0780	0850	0812	0556	1032							
26.1 116.2	BEAM B3							0791	0498	0670	0875	1125	1033	0645	0481	.0872						
	BEAM B4			0210			0813	0675	0360	0780	0810	1063	0975	0558	0405	0572	0752			0180		
	BEAM B5					0542	0572		0524	0824	0984	0928	0976	0872	0648		0511	0628				
	BEAM B6				0195		0329		0498	0841	0817	0976	0737	0771	0570		0374		0195			
	BEAM B1								1340	0667	0992	1082	1218	0618	1356							
	BEAM B2								1245	0694	0890	0975	0942	0675	1210							
28.7 127.8	BEAM B3							0978	0581	0750	1022	1252	1125	0735	0542	1038						
	BEAM B4			0345			0946	0835	0420	0855	0917	1175	1080	0660	0465	0748	0913			0345		
	BEAM B5					0698	0694		0613	0900	1100	1049	1095	0961	0736		0617	0756				
	BEAM B6				0273		0450		0565	0952	0946	1094	0839	0884	0640		0498		0300			
	BEAM B1								1542	0765	1125	1176	1335	0720	1532							
	BEAM B2								1426	0780	1005	1066	1052	0750	1365							
31.3 139.4	BEAM B3							1200	0651	0840	1125	1362	1230	0840	0630	1262						
	BEAM B4			0465			1098	0988	0470	0960	1020	1270	1185	0750	0565	0926	1052			0436		
	BEAM B5					0824	0800		0689	0982	1222	1170	1222	1050	0825		0736	0925				
	BEAM B6				0450		0563		0648	1053	1050	1226	0961	0991	0722		0600		0482			

TABLE C.3 (continued)

TENSILE STRAINS ALONG #6 REINFORCING BAR (MICRO IN/IN)

DISTANCE FROM CENTRE	in			47	44	40	36	34	28	20	8	CENTRE	8	20	28	34	36	40	44	47		
	cm			119.4	111.8	101.6	91.4	86.4	71.1	50.8	20.3	0	20.3	50.8	71.1	86.4	91.4	101.6	111.8	119.4		
LOAD	GAUGE NUMBER			22	23	24	25	26	27	28	29	30	31	32	33	34	35	36	37	38		
kips kN																						
	BEAM B1								1782	0870	1245	1290	1470	0825	1770							
	BEAM B2								1653	0872	1100	1208	1160	0854	1560							
34.0 151.0	BEAM B3							1435	0728	0946	1232	1482	1365	0933	0690	1472						
	BEAM B4			0557			1256	1140	0555	1035	1128	1364	1289	0840	0585	1078	1200			0532		
	BEAM B5					0947	0931		0782	1064	1350	1305	1320	1148	0910		0858	1041				
	BEAM B6				0587		0663		0722	1156	1176	1340	1098	1088	0800		0690		0629			
	BEAM B1								1978	0960	1380	1342	1575	0908	1992							
	BEAM B2								1882	0958	1226	1350	1278	0930	1742							
36.6 162.7	BEAM B3							1635	0805	1076	1350	1580	1485	1026	0780	1678						
	BEAM B4			0652			1389	1290	0600	1128	1230	1455	1394	0930	0630	1238	1336			0616		
	BEAM B5					1053	1043		0870	1170	1470	1425	1438	1252	0940		0990	1170				
	BEAM B6				0733		0750		0809	1246	1282	1455	1184	1196	0885		0779		0751			
	BEAM B1								2013	0978	1412	1397	1592	0930	2040							
	BEAM B2								1920	0970	1241	1370	1305	0946	1780							
37.0 164.6	BEAM B3							1680	0820	1095	1370	1606	1500	1050	0798	1722						
	BEAM B4			0672			1412	1322	0615	1143	1250	1470	1411	0945	0645	1262	1371			0632		
	BEAM B5					1078	1066		0886	1187	1486	1451	1458	1268	0954		1006	1183				
	BEAM B6				0750		0766		0825	1282	1314	1476	1209	1211	0900		0788		0768			
	BEAM B2								2070	1050	1350	1440	1410	1018	1950							
39.0 173.5	BEAM B3							1855	0885	1185	1467	1692	1588	1145	0867	1890						
	BEAM B4			0737			1539	1444	0660	1218	1335	1540	1486	1010	0690	1380	1486			0706		
	BEAM B5					1170	1156		0955	1275	1590	1545	1542	1342	1059		1096	1276				
	BEAM B6				0861		0835		0880	1361	1598	1570	1324	1289	0946		0864		0892			

TABLE C.3 (continued)

TENSILE STRAINS ALONG #6 REINFORCING BAR (MICRO IN/IN)

DISTANCE FROM CENTRE	in	47	44	40	36	34	28	20	8	CENTRE	8	20	28	34	36	40	44	47
	cm	119.4	111.8	101.6	91.4	86.4	71.1	50.8	20.3	0	20.3	50.8	71.1	86.4	91.4	101.6	111.8	119.4
LOAD	GAUGE NUMBER	22	23	24	25	26	27	28	29	30	31	32	33	34	35	36	37	38
kips kN																		
40.0 177.9	BEAM B3					1950	0900	1230	1500	1725	1620	1170	0885	1992				
	BEAM B4	0772			1584	1500	0675	1248	1380	1580	1524	1051	0705	1430	1546			0736
	BEAM B5			1215	1200		0980	1307	1622	1596	1590	1380	1089		1136	1321		
	BEAM B6		0915		0871		0913	1394	1444	1618	1367	1321	0974		0886		0938	
41.8 185.9	BEAM B4	0834			1672	1595	0720	1305	1455	1652	1605	1095	0750	1561	1637			0796
	BEAM B5			1307	1272		1049	1382	1696	1682	1681	1454	1158		1226	1412		
	BEAM B6		1018		0929		0938	1462	1528	1688	1442	1412	1021		0948		1037	
44.4 197.5	BEAM B4	0918			1828	1750	0790	1398	1560	1741	1710	1200	0810	1710	1772			0885
	BEAM B5			1426	1398		1127	1488	1832	1801	1787	1547	1246		1336	1518		
	BEAM B6		1158		1021		1022	1570	1642	1789	1560	1509	1100		1036		1175	
45.0 200.2	BEAM B4	0948			1860	1796	0820	1425	1580	1770	1740	1215	0840	1768	1830			0915
	BEAM B5			1454	1437		1158	1518	1858	1828	1817	1567	1273		1366	1542		
	BEAM B6		1183		1039		1042	1594	1684	1818	1592	1547	1123		1064		1209	
47.0 209.1	BEAM B4	1020			1972	1921	0857	1489	1668	1840	1817	1291	0885	1894	1928			0975
	BEAM B6		1273		1103		1110	1674	1753	1892	1666	1618	1172		1126		1304	
49.5 220.2	BEAM B6		1422		1192		1160	1779	1872	1997	1802	1722	1248		1213		1446	

TABLE C.4

CONCRETE STRAINS AT 1.5 IN. (3.8 cm) FROM TOP COMPRESSION FIBER

DISTANCE FROM CENTRE	in	40	36	34	28	8	4	CENTRE	4	8	28	34	36	40
	cm	101.6	91.4	86.4	71.1	20.3	10.2	0	10.2	20.3	71.1	86.4	91.4	101.6
LOAD	GAUGE NUMBER	39	40	41	42	43	44	45	46	47	48	49	50	51
kips kN														
2.6 11.6	BEAM B1						-0036	-0040	-0030					
	BEAM B2						-0030	-0037	-0028		-0020			
	BEAM B3			-0020			-0035	-0042	-0030			-0022	-0015	
	BEAM B4			-0025		-0035	-0048	-0038	-0045	-0042		-0024		
	BEAM B5	-0016				-0039	-0050	-0045	-0045	-0038				
	BEAM B6	-0018	-0024			-0045	-0045	-0050	-0041	-0035			-0025	-0018
5.2 23.2	BEAM B1						-0070	-0080	-0068					
	BEAM B2						-0075	-0085	-0064		-0045			
	BEAM B3			-0038			-0068	-0075	-0062			-0038	-0030	
	BEAM B4			-0040		-0045	-0067	-0080	-0067			-0035		
	BEAM B5					-0055	-0084	-0088	-0080	-0070				-0029
	BEAM B6	-0028	-0032			-0050	-0068	-0095	-0075	-0060			-0030	-0025
7.8 34.9	BEAM B1						-0180	-0195	-0187					
	BEAM B2						-0175	-0190	-0185		-0120			
	BEAM B3			-0082			-0163	-0180	-0170			-0086	-0072	
	BEAM B4			-0091		-0175	-0182	-0188	-0170	-0170		-0090		
	BEAM B5	-0060				-0185	-0190	-0200	-0188	-0170				-0061
	BEAM B6	-0065	-0075			-0184	-0180	-0195	-0190	-0180			-0070	-0060
10.4 46.5	BEAM B1						-0220	-0230	-0224					
	BEAM B2				-0140		-0215	-0245	-0220		-0150			
	BEAM B3			-0129			-0218	-0240	-0235			-0130	-0110	
	BEAM B4			-0125		-0230	-0235	-0240	-0228	-0220		-0138		
	BEAM B5	-0085				-0220	-0220	-0230	-0235	-0220				-0088
	BEAM B6	-0095	-0110			-0210	-0228	-0250	-0240	-0231			-0125	-0090

TABLE C.4 (continued)

CONCRETE STRAINS AT 1.5 IN (3.8 cm) FROM TOP COMPRESSION FIBER														
DISTANCE FROM CENTRE	in	40	36	34	28	8	4	CENTRE	4	8	28	34	36	40
	cm	101.6	91.4	86.4	71.1	20.3	10.2	0	10.2	20.3	71.1	86.4	91.4	101.6
LOAD	GAUGE NUMBER	39	40	41	42	43	44	45	46	47	48	49	50	51
kips kN														
	BEAM B1						-0255	-0270	-0260					
	BEAM B2						-0270	-0285	-0290		-0170			
13.1 58.1	BEAM B3			-0140			-0260	-0280	-0275			-0145	-0130	
	BEAM B4			-0160		-0160	-0290	-0310	-0295	-0170		-0155		
	BEAM B5					-0170	-0250	-0300	-0285	-0175				-0090
	BEAM B6	-0105	-0095			-0180	-0240	-0290	-0280	-0175			-0090	-0100
	BEAM B1						-0270	-0300	-0260					
	BEAM B2						-0280	-0320	-0290		-0210			
15.7 69.7	BEAM B3			-0150			-0300	-0350	-0310			-0160	-0148	
	BEAM B4			-0140		-0300	-0320	-0365	-0330	-0305		-0170		
	BEAM B5					-0290	-0340	-0360	-0337	-0300				
	BEAM B6	-0140	-0150			-0320	-0330	-0380	-0340	-0330			-0145	-0130
	BEAM B1						-0385	-0420	-0390					
	BEAM B2						-0390	-0430	-0400		-0240			
18.3 81.3	BEAM B3			-0230			-0375	-0430	-0400			-0210	-0200	
	BEAM B4			-0220		-0370	-0390	-0420	-0400	-0380		-0220		
	BEAM B5	-0135				-0390	-0400	-0420	-0390	-0390				-0140
	BEAM B6	-0140	-0170			-0400	-0420	-0450	-0410	-0385			-0160	-0150
	BEAM B1						-0470	-0500	-0460					
	BEAM B2						-0485	-0510	-0490		-0270			
20.9 92.9	BEAM B3			-0230			-0450	-0480	-0420			-0210	-0200	
	BEAM B4			-0250		-0450	-0465	-0490	-0440	-0410		-0230		
	BEAM B5	-0160				-0440	-0480	-0505	-0470	-0420				-0180
	BEAM B6	-0180	-0160			-0460	-0485	-0520	-0490	-0415			-0240	-0200

TABLE C.4 (continued)

CONCRETE STRAINS AT 1.5 IN (3.8 cm) FROM TOP COMPRESSION FIBER

DISTANCE FROM CENTRE	in					40	36	34	28	8	4	CENTRE	4	8	28	34	36	40				
	cm					101.6	91.4	86.4	71.1	20.3	10.2	0	10.2	20.3	71.1	86.4	91.6	101.6				
LOAD	GAUGE NUMBER					39	40	41	42	43	44	45	46	47	48	49	50	51				
kips kN																						
	BEAM B1										-0520	-0550	-0515									
	BEAM B2								-0340		-0540	-0570	-0520		-0350							
23.5 104.6	BEAM B3							-0300			-0510	-0560	-0520			-0290	-0275					
	BEAM B4							-0320		-0510	-0540	-0560	-0500	-0480		-0280						
	BEAM B5					-0190				-0520	-0550	-0570	-0540	-0500				-0180				
	BEAM B6					-0195	-0220			-0500	-0540	-0580	-0530	-0510			-0235	-0200				
	BEAM B1										-0540	-0610	-0520									
	BEAM B2										-0540	-0630	-0600		-0380							
26.1 116.2	BEAM B3							-0330			-0580	-0600	-0570			-0330	-0310					
	BEAM B4							-0335		-0590	-0560	-0620	-0600	-0580		-0350						
	BEAM B5					-0200				-0580	-0560	-0600	-0580	-0560				-0205				
	BEAM B6					-0220	-0200			-0560	-0600	-0640	-0590	-0575			-0240	-0210				
	BEAM B1										-0680	-0700	-0670									
	BEAM B2										-0650	-0720	-0680		-0375							
28.7 127.8	BEAM B3							-0350			-0678	-0700	-0668			-0320	-0300					
	BEAM B4							-0370		-0605	-0688	-0730	-0655	-0612		-0345						
	BEAM B5					-0200				-0640	-0675	-0700	-0670	-0622				-0205				
	BEAM B6					-0210	-0225			-0635	-0695	-0725	-0690	-0637			-0208	-0240				
	BEAM B1										-0700	-0750	-0710									
	BEAM B2										-0760	-0800	-0740		-0430							
31.3 139.4	BEAM B3							-0405			-0770	-0770	-0750			-0400	-0380					
	BEAM B4							-0435		-0700	-0790	-0780	-0750	-0710		-0410						
	BEAM B5					-0250				-0690	-0785	-0750	-0725	-0750				-0260				
	BEAM B6					-0270	-0250			-0750	-0725	-0800	-0698	-0800			-0241	-0251				

TABLE C.4 (continued)

CONCRETE STRAINS AT 1.5 IN (3.8 cm) FROM TOP COMPRESSION FIBER

DISTANCE FROM CENTRE	in	40	36	34	28	8	4	CENTRE	4	8	28	34	36	40
	cm	101.6	91.4	86.4	71.1	20.3	10.2	0	10.2	20.3	71.1	86.4	91.4	101.6
LOAD	GAUGE NUMBER	39	40	41	42	43	44	45	46	47	48	49	50	51
kips kN														
34.0 151.0	BEAM B1						-0760	-0800	-0765					
	BEAM B2						-0795	-0850	-0805		-0460			
	BEAM B3			-0420			-0800	-0840	-0810			-0420	-0330	
	BEAM B4			-0400		-0800	-0840	-0870	-0850	-0800		-0435		
	BEAM B5	-0280				-0845	-0810	-0830	-0840	-0810				-0310
	BEAM B6	-0300	-0320			-0860	-0850	-0870	-0800	-0780			-0350	-0320
36.6 162.7	BEAM B1						-0880	-0910	-0870					
	BEAM B2						-0885	-0940	-0870		-0510			
	BEAM B3			-0485			-0950	-0900	-0910			-0465	-0320	
	BEAM B4			-0495		-0850	-0870	-0930	-0900	-0810		-0480		
	BEAM B5	-0330				-0800	-0870	-0900	-0850	-0815				-0280
	BEAM B6	-0310	-0290			-0930	-0850	-0940	-0900	-0870				-0300
37.0 164.6	BEAM B1						-0885	-0915	-0875					
	BEAM B2						-0886	-0946	-0872		-0515			
	BEAM B3			-0488			-0958	-0907	-0915			-0470	-0326	
	BEAM B4			-0502		-0852	-0878	-0936	-0911	-0817		-0483		
	BEAM B5	-0338				-0816	-0873	-0907	-0854	-0819				-0282
	BEAM B6	-0316	-0350			-0935	-0858	-0941	-0912	-0878			-0338	-0312
39.0 173.5	BEAM B2						-0915	-0990	-0920		-0520			
	BEAM B3			-0512		-0850	-0900	-0997	-0940			-0485	-0450	
	BEAM B4			-0524		-0870	-0930	-1018	-0925	-0870		-0475		
	BEAM B5	-0320				-0980	-0975	-1000	-0970	-0940				
	BEAM B6	-0335	-0355			-0960	-0920	-1010	-0900	-0870			-0360	-0340

TABLE C.4 (continued)

CONCRETE STRAINS AT 1.5 IN (3.8 cm) FROM TOP COMPRESSION FIBER

DISTANCE FROM CENTRE	in					40	36	34	28	8	4	CENTRE	4	8	28	34	36	40				
	cm					101.6	91.4	86.4	71.1	20.3	10.2	0	10.2	20.3	71.1	86.4	91.4	101.6				
LOAD	GAUGE NUMBER					39	40	41	42	43	44	45	46	47	48	49	50	51				
kips kN																						
	BEAM B3							-0524		-0858	-0920	-1000	-0950			-0505	-0465					
40.0 177.9	BEAM B4							-0530		-0876	-0936	-1022	-0930	-0880		-0478						
	BEAM B5					-0327				-0988	-0980	-1010	-0978	-0947								
	BEAM B6					-0348	-0362			-0973	-0932	-1022	-0913	-0877			-0366	-0354				
	BEAM B4							-0535		-0960	-0980	-1050	-0960	-1005		-0570						
41.8 185.9	BEAM B5					-0338				-0970	-1000	-1070	-0975	-0920				-0346				
	BEAM B6					-0360	-0390			-0980	-1020	-1100	-0950	-0890			-0405	-0350				
	BEAM B4							-0585		-0950	-1027	-1150	-1012	-0943		-0605						
44.4 197.5	BEAM B5									-0986	-1068	-1140	-1032	-1000								
	BEAM B6					-0400	-0452			-1006	-1058	-1160	-1070	-0987			-0428	-0350				
	BEAM B4							-0588		-0958	-1035	-1157	-1030	-0952		-0620						
45.0 200.2	BEAM B5									-0996	-1080	-1145	-1043	-1018								
	BEAM B6					-0409	-0458			-1015	-1065	-1168	-1077	-0995			-0436	-0359				
47.0 209.1	BEAM B4							-0620		-1002	-1105	-1218	-1180	-1073		-0650						
	BEAM B6					-0425	-0500			-1078	-1195	-1280	-1200	-1150			-0485	-0410				
49.5 220.2	BEAM B6					-0467	-0588			-1027	-1298	-1387	-1250	-1028			-0612	-0495				

TABLE C.5

CONCRETE STRAINS AT 3 IN (7.6 cm) FROM TOP COMPRESSION FIBER

DISTANCE FROM CENTRE	in	40	34	28	8	4	CENTRE	4	8	28	34	40
	cm	101.6	86.4	71.1	20.3	10.2	0	10.2	20.3	71.1	86.4	101.6
LOAD	GAUGE NUMBER	52	53	54	55	56	57	58	59	60	61	62
kips kN												
2.6 11.6	BEAM B1					-0030	-0035	-0031				
	BEAM B2			-0024		-0027	-0038	-0030		-0025		
	BEAM B3		-0015			-0030	-0035	-0026				
	BEAM B4		-0019		-0015		-0040		-0025		-0020	
	BEAM B5	-0013				-0021	-0035	-0025				-0015
	BEAM B6					-0030	-0038	-0027				
5.2 23.2	BEAM B1					-0050	-0075	-0058				
	BEAM B2			-0040		-0061	-0070	-0060		-0035		
	BEAM B3		-0025			-0058	-0070	-0055				
	BEAM B4				-0065		-0078		-0060		-0040	
	BEAM B5	-0020				-0055	-0072	-0062				-0018
	BEAM B6					-0065	-0080	-0071				
7.8 34.9	BEAM B1					-0080	-0090	-0085				
	BEAM B2			-0046		-0075	-0090	-0078		-0050		
	BEAM B3		-0030			-0090	-0085	-0080				
	BEAM B4		-0038		-0050		-0098		-0055		-0045	
	BEAM B5	-0030				-0082	-0090	-0075				-0035
	BEAM B6					-0075	-0095	-0080				
10.4 46.5	BEAM B1					-0086	-0108	-0090				
	BEAM B2			-0070		-0095	-0120	-0105		-0065		
	BEAM B3		-0035			-0088	-0115	-0107				
	BEAM B4		-0045		-0105		-0125		-0120		-0040	
	BEAM B5	-0042		-0098		-0098	-0110	-0087				-0050
	BEAM B6					-0115	-0130	-0120				

TABLE C.5 (continued)

CONCRETE STRAINS AT 3 IN (7.6 cm) FROM TOP COMPRESSION FIBER

DISTANCE FROM CENTRE	in	40	34	28	8	4	CENTRE	4	8	28	34	40
	cm	101.6	86.4	71.1	20.3	10.2	0	10.2	20.3	71.1	86.4	101.6
LOAD	GAUGE NUMBER	52	53	54	55	56	57	58	59	60	61	62
kips kN												
13.1 58.1	BEAM B1					-0110	-0125	-0105				
	BEAM B2			-0080		-0120	-0135	-0106		-0070		
	BEAM B3		-0085			-0094	-0125	-0104				
	BEAM B4		-0080		-0128		-0140		-0140		-0090	
	BEAM B5	-0050				-0105	-0140	-0115				-0048
	BEAM B6					-0125	-0160	-0130				
15.7 69.7	BEAM B1					-0140	-0150	-0135				
	BEAM B2			-0100		-0150	-0165	-0145		-0095		
	BEAM B3		-0075			-0100	-0125	-0105				
	BEAM B4		-0095		-0135		-0150		-0090		-0086	
	BEAM B5	-0060				-0145	-0170	-0160				-0070
	BEAM B6					-0160	-0190	-0170				
18.3 81.3	BEAM B1					-0180	-0190	-0180				
	BEAM B2			-0120		-0205	-0220	-0190		-0110		
	BEAM B3		-0090			-0185	-0215	-0195				
	BEAM B4		-0098		-0200		-0230		-0185		-0110	
	BEAM B5	-0070				-0190	-0205	-0185				-0080
	BEAM B6					-0195	-0220	-0205				
20.9 92.9	BEAM B1					-0200	-0220	-0205				
	BEAM B2			-0140		-0215	-0230	-0210		-0125		
	BEAM B3		-0125			-0206	-0215	-0200				
	BEAM B4		-0120		-0220		-0240		-0210		-0130	
	BEAM B5	-0080				-0205	-0235	-0216				-0095
	BEAM B6					-0220	-0250	-0216				

TABLE C.5 (continued)

CONCRETE STRAINS AT 3 IN (7.6 cm) FROM TOP COMPRESSION FIBER

DISTANCE FROM CENTRE		in	40	34	28	8	4	CENTRE	4	8	28	34	40
		cm	101.6	86.4	71.1	20.3	10.2	0	10.2	20.3	71.1	86.4	101.6
LOAD	GAUGE NUMBER		52	53	54	55	56	57	58	59	60	61	62
kips kN													
	BEAM B1						-0255	-0270	-0260				
	BEAM B2				-0155		-0250	-0275	-0245		-0165		
23.5 104.6	BEAM B3			-0135			-0240	-0260	-0225				
	BEAM B4			-0145		-0250		-0290		-0265		-0128	
	BEAM B5		-0100				-0265	-0280	-0245				-0090
	BEAM B6						-0270	-0300	-0275				
	BEAM B1						-0280	-0300	-0275				
	BEAM B2				-0170		-0320	-0300	-0270		-0186		
26.1 116.2	BEAM B3			-0150			-0295	-0310	-0283				
	BEAM B4			-0160		-0310		-0305		-0325		-0165	
	BEAM B5		-0100				-0280	-0305	-0290				-0110
	BEAM B6						-0305	-0330	-0300				
	BEAM B1						-0310	-0325	-0310				
	BEAM B2				-0190		-0305	-0335	-0315		-0200		
28.7 127.8	BEAM B3			-0170			-0310	-0325	-0299				
	BEAM B4			-0185		-0310		-0345		-0300		-0195	
	BEAM B5		-0120				-0325	-0360	-0335				-0130
	BEAM B6						-0350	-0360	-0300				
	BEAM B1						-0350	-0360	-0345				
	BEAM B2				-0213		-0355	-0370	-0330		-0208		
31.3 139.4	BEAM B3			-0185			-0325	-0370	-0350				
	BEAM B4			-0195		-0350		-0385		-0340		-0190	
	BEAM B5		-0130				-0338	-0375	-0348				-0135
	BEAM B6						-0380	-0400	-0360				

TABLE C.5 (continued)

CONCRETE STRAINS AT 3 IN (7.6 cm) FROM TOP COMPRESSION FIBER												
DISTANCE FROM CENTRE	in	40	34	28	8	4	CENTRE	4	8	28	34	40
	cm	101.6	86.4	71.1	20.3	10.2	0	10.2	20.3	71.1	86.4	101.6
LOAD	GAUGE NUMBER	52	53	54	55	56	57	58	59	60	61	62
kips kN												
34.0 151.0	BEAM B1					-0400	-0420	-0390				
	BEAM B2			-0230		-0390	-0410	-0380		-0240		
	BEAM B3		-0192			-0375	-0405	-0385				
	BEAM B4		-0205		-0380		-0400		-0370		-0200	
	BEAM B5	-0145				-0390	-0405	-0375				-0155
	BEAM B6					-0415	-0425	-0440				
36.6 162.7	BEAM B1					-0420	-0450	-0425				
	BEAM B2			-0250		-0429	-0440	-0422		-0260		
	BEAM B3		-0200			-0419	-0440	-0411				
	BEAM B4		-0225		-0400		-0460		-0390		-0210	
	BEAM B5	-0160				-0435	-0450	-0415				-0165
	BEAM B6					-0454	-0470	-0443				
37.0 164.6	BEAM B1					-0425	-0455	-0430				
	BEAM B2			-0255		-0433	-0442	-0424		-0262		
	BEAM B3		-0204			-0423	-0444	-0416				
	BEAM B4		-0229		-0403		-0464		-0393		-0217	
	BEAM B5	-0165				-0439	-0458	-0422				-0168
	BEAM B6					-0458	-0477	-0446				
39.0 173.5	BEAM B2			-0270		-0465	-0490	-0470		-0280		
	BEAM B3		-0218			-0452	-0485	-0465				
	BEAM B4		-0238		-0440		-0500		-0430		-0245	
	BEAM B5	-0165				-0450	-0475	-0455				-0170
	BEAM B6					-0490	-0515	-0540				

TABLE C.5 (continued)

CONCRETE STRAINS AT 3 IN (7.6 cm) FROM TOP COMPRESSION FIBER

DISTANCE FROM CENTRE	in	40	34	28	8	4	CENTRE	4	8	28	34	40
	cm	101.6	86.4	71.1	20.3	10.2	0	10.2	20.3	71.1	86.4	101.6
LOAD	GAUGE NUMBER	52	53	54	55	56	57	58	59	60	61	62
kips kN												
40.0 177.9	BEAM B3		-0226			-0460	-0496	-0468				
	BEAM B4		-0248		-0447		-0508		-0440		-0252	
	BEAM B5	-0170				-0461	-0482	-0462				-0178
	BEAM B6					-0497	-0523	-0548				
41.8 185.9	BEAM B4		-0270		-0480		-0535		-0500		-0280	
	BEAM B5	-0190				-0500	-0520	-0480				-0180
	BEAM B6					-0532	-0550	-0599				
44.4 197.5	BEAM B4		-0300		-0605		-0610		-0572		-0295	
	BEAM B5	-0200				-0595	-0580	-0575				-0220
	BEAM B6					-0663	-0590	-0607				
45.0 200.2	BEAM B4		-0307		-0612		-0618		-0590		-0302	
	BEAM B5	-0208				-0601	-0589	-0584				-0228
	BEAM B6					-0671	-0597	-0615				
47.0 209.1	BEAM B4		-0351		-0668		-0625		-0607		-0360	
	BEAM B6					-0778	-0640	-0700				
49.5 220.2	BEAM B6					-0886	-0700	-0742				